ARCHAEOMETRIC INVESTIGATION OF THE CONSTRUCTION MATERIALS
OF ROMAN (CARACALLA) BATH IN ANKARA

A THESIS SUBMITTED TO
THE GRADUATE SCHOOL OF NATURAL AND APPLIED SCINCES
OF
MIDDLE EAST TECHNICAL UNIVERSITY

BY

ZEYNEP TANRIVERDİ

IN PARTIAL FULFILLMENT OF THE REQUIREMENTS
FOR
THE DEGREE OF DOCTOR OF PHILOSOPHY
IN
ARCHAEOMETRY

DECEMBER 2018

Approval of the thesis:

ARCHAEOMETRIC INVESTIGATION OF THE CONSTRUCTION MATERIALS OF ROMAN (CARACALLA) BATH IN ANKARA

submitted by **ZEYNEP TANRIVERDİ** in partial fulfillment of the requirements for the degree of **Doctor of Philosophy in Archaeometry Department, Middle East Technical University** by,

Prof. Dr. Halil Kalıpçılar
Dean, Graduate School of **Natural and Applied Sciences**   _____

Prof. Dr. Musa Doğan
Head of Department, **Archaeometry**   _____

Prof. Dr. M. Ümit Atalay
Supervisor, **Mining Engineering Dept., METU**   _____

Assoc. Prof. Dr. Ali Akın Akyol
Co-Supervisor, **Con. and Res. of Cult. Prop. Dept., GU**   _____

Examining Comittee Members:

Prof. Dr. Suna Naziyet Güven
History of Architecture Dept., METU   _____

Prof. Dr. M. Ümit Atalay
Mining Engineering Dept., METU   _____

Assoc. Prof. Dr. Çiğdem Atakuman
Settlement Archaeology Dept., METU   _____

Prof. Dr. Yusuf Kağan Kadıoğlu
Geological Engineering Dept., AU   _____

Prof. Dr. Kutalmış Görkay
Archaeology Dept., AU   _____

Date: 07.12.2018

I hereby declare that all information in this document has been obtained and presented in accordance with academic rules and ethical conduct. I also declare that, as required by these rules and conduct, I have fully cited and referenced all material and results that are not original to this work.

Name, Surname: Zeynep Tanrıverdi

Signature:

ABSTRACT

ARCHAEOMETRIC INVESTIGATION OF THE CONSTRUCTION MATERIALS OF ROMAN (CARACALLA) BATH IN ANKARA

Tanrıverdi, Zeynep

Ph.D. Graduate Program of Archaeometry

Supervisor: Prof. Dr. M. Ümit Atalay

Co-Supervisor: Assoc. Prof. Dr. Ali Akın Akyol

December, 2018, 257 pages

In this study, the characteristics, technologies, provenance, compatibility, durability and deterioration problems of the original materials (stone, stone tessera, brick, mortar, and plaster) used in the construction of the Roman Bath in Ankara are identified through archaeometric methods, such as basic physical and physicomechanical tests (bulk density, effective porosity, water absorption capacity, ultrasonic pulse velocity, hardness tests), and compositional, mineralogical, and chemical analyses (binder-aggregate ratio and particle size distribution analyses, gravimetric analysis, salt content tests – spot salt analysis and electrical resistivity – petrographical thin section optical microscopy analysis, Raman analysis, SEM-EDX analysis and, XRF analysis). Firstly, stones are classified into five groups as andesite, limestone, marble, sandstone, and tuff. The provenance of the stones is Hüseyingazi-Kale for andesite, Haymana for limestone, Afyon marble quarry (Antique Marble Quarry) for marble and, Memluk Yuva Village for sandstone and tuff. The durability is low for andesite, sandstone, and tuff while for marble is moderate and for limestone is high. Salination (as phosphate, sulphate and carbonate salts) is the most important deterioration problem for all types of stones. Stone tesserae are in radiaolarite rock group from Elmadağ Irmak Village and low durability. Secondly, the brick work results show that the raw material characteristics and sources of clay in all bricks (structural brick, *pilae*, and pipe) are the same and local formation. It is the conclusion that the bricks were produced in the same mills, ateliers and in the same period. All original bricks have firing temperature

of around 900°C, a porous texture, and a rich composition as to minerals and rock type. However, structural bricks are more durable compared by *pilae*. The source of the clay material used was found to be METU forest and environs of Cevizlidere for Brick Gr1, Brick Gr2, Brick Gr4, and Brick Gr7, Yenidoğan for Brick Gr3, Brick Gr5, and Brick Gr6, and Tandoğan for Brick Gr8. On the other hand, the aggregates used in the production of the brick materials are basically andesite, granite, and metagrovac, which originate from the local formations of Hüseyingazi Kale, Bala Köprüköy, and southern Ankara, respectively. Besides, all bricks have low durability and the sources of their deterioration are mostly salt, moisture, and biological factors. Thirdly, mortars and plasters composed of traditional 2:1 aggregate:binder ratio have rich, homogeneous particle distribution the majority of which are angular coarse aggregates. The production technology of the structural mortars is of more quality than the *pilae* mortars. However, the structural mortars in Caldarium (hot room) are more qualified than the ones used in Tepidarium (warm room). While the raw material characteristic, source, and production technologies of the mortars are varied according to in which section of the Bath and for which function they are used, these properties are similar for all original plasters. Thus, the plasters probably were produced in local ateliers and around the same time. Binder material for the mortars and plasters are lime with brick fragments. The lime types of mortar and plaster are cement or natural cement (C/NC) category and highly durable. Finally, the results of garnered for each type of material are evaluated together, and the contributions made by each of the materials to the architecture, construction, and heating and water supply system of the Bath are determined.

Aside from this, these findings are reevaluated in terms of social context,revealing new knowledge about the history, archeology, architecture of the Bath, and enabling the reformulation of views on social, cultural, economic, and political life in Roman Period's Ankara.

Keywords: Roman Baths, Material Analysis, Archaeometry and Methods, XRF

ÖZ

ANKARA ROMA (CARACALLA) HAMAMI YAPI MALZEMELERİNİN ARKEOMETRİK İNCELEMELERİ

Tanrıverdi, Zeynep

Doktora, Arkeometri Programı

Tez Yöneticisi: Prof. Dr. M. Ümit Atalay

Ortak Tez Yöneticisi: Doç. Dr. Ali Akın Akyol

Aralık 2018, 257 sayfa

Bu çalışmada; Ankara Roma Hamamı'nın yapımında kullanılan özgün malzemelerin (taş, taş tessera, tuğla, harç ve sıva) malzeme karakteristikleri, üretim teknolojileri, hammadde kaynakları, uyum, dayanıklılık özellikleri ve bozulma problemleri; temel fiziksel ve fizikomekanik testler (birim hacim ağırlığı, gözeneklilik, su emme kapasitesi, ultrasonik hız, sertlik testleri) bileşimsel, mineralojik ve kimyasal analizler (bağlayıcı-agrega oranı ve agregada tane boyutu dağılımı analizleri, kızdırma kaybı analizi, tuz içeriği analizleri–spot tuz testi ve elektriksel iletkenlik - petrografik ince kesit optik mikroskop analizi, Konfokal Raman analizi, SEM-EDX analizi ve XRF analizi) gibi arkeometrik yöntemlerle tanımlanmıştır.

İlk olarak taşlar andezit, kireçtaşı, mermer, kumtaşı ve tüf olmak üzere beş gruba ayrılmaktadır. Taşların kaynağı, andezit için Hüseyingazi-Kale, kireçtaşı için Haymana, mermer için Afyon mermer ocağı (Antik Mermer Ocağı) ve kumtaşı ve tüf için Memluk Yuva Köyü'dür. Dayanıklılık, andezit, kumtaşı ve tüf için düşük iken mermer için ise ortalama ve kireçtaşı yüksek düzeydedir. Tuzlanma (fosfat, sülfat ve karbonat tuzları gibi) her türlü taş için en önemli bozulma problemidir. Radyolarit kayaç grubundaki taş tesseralar Elmadağ Irmak Köyü'ndendir ve düşük dayanıklıktadır. İkinci olarak, tuğla çalışma sonuçları göstermiştir ki, tüm tuğlaların (yapısal tuğla, pilae ve künk) kil hammadde karekterleri ve kaynakları benzer ve yerel formasyona aittir. Bu durum, tuğlaların aynı atölyelerde veya aynı dönemde üretildiğine işaret etmektedir. Tüm özgün tuğlalar, yaklaşık 900°C pişirme sıcaklığına,

gözenekli bir dokuya ve zengin türde mineraller ve kayaç bileşimine sahiptir. Ancak, yapısal tuğlalar pilaelerle kıyaslandığında daha yüksek dayanıma sahiptir. Kullanılan kil malzemenin kaynağı Tuğla Gr1, Tuğla Gr2, Tuğla Gr4 ve Tuğla Gr7 için ODTÜ Ormanı ve Cevizlidere Çevresi, Tuğla Gr3, Tuğla Gr5 ve Tuğla Gr6 için Yenidoğan ve Tuğla Gr8 için Tandoğan bölgesidir. Öte yandan, tuğla malzemelerin üretiminde kullanılan agregalarda temelde andezit, granit ve metagrovak kökenli ve aynı sıralamayla Hüseyingazi Kale, Bala Köprüköy ve Ankara'nın güney bölgesine ait yerel formasyonun ürünleridir. Ayrıca, tüm tuğlalar düşük dayanıma sahiptir ve bozulma nedenleri çoğunlukla tuz, nem ve biyolojik faktörlerdir. Üçüncü olarak, geleneksel 2:1 agrega: bağlayıcı içeriğe sahip harç ve sıvalar, çoğunluğunu hayli köşeli kaba agregaların oluşturduğu zengin, homojen agrega dağılımına, sahiptir. Yapısal harçların üretim teknolojisi, pilae harçlarından daha kalitelidir. Ancak Caldarium'daki (sıcaklık) yapısal harçlar, Tepidarium'dakinden (ılıklık) daha niteliklidir. Harçların hammadde karakteristiği, kaynağı ve üretim teknolojileri onların hangi hamam bölümünde ve hangi işlevde kullanıldığına göre çeşitlenirken, bu özellikler tüm özgün sıvalar için de benzer niteliktedir. Bu nedenle, sıvalar muhtemelen yerel atölyelerde ve aynı dönemde üretilmiştir. Harç ve sıvaların bağlayıcısı tuğla kırık katkılı kireçtir. Harç ve sıvaların kireç türleri çimento/doğal çimento (Ç/DÇ) kategorisinde ve oldukça dayanıklıdır. Sonuç olarak her bir malzeme türü için elde edilen veriler üzerinden malzemenin hamamın mimari, yapım, ısıtma ve su temin sistemine olan katkıları belirlenmiştir.

Bunun yanı sıra, bu bulgular; hamamın tarihi, arkeolojisi ve mimarisi hakkında yeni bilgileri ortaya çıkarmak ve Roma Ankara'sının, sosyal, kültürel, ekonomik ve politik yaşamına ilişkin görüşlerin yeniden şekillenmesini mümkün kılmak için sosyal bağlamda tekrar değerlendirilmiştir.

Anahtar Kelimeler: Roma Hamamları, Malzeme Analizi, Arkeometri ve Yöntemleri, XRF.

To the memory of my mother...

ACKNOWLEDGMENTS

TABLE OF CONTENT

LIST OF TABLES

LIST OF FIGURES

xvi

CHAPTER 1

INTRODUCTION

Conservation refers to all of the necessary precautions taken for the survival, maintenance and repair of objects, structures, groups of structures, or areas of historical, architectural or artistic value. Throughout history, varying conservation measures have been developed in different periods aiming at preserving historic heritage, and today, global conservation approaches seek to extend the lifetime of the historic asset to be passed on to the future generations.

In conservation studies, historical materials that bear witness to the technologies of past generations have an important position in discovering and protecting past knowledge. Today, material studies are conducted in many areas and by different disciplines, such as architecture, art history, archaeology, restoration, conservation, geology, chemistry, physics, biology, and material science. Scientific investigations of historical materials in particular, are examined both *in situ* and in a laboratory environment, and this is also the case in archaeological science. The importance of laboratory processes in the identification of historical materials is increasing every day. To begin with, Viscount Cherwell and Professor Christopher Hawkes had the vision and foresight of the necessity of laboratory research for archaeology and art history (University of Oxford) in Britain, if not in the world, and they were followed by Professor Teddy Hall who, with Professor Martin Aitken, brought laboratories up to international standards (Tite, 1991:139).

The main areas of Archaeological Science are dating, artefact studies, man and the environment, mathematical methods, remote sensing, and conservation. However, in the present thesis, artefact studies and archaeological conservation areas are given priority. The aim of artefact studies is to determine the provenance (source), production technology, usage, and durability (decay processes) of raw materials, and

based on the results of such studies, correct restoration and conservation techniques are applied to the artefact to preserve its "authentic value" for future generations (Tite, 1991:140).

The present study begins by making an assessment of provenance which involves characterizing and locating the natural sources of raw materials used to create the trade or exchange artefacts or buildings. Then, based on this assessment, a cultural-historical, economic-ecological, or processual contextual approach between different cultural groups is estimated.

In the provenance study, every possible analytical and microscopic technique can be used. That is to say, determining the link between the artefact or building material and the source of its raw materials on the basis of trace element composition, mineralogy or isotopic composition is not easy. The determination of the location of possible natural raw material sources (e.g. mines, quarries, clay beds) involves long-term study, and sources that are separated in geological maps may have similar trace element compositions, mineralogies or isotopic compositions. Furthermore, the character of some raw materials may change during the production of the artefact (Tite, 1991:143).

Second, technological studies are carried out to identify the materials and techniques used in the production of artefacts or building materials. The role of physical sciences is important in the technological study of certain artefacts or building materials, such as pottery, brick, plaster, metal and glass due to the chemical or structural alterations that may occur in raw materials during the manufacturing process. In contrast, the contribution of the physical sciences is limited in the case of those technologies of the artefacts such as stone, wood and bone due to the mechanical modifications of raw materials. Such science-based technologies have been studied using a wide range of analytical and microscopic techniques, and the objective of these studies has been twofold. First, it is of prime importance to find out the types of raw materials, and the processing techniques applied to the artefacts or building materials. Second, it is necessary to identify the reasons why particular materials and production methods were used and causes of changes in technologies. The production processes of materials represent important scientific evidence in investigations of ancient technologies when they are correlated with those described

in contemporary ancient writings such as those of Pliny (1st century AD) (1857) and Theophilus (12th century AD) (Smith, 1870). Furthermore, it is desirable to recreate production processes through scientific examinations in the field or laboratory so as to test their effectiveness. For example, experimental pottery or brick kilns may be reconstructed in the laboratory to understand the production process (Tite, 1991:144-146).

Third; usage studies are conducted in order to investigate the ways artefacts or building materials were used. In these studies, the mechanical properties of the objects, such as their plasticity, malleability, fragmentation and thermal and mechanical shock resistance are important factors in the choice of materials used in artefacts or building materials (e.g., Anders et al., 1992, Bradley et al., 1992; Kilikoğlu et al, 1998; Jones, 2004:334). Usage studies on artefacts require less scientific effort than provenance and technological studies and generally focus on the examination of the surface appearance of materials. Through such studies, it is possible to obtain useful information about the tools used. For example, a microwear analysis is applied to the surfaces of Paleolithic stone tools to identify the materials (wood, bone, meat) on which the tools were used (Keeley, 1980; Tite, 1991:146-147).

Fourth, durability studies are carried out to determine the performance characteristics of artefacts or building materials. The materials are chosen to make artefacts depending on their durability. According to Miller (1994), the meaning of the objects is related to their temporal connection to people, and whether they have longevity or a temporal relationship. This temporal connection provides information about the physical characteristics of the objects. For example, in the modern world, people might expect transient artefacts to be made out of plastic while enduring artefacts would be made of stone or concrete, but the durability of materials does not simply relate to utility or function. Materials have a social meaning for the quality of artefacts; for instance; how artefacts are valued, used or exchanged or which artefacts are involved in commercial acts (Jones, 2004:335).

In this context, to obtain valid and accurate information from studies of all areas of archaeological science, collaboration between science and archaeology is necessary. Archaeometry is a scientific branch of archaeology that seeks to come up with

solutions to archaeological problems through the application of scientific methods in natural and applied sciences. The physical and mechanical properties of archaeological materials are the prime concern of archaeometry and science-based archaeology. Actually, archaeometric and material based approaches to archaeology were introduced by experts imported from physical sciences such as chemistry, physics (Tite, 1972:148), and geology (Peacock, 1969a,b; 1982) and the success of these approaches is perhaps based on the useful translation of tried and tested techniques in the characterization of materials such as petrology (Peacock, 1969a,b; 1982). The adoption of techniques from physical sciences has been maintained through refined methods in the determination of the chemical, physical, and mechanical properties of artefacts (Cotterell, Kamminga 1990; Kingery, 1996; Pollard, Heron, 1996; Henderson, 2000; Jones, 2004:331).

Today, archaeometric studies contribute to archaeological studies, but the following problems need to be addressed. First, the balance between new techniques and the application of established techniques is necessary in the resolution of problems.

Second, different components of different disciplines arguably talk in different languages (Schiffer, 1996; Brown, Pluciennik, 2001), and one of the most significant problems faced by archaeological theorists and archaeological scientists relates to communication (Edmonson, 1990; O' Conor, 1991; Dunnel, 1993). Accordingly, an improved meaningful dialogue is essential between scientists and archaeologists who are useful in obtaining information. While scientists should be taught to understand the aim, methodology and framework of archaeology, archaeologist should be trained to understand the potentials of and restrictions to the application of science.

Third, both archaeologists and scientists must understand the limitations of scientific data and should assess the accuracy of such data.

Fourth, when developing new techniques, scientists should not concentrate only on high technologies as these can provide detailed and sophisticated data only on a small proportion of the artefactual records. On the other hand, some emphasis should be given to the low technologies which are capable of providing data for the complete artefactual record that is for all artefacts as pottery, flint or obsidian from a site. Success in tackling with all of the above problems will lead to future developments in archaeological and archaeological science (Tite, 1991:148-149).

1.1 Problem Statement

Archaeological structures or ruins are the main sources of information on architectural, construction technologies and building functional systems (heating, water supply and drainage system etc) of past achievements. It is necessary to retain their authenticity and to pass them on to future generations, and to this end, Roman baths are highly unique structures due to their original (authentic) architectural, constructional technologies and functional systems (heating, water supply and drainage system) of their time. In the Roman era, baths were constructed to respond to different demands such as for bathing, health and, socializing based on parameters such as geography, climate and tradition.

It is known that bath buildings have been constructed since ancient times (e.g. by the Greeks and Romans), and there have been a number of studies of baths and bathing culture (Yegül, 2010, 2006; 1992; Fagan, 2001, 1999; Farrington, 1995; Nielsen, 1993; Brödner, 1983). However, there is lack of knowledge on the material properties of their architecture, construction, and functional systems (in heating and water supply system). Roman baths are based on archaeometric methods (Oğuz, et al., 2014; Stefanidou, et al., 2014; Marey Mahmoud, et al., 2011). There is, therefore, a need to conduct research in order to determine the characterization and source (provenance) as well as the technological and usage properties of materials. Knowledge of the material technologies is also essential in the maintenance and conservation of Roman baths with authentic values, although this requires collaboration among a multidisciplinary group of architects, engineers, archaeologists, scientists, and specialists.

Generally, in Roman baths, the remains of foundations as an original part of the structure provide clues into the technology of the architecture, construction and functional system. Although the actual plans of the Roman baths may not change in many cases, they may lose their original constructional and material technologies due to incorrect interventions such as using incompatible contemporary materials. In addition, due to the lack of conservation studies in archaeological areas, archaeological structures or ruins suffer from serious problems, such as rising damp, atmospheric pollution, and salination. To eliminate or minimize the damaging effects of such problems, correct diagnostic studies should be carried out to establish

maintenance and conservation programs.

This study of a Roman (Caracalla) Bath was carried out in Ankara, the capital city of Turkey. The ruins of the bath building and its archaeological surroundings are unique in Ankara; and the site still provides clues to the original architecture, construction, heating and water system, and material properties of Roman period baths. Accordingly, the site has been selected for an examination of original materials (stone, brick, mortars and plasters) and constructional techniques from the Roman period, making use of archaeometric methods.

Archaeometric approaches are important in identifying the characteristic, provenance, technological and usage properties of materials of archaeological sites. Accordingly, the study was conducted using archaeometric methods involving a collaboration of science and archaeology. The scientific examination of the study was carried out in a laboratory setting, and the archaeological survey was carried out *in situ*.

1.2 Aim and Objectives

This study was carried out to identify the original material properties of the Roman Bath in Ankara using archaeometric methods, with particular emphasis on their contribution to construction technologies and performance. Such knowledge is essential in gaining a better understanding of the material technologies used in the construction of Roman baths in establishing their particular constructional and functional technological features and maintaining these inherent technological features as long as possible through well-planned maintenance and conservation programs.

The main objectives of the study were to improve material analysis methods through the use of archaeometric methods, with emphasis on:

1. Discovering the characteristic properties and sources of the natural raw materials used in the construction of the Roman Bath through provenance studies, and petrographical, mineralogical, and chemical analyses,

2. Identification of the material technologies of the Roman Bath through compositional, mineralogical, and chemical, analyses. In other words, to find out the different types of raw materials and the processing techniques which are used on the

architectural component. Furthermore, identifying the rationale behind the use of particular materials and production methods, and the reasons for technological changes,

3. Determination of the compatibility and durability of materials used in the architectural, constructional, and functional system (water, heating, drainage etc.) of the Roman Bath through physical, physicomechanical, petrographical, mineralogical, and, chemical analyses,

4. Observation of the present condition and deterioration factor of the material structure of the Roman Bath by way of an in situ survey.

5. Creation of a database for the production of repair materials that are similar to those used in the original structure for the future restoration and conservation works of the Bath,

6. Determination of the contribution of the materials to the architecture, construction techniques, and heating and water supply systems of the Bath,

7. Obtaining new knowledge about history, archaeology, architecture etc. of the Bath,

8. Filling the gap in the literature concerning material analysis in other Roman baths in Anatolia,

9. Uncovering information about historical, social, cultural, economic and political life in Roman-era Ankara,

In summary, the constructional materials of Roman (Caracalla) Bath in Ankara were examined using archaeometric methods to gain knowledge and experience, based on the objectives mentioned above.

1.3 Procedure

The study was designed to determine the material properties of the Roman Bath through the use of archaeometric methods. Initially, a comprehensive review of the literature was made on baths from the Roman Era, in terms of their bathing, heating and water supply systems, their architecture and construction techniques and the material characteristics.

Secondly, information on the Roman (Caracalla) Bath in Ankara was documented, highlighting its historical, archaeological, architectural, constructional and material

properties and its heating and water supply system. Then, in order to determine the present condition of the Roman Bath, several field observations were made. At the same time, to obtain visual, documents, reports and measured drawings of the Bath, the General Directorate of Pious Foundations and a conservation architect were contacted. The background information for the study was compiled from all available sources.

Thirdly, archaeometric methods were determined for the materials used in the construction of the Roman Bath, and these methods were reviewed in a literature survey. Material samples were taken during a field study and prepared for laboratory studies. In the laboratory, a set of archaeometric studies comprising physical and physicomechanical tests, and compositional, chemical, and mineralogical, analyses were applied to the samples. The physical and physicomechanical tests were performed to determine the strength of materials, while the compositional and chemical analyses were then applied to identify the material characteristics and technologies. The mineralogical analyses were used to discover the provenance characterizations and the sources of the raw materials. In all tests and analyses, the relevant standards used for the calculations were obtained from the Turkish Standards Institution.

All related documents were reviewed collectively to explore the characteristics, technologies, provenance, usage, compatibility and durability of the construction materials in the Roman Bath. All cases were examined according to predetermined parameters garnered from existing literature so as to allow an easy comparison. Thereafter, all the results were reevaluated in the result and discussion section to obtain an accurate conclusion. For the conclusion, the author and experts from natural sciences and social sciences interpreted all the results together, coming up with some new results about the Roman (Caracalla) Bath in Ankara and Roman Era Ankara.

1.4 Disposition

The study is presented in six chapters, beginning with this introduction.

In the second chapter, the literature survey is presented on the general aspects of Roman baths, together with the bathing system, heating and water supply systems,

the architecture and construction techniques, and the material characteristics.

In the third chapter, a more comprehensive literature survey is carried out on the Roman (Caracalla) Bath in Ankara. Its historical, archaeological and architectural construction technologies, material properties, and functional systems (heating and water supply systems) applied are reviewed.

The fourth chapter describes the materials used in the construction of the Roman (Caracalla) Baths in Ankara, and more detailed information of the methods applied to the materials is provided. The first phase of the analysis method provides information about the determination of the colors of the materials through a chromametric analysis. In the second phase, physical and physicomechanical tests, such as bulk density, effective porosity, water absorption capacity, ultrasonic pulse velocity and hardness (Schmidth hammer) tests are discussed. The final section comprises such compositional, mineralogical and chemical analyses as binder-aggregate ratio, particle size distribution, gravimetric analyses (LOI); quantitative analysis of soluble salts as conductivity measurements and spot test for anions; petrographical thin section optical microscopy, confocal Raman microscopy and spectroscopy, and SEM-EDX and PED-XRF, analyses.

In the fifth chapter, the results obtained from the basic physical and physicomechanical tests, and the compositional, mineralogical and chemical analyses are presented in tables, figures, drawings and charts. The results obtained from the tests and analyses are then evaluated and discussed in terms of the characteristic, provenance (location), technology, usage, compatibility and durability properties of the materials. The chapter ends with a conclusion in which all the findings are summarized and interpreted together by the author and social-natural sciences experts, and their comments and recommendations are offered for further research work.

1.5 Literature Survey

Baths are among the finest historic structures from ancient history, with remarkable characteristics that reflect the cultural, social, religious and technological habits of a certain era. Accordingly, the remains of baths have attracted significant attention and have been the subject of broad studies by researchers in the archaeological,

restorational-conservational and/or archaeometric areas who aim to evaluate the role of materials in the past. Some of these can be summarized as follows:

Stefanidou et al. (2014) made an analysis and characterization of the hydraulic mortars of ancient cisterns and baths in Greece. In the study, structural mortars and plasters from cisterns and baths (thermae) from the Roman, Byzantine and Ottoman periods were investigated to determine their physicomechanical, chemical and microstructural characteristics. It was revealed that coherent and dense structure of the samples arose from the selection and combination of raw materials and their interaction with the environment. The binding system consisted of a combination of hydrated lime and natural pozzolan or brick dust forming a continuous micro-crystalline matrix with a high degree of hydraulicity. The porous structure of the mortars provided the space where there was the secondary crystallization of calcite. Therefore, it created a more compact and dense structure. In addition, the environment of cisterns and baths could have a positive effect on these reactions of the materials, in that moist and hot conditions were suitable for the dilution of the calcite. According to the mortar or plaster type, aggregates of both siliceous and brick fragments had different granulometries. The technology behind was different granulometry in mortar and plaster providing a reactive, compact and impermeable structure. The production technology of the mortars and plasters in baths and cisterns showed that the builders had advanced knowledge of material behaviors and were able to build durable structures highly resistant to deterioration.

Another paper (Kramar et al., 2011) discussed the characterization of mortars from the bath complex of a Roman villa rustica from an archaeological site near Mošnje (Slovenia), and analyzed the layers of mortar below mosaics and wall paintings, as well as the mortar floors. The mineralogical and petrographic properties of the mortars were determined via optical microscopy, X-ray powder diffraction and FTIR spectroscopy. With the help of a SEM-EDX analysis, the aggregate-binder interfaces were revealed, while the acid-soluble fractions were determined using ICP-OES to identify the hydraulic characteristics of the mortars. Moreover, the brick fragments contained within a special mortar aggregate were studied. To assess the content of the brick fragments, Hg-porosimetry and gas sorption isotherms were used, and the results revealed that higher content brick fragments in mortars exhibited a higher

porosity and a greater BET surface area, but a lower average pore diameter when compared to mortars with lower amounts of the special aggregate. The study reported that all of the mortar samples investigated had similar petrographic and mineralogical compositions.

In the study by Marey Mahmoud et al. (2011), the characterization of plasters from the Ptolemaic Baths near the Karnak Temple Complex in Upper Egypt was conducted by means of an optical microscopy (OM), a scanning electron microscopy (SEM) equipped with an energy-dispersive X-ray detector (EDS), an X-ray diffraction analysis (XRD) and a Fourier transform infrared spectroscopy (FT–IR), through which the chemical compositions and structures of the plasters were determined.

The paper entitled "Provenance of white marbles from Ptolemaic Baths: New excavations near the Karnak Temple Complex, Upper Egypt (Abu-Jaber et al., 2012) seeks to determine the source (provenance) of the marble in the baths through petrological, textural, geochemical and isotopic analyses. In particular, the marble samples from the baths at Qasr al Bint and the Colonnaded Street were studied, and the results differentiated between four different types of imported marble. The first was a coarse grained dolomitic marble, which was highly durable and came from the Thasos 3 quarry site; the second was a coarse grained hard grayish calcitic marble from Proknnesos; the third was also a course grained hard calcitic marble, sourced from the Penteli; and the fourth one was of a finer grained friable variety that resembles calcarenite in thin sections from the Dokimeion quarries. As a result, the study revealed that marble had been sourced from Asia Minor and Greece. The choices of marble were based on their desired utilitarian and aesthetic function, and from this, it can be understood that the trade of stone materials was part of the cultural relationships of that period.

Another paper making a provenance analysis was penned by Lancaster et al. (2009), and was entitled "Provenance of lightweight volcanic stones used in Ancient Roman concrete vaulting: Evidence from Turkey and Tunisia". The use of lighter rocks for the vaults and heavier rocks for the foundations could be traced back to the mid-1st century BC in Rome, although the systematic usage of these rocks started in the early 2nd century AD under Trajan (Lancaster, 2005). The system then spread

throughout the Empire to areas with local sources of lightweight volcanic material. The authors sought to determine the provenance of the lightweight stones used in vaulting of two areas of the Mediterranean – modern Turkey (ancient Cilicia) and Tunisia (ancient Africa Proconsularis) and involved the collected samples which were analyzed in thin sections under an optical microscope to detect their mineral phases and textural features. The samples were also subjected to an XRF and (ICP–MS) analysis to determine the elemental composition and concentrations of the major and selected trace elements. The geochemical results revealed that the source of the scorias from Anazarbos and Elaeussa Sebaste were the Ceyhan-Osmaniye volcanoes of Delihalil Tepe, Üçtepeler and Gertepe.

A paper by El-Gohary (2009) entitled "Characterization of Bricks used in the external casing of Roman Bath walls Gadara, Jordan" deals with the brick units used in one of the Roman baths at the Gadara archaeological site. The study investigated different raw material characteristics of the bricks and the different technological measurements of the brick units, including shapes, dimensions and visual descriptions. The construction techniques and deterioration problems of the bricks were also examined, making use of scientific techniques and analytical procedures, such as EDX, to define the elemental and chemical characteristics; a polarizing microscope and XRD to study the mineralogical components, and SEM to identify the morphological characteristics of the samples. In addition, the physical, mechanical and thermal properties of the brick samples were determined using different scientific techniques and standard tools, such as digital camera, magnifying glass, and mechanical sieves. As a result of the study, the chemical, physical, mechanical and thermal properties and deterioration cycles of the brick samples, as well as brick types, shapes, dimensions, firing temperatures were determined.

Degryse et al. (2002) carried out a facies analysis and provenance studies on the building materials used in the construction of the Roman Sagalassos (SW Turkey). In this study, the different types of building stone used in the ancient city of Sagalassos were analyzed through macroscopic and petrographic studies. According to the study, the natural stones of the buildings were limestone, conglomerate, breccia, marble, travertine, granite, sand, and siltstone, and they had different qualities. Besides, the provenance of the building stones was most probably the lithological

12

units both in the surroundings of the city and further away in the area of Burdur. While travertine and volcanic building stones were brought from Başköy and Selçuk respectively, the marbles were transported from the Docimian quarries 250 km to the north of the site. On the other hand, the sources of some other building materials, including brown-grey and greyish granite, were not identified.

In Turkey, the building materials used in the construction of Ottoman Baths and Roman buildings have been widely analyzed in terms of their raw material characteristics, provenance, and technologies, although there have been limited material analyses of Roman baths.

The paper entitled "Construction Materials Used in the Historical Roman Era Bath in Myra" (Oğuz et al., 2014) discussed the physical, chemical and mechanical properties of the mortars and bricks used in the historical Roman Era Bath in Myra, within the boundaries of the Antalya Province, during the Roman era. In this study, firstly the sample picked points were marked on the air photograph and the plan of the buildings and then the all samples were photographed. After that, the laboratory analyses were carried out on the samples. Petrographical studies of the construction materials (mortar, brick) were made with a stereo microscope to determine their mineralogical properties. Concurrently, physical (unit volume, water absorption by mass, water absorption by volume, specific mass, compacity and porosity), chemical (acid loss and sieve analysis, salt analyses, pH, protein, fat, pozzolanic activity and conductivity analyses) and mechanical (compressive strength, point loading test, and tensile strength at bending) analyses were carried out on the samples. The results of the analyses showed that the binders and aggregates in the mortars have good adherence with each other. Furthermore, the mechanical analysis results of the bricks revealed that they were produced using appropriate techniques against negative environmental and atmospheric effects and so they have preserved their originality until today.

Other papers reporting on material analyses of Ottoman Baths in Turkey have been prepared by experts from the Izmir Institute of Technology. The first of these studies analyzed the use of brick-lime plasters and their relevance to the climatic conditions of historic bath buildings (Böke, Uğurlu, 2009). In this study, the brick-lime plasters used in the construction of Ottoman Baths were investigated in terms of the suitability

suitability against the hot and humid environmental conditions of the baths. To this end, the raw material compositions and basic physical, mineralogical, microstructural and hydraulic properties of the brick-lime plasters collected from some of the historic bath buildings in Izmir (Turkey) were examined by way of XRD, SEM-EDX, AFM, and chemical analyses. The results showed that the brick-lime plasters were durable against the moist, humid and hot conditions of the baths, due to the formations of calcium silicate hydrate and calcium aluminate hydrate on the surfaces and in the pores of the brick aggregates. The formations were formed as a result of the chemical reaction between the lime and the brick aggregates and they provided a strong adhesive bond between these two materials. Therefore, the brick-lime products were more durable and stiff in the humid and hot environmental conditions of the baths. The second such paper analyzed the "characteristics of brick used as aggregate in historic brick-lime mortars and plasters" (Böke et al., 2006). In the study, seven brick-lime plasters, one dome mortar and three dome bricks collected from the Ottoman bath buildings which were constructed in the 14th and 15th centuries in the cities of Edirne (Saray and Beylerbeyi) and Bursa (Ördekli) in Turkey were studied to determine their raw material compositions (based on dilute hydrochloric acid and sieving analyses), basic physical (based on bulk density and porosity, uniaxial compressive strength analyses), mineralogical (based on an XRD analysis), chemical, microstructural (based on SEM-EDS and AFM analyses) and hydraulic (based on a TGA analysis) properties. The analyses revealed that the historic brick-lime mortars and plasters used in the construction of the Ottomans bath had high durability against the moist and hot environments. Their utility for use in the moist environment was explained by their hydraulic properties due to lime-binder products which were created by the chemical reaction between the lime binder and brick aggregates and the pores of the bricks. These products facilitated strong adhesion bonds, which make the mortar and plaster samples durable. While the brick used in the aggregate of the mortar and plaster samples had good pozzolanicity due to its amorphous clay minerals, the brick samples used for the construction of the domes in the bath buildings had poor pozzolanicity due to their different mineralogical and chemical compositions from the bricks used in mortars and plasters. Accordingly, pozzolanic bricks were used predominantly in the production of hydraulic mortar and plasters.

14

In the third such paper, the focus is on the "ettringite formation in historic bath brick – lime plasters" (Böke, Akkurt, 2003). In the study, two types of hydraulic brick-lime plasters or Horasan plasters were collected from the interior walls of warm space of an Ottoman bath that had been constructed in 1375 in Edirne, Turkey and repaired in 1565, and again in the 18th century. The samples were investigated to understand their production technologies and compatibility for use in such applications. Although the two types of plasters were exposed to the same environmental conditions, they deteriorated differently. As the first type is the original plaster and structurally sounds, the second type is repair plaster and is found to have deteriorated in such a way that it was hard to identify the difference between the two. The raw material compositions and the pozzolanic activity of the brick powders used in the plasters were compared through a number of analyses. Although the analyses results showed no significant differences, ettringite crystals were identified in the historic repair materials using XRD, FTIR and SEM-EDS techniques, and this fact could be explained by the repair plaster losing its integrity because of the growth of ettringite crystals in the plaster. The growth caused an expansion of the repair plaster sample, causing deterioration, and so a decision was made to repair such buildings using plaster containing gypsum to protect it from moisture and to avoid ettringite formation. Güleç and Ersen (1998) discussed the characterization of ancient mortar samples taken from the Tahtakale Bath in İstanbul in an effort to understand ancient lime technologies, the processes of deterioration and the morphologies using both simple analyses (ignition loss test, acid loss test, sieve, water soluble salts and petrographic analysis, and physical and mechanical tests) and sophisticated techniques (XRD, SEM, EDXA). The studies provided explanatory information about the ancient mortars prior to the carrying out of conservation works.

Our literature survey identified a gap in the research of the material characteristics, techniques and provenance of the Roman baths in Turkey. As a significant location in Roman culture, Anatolia (or modern Turkey) can be considered an appropriate site for the exploration of materials used in the construction of Roman baths. The archaeological site containing the Roman Bath in Ankara was selected due to its uniqueness in Ankara. The Bath has survived with its original architectural form, construction, and heating and water system, making it ideal for a study of the

material properties of Roman-Era baths.

Through this study, the characteristics, technologies, provenance, compatibility, durability and deterioration problems of the original materials (stone, brick, mortars and plasters) used in the construction of the Roman Bath in Ankara are identified through archaeometric methods, such as basic physical and physicomechanical tests (bulk density, effective porosity, water absorption capacity, ultrasonic pulse velocity, hardness tests), and compositional, mineralogical, and chemical analyses (binder-aggregate ratio and particle size distribution analyses, gravimetric analysis, salt content tests – spot salt analysis and electrical resistivity – petrographical thin section optical microscopy analysis, Raman analysis, SEM-EDX analysis and, XRF analysis). In the following stage, the results are gathered for each type of material and are evaluated together. Consequently, the contributions made by each of the materials to the architecture, construction, and heating and water supply system of the bath are determined.

Besides, the results of the tests and analyses in the study will be referred to when deciding upon the materials used for repairs in the future restoration and conservation projects of the Bath and these results will pave the way for filling the gap in the literature concerning material analysis of other Roman baths in Anatolia.

The results are also reevaluated in terms of social context, revealing new knowledge of the history, archaeology and architecture of the Bath, and the social character of Roman-era of Ankara and so, it will serve as a supplementary resource for researchers studying the Roman Baths and the Roman era in Ankara.

CHAPTER 2

GENERAL ASPECTS OF ROMAN BATHS

Bathing in Roman culture was a daily practice that was deeply rooted in history. Ablutions at the baths in the Roman lifestyle were considered physically and physiologically satisfying and also a form of entertainment. In the typical day of a Roman citizen, the afternoon was set aside as leisure time, and even at the end of the Republic Period, spending the afternoon at the baths after a light lunch and a quick nap were customary. This lifestyle was a part of city life and part of the Roman national identity (Yegül, 2010:29) and was summarized in a graffito as "Bathing, wine and love spoiled our bodies, but bathing, wine and love make up life" (Nenova, 2015; Daşbacak, 2006; Eliav, 2000; Yegül, 1992; Dunbabin, 1989).

Roman period thinkers used many words to refer to public bathing facilities, such as *Balineae, balneum, balineum, thermae, balaneion, Loetro / n, Loutro*/ n., as a clear indication of the importance of washing in Roman life. Describing the private bathing activity, the term *balanei* was adopted from *balaneion, balineum* or *balneum*. While balneum and balaena refer to places for bathing, balnearius means things pertaining baths (Rich, 1873; Sevimli, 2005:49-50). "Balneator" or "conductor baline" were terms used for the administrative officer of the bath, who had a service agreement that consisted of the bath rules and responsibilities of the administrative officer (Kula Say, 2007: 11).

M. Valeri Martialis suggested that the baths were similar to the thermal baths of the Etruscans. In Martial Epigrams (Martial, 1919) he suggested that the term "*balneum*" should be used not to refer to the entire building, but only for the washing room within the building. Along with the adoption of this understanding, the work *thermal* appeared in the Roman literature. Juvenal (1974) adopting a similar approach, used the expression "thermae (qe / rmai)" in his work entitled "Satura (VII.232-234)",

mentioning that such places belonged to Apollo, the god of healing, and he used the word to describe hot and hot water baths (Sevimli, 2005:56).

In brief, Roman baths comprised two basic bathing establishments – being *balnea* and *thermae* – referring to different ownership statuses and scale (Meiggs, 1973:416; Yegül, 1992:43). *Balneas* were small and private, while *thermaes* were very large public bathing complexes. While the *balnea* was solely for bathing, the *thermae* had, at minimum, also areas for sport, like the Greek *palaestra* (Nielsen, 1999:35). Fagan mentions that *balneas* would be relatively unadorned, while *thermaes* would be luxurious and ornately decorated (Fagan, 1999:14-15).

A thermae was a huge complex that would include lecture halls, libraries, pools, art galleries and many other practical facilities. According to some scholars, baths could be described as "a city within a city" or a "microcosm" within the Roman Empire (Zajac, 1999:103). The Romans used new technologies in *thermaes* (Smolijaninovaite, 2007:14).

The primary reason for the widespread popularity of the baths was their ability to make the user feel light and positive. The bathing experience induced relaxation through the use of clean water, steam, the odor of the oils and the massages that stimulated the senses, thus calming the mind. Relaxation was of course intensified by the magnificent bathing environment. "Thermae" that usually refer to the large imperial bath complexes in the Roman were known especially for their luxurious interiors. Vivid depiction of Bath interiors, shiny and colorful marbles, mosaics, plaster adornments, bronze equipment, sculptures, columns and high, light vaults and domes created the backdrop for architectural style in ancient in that era (Yegül, 2010:23-24).

As a secondary purpose, it was believed that baths were good for one's health, and so had medical and treatment functions. It was thought possible to cure illnesses through the application of a program of hot, cold and warm baths in sequence. Greek and Roman doctors and health experts were unanimous in their belief that natural hot springs and thermo-mineral baths were good for one's health. In ancient times, when there were only limited means of fighting illnesses, and when the average lifespan was 30 to 35 years, baths were considered an important preventive measure in regards to health. Furthermore, light physical exercise while bathing in the Greek

gymnasium was considered to be an effective but simple method of keeping in shape and staying healthy (Yegül, 2010:27).

Baths were further prioritized in daily Roman life as places where people could socialize while engaging in different kinds of social and fun activities. Popular activities included reading poems, playing music and singing, in both professional and amateur ways, and eating and drinking were also permitted. For regulars, chatting and gossiping while eating light snacks before dinner was a common social activity (Wheeler, 2004:14; Yegül, 2010:36).

In social gathering places such as theaters, amphitheaters, stadiums, and circuses, all seating was segregated into different social subclasses, while in contrast, the baths were unique in their democratic nature, making no discrimination with respect to sex, color, class or wealth. The single exception to this rule would be the slaves in the baths: slave labor was a key factor in entertainment during the Roman era, and many slaves were used to operate the baths (Strickland, 2010:41-43).

The baths were open to the general public for a low entrance fee, and so the emperor and politicians would use the baths to garner public support and to raise their popularity (Yegül, 2010:51-52).

Finally, there was also an economic reason behind the prevalence of Roman baths in the Roman lifestyle. The baths were a profitable and favorable investment. Improvements in building technologies and water transportation systems (especially the widespread usage of Roman concrete, which is widely used in the baths) cut costs, and these technical and economic advantages led to the proliferation of baths in city life and also in the rural areas. Even though the baths were built for profit, entrance fees were so low that even the poor could make use of them (Yegül, 2010:27-28).

2.1 Bathing System in Roman Baths

The bathing system in Roman baths generally involved moves from warm water to hot water through a sequence of connected rooms at different temperatures. One of the main stops in this sequence of rooms was the warm room *(tepidarium)* with medium temperatures. The sequence continued with the hot room *(caldarium),* which had high temperatures, and bathing ended in the cold room *(frigidarium)*, in which

there was a large pool containing cold water *(piscina)* (Yegül, 2010:34-35).

The sequence would thus be as follows: the bathers began their ablutions in the clothes-changing room *(apoditerium)* at the entrance to the bath where they changed clothes and then entered into the cold room (*frigidarium),* plunging into the cold water pool *(piscina)*. Then, they would pass into the warm room *(tepidarium)* and then into sweating rooms *(sudatorium* or *sudatorium)* where they sweated and were massaged. After that, they would enter the hot room (*caldarium)* where they bathed in hot water and then returned to the cold room (*frigidarium)*, where they would plunge into the pool *(piscina)* again. While some bathers would be dried at this point and return to the changing room *(apoditerium)* before leaving the bath, others preferred to return to the sweating rooms *(laconicum* or *sudatorium)* for more sweating and massage (Ürük, 2016:194), (Figure 2.1) (Yegül, 2006:67).
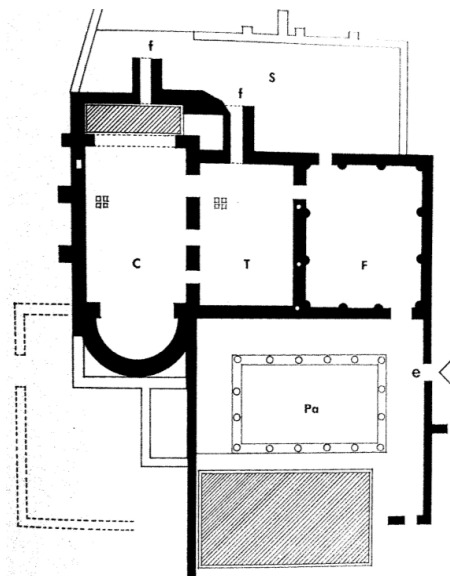
Figure 2.1 City Baths in Rome, Glanum (Saint-Remy-de-Provence, France) (Yegül, 2006:67)

Although it was not definite information, the bathing system took inspiration from ancient medical traditions. In ancient times it was believed that the final bathing step, passing from the hot room (*caldarium)* to the cold room (*frigidarium)* and plunging into the cold water pool served to open the closed pores, strengthen the body and boost bodily energy (Ürük, 2016:194). Furthermore, the *caldarium* and *frigidarium* carried also some symbolic and psychological meanings. The high temperature in the *caldarium* softened and relaxed the body, while the cold *frigidarium* woke, revived

and strengthened the user. It was accepted that the death of the elderly body in the *caldarium* from the excessive heat was followed by rebirth in the *frigidarium*. In this regard, the *frigidarium* was host to somewhat of a resurrection ceremony (Yegül, 2006:85).

The temperature for all bathing steps in all sections of the baths was tried to be measured by experts. The temperature in the warm room, according to Rook (1978) and Joria (1978-1979), would be between 30°C and 55°C, while the estimated temperature in the hot room is a source of contention among Kretzschmer (2000), Rook and Joria who estimated the temperatures to be 55°C, 70°C or 35°C values respectively (Başaran, 1997:1010-1011).

There are many different opinions regarding the base and air temperatures in each of the bathing sections. Yegül claims that speculations cannot be used to determine the exact temperature of the different sections of the bath. Modern experiments into how much a Roman bath is heated do not take into account the subjective sensitivity of the human body to heat and relaxation, and the physiological effects of heat loss (Yegül, 2006:114).

2.2 Heating System in Roman Baths

The main means of heating in Roman baths is via the floors, walls and sometimes even vaults, although significant heat also came from solar sources. According to Vitruvius (1914, 1990) this can be achieved by orienting the heated rooms in a south or southwest direction, and by having several windows. This heating system made significant contributions to ancient technology, and it can be seen that the locations of the bath are cleverly and creatively designed to make use of such technologies. The organization of the bath takes the form of a sequence of rooms with increasing temperature levels, with the visiting bather starting in the cold room before moving through warm and hot rooms. The system provides a clear separation between rooms with heating and those without. This heating system is referred to as *"hypocaust"*, meaning literally meaning "the furnace heated from below". As the name implies, the basic aim of the system was to heat the surfaces on which the bathers would walk (Ring, 1996; Yegül, 2010). Though it has not been fully corroborated (Fagan, 1997), according to ancient writers, notably Pliny the Elder (1857) the hypocaust system

was invented by architect Sergius Orata in the 1st century (Smith, 1870). Pliny's (1857) belief in this regard is based on the similarity between the Orata's "hanging baths" application to cultivate oysters, and the hypocaust system. In fact, Orata had no heating technology under the baths, he only invented building commercial oyster beds in 90–80 BC. The most accurate data on the hypocaust system comes from the Stabia Baths in Pompei (Figure 2.2) which date back to the end of the 2nd century BC and from the Greek Baths of Olympia in the 5th century BC (Mallwitz, 1972; Ürük, 2016). If it is true that the invention of the hypocaust system in the Olympia Baths in Greece dates back to 100 BC, it would have been impossible for Orata, who lived between 90–80 BC to have invented the hanging baths (Yegül, 2006: 111).
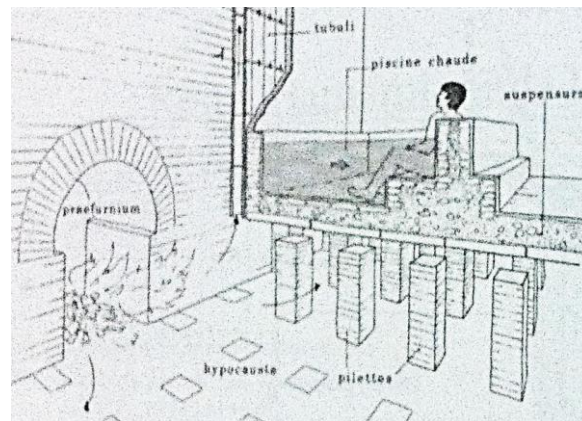
Figure 2.2 The *hypocaust* system of Stabia Baths in Pompeii (Yegül, 2006:90)

While the data from the Greek Baths of Olympia suggest that the origin of the hypokaust system belongs to Greeks, the new evidence collected from the Baths of Stabian in Pompeii supported that the system was compatible with the general view of the Late Republican period of Roman. According to Yegül, identifying the inventor of the hypokaust system is not easily solved with a simple Greek and Roman polarization, as there are many complex, cultural and historical perspectives reflecting archaeological data in the world. Yegül also claims that more primitive forms of this floor heating system have often been found in the Eastern Mediterranean, indicating a very ancient history. For example, in the Gortys Baths of Arcdia in Greece, built at the beginning of the 3rd century BC, heating channels were used under some pools and apse. According to Yegül, therefore, it would be a more

sensible approach not to attribute the invention of the hypocaust system to a single source or culture (Yegül, 2006:111-112)

Vitruvius (1914) wrote about the construction of a suspended floor that allowed heat to be circulated beneath the floor, and thus regulating the temperature, in *Ten Books on Architecture* as the follows:

First, the floor is laid with one and one-half foot tiles that incline toward the furnace, so that if a ball is thrown in it cannot stay in place, but returns to the furnace on its own accord. In this way flame will circulate more easily under the suspended floor. On top of this piers of eight inch tiles should be placed so that two foot tiles can be placed over them. The piers should be two feet high and they should be mortared with clay mixed in with hair and over them place the two foot tiles, which will hold up the pavement p.157.

His instructions provide insight into the construction of the heating system used in Roman baths, which can easily be achieved by locating channels below the floor to allow the hot air to circulate. The floor is raised above the ground on small columns. Within the system, air at high temperature passing from the furnace circulates through the system between supports called *"pilae"*. These *pilae* are usually made of bricks with hydraulic properties, being made sometimes from resistant volcanic stones based on basalt, limestone etc., shaped into a cylindrical or square shape. The height of the *pilae* varies between 0.70 and 1.40 meters, and they are set around 0.80 meter interval from the center. The floor is called a *suspensuare* supported by the *pilae* carrying the form of square tiles of 0.60 meter upon which is a 0.30–0.40 meters layer of tile mortar, upon which paving stones are laid. This thick structure is the reason why it took an entire day to heat the system (Figure 2.3) (Yegül, 2010:105-106).
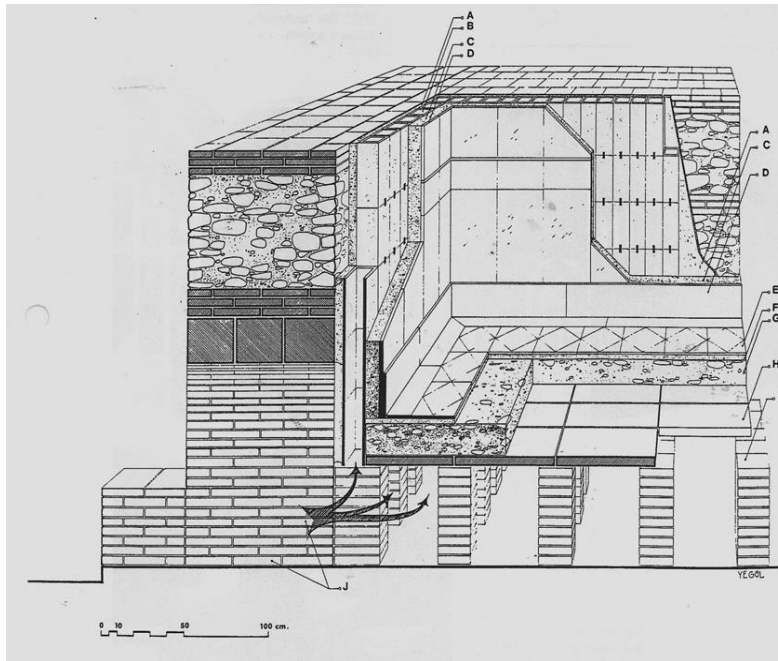
A: Lime mortar B: Tubuli C: Brick mortar D: Marble coating E: Ground floor F: Light weight mortar
G: Under floor heavy weight mortar H: Floor tiles (bipedales) I: *Pilae* (stone pillar) J: Furnace

Figure 2.3 Drawing of the *hypocaust* system in Roman baths (Yegül, 2010:105)

In the *hypocaust* system, the components and typical elements changed in line with regional requirements or availability. For instance, stone *pilae* were used instead of brick in the hypocaust systems of the eastern baths in the upper gymnasium at Pergamon. Some of the brick supports (*pilae)* were connected with arches in the huge Caracalla Bath in Ankara (Figure 2.4) (Yegül, 2010:107).
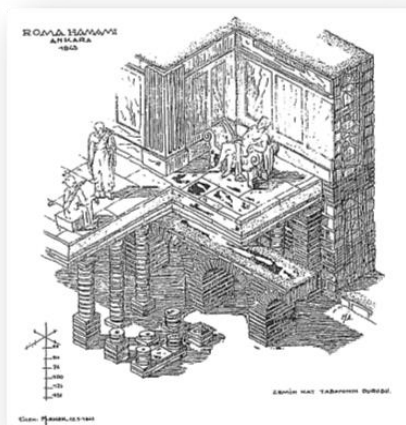
Figure 2.4 *Hypocaust* system of Roman (Caracalla) Bath in Ankara (Akok, 1955; Yegül, 2010:107)

24

The walls are heated by making use of the empty space behind the outside plaster (stucco) covering. The hot air and gases that circulate in this empty space are produced in the same furnace as the one heating the *hypocaust.* The air and gases are ventilated via holes below the eaves, allowing the hot gasses to be reused and making it possible for visitors to lean on the wall of the bath (Yegül, 2010:109).

The void walls in baths are created using terra cotta tiles *(tegulaemammatae)* with notches, although an improved *"tubuli"* tile version was later invented. "*Tubuli"* tile is a kind of hollow tubular brick. When placed on top of each other, these tiles form vertical holes that allow the warm air to circulate inside the walls. Almost all *"tubuli"* is closed and have very low drainage capacity, indicating a very economic system (Figure 2.5). As in the *hypocaus*t system *"tubuli"* tiles were used for the first time in the Stabia Baths in Pompei. These tiles were built into the walls to provide more effective and equal heat dissipation, and they were connected to the wall with metal clamps, mortar or both. They were then plastered over with mortar to a thickness of 3–6 cm and covered with marble slabs or Stucco (Yegül, 2010:110-111).
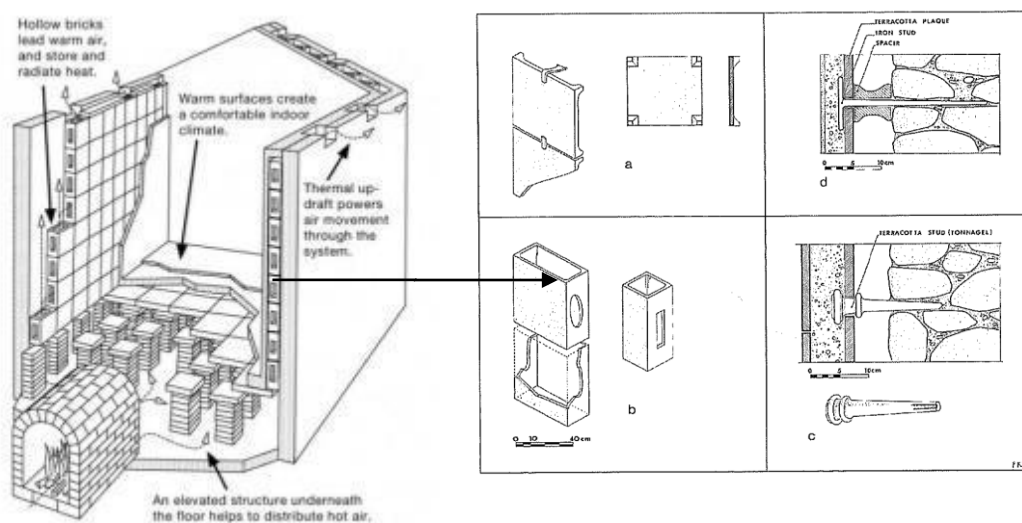
a: *tegulaemammatae* b: *tubuli* c: *terra cotta stakes* d: *terra cotta* connector iron nails

Figure 2.5 Wall heating system in Roman baths (Pinterest, n.d.; Yegül, 2010:110)

The baths were heated by a furnace called a "*praefurnium*". *Praefurnium* were generally built out of firebrick with refractive properties that were square in shape (about 0.50 x 0.50 m). The connection between the furnace and the underfloor space

of the bath was provided by a pair of short walls by which it was possible to canalize the flaming gases and to increase tractive effort. Grill which allows the oxygen to enter was not used in furnaces of the bath. Therefore, the slow-burning system which is suitable to run for long periods with heating requirements of Roman baths was obtained (Başaran, 1997:1012; Yegül, 2010:112-113). According to Yegül, heating Roman baths for 24 hours a day, keeping the furnaces in operation at low levels, is more economical and efficient than allowing them to go out between bathing hours (Yegül, 2006:113).

Furnaces would typically be located as an array on the outer walls of one of the heated rooms or arranged in all the heated locations of the bath. This second arrangement can clearly be seen in *thermae* and big baths, in that the large hot rooms or *caldariums* in these buildings require more than one furnace. Normally, the floors of the furnaces are raised by around 0.50–0.80 m, which is a suitable height for manually keeping the furnace stocked with fuel. The fuel would be mostly wood or rarely charcoal and the ash would be funneled down a slope in the floor. In the larger baths, such as Imperial Baths in Trier and the Roman (Caracalla) Bath in Ankara, the furnaces were connected to a service hall built with a high and wide stone vault. In the Roman Caracalla Baths in Rome there were four parallel and unconnected underground service galleries, measuring 4–6 m in width and located along the entire southwestern facade of the gigantic bath. In the service halls of all baths, servants and slaves worked in teams under difficult conditions to ensure that the bath worked in harmony (Yegül 2010:114).

In addition, the heating of water and cauldrons within the baths was also carried out in the furnace. The cauldron system used to heat the water was described by Vitruvius (1914) as the follows:

Three bronze cauldrons are to be set over the furnace, one for hot, another for tepid, and the third for cold water placed in such positions that the amount of water which flows out of the hot water cauldron may be replaced from that for tepid water, and in the same way the cauldron for tepid water may be supplied from that for cold. The arrangement must allow the semi cylinders (testidunes alveolorum) for the bath basins to be heated from the same furnace. p.157

Infact, Vitruvius (1914) describes two different systems that are heated by the same

furnace. The first one consists of three cauldrons that are interconnected with each other and cold water reservoirs. These are the sources of the hot and cold waters at the basins, taps and pools of the baths. The second one is mentioned in the last sentence *testidunes alveolorum* is an instrument that was used to heat the water and to keep hot water in the pool. Considering the thickness of the stone walls surrounding a typical Roman bath, it is a difficult to heat water and to keep hot water in the pool without such an instrument, which takes the form of a semi-cylindrical metal chamber, one edge of which is open and the other is closed (Its turtle shape led it to be named *testudo* in Latin) The open edge of the *testudo* opens into the pool, while the bottom metal edge is in direct contact with the fire. This allows the water in pool to be kept much warmer than with the thick concrete floor of the *hypocaust* system.

The two systems are both mentioned by Vitruvius (1914) as being used in the Stabia Baths in Pompei. There were three cauldrons in the service area located between the men's and women's sections. The cauldrons were shared by the both departments, to great effect, with two located over the furnaces serving the *hypocaust* of the bath, and the third cauldron, or reservoir, containing cold water placed over the furnace at the same level as the other cauldrons. Besides, the earliest use of the *testudo* is in the Stabia Baths in Pompei. Thus, it can be said that the invention of the instrument was in the early 1st century B.C. The *testudo* was used in the women's section of the bath. According to archaeological data, the *testudo* was in common use in the baths of Rome, although there is no evidence of *testudos* in the other well-preserved baths. In this regard, the use of a *testudo* in the baths was not universal (Yegül, 2010:115-116).

2.3 Water Supply System in Roman Baths

In order to describe the system for the supply of water to the Roman baths, it is first necesseray to understand Roman city planning. Romans generally sought to establish their cities in healthy areas, avoiding swamp lands due to the associated negative effects. Accordingly, they established some conditions to direct the location of their cities with inputs from writers, engineers, and thinkers like Strabo (2000), Columella (1941), Vitruvius (1914, 1990). These conditions were as follows, 1) The site should

be healthy, 2) It should have no nearby swamplands and be distant from very hot, cold or foggy climates, 3) The morning sun should rise on the city, 4) The wind must blow without disturbing the people and 5) There must be a natural water source. Therefore, based on these conditions, Romans designed their cities satisfied the needs of the people in the best possible way (Gültekin, 1998; Hodgkinson, 1985; Yegül, 1995; Sevimli, 2005:46).

Many Roman-period writers mentioned the importance of the infrastructures and superstructures required for water management in the maintenance of hygienic and healthy lifestyles. Structural systems and components were developed to this end, including cisterns, aqueducts, waterways, water reservoirs, water storage dug into rock, dirty and clean water channels below the streets and sewerage system. In addition, public baths and latrines were built in the cities (Anabolu, 2001; Sevimli, 2005:61-62).

In the small- and medium-sized Roman baths, the water for bathing was generally came from deep wells, roof water reservoirs and cisterns. These baths are very economical, and could be operated using surprisingly little amounts of water. According to Vitruvius (1914, 1990), bathing water had to be clean and was ideally brought in from the mountains, but also had to be rested and filtered in the tanks or the cisterns before public use (Prioreschi, 1991).

The water used in the Roman baths was refined in the three cisterns. Within the cistern system, water was not drawn directly from the reservoir, as it was first expected to pass through the clay walls and then to be transferred to the second and third reservoirs. Under normal conditions, the water in the third reservoir should have been used, although the water in the first and second reservoirs was used should the need arise (Landels, 2000; Sevimli, 2005:54-55).

In the imperial baths, however, aqueducts played an important role in the supply of water (Mitchell, 1993). According to Yegül (2010), aqueducts were one of the most important technical achievements of the ancient world, and the invention of the aqueduct system allowed for the construction of baths in the most arid regions of the Empire. The first aqueduct (Aqua Appia) was built in Rome in 312 BC. The construction of aqueducts was continued quickly, but by the beginning of the 2nd century, Rome was being served by nine aqueducts, carrying 1 million cubic meters

of water daily (Yegül, 2010:122).

Aqueducts were constructed with a gentle downward gradient to supply water to the baths through the use of gravity (Fagan, 1999:42-44). In other words, the water was always sourced in the uplands and run down the slopes with no additional pressure requirements. In this construction method, aqueducts were built underground in tunnels and above ground as bridges using accurate surveying and building techniques (Mitchell, 1987:352-353; Kretzschmer, 2000:74), The aqueducts initially carried water to the *castellum* (water distribution tower) at the highest point of the city, after which the water fed from the water tower would split into three branches taking different routes. The first branch of this system was used for the distribution of water to private houses; the second branch carried the water to such public buildings as baths; and the third branch provided water for official facilities as state house (Kretzschmer, 2000:74-77) (Figure 2.6).

Although the large baths took their waters directly from the *castellum* at the highest point of the city as an optimum approach, a free cistern was also necessary. The free cistern contained a large supply of ready water to meet the varying needs of the different bath sections. For instance, the water requirements of the Baths of Caracalla in Rome was supplied by one of the most impressive of all the cisterns, where the Aquae Antoniniana water branch ended (Yegül, 2010:122-123).
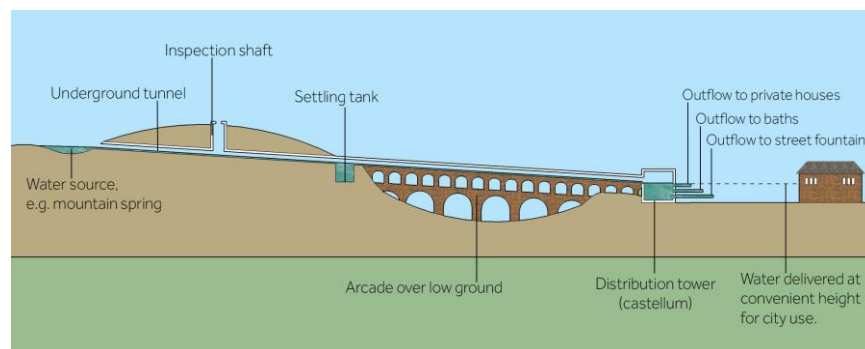
Figure 2.6 The elements of a Roman aqueduct system (Nicholls, n.d.)

In addition, within the bath, the water was distributed by water pipes, culminating at faucets. Many Roman thinkers mentioned the quality of the water pipes, and argued about which was healthier, clay pipes or lead pipes. Vitruvius (Vitruvius, 1990) who was one such thinker, suggested both lead and terracotta pipes be used in baths with

closed systems (Scarborough, 1969) and voiced his concern at the use of lead pipes after seeing some of the diseases that were common among people who worked in lead smelting and casting (Landels, 2000). Accordingly, he recommended the use of terracotta pipes for the distribution of water within the bath (Vitruvius, 1990).

The Romans were also aware of the importance of a working sewerage system for human health, and so paid close attention to the construction of extensive sewers for the removal of waste water and other waste. The sewerage system consisted of wide underground channels that were mostly arc-shaped, and that carryied the city's waste into nearby streams or the sea (Anabolu, 2001; Sevimli, 2005:70). In the Roman baths, waste water was carried away in channels below the floor that were connected to a branch of sewerage system. An analysis of the water supply systems in the Roman baths in Anatolia (Asia Minor) identifies a similar approach to that seen in Roman cities. The planning of Roman cities in Anatolian took into account hygiene and health, as expressed in the "Laws" of Platon (1998). Romans mostly designed their cities as a grid to facilitate the circulation of air and wind through the city. In the planning of cities, many public works (thermae, baths, theathers gymnasions, collanned streets, street fountains, cisterns, waterways, aqueducts, latrines, sewerage systems) were carried out by the city administrators (Gültekin, 1998; Hodgkinson, 1985; Yegül, 1995; Sevimli, 2005:60-61) to respond to the needs of the people.

One of the most important of these is the *thermae,* which would usually be located on a hillside overlooking the valley and the scenery. The baths attracted those who wanted to bathe in gorgeous, clean scented air, surrounded by glittering polychrome marble, fountains, vases, gardens and waterfalls (Sevimli, 2005:57).

The water need of these baths was supplied by aqueducts similar to those in the Rome. The Romans built aqueducts with one or more storeys in Anatolia to carry water from the source to the cities, with more water transferred than was actually needed. Changing construction technologies in the designing of the aqueducts system was mentioned by Sextus Iulius Frontinus (1922) in his work "De Aquaductu Urbis Romae Liber Primus". The Romans first skirted the edges of the valleys with underground channels and then, depending on the height, shortened the routes of the aqueducts by passing the valleys through both full and empty structures. Once reaching the city, the water would be distributed in a balanced way (Fro. Aqua.

XVIII). Among the main aqueducts in Anatolia were those of Aspendos, Cilicia Andriake, Balbura, Idebessus, Myra, Oenoanda, Patara, Pynda/Cynda, Rhodiapolis, Xanthus and Valens (Dinç, 2003; Farrington, 1995; Prokopios, 1994; Sevimli, 2005:69).

The other water supply systems feeding the baths and, cisterns were used not only for the collection of water, but also for filtering and refining. Vitruvius explained that bathing water should be clean as other Roman thinkers; it was suggested to bring the water from the mountains to the baths in the stores or cisterns. He also prohibited the use of river water for the washing purpose due to infant and young deaths unknown reasons at that time. The water used in the Roman baths was obtained by means of the triple cistern mechanism in which the water was first filtered to remove particles, after which rested and lastly ventilated before being distributed (Umar, 1989). There are many cisterns in Anatolia, the most important of which were the Cistern of Philoxenos, which was built by Senator Philoxenos in AD 336–337, and Basilica Cistern which was built by Emperor Justinian in AD 527–565 (Landels, 2000; Prokopios, 1994; Sevimli, 2005:66)

Finally, in the Roman baths of Anatolia, clean water was generally distributed via terracotta pipes beneath the ground floor, while waste water was carried out via underground channels connected to the city's sewer system.

2.4 Architecture of Roman Baths

Although it was the Romans that built the largest baths in history, they were inspired by the technologies and designs of the Greeks. As the Roman Empire grew and the population increased, a large number of aqueducts, dams, and pools were built, supplying hundreds of baths in which 3000-4000 people could be washed daily. Romans baths are works of art that had a significant impact and played a pioneering role in the development of Roman Architecture. The plan layouts of Roman baths were determined based on the sequences of the bathing areas within the traditional bathing system.

The main functional sections in Roman baths were the *apoditerium, frigidarium, tepidarium, sudatorium, laconicum, caldarium destrictarium/unctorium, heliocaminus* and *palaestra*.

The *apoditerium* (clothes-changing) is the first place in the closed bath buildings. Here the bathers would change their clothes and would store their personal belongings in the shelves, and niches built into the wall (Ürük, 2016:192-193).

The *frigidarium* (cold room) was the coldest and one of the most luxurious rooms in the bath and was not heated. It could contain one or numerous cold pools *(piscina)* with steps leading down into them where bathers could sit. Entertainment was usually carried provided here. The room generally had semi circular and arched windows to allow the entrance of daylight (Kula Say, 2007:12).

The *tepidarium* (warm room) section was found between the changing room and the hot room and was where bathers could adapt to temperature changes and to rest. The *sudatorium and laconicum* (sweating rooms) sections were used by the bathers for sweating respectively in dry air and moisturized steamy air. These rooms were suitable for resting.

The *caldarium* was the hottest and another of the most luxurious rooms in the bath containing hot water pools, niches seating areas, and bathrooms. The bathers could sit and, enjoy the heat or immerse themselves in heated pools (Yegül, 2010:34-35, Ürük, 2016:193). This area was usually enclosed with high vaults and had large semi-circular or arched windows, providing light during the day, but closed at sunset (Kula Say, 2007:12).

The *destrictarium/unctorium* (massage room) section was used for rubbing and oiling of bathers' bodies with hot oil. Bathers would use a curved metal tool called a strigil to scrape the oil from their bodies, leaving behind clean and smooth skin (Whitmore, 2013:18). In this area, massages were carried out by a professional masseuse or slaves working in the baths (Staggs, 2014:45).

The *heliocaminus* was a special room, found only in some baths, that was used for sun-bathing, facing south, southwest and containing wide windows with no glass (Kula Say, 2007:12; Ürük, 2016:193). Aside from these, the facilities also contained toilets *(latrina)* and shaving rooms in appropriate areas of the bath.

The *palaestra* (colonnaded spaces) was an open area in the bath, where bathers, before entering the bathing area, would partake in such exercise as ball games, running, boxing, wrestling, fencing or weightlifting (Figure 2.7) (Yegül, 2010:32). The gymnasium was generally a square or rectangular peristyle court (MacDonald, 1986:115).
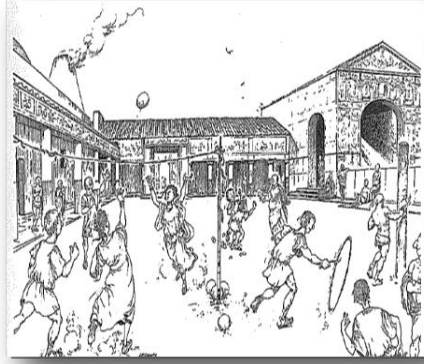
Figure 2.7 Drawing of play and sport activities in the *palaestra* (Yegül, 2010:35)

The Plan Categories and Types of Roman Baths

When the plan types of Roman baths are analyzed, the centralized or semi-centralized layouts are seen depending on curvilinear and circular elements and curved grouping rooms, which are mostly used in the construction and designing of the baths. In fact, the aim of these layouts is to reduce the surface areas of the baths and so to reduce the heat loss (Kula Say, 2007:14).

The basic plan types of the Roman baths included both asymmetrical and symmetrical layouts. Those with an asymmetric plan were built in 1 BC, but the advent of new construction technologies brought the construction of huge baths with a symmetric plan in the AD 1 (Ertuğrul, 2009:244-245).

Asymmetric Plan: This layout was used mostly in *balneums* (small baths). This important type sometimes is referred to as the "Pompeii Type"(Figure 2.8) emerged in Campania at the beginning of the 19th century BC with the earliest known example being the Stabia Baths in Pompei (Figure 2.9) (Yegül, 2006:163). This plan type could also be found in the houses and villas of the Late Republican period (Yegül, 2006:162).
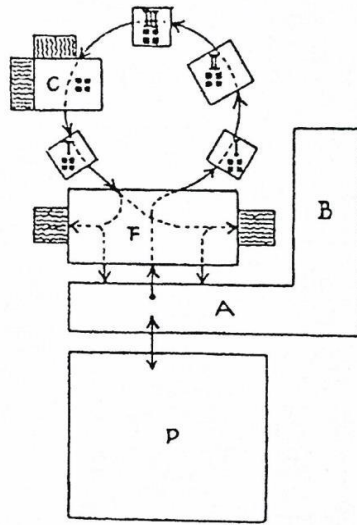
Figure 2.8 Asymmetric Bath Type "Pompeii Type"(Yegül, 2006:163).

The Stabia Bath in Pompei was built in 150 BC and was expanded with additional constructions in later periods (Eyice, 1997:403). The arrangement of the rooms was associated with the bathing system, with the *apoditerium*, *frigidarium, tepidarium,* and *caldarium* located on the eastern and north eastern sides of the bath in an asymmetrical layout. The small rooms to the west and south housed such facilities as shops, unconnected to the main function of the bath (Figure 2.9) (Whitmore, 2013:18-19).
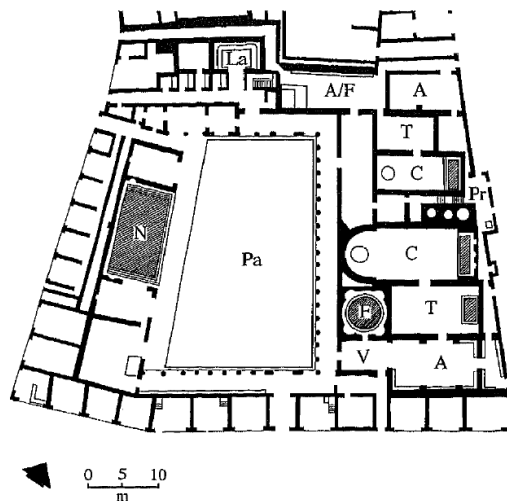
Figure 2.9 Plan of Stabian Baths, Pompeii (Yegül, 2006:59; Whitmore, 2013:19).
A: *apodyterium*, **V:** vestibule; **T**: *tepidarium*, **C**: *caldarium*, **Pr**: *praefurnium,* **F**: *frigidarium*
N: *natatio*, **Pa**: *palaestra,*

34

Symmetrical Plan: This plan organization was common among the large bathhouses, with the more detailed examples being known as "Imperial Baths" *(Thermae)*. Aside from bathing areas, these facilities contained also libraries, conference rooms, columned passages, walkways, and gardens, indicating additional cultural and intellectual functions within the baths (Yegül, 2006:163).

The plan layout would feature many rooms and halls on either sides of the symmetrical axis of the bath. The axis was intersected by the *frigidarium* containing a pool called *piscina.* Near the *frigidarium* was the *apoditerium* the changing room, and then there were some smaller rooms of the *tepidarium* for sweating and massage in appropriate places. The *caldarium* which usually lay at the center of the bath was surrounded by a series of hot rooms located to the south or southeast direction to benefit from direct sunlight. The *frigidarium* and *caldarium* were often covered with a cross vault system, but rarely with a barrel vault. In some examples, the round *caldarium* enclosed with a high dome (Figure 2.10) (Kula Say, 2007:14-15).
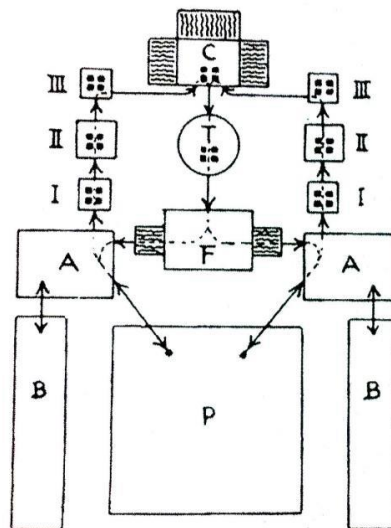
Figure 2.10 Symmetrical Bath Type "Imperial Baths"(Yegül, 2006:163).

Morever, the axial and symmetrical plan organization was preferred in the large bathhouses or *thermae* due to economic and functional reasons. For example, some symmetrical parts of these baths were closed for cleaning or maintenance, while the remaining parts could stay open. Similarly, in extraordinary winter conditions or in times of economic difficulty, the remaining areas could keep working at half of the

cost. The best examples of imperial baths are those at Caracalla and Diocletianus (Figure 2.11-2.12) (Yegül, 2010:127-128).

In terms of its physical appearance and plan organization, the Baths of Caracalla built in AD 200 was the second largest Roman bath complex in Rome, and it could accommodate 1600 bathers at a time. The total bath area occupies 120000 square meters with some cultural and intellectual activity areas such as libraries, theaters and dining halls, while only the bath building covered an area of 25000 square meters (Yegül, 1992:146) (Eyice, 1997:403). In spite of its vast scale, the *thermae* of Caracalla had simplicity in planning. The plan organization contained separate sections for women and men with all sections on either side of the symmetrical axis being identical. The bath was divided longitudinally into five parts. The central part contained the *caldarium* (hot room)*, tepidarium* (intermediate room)*, frigidarium* (cold room) and, *piscina* (a cold pool) while the end part contained the *palaestra* where sporting activities would be undertaken. The service areas and changing rooms were situated between these functional rooms (Smolijaninovaitė, 2007:15) (Figure 2.11)

The Diocletianos Bath, which was built in AD 300, covered an area of 120000 square meters and contained gardens that were thought to have been of sufficient size to accommodate 3000 people (Eyice, 1997:403). The Diocletianos Bath was equal in size to the Caracalla Baths although its bath buildings occupied a larger area (Yegül, 2006:191). The plan organization of the Diocletianos Baths was also similar to that of Caracalla, with separate sections for women and men with symmetrical layouts on either side of the central axis. The *caldarium* (hot room)*, tepidarium* (intermediate room)*, frigidarium* (cold room)*, apoditerium* (clothes-changing room), and other rooms were located in accordance with bathing order (Figure 2.12).
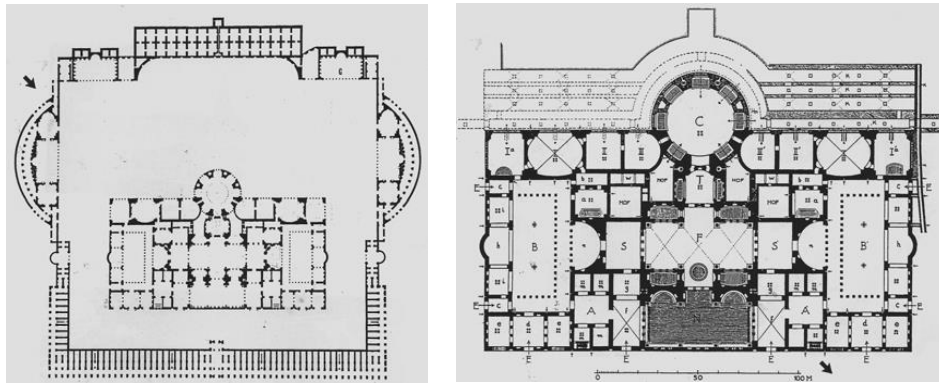
Figure 2.11 The plans of Caracalla Baths in Rome (Yegül, 2010:134-135)
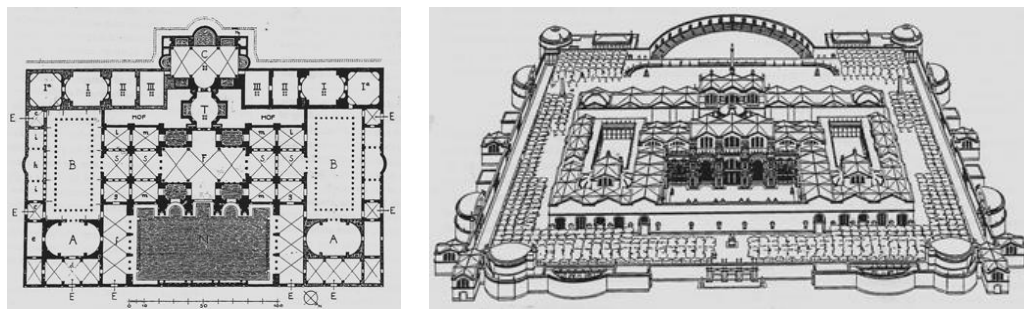
Figure 2.12 The plan and perspective of Baths of Diocletainaus in Rome by Paulin 1890 (Yegül, 2006:192; Yegül, 2010:127)

2.4.1 Architecture of Roman Baths in Anatolia

As analysis of the Roman baths in Anatolia (Asia Minor) reveals that many baths were built by the Romans. Anatolia's fertile lands and geographical position attracted the Romans due to their economic, political and cultural aspects, leading the Romans to invade the region in 190 BC. The first Anatolian province to be settled by the Romans was Pergamon, by the will of Attalos III in 133 BC. Under Julius Caesar (63-44 BC) the colonies that formed part of the Roman World (Orbis Romanium) were established and spread across the whole of Anatolia, such as the Cilicia State (12 BC) in Eastern Mediterranean and Toros, the Bithynia State (74 BC) and the Bithyiana Pontus State (64 BC) in the Marmara region, (Magie, 1948, 2001) the Galatia State (25 BC) and following the Cappadocia State in Ankara, Niğde and Kayseri, the Lycia-Pamphylia State (AD 43), and the Thracia State (AD 46) in the South Aegean and Antalya. In short, the Roman era began through the colonies

37

established in Anatolia (Magie, 1948, 2001; Mitchell, 1993; Livius, 1994; Sevimli, 2005:45). In the Roman era, public works were carried out quickly by the rulers of the Roman states, and many public buildings were built. The most important of these, the *thermae* were constructed in different regions of Anatolia (Asia Minor).

The Roman baths were named after the rulers of the period such as Maecenas (the first baths were built in his period), Agrippa (AD 10), Nero (AD 64), Vespatian (AD 68), Titus (AD 75), Trajan (AD 110), Hadrian (AD 120), Faustina (the wife of Emperor Marcus Aurelius, AD 161–180), Commodus (AD 188), Caracalla (AD 217), Alexander Severus (AD 230), Aurelian (AD 272), Diocletian (AD 295), Constantine (AD 324), and Domitian (AD 337) (Aru, 1949; Sevimli, 2005:57).

Today, the most important examples of Roman baths can be found in the Çankırı Kapı district of Ankara (see Chapter 3), and in the ancient sites of Ephesus, Miletus, Pergamon, Magnesia, Hierapolis, Perge, and Aphrodisias. Furthermore, the Lycia region contains many baths that were built after it became part of the Roman Empire in AD 43 (Farrigton, 1995:23; Ertuğrul, 2009:245). Examples of the baths found in Anatolia (Asia Minor) are briefly explained below, along with the ancient cities in which they were built.

Ephesus: Ephesus was one of the four most important Anatolian cities in the Roman Empire. It is located in southwest Anatolia, 3 kilometers from Selçuk in İzmir (İİKVTM, n.d.). The city flourished after coming under the control of the Roman state in 129 BC (Ladstatter, Zabrana, n.d.). Ephesus was supplied with via underground channels from Kenchrios, the Marnas Creek and the Küçük Menderes (Maiandros) River using wells and cisterns (Scherrer, 2000). The city was also served by at least six aqueducts of various sizes supplying water to different parts of the city (Crouch, Ortloff, 1997). The city's four Roman bath complexes, Harbour Bath-Gymanasium, Eastern Baths, Theater Baths, and Vedius Bath-Gymnasium, were one of its most remarkable features, and their location is of particular importance. For instance, the bath was the first building to be seen by travelers entering Ephesus from the north-eastern, Koreos Gate, and in the same way, was the last building to be seen when leaving the city (Sevimli, 2005:63), (Figure 2.13).

An analysis of the plan of Harbour Gymnasium Bath, another of four baths in Ephesus reveals that the building was 360 meters in length, and contained two

palaestras, one of which was 90 square meters in area and the other which measured 20 m x 240 m. Construction of the bath probably started and was completed in the reign of Emperor Domitian (AD 81-96). In Hadrian's time (AD 117-138), the entire *palaestra* was clad with marble slabs and, it has been confirmed that 13 different kinds of colored marble were used (Akurgal, 1970:157). The slabs themselves are no longer in place, with only the clamp holes in the walls still evident. The hall in the northern section of the *palaestra* must have been dedicated to the cult of the emperor, while the hall to the south, containing a fine Roman copy of a Greek bronze statue an athlete, was most probably used for lectures and meetings. The ruins of the bath section of the building indicate a complex of immense proportions (Akurgal, 1970:157).

Miletus: Miletus was a harbor city in southwest Anatolia, lying at the mouth of the Maiandros River, and which is now 9 km from the sea. The Roman period of the city began in 133 BC. The Faustina Bath in the city was built in AD 2 by Roman Emperor Marcus Aurelius for his wife Faustina (Stilwell et al., 1999) (Figure 2.13). The bath has survived to the present day in a very good condition, with its *palaestra* almost square in shape, measuring 77.7 m x 79.41 m. The columns surrounding the courtyard were of the Corinthian order. The sequence and grouping of the rooms in the bath is axially symmetrical. (Akurgal, 1970:220) After the *palaestra*, bathers entered the *apoditerium*. From here, the bathers passed into a three-roomed *frigidarium* section containing a large pool with two fountains depicting the River God and a Lion that are still in place today. The *frigidarium* then opened into the *caldarium* comprising two large rooms with apses in the south-eastern part of the bath. The *caldarium* was heated from below by hot air flowing from the furnaces to the south to the spaces beneath the floor, and the rooms gained further heat from the hot air passing through earthenware pipes concealed in the walls (Akurgal, 1970:221). From the *caldarium,* the bathers proceeded to the *tepidarium*, and then finally back to the *apoditerium* before leaving the bath (Akşit, 2009:147).

Figure 2.13 Ephesus and Miletus Baths (İİKVTM, n.d.; AİKVTM, n.d.)

Pergamon: Pergamon was a prosperous and powerful ancient city (Aksit 2009:195) located on the north side of River Caicus (modern-day Bakırçay) in northwest Anatolia. Pergamon became the capital city of the Roman state in 133 BC (UNESCO, n.d.) and in this period, the gymnasium built in the Hellenistic period was converted into bath-gymnasium complexes with the addition of bath buildings. The four baths that existed in the 1st century were increased to five during the reign of Emperor Augustus, and the number reached seven during the reign of Hadrianus in the 2nd century (Radt, 2001; Sevimli, 2005:64).

The Roman baths were an integral part of the upper gymnasium having been constructed during the Roman times. The courtyard, measuring 74 m x 36 m, was floored only with earth being athletics training ground. Architectural fragments reveal that the stoas erected on all four sides were in the Doric style, dating to the Hellenistic times, while those in Roman times were in the Corinthian style. The bath buildings were located to the west of the gymnasium. These buildings were supplied with water from a cistern built on high ground sourced by water brought from the west (Akurgal, 1970:96-97).

Magnesia Ad Maeandrum: Magnesia was the ancient city of Lydia, located in Tekinköy near Ortaklar district of Aydın in southwest Anatolia. After 133 BC, the Kingdom of Pergamon was joined to the Roman state through inheritance. Thus, Magnesia became a Roman city (Bingöl, 1998; Sevimli, 2005:64). There were two bath-gymnasium complexes in the city: the "Caserma Bath" and the "Gymnasium Bath". The Caserma Bath was located on the eastern side of the city and was in the typical bath-gymnasium complex. On the other hand, the Gymnasium Bath was

located in the west end of the city. Most parts of the bath are today under thick vegetation. However, experts believe that it must be asymmetrical in plan, based on the evidence provided by some of the ruins (Yegül, 2006:244).

Aside from the bath, the site contains some evidence of the infrastructure systems such as clean water channels and elements of the sewage system that would have served the needs of the city (Bingöl, 1998; Sevimli, 2005:64)

Hierapolis: Hierapolis, which means "holy city", is in the Denizli province. In 129 BC, the city was joined to the Asian province of Roman Empire and administrated by proconsuls. Due to the warm healing waters, the site became a pilgrimage destination for worship and health. Like in the other Roman cities, the site featured a gymnasium in the Hellenistic period that was then converted into a bath- gymnasium complex with the addition of bath houses in the Roman period (Şimşek, 1996; Sevimli, 2005:64-65) (Figure 2.14). The Tripolis Bath in the ancient city has been very well preserved, after being built in the 2nd century AD, oriented in a north-south direction, side by side and with parallel lined rooms. The structure was constructed out of travertine blocks in rectangular form (Daşbacak, 2006:958). The *palaestra,* measuring 36.13 m by 52.25 m, was located on the eastern part of the site, and the two rooms located to the north and south of the *palaestra* were reserved for the emperor and for ceremonial use. A large hall stretching the length of the western side of the *palaestra* was used by athletes as a gymnasium, and this hall led into the *frigidarium* from which one entered the *caldarium* rooms. The rooms were covered with barrel-vaults (Akurgal, 1970:177; Aksit 2009:203-204).

Perge: Perge was one of the most important cities in ancient Pamphylia, located in the Attalia (Antalya) province on the southwestern Mediterranean coast of Anatolia. The ancient city ruins revealed two baths, the first of which the northern bath, was built in the 3rd century AD, and is one of the finest examples of a Roman bath in the Pamphylia region. The organization of the bath is as in the typical Roman city. The architectural fragments of the bath include several arches and travertine walls (Miszczak, 2017) The second bath is located on the west side of the Hellenistic gate of the ancient city. The bath site contains bath building and a *palaestra* found on the west part of the main street, and is square in shape, measuring 76 m by 76 m (Aksit, 2009:227). The bath building consists of sequence of the bathing rooms as in the first

Roman bath in Perge. The thin marble slabs used to cover the walls and the brick pillars that form the hypokaust system can be seen among the ruins of the city (Miszczak, 2017) (Figure 2.14)

Figure 2.14 Hierapolis and Perge Baths (DİKVTM, n.d., Miszczak, 2017)

Aphrodisias: Aphrodisias was not a Roman city although it served both Caesar and Augustus. Accordingly, it both influenced Roman culture and was also influenced by it. The remains of Aphrodisias were found in the village of Geyre in Dandalas Valley, south of the Maiandros River. In Aprodisias, the Hadrian Baths were named after Emperor Hadrianus (Erim, 2002; Sevimli, 2005:64), (Figure 2.15) and were located to the west of the Agora. The baths featured at least five large galleries and a *palaestra* which was built and decorated with magnificent reliefs and statues in Hadrian period. The bath sections of the building consist of many bathing stages, including a *caldarium, tepidarium, sudatorium* etc (Akurgal, 1970:174-175).

Sardis: Sardis was a rich and powerful ancient city; it lies within the boundaries of the Sard province in the Salihli District of Manisa (MİKVTM, n.d.) (Figure 2.15). Sardis enjoyed its greatest prosperity during Roman times, and many of its ruins can be seen today as a reflection of the period (Akşit, 2009:124-125). The Sardis Bath-Gymnasium complex covers an area of 23000 square meters and resembles the typical imperial bath plan type that can be found at other sites in Asia Minor, such as in Ephesus. The rooms within the baths were arranged in an axial symmetrical pattern, and there was an open, almost square courtyard (*palaestra)* in the eastern half of the complex. The complex was most probably completed in the late 2nd or 3rd century AD. Repairs and modifications to the bath continued in later centuries, but the site fell into ruin in the 7th century AD (Yegül, 1986).

Figure 2.15 Aphrodisias and Sardis Baths (AİKVTM, n.d., KVVMGM, n.d.)

The Plan Categories and Types of Roman Baths in Anatolia

The planned organizations of the baths in Anatolia were categorized by Yegül, who emphasized especially the new bath type being the bath-gymnasium complex. This new type brought together the properties of the Greek gymnasium and the Roman bath and featured large rooms serving the educational, athletic, bathing and entertainment needs of society. Even though grandiose symmetric axial compositions dominated in planning, there are also examples of non-symmetrical plans (Figure 2.16- 2.17) (Yegül, 2010:181-183).
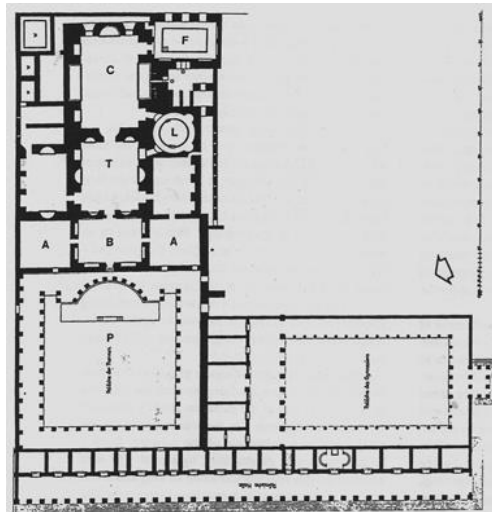
Figure 2.16 Virgilius Capito Bath and Hellenistic Gymnasium Plan in Miletus
(Yegül, 2006:220)
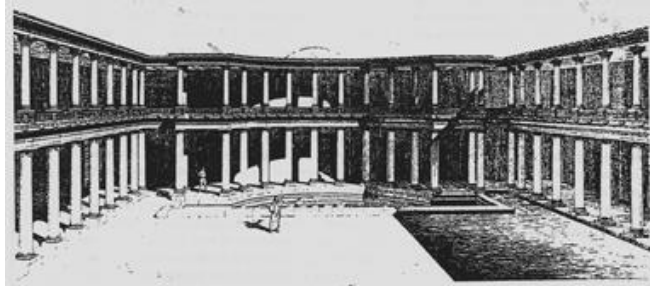
Figure 2.17 Restitution perspective from the east of Virgilius Capito Bath in Miletus
(Yegül, 2006:221)

In Anatolia, linear and orthogonal plans were prominent in contrast to the tendency for curvilinear plans for the baths in Rome. The use of curves in the plans was seen only in niches and small circular rooms. Even though they were influenced by the symmetrically planned *thermae* in Rome, there were no examples of a central *caldarium* with several *abscissa* in Anatolia. According to Yegül, therefore, three different symmetrical plan forms can be found in Anatolia 1) Double Row Places, 2) U-Planed Halls and Reverse Circulation, and 3) The Combination of Bath Buildings and *Palaestra* on the same axis (Yegül, 2006:236; Kula Say, 2007:16).

The first plan type contains an arrangement of rooms in two rows, as exemplified in the Ephesus Port Bath Gymnasium, the Gymnasium Bath in Magnesia ad Meandrum, and the Caracalla Bath Gymnasium in Ancyra (Figure 2.18-2.19-2.20).

In the Ephesus Port Bath, while the outer row rooms were used for bathing activities, the inner rooms served as the entrance and exit, the changing room and the inner exercise activity area. The outer row rooms in the bath were hot places and were located on the western side of the bath. All rooms were enclosed with barrel vaults. The *caldarium* was a projection and located in the middle row room of the outer row. The inner row rooms were located on the east side of the bath and were not served by a heating system. The *frigidarium* was located in the middle row room of the inner row. The *piscina* in the *frigidarium* was shared by the two rows of rooms (Figure 2.18) (Yegül, 2006:237; Kula Say, 2007:16).
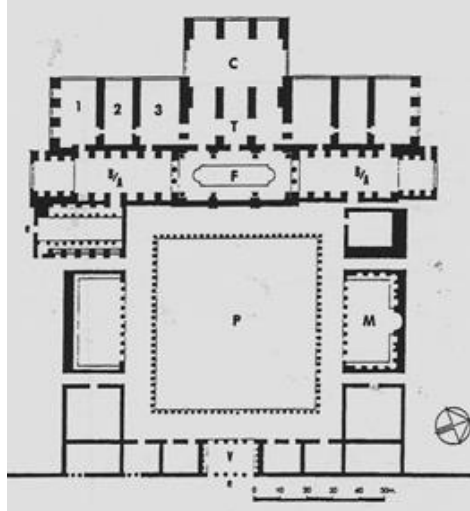
Figure 2.18 Ephesus Port Bath Gymnasium Plan (Yegül, 2006:238)

The Gymnasium Bath in Magnesia ad Meandrum is one of the two -gymnasium complex types in the area and of the imperial type (Yegül, 2006:243). The first drawings of the bath, prior to excavation from under the dense vegetation, were made by Humann in the early 20th century, and indicated a noteworthy small arrangement of rooms (a-b-c) between the inner and outer rooms. There is a single long hall (B/A) in the inner series. The hall extends outwards with a projection carried by pillars that are connected with the arches. This outward projection causes the general symmetrical scheme to be disrupted (Figure 2.19) (Yegül, 2006:243-244).
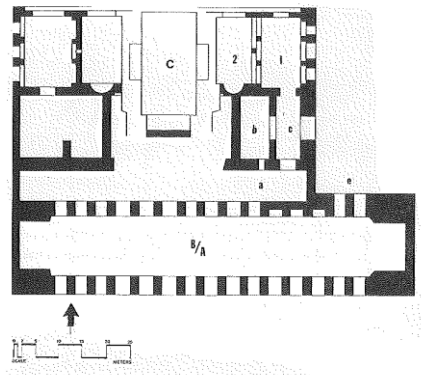
Figure 2.19 Magnesia ad Meandrum Bath of Gymnasium Plan (Yegül, 2006:243)

Although the Roman Caracalla Bath in Ankara on the Central Anatolian plateau is quite remote from the Magnesia ad Meandrum located in Tekinköy near Ortaklar

district of Aydın in southwest Anatolia, the Bath has similar basic plan features to a bath-gymnasium complex in the Magnesia ad Meandrum. This bath structure contains more complex and impure design features, containing two rows of smaller and larger spaces placed between the outer and inner row rooms. The secondary halls of the bath are of the typical type to Anatolian bath architecture, and do not disrupt the basic functional relationship between the inner and outer row rooms and the *palaestra.* The Bath complex in Ankara must be the largest example of its kind, in that the parts that have been excavated to date indicate a half symmetrical plan of the structure (Figure 2.20) (Yegül, 2006:244).
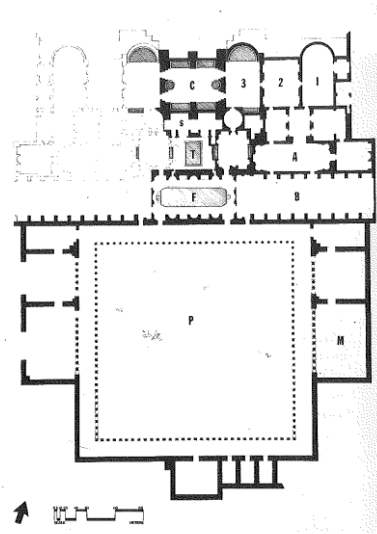
Figure 2.20 Caracalla Bath Gymnasium Plan in Ancyra (Yegül, 2006:244).

The second plan type features an arrangement of rooms and a U-shaped corridor with reversed circulation, as in the Ephesus East Bath Gymnasium (Figure 2.21). In this bath, the U-shaped corridor surrounds three sides of the bath block and changes the relationship between the bath and the *palaestra.* The entrance to the bath was via the *palaestra,* after circulating U-shaped corridor, finally reaches again the *palaestra.* The *frigidarium* lies at the point furthest from the *palaestra,* and so was not shared by the bath and gymnasium. On the other hand, the *tepidarium* and *caldarium* were placed around the U-shaped corridor according to the order of bathing (Yegül, 2006:245; Kula Say, 2007:16).

46
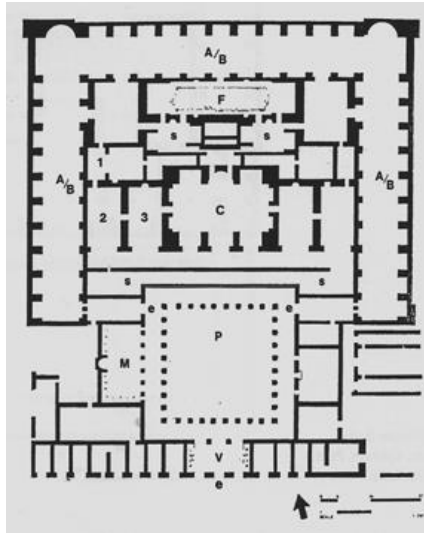
Figure 2.21 Ephesus East Bath Gymnasium Plan (Yegül, 2006:245)

The third plan type features the combination of a bath building and a *palaestra* on the same axis, as in the Sardis Bath-Gymnasium (Figure 2.22). The main axis in the east-west direction of the bath passed through the *caldarium* and the *palaestra*. The *palaestra* was easily reachable from the street and was connected to the outer hot rooms via the inner row of rooms. The circulation continued in a straight line to the hot rooms, after which the recirculation ended at the *frigidarium* located between the *palaestra* and the *caldarium* (Yegül, 2006:248; Kula Say, 2007:17).
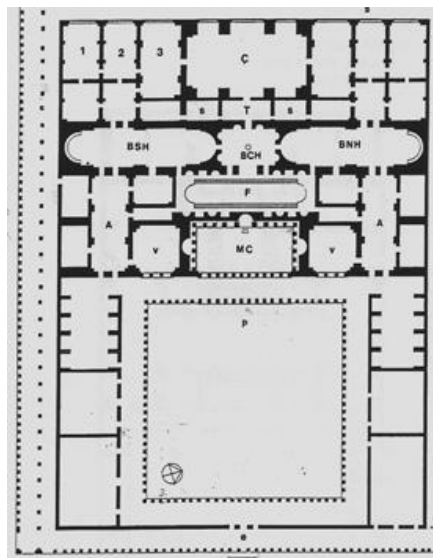
Figure 2.22 Sardis Bath-Gymnasium Plan (Yegül, 2006:249)

47

An asymmetrical plan type could also be found in Anatolia in the Perge South Gate Baths (Figure 2.23). These baths featured a series of rooms with parallel vaults, three of which had an *apse* projection. The southern room was *caldarium,* while the *frigidarium* with a *piscina* was located in the north. The Bath in Anemurium (Figure 2.23) stands as an interesting example, being a blend of both the *palaestra* and the local bath building (Yegül, 2006:267-268; Kula Say, 2007:17).
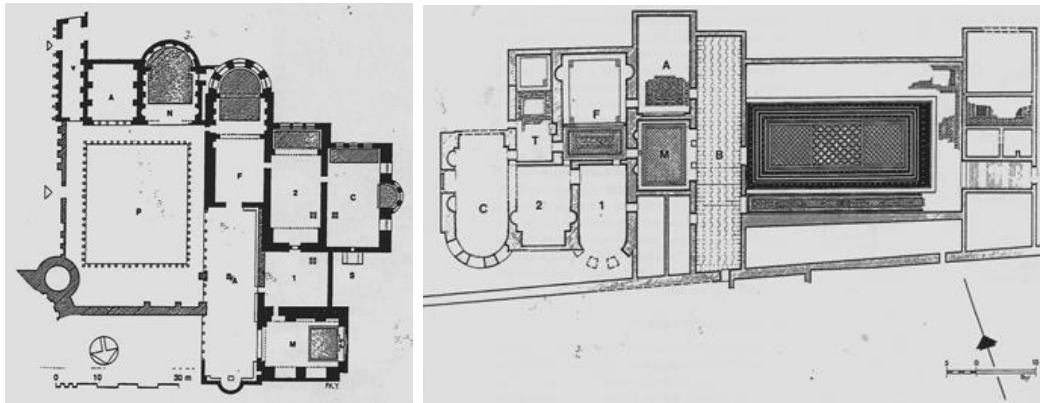
Figure 2.23 Perge South Gate Baths and Anemurium 3 numbered Bath Plan
(Yegül, 2006:261, 269)

2.5 Construction Techniques and Materials of Roman Baths

Roman imperial baths – *thermae* – played a pioneering role in the development of Roman construction technologies. The era in which Roman construction technologies saw rapid development coincided with the construction of Roman imperial baths, and this indicates that the construction of the Roman baths and the development of new construction techniques supported each other (Yıldız, 2017).

The invention of concrete *(opus caemeticum)* brought about the construction of the earliest Roman arches, vaults and domes in the Roman imperial baths. *Opus caemeticum* was similar to modern concrete, being composed of aggregate (gravel, chunks of stone, rubble, broken bricks, etc.), a binding material (lime, gypsum, pozzolan) and water (Adam, 1994:65; Yegül, n.d.). Pozzolan, referring to volcanic sand or dust, was the primary binding material (Kretzchmer, 2000:31). The pozzolan containing both silica and alumina created a chemical reaction that formed a very strong bond with the aggregates (Labate, 2016). Also, the elastic feature of the Roman concrete containing pozzolan facilitated the construction of curved elements

such as arches, vaults and domes.

The other important material that was used in the walls of Roman imperial baths was fired clay brick. The brick-making techniques developed by the Romans in the 1st century led bricks to become the primary building material for the walls of Roman baths. In the Roman imperial baths, fired clay bricks made of clay and water were produced as follows: first, the clay was extracted from deposits in the ground and rested, after which it was mixed with water and shaped into the form of bricks. The bricks were then dried away from direct sunlight to avoid cracking, and then fired in chamber at temperatures of around 1,000°C (Labate, 2016). It is known, however, that the brick kilns in the Roman period were unable to be heated to the necessary internal temperature. In the furnaces, the areas close to the heat source reached 1,100°C, but there was a drop-off in the upper parts to about 800°C. Accordingly, some of the fired bricks were exposed to different temperatures (Adam, 1994:62-63; Sağın, 2017). The ideal firing temperature for fired brick is between 850–950°C (Işık, 2010). The temperature should be above 450°C for the durability of brick (Çördük, 2006:61). The clay bricks were initially green, but became red-brown after the oxidation of the iron minerals that occur naturally in clay (Labate, 2016). Therefore, depending on the devolopment of these materials, the new construction techniques emerged in Roman architecture as follows.

Firstly, with the discovery of *Opus caemeticus,* Romans started building walls made of concrete at a much faster pace than with cut stone constructions (Labate, 2016). Besides, they used many types of facings for the coating of the walls - *opus tastaceum*, *opus reticulatum, opus quadratum, opus incertum, opus mixtum* (Anabolu, 1996) due to stone and brick being expensive materials. The concrete core and facing parts of the wall were built as follows: Initially, the space between the timber molds was filled with a certain mix of crushed stone, quicklime, and water and then faced with stone blocks and brick materials (Kretzchmer, 2000:31; Çördük, 2006:58-59; Ekinci et al., 2012). All facing materials became firmly bonded to concrete core and could be coated with a more decorative material, such as plaster or *stucco,* made out of lime, sand, and marble dust (Yegül, n.d.).

The walls of Roman imperial baths were constructed using the *opus tastaceum* method (Figure 2.24), comprising a concrete core with brick cladding (Fletcher,

1961) similar to the huge walls of the *frigidarium, tepidarium* and *caldarium* sections of the Caracalla Baths, which were constructed in the same way. After that, the inside walls were coated with slabs of marble, glass mosaic and painted *stucco,* while the outside surfaces were coated with white *stucco* (an outdoor plaster) imitating blocks of white marble (DeLaine, 1992:269-270). The walls of the heating rooms were built with hollow areas behind the outer covering to allow the circulation of hot air (DeLaine, 1992:183).
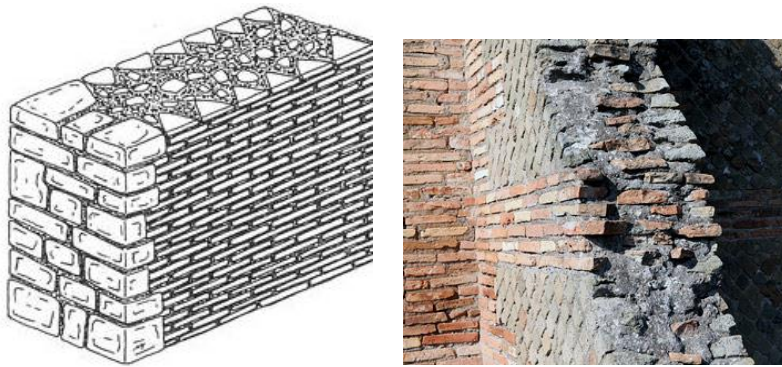
Figure 2.24 *Opus tastaceum* -brick and tile faced concrete-
(Sharo, 2016; Muench, 2017)

Secondly, concrete vaults and domes were constructed to cover wide expanses in the Roman baths (Dirlik, 2017). The vaults of Roman imperial baths were almost entirely made of concrete with a single homogeneous mass form, and were not subjected to any horizontal compressive forces once in place, which is the secret of the success of the vault system. The most common vault types found in Roman baths are barrel and cross vaults (Thorpe, 2002:106). A barrel vault is obtained by increasing the depth of an arch, and the *apoditerium, tepidarium* and *caldarium* sections of the Stabian Baths in Pompei all offer good examples of a barrel vault. A cross vault is formed at the intersection of two equal barrel vaults (Çördük, 2006:84). The high main hall of the *frigidarium* section of Caracalla Baths features triple cross vaults (Yegül, 2010:137) (Figure 2.25).

Similarly, the dome of huge halls in the Roman imperial baths was built out of concrete *(opus caementicum)* (Conti et al, 2009) depending on the natural development of the vault (Çördük, 2006). One of the best-known examples of such a dome can be found at the Caracalla Baths in Rome. The circular *caldarium* section of

the Caracalla Baths was capped by a dome measuring 35 m in diameter and 44 m in height, which makes it similar in size to the dome of the Pantheon, which are 43.3 m in diameter and 44 m in height. The weight of the dome was carried by eight stone columns, and it was built with a concrete core with brick cladding, while its drum had a series large brick arched windows allowing in plenty of sunlight (Yegül, 2010:137)

Figure 2.25 Perspective drawings and the ruins of the *frigidarium* of Caracalla Baths in Rome (Ivanov, Hülsen, 1898; Yegül, 2010:138-139)

Aside from these, decorated stone columns (Figure 2.26) were erected in the large interior spaces of the baths and in the half-open areas of the *palaestra*. While these columnar orders had mostly a decorative function, they were incorporated into a concrete structure (DeLaine, 1992:237). The columns were connected to each other with horizontal beams or arched architectural components, and this arched application would be applied to eliminate the risks associated with crossing large openings with columns (Thorpe, 2002:104).

Figure 2.26 Before and after - the decorated stone columns of Caracalla Baths in Rome by virtual reality goggles (Squires, 2017)

2.5.1 Construction Techniques and Materials of Roman Baths in Anatolia

An analysis of the construction and material properties of the Roman baths in Anatolia reveals that they were constructed using local materials and craftsmanship, in that it was much easier and more economical to transport construction plans and descriptions of structures rather than materials and workmen. In other words, the materials and construction techniques used in the Roman examples were imitated in Anatolia (Sherwood, 2000:178-179).

The first difference in the baths in Rome and those in Anatolia is that the Roman concrete trend was never transported to Anatolia, as, for example, the special and strong pozzolan binding material found in volcanic region of Central Italy was absent in Anatolia, or the volcanic region in which it could be found was unknown in that period. Instead of that, a lime-based rubble fill mortar was used for the same purpose, although its durability was lower than that of pozzolan. In order to add strength to the mortar, the lime content was increased to an optimum rate, and the durability of this material can be seen in the barrel vaults spanning 12–18 m that were common in Anatolia (Yegül, 2010:184-185).

The other major difference between the materials used in Rome and those in Anatolia was the fired bricks. According to the study of Sağın (2017) entitled "Characteristics of Roman period building bricks in Anatolia", the fired brick of Anatolia was weaker than that produced in Rome. Several Roman bricks from Serapeum (Red Courtyard) and from different buildings in the ancient cities of Agia and Nysa in Pergamon were examined using analytical methods, and it was found that the bricks were fired at low temperatures, due to the limitations of the Roman brick kilns and their inhomogeneous internal temperature distribution. Besides, the clay content of the fired bricks was low due to the sparsity of the local raw materials used in their manufacture (Sağın, 2017).

Thus, there were differences in construction techniques depending on the material differences used in the baths in Rome and Anatolia. The most significant difference between the construction styles of the baths in Rome and those in Anatolia was the curved grouping of rooms that were prevalent in Rome, but not so popular in the baths of Anatolia. The use of curvilinear elements in Anatolia was limited to small circular rooms or niches carved into the walls, in that the Roman concrete

construction techniques mentioned earlier were unknown in Anatolia, where the predominant materials were cut stone and block. Furthermore, unlike in Rome, all brickwork was structural, and the brick walls in Anatolia were massive (Kula Say, 2007:16; Yegül, 2010:185).

Moreover, when the baths in Anatolia are investigated regionally, several construction techniques can be seen according to the characteristics of regional material and workmanship.

As is still the case to this day, stone is the ideal material for the western and southern coastal regions of Anatolia, and there are application differences even between the stone bath buildings within the region of Anatolia. For example, in the Arycanda Baths in the central part of Lycia, the partition walls were constructed out of irregular stone blocks. The masonry wall resembles a polygonal structure due to the use of irregular stone blocks, while the masonry facade was constructed using rectangular shaped stones (Yegül, 2006:223).

In the small mountain settlements of Caria, Lycia and Pisidia, generally, all the structures of the small- and medium-sized baths were constructed out of irregularly shaped stone blocks. Only the important parts of the bath building, such as the facade, were built using regular rectangular stone or using a masonry technique in which cut stones were placed between the stone arranged regularly (Yegül, 2006:223).

In Kaunos, on the coast between Caria and Lycia, the load-bearing walls of the main halls of the baths were constructed out of regular stone, while in all the secondary walls, irregular river stones were used in a technique that can be defined as "rubble with mortar", being a local version of *opus caementicum.* The walls were constructed using medium-size rectangular stones in the Great Baths (Vespasian) and Small Baths on the coast of Lycia and in the bath-gymnasium complex near the South Gate in Perge. It is worth mentioning that the use of bricks in all of the above-mentioned settlements is out of the question, as all arches and vaults were constructed using cut facing stones with rubble filling the void behind. (Yegül, 2006:223). Besides, both baths in Magnesia ad Meandrum (the so-called Caserma Bath and the Gymnasium Bath) contain massive walls made of mortar and rubble constructed over the cut stone masonry walls (Yegül, 2006:231).

The best examples of the building technique using high-quality rectangular stones can be found in Hiearapolis, Laodiceia and Tripolis, located in the eastern Karia highlands. The large, smooth cut stone blocks produced from local limestone were applied in a standard manner to the walls, free standing pillars and barrel vaults of the buildings at these sites (Figure 2.27) (Yegül, 2006:223; Yegül, 2010:183-184). The bath-gymnasium complex of Termesus, one of the leading mountain settlements in Psidia, has carefully-built walls made from rectangular cut stone blocks (Figure 2.27). On the facade of the baths in Oenoanda, which is the mountain settlement of Lycia, the two-story arched walls constructed with rectangular stone blocks are similar to those in Termessus, although the quality of the rectangular stone blocks is lower (Yegül, 2006:223).
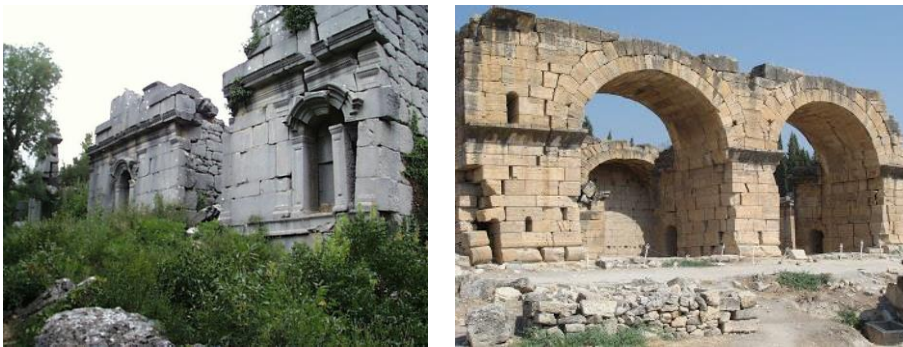
Figure 2.27 Cut stone masonry walls of Termessus and Hierapolis Bath-Gymnasium (Yegül, 2010:185; Daşbacak, 2002:964)

Similar quality stone walls were also used in the Hadrianus Bath-Gymnasium in Aphrodisias, which is one of the cities of Karia (Yegül, 2006:223) and in the other western Anatolian coastal cities of Ephesus, Miletus and Sardis.

Aside from this, in the four major bath-gymnasiums, being the Harbor Bath-Gymnasium, the Eastern Baths, the Theater Baths and the Vedius Bath-Gymnasium of the Imperial Period in Ephesus, brick was used as the basic building material. In the first three of these structures in particular, massive brick walls, which again carried massive brick vaults, were constructed over the heavy stone walls at the lower levels (Yegül, 2006:229). In all of these structures, the stone walls at the lower levels reflect the *petit appareil* wall technique of using large, medium, and small rectangular stones, which is, more or less, a more economical form of construction.

The wall construction technique in which small rectangular stones are laid carefully in horizontal courses was typical of Italy and the western states in the early Imperial Period (Yegül, 2006:231).

In the Sardis Bath-Gymnasium complex, this wall construction style (large, medium and small rectangular stones) was also adopted as the basic construction method. In the Sardis Bath, the upper levels of the walls were carefully constructed out of rubble, separated by bricks at regular intervals. This system, which is generally associated with late ancient structures, can also be seen in the Eastern Bath-Gymnasium in Ephesus, in the Large Bath in Aspendos, in the Three Eyes Baths in Tralles, in the 2B Bath in Anemurium 3, in the North and South Baths in Perge and in the Large Bath in Hierapolis (Yegül, 2006:229-231; Farrington, 1995; Çoşkun, 2004; Lancaster, 2009). On the other hand, in the Faustina Baths, brick materials were used only in the heating system elements. Aside from that, while the lower level walls of the more important building sections were constructed out of medium-sized rectangular stones, the upper level of walls was constructed out of smaller stones in horizontal but loose courses (Yegül, 2006:231).

In short, the stone workmanship seen in the Roman baths in Anatolia can be considered a distinctive feature, as materials were shaped differently and varied from region to region. Secondly, the economic and structural characteristics of local materials, such as their load bearing capacities, durability and their hierarchical relationships with various types of materials are taken into account in all applications. The walls formed out of marble and large high-quality limestone blocks are at the top of the structural hierarchy, while walls made from rubble and mortar represent the lowest level of the scale. Walls made of small stone blocks, bricks and/or stone-brick can be found at a central level of this hierarchy (Yegül, 2006:235).

CHAPTER 3

ROMAN (CARACALLA) BATH IN ANKARA

The Roman (Caracalla) Bath is one of the most important ancient historical sites in Ankara. In order to understand and evaluate the Roman Bath, it is first necessary to grasp its context, and so this section will provide some brief information about Roman Ankara, after which the topographical and historical characteristics of the city will be described.

Ankara is located in Central Anatolia (Asia Minor), offering good access to other parts of the Anatolian peninsula in all directions. It is surrounded by different geological and topographical forms, including plateaus and mountains, and its strategically important location led many civilizations to settle in the area. The history of Ankara dates back to the Paleolithic age and was inhabited by the Hittites in the Bronze Age, and the Lydians and Persians in the Iron Age, up until the arrival of Alexander the Great. Ankara then fell under the rule of the Tektosag tribe of the Galatians, and it was the capital of the Galatian Province until the Romans settled there. Ankara hosted many different civilizations in its history but lived its most prosperous period under Roman rule (Mutlu, 2012:83). According to Güven, the city of Ankara was relatively unknown in the earlier ages but became important with the diminishing of the power of Gordion in the Roman era, primarily in the military, cultural, architectural, commercial and wool production areas (Güven, 1994:55; Mutlu, 2012:83).

Archaeological excavations have uncovered a few remains from the Phrygian period, although most of the remains uncovered in Ankara date to the Roman era, and provide the bulk of information for Ankara's history.

3.1 Roman Remains in Ankara Today

Although Ankara has a long history in which it has hosted many different civilizations, the only archaeological remains that are still visible in-situ in the city today are from the Roman era. The remains of monumental buildings of Roman origin in Ulus – the historic town center of Ankara – offer a good indication of the wealth and power of the Roman Empire, including the Augustus Roman Temple; the Roman Bath in Ankara and one section of the Colonnaded Street; the Roman Theatre; and the remains of a Roman street that is thought to be "Cardo Maximus" – one of the two main thoroughfares in the street system of Roman cities (Figure 3.1) (Mutlu, 2012:69).
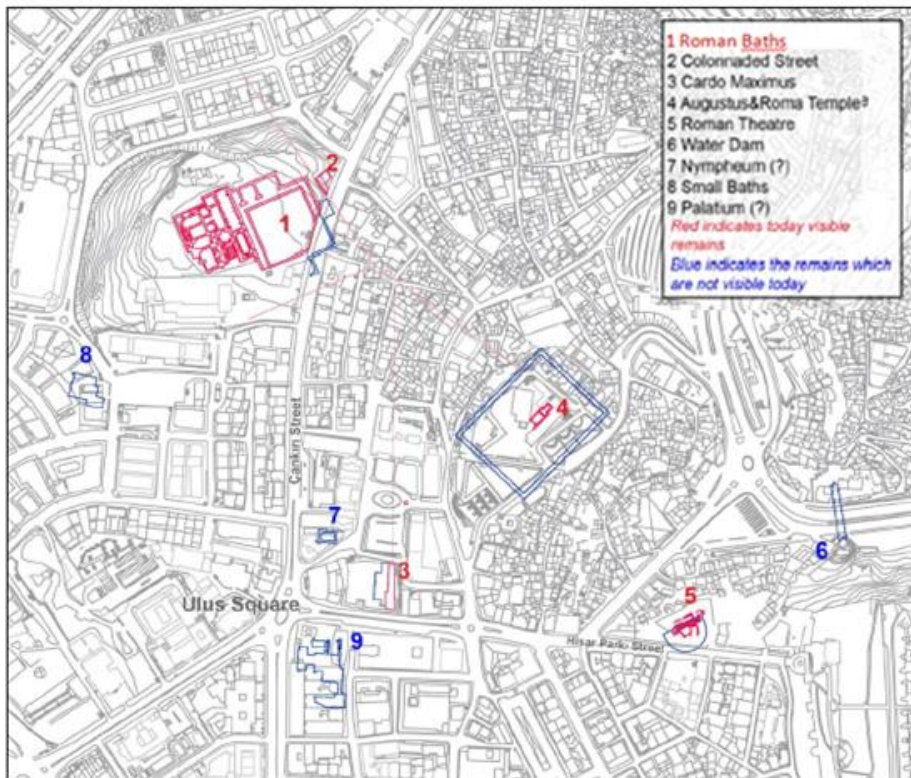
Figure 3.1 Known Roman structures and roads superimposed with contemporary Ankara

The plan is prepared by taking the archaeological information from Kadıoğlu, Musa; Görkay, Kutalmış (Kadıoğlu, Görkay, 2007; Mutlu, 2012:69)

The topography of Ulus, where the in-situ Roman remains (Figure 3.2) can be found, features two high hills with steep slopes, with the Roman sites lying to the west. The

Augustus Temple is located at a relatively higher level than the other sites, which are almost on the same level. The Roman (Caracalla) Bath in Ankara, as one of the four in-situ Roman Remains in Ulus, occupies the largest area of all the Roman sites in the district (Mutlu, 2012:83), sitting on a tumulus approximately 2.5 meters in height on Çankırı Street, about 400 meters from Ulus, the old town center of Ankara (Figure 3.3).
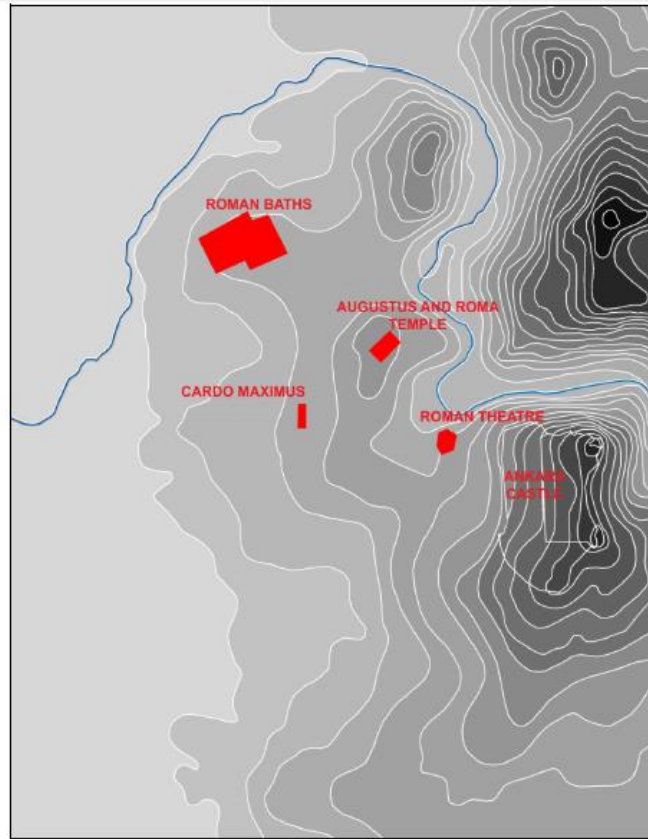
Figure 3.2 Extant Roman remains on the topographic map of Ulus (Mutlu, 2012:84)

The site is very close to the other heritage sites in Ulus, being only around 1.5 km from Ankara Castle and the historic residential urban tissue, and is, therefore, an important part of the cultural heritage of Ankara (Mutlu, 2012:90).

Building lot number and plot number of the site are 2738 and 3 respectively, and the plot is the property of the state, assigned to the Ankara Ministry of Culture and Tourism as the Roman Baths Open-air Museum (KVKBK, 2005; Mutlu, 2012:88). The visitor's entrance to the Bath is from Çankırı Street, the primary axis of the city, which lies to the east side of the site. As the street connects the old and new centers,

and also the residential areas and airport to the north, it has a relatively high traffic density. Another entrance from the northeast corner of the site is used for only service vehicles to the archaeological site. There is a high school to the south of the site, while the western side of the site is surrounded by car mechanic workshops. The east of the area has a mix of various commercial activities, including hotels, shops, casinos, and private offices (Drawing B.1 in Appendix B). The site is surrounded by stone walls that were built to provide security to the site, and the height of the walls changes depending on the topography and differences in levels between the site and the street, varying between 1.10 to 1.80 meters at the eastern elevation of the site (Mutlu, 2012:91-92) (Drawing B.2 in Appendix B).

(a)

(b)   (c)
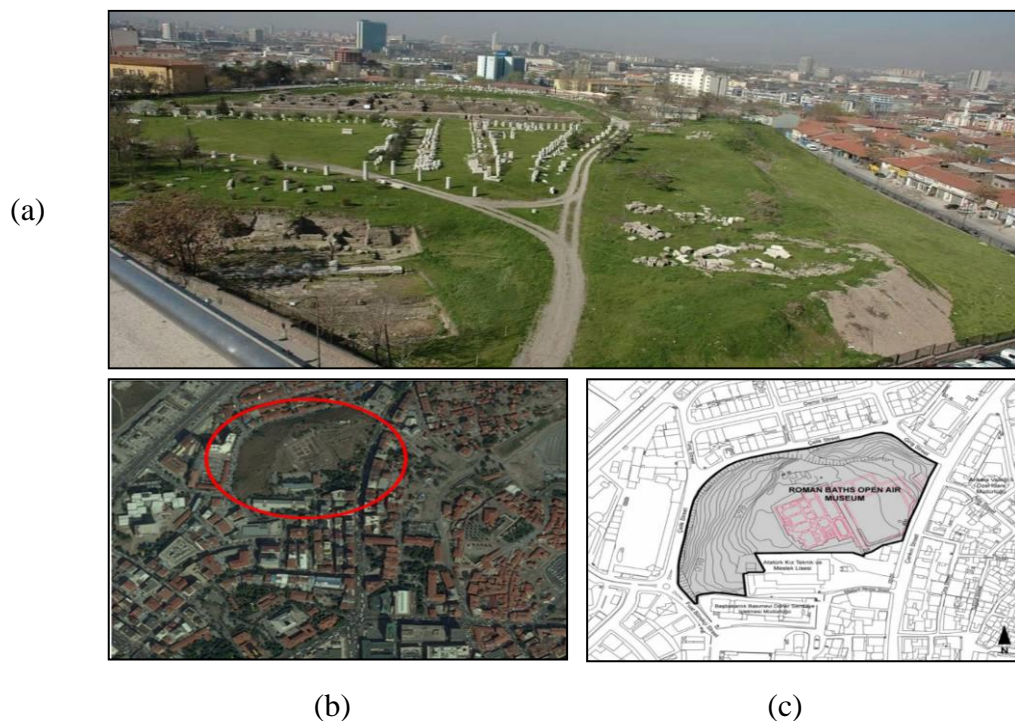
Figure 3.3 The location of the Roman (Caracalla) Bath in Ankara in north-east (a) Aerial photo (b) and the Ulus historical city center (c) (AAMM, n.d.; www.google.com-earth, n.d.; Mutlu, 2012:90)

3.2 History and Archaeology of Roman (Caracalla) Bath in Ankara

The existence of a Bath in Ancient Ancyra is indicated from an inscription carved in various parts of the city by 12 phyles of Ancyra, although only five copies of this inscription survive today. The inscription states that a temple priest named Tiberius

60

Iulius Iustus Iunianus built a bath, and served the city in many ways (Bosch, 1967:317-322; Mitchell, 1977:72). Although it is not certain that the bathing structure mentioned in the text may be the Roman Bath in Ankara, it has been accepted by many researchers (Bosch, 1967:317-322; Mitchell, 1977:72-75; Kadıoğlu et al., 2011:179). Traveler J.M. Kinneir who came to Ancyra on September 19, 1813 (Kinneir, 1818:104), spoke about architectural fragments and the remains of a building, describing a building on a hill overlooking the plain with walls of 30 feet high. It is assumed that this must have been the Roman Bath. Tournefort, who visited Ancyra in 1701 depicted the Roman Bath with high walls on the same hill in his Ancyra engraving (Figure 3.4) (Tournefort, 1717:442-446, 2005). The walls were destroyed by dynamite for the construction of the Ministry of Defense in 1926 (Dolunay, 1948:213; Akok, 1968:5), and the single and last picture showing the walls of the Roman Bath was drawn by Jerphanion (Figure 3.5) (De Jerphanion, 1928:226) (Kadıoğlu et al., 2011:179-180).
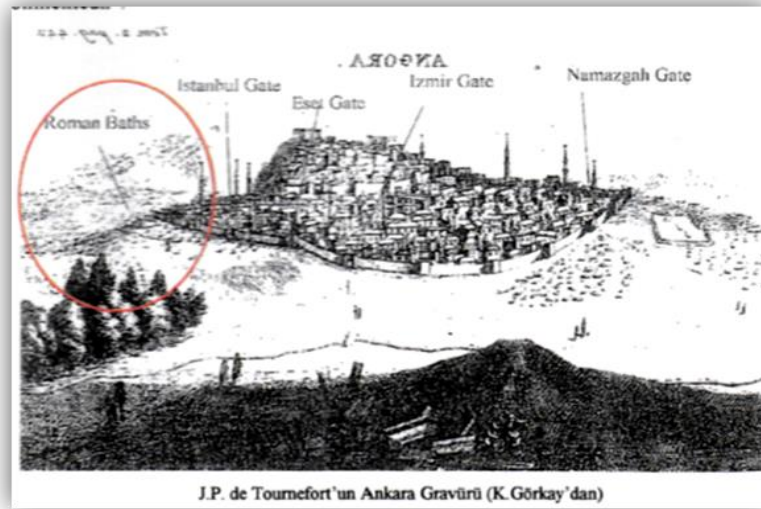
Figure 3.4 Engraving of Ancyra by Tournefort in 1701 (Kadıoğlu et al., 2011:110)

Hamamdan bir görüntü-(De Jerphanion 1928, lev.120-K.Görkay'dan)

Figure 3.5 View from the Bath (De Jerphanion 1928; Kadıoğlu et al, 2011:180)

Based on archaeological findings including coins, it has been thought that the Bath was constructed during the reign of the emperor Caracalla (Dolunay, 1941:266; Erzen, 1946:98-99). Erzen has considered the inscriptions for dating the bath (Erzen, 1946:99-100). On the other hand, Bosch who studied the inscriptions found in Ankara in 1967 also gives information about the construction date of the bath based on the coins (Bosch, 1967:321). He also argues that the earliest city coins that were found in that location were minted in honor of Caracalla and his mother Julia Domna, and claims further that the Bath was constructed as a dedication to Asclepius, the God of Health, based on the fragments of a sculpture of Asclepius found during the excavations. Another factor dating the Bath to the Caracalla period is the likelihood that emperor visited Ancyra on his way East (Bosch, 1967:243; Mitchell, 1977:64-65; Kadıoğlu et al., 2011:188), and so the Bath may have been completed before his arrival and dedicated to him. Bosch also suggests that the Megala Asklepia Soteria games that were held in the area were organized to celebrate Emperor Caracalla's recovery from illness at the time. Besides, there are also inscriptions honoring the emperor wishing him a rapid recovery (Bosch, 1967:322-323; Kadıoğlu et al., 2011:188-189). The most important inscription mentions the relationship between Asclepius and Caracalla and provides information about Agonothetes Titus Flavius Gaianus, who was the local ambassador of Caracalla, and who organized health contests in the name of the emperor (Bosch, 1967:310-313; Kadıoğlu et al., 2011:190).

Ancyra was also known as the venue of a long-distance running race in that period as is known from another inscription found in Aphrodisias (Robert, 1960:358; Roueché, 1993:198; Gagniers et al., 1969:293-294). Aside from the inscriptions, agonistic coins minted in Ancyra related to the *Isopythia Asklepia Soteria* and *Pythia* games prove the existence of the games (agonistic) organized in the city (Görkay, 2006:243; Arslan, 2004:150; Kadıoğlu et al., 2011:109-110). According to researchers, inscribed architrave blocks found in the colonnaded street excavations leading towards the entrance gate of the Bath may have belonged to the *palaestra* of the Bath, and the features of the inscription indicate that the *palaestra* could have been built during the Hadrian period (Dalman, 1933:130; Bosch, 1967:185-186; Cooke, 1998:56; Bennett, 2003:7; Bennett, 2006:210; Kadıoğlu et al., 2011:190). Cooke (1998), on the other hand, states that the bricks used in the building may have been produced as part of a single project, while standard-sized bricks may date back to the Hadrian or Caracalla periods, according to the measurements made by Dodge (Cooke, 1998:57). In contrast, Bosch (1967) claims that the building may have been built at an earlier time after examining two other inscriptions found in Ankara that mention of a Polyeidos Gymnasium in the city. Bosch, along with some other researchers, claims that the Roman Bath in Ankara is actually the site of the Polyeidos Gymnasium, given that the Bath has a large *palaestra* section that resembles a gymnasium (Bosch, 1967:351; Foss, 1977:63; Görkay, 2006:264-265). This suggests that the gymnasium was converted into a bath-gymnasium complex with additional construction work. Although this idea has not been proven, the presence of a bath-gymnasium complex at most of the Roman Baths in Anatolia supports this suggestion (Görkay, 2006; Kadıoğlu et al., 2011:190).

The first scientific excavations of the Bath were made in 1931 after architectural fragments were found on the Colonnaded Street during the construction of Çankırı Street in Ulus (Figure 3.6). The Ministry of Education asked the German Archaeology Institute to help document the remains, and Dr. K Bittel and Dr. K. O. Dalman were assigned to the task (Dalman et al., 1932:233-261; Dalman, 1933:121-133). During their excavations, the south-eastern corner of the *palaestra* (open area), whose connections with the bath were unknown, was excavated together with the Colonnaded Street (Kadıoğlu et al., 2011:180-181).

1931 Yılı Çankırıkapı kazısından (K.Görkay'dan)

Figure 3.6 The Çankırıkapı excavation undertaken in 1931 -DAI Istanbul Archive, K. Bittel- (Kadıoğlu et al., 2011:181)

In 1937, R. O. Arık made *sondage* excavations to the Bath on the northern skirts of the hill, and uncovered Phrygian, Roman, Byzantine, Seljuk, and Ottoman ceramics that were used for the identification of the phases of the mound (Arık, 1937:47-57; Dolunay, 1941:261-263; Dolunay; 1948:212-214). In 1938, the Turkish Historical Society and Monuments and Museums carried out excavations to find the early Phrygian layer, and in the same year, on July 18–August 31, the excavations were continued with the attendance of archaeology students from the Ankara University Faculty of Letters, directed by H. H. Von der Osten (Dolunay, 1938:495). "A" trench was opened into the northwest of the mound, and 40-50 cm of thick fill was removed revealing a 2.50 m deep cultural layer. In addition, in 1938 another *sondage* (5.00 x 10.00 meters) was made into the center of the mound in the same direction as "A" trench, revealing the *hypocaust* and *caldarium* of the Bath (Figure 3.7) (Dolunay, 1941:262; Kadıoğlu et al., 2011:181-182).

Büyük Hamam Kuzeyden Görünüş(1938 kazılarından) (K.Görkay'dan)

Figure 3.7 The Bath, view from north in 1938 (Dolunay, 1941:262; Kadıoğlu et al., 2011:182)

In 1939, the same group worked on the *caldarium* and *praefurnium* of the Bath, and most of the Bath was uncovered over a six-month period spanning 1940 and 1941 (Dolunay, 1941:263; Dolunay, 1948:212-218). After that, the excavations were continued by H.Z. Koşay and N. Dolunay until 1943, during which the northern wing of the Bath and the *palaestra* were uncovered (Dolunay, 1948:213). Further remains were found during the construction of new buildings around the Bath in 1944–1947, and remains that may have belonged to the Bath were examined and documented under the supervision M. Akok. Later excavations were made aimed at understanding whether the Bath was symmetrical in plan in its southern wing although the results were not as expected (Akok, 1955:311). The uncovered walls were not symmetrical with the northern wing, and so it was suggested that the southern part of the bath had possibly not been completed (Akok, 1955:311; Kadıoğlu et al., 2011:182-184).

Between 1996 and 2001, exhibition and restoration works related to the Roman (Caracalla) Bath in Ankara were carried out under the direction of the Museum of Anatolian Civilizations. Following this, Roman Bath in Ankara was converted into Open-Air Museum. To uncover the outer walls of the Ankara Castle, the south-western side of the Bath was excavated between 2000 and 2006, and excavation of the Colonnaded Street started in 2007 (AAMM, n.d.). In the following period, some restoration works were carried out by architectural firms. Then, the most extensive

studies were carried out between 2011 and 2014, in which a pre-study was made of the characteristic, type and deterioration problems of the construction materials. The first comprehensive laboratory analysis was also carried out at this time (Akyol, 2012).

3.3 Architecture of Roman (Caracalla) Bath in Ankara

The building was constructed in two parts: the *palaestra* (open space or area) and the bath building (enclosed space). The bath building measured around 140.00 x 180.00 m, while the *palaestra* to the northeast of the site was 95.00 x 95.00 m (Yegül, 1992:279) (Figure 3.8-3.9). There were porticos with 32 columns, including *postaments* on *stylobates,* unfluted column shafts, and Corinthian capitals, surrounding each side of the *palaestra*. The large area in the center of the northeast part of the *palestra* or in the central area of the strolling hall of the *portico* was probably the location of a large doorway providing direct entrance to the building. During the construction of Çankırı Street, some *architrave* blocks were unearthed that most probably came from the gate building. Entry to the *palaestra* was via the gate building (Bosch, 1967:185). According to Cooke the *architrave* fragments belonged to the *palaestra* (Cooke, 1998:55-56), although further measurements indicated otherwise (Kadıoğlu et al., 2011:184-185). During the excavation, a statue of a naked male was found in the *palaestra,* which is believed to have once adorned the gate building of the *palaestra*. Although the function of the covered spaces on the southeastern edge of the *palaestra* remains unknown, it is thought to contain a xystos used for warming to exercise on rainy days. On the other hand, Yegül suggests that the northernmost of the covered spaces was the hall of Emperor (Yegül, 1992:289). Perhaps the space was the gate building, mentioned above, in which there was a naked statue of an emperor built in honor of the elites, emperors and their families.

The other rectangular covered space located in the southeast part of the *palaestra* was probably also used as an exit from the *palaestra*, and this notion is supported by 1944 excavation. During the excavation, a street and staircase were uncovered to the south of the Bath and a door was identified (Akok, 1955:313; Kadıoğlu et al., 2011:185-186) (Figure 3.10).
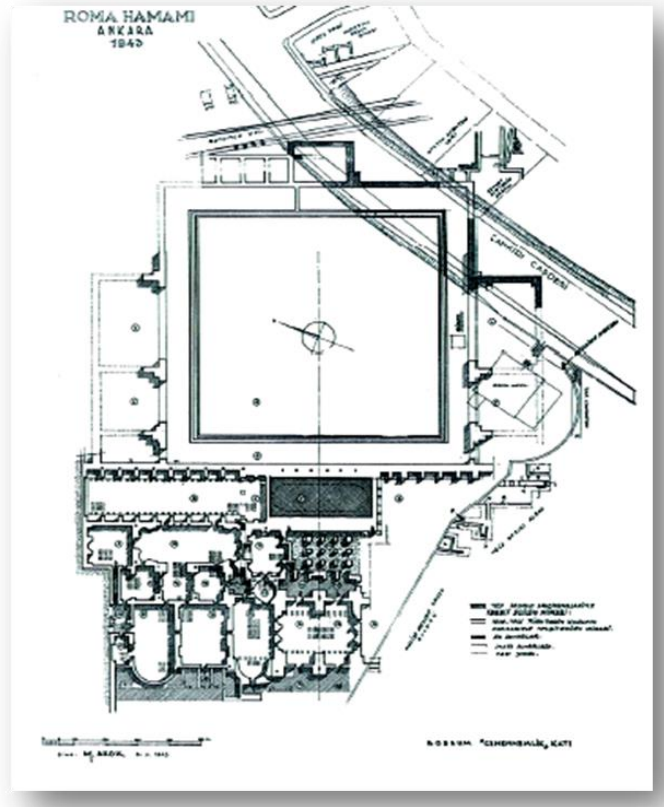
Figure 3.8 Plan of the Bath (Akok, 1968:25)
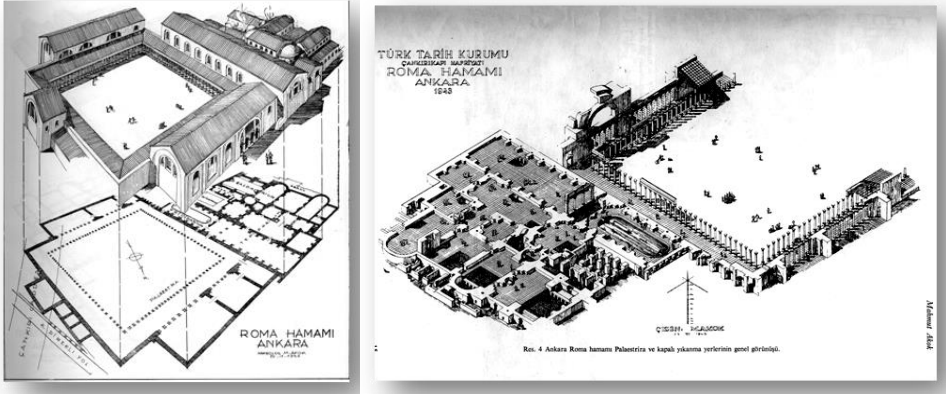
Figure 3.9 Plan and perspective drawings of the Bath (Akok, 1968:15, 29)
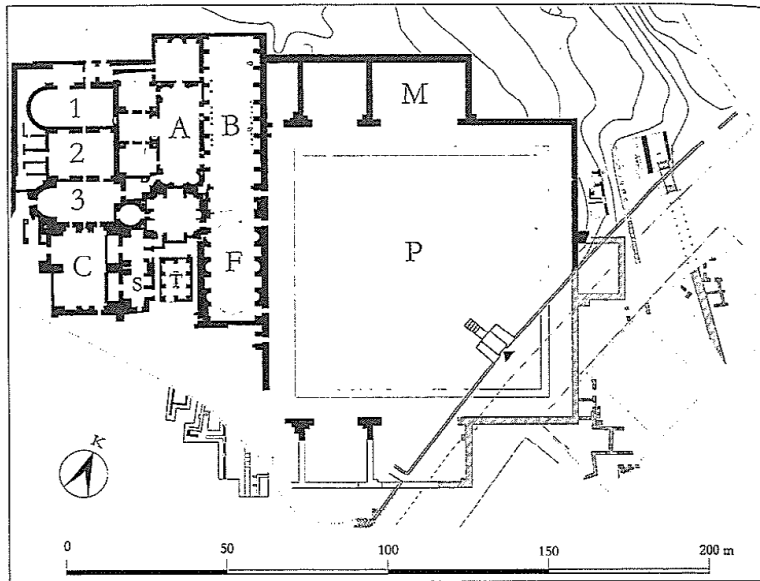
C-*Caldarium,* 1-2-3-*Tepidarium,* S-Service Halls, B-*Basilica* (Closed *Palaestra*)

A-*Apoditerium,* F-*Frigidarium*, M-The Hall of Emperor, P-*Palaestra*

Figure 3.10 Plan of the Bath (names of spaces from Yegül, 1992; Kadıoğlu et al., 2011:184)

Scholars believe the *palaestra* was also used for festivals, celebrations and religious ceremonies (Dolunay, 1941:264; Erzen 1946:99; Akok, 1968:13, Cooke, 1998:55), and especially during the agonistic Megala Asklepia Soteria games in the Caracalla Period; the bath area (palaestra) was also used as a gathering place for the people (Cooke, 1998:55). On the other hand, according to experts it is likely that people accessed such festivals through the inscribed gate to the east of the Bath, and then proceeded to the *stadion* through the south gate. Although the exact position of the *stadion* is not known in Ancyra, it is thought have been linked to the Bath. The existence of several *stadions* and baths on the same site in Anatolia supports this view (Görkay, 2006; Kadıoğlu et al., 2011:114-115).

Some of the archaeological remains of the *stadion* of ancient Ancyra – andesite seat blocks – are today piled up on the edge of the site to the west of the Roman Bath. The dense use of the seat blocks in 3rd century A.D city walls, both in Bath location and also to the west of the Bath; suggest that the *stadion* was in the southern part of the Bath (Görkay, 2006:247-271; Kadıoğlu et al., 2011:110-111). According to Görkay (2006), it is also possible that the limestone seat blocks reused in the 3rd

century city walls, found during the excavation of the Bath, may have belonged to the *stadion.* Thus, two different materials (andesite and limestone) were used for seat blocks in the *stadion.* In other words, different materials were added to the *stadion* in different periods. Especially the situation may have been a result of increasing demand for seats during the Agontistic games of the Caracalla Period (Görkay, 2006:247-271; Kadıoğlu et al., 2011:115).

The covered spaces or the main building complex of the Bath, contain some specific facilities, including a *caldarium*, *tepidarium, frigidarium* containing *apoditerium* and *piscina* (Figure 3.11-3.13-3.14).

While the *frigidarium* measured around 15.00 x 35.00 m, the *tepidarium* and the *caldarium* spaces measured around 11.00 x 25.00 m and 25.00 x 25.00 m, respectively. The *frigidarium* which was located near the entrance to the *palaestra*, contained a *piscina* (cold water pool) and an *apoditerium* (changing room). The *piscina* was designed in rectangular form with two of the corners constructed in a half circle and the length coming to the height of a person. (Akok, 1968:8-11). The floor of the *piscina* was laid with mosaics in a regular octagonal and square *opus sectile* organization (Kadıoğlu, 1997:361-362, Çoşkun, 2004:70). The *apoditerium* was located near the *piscina.* There is also a *hypokaust* system below the *apoditerium* part (Akok, 1968:8) which would be needed both to keep people warm, and also to prevent loss of heat from the overall building during the cold periods in Ancyra. On the other hand, the *tepidarium* (warm room) and *caldarium* (hot room) were located on the southwest side of the site, rather than to the south, as suggested by Vitruvius (1914:157, 1990:116; Brödner, 1983:250).

In addition, there was a *sudatorium* containing a hot dense vapor room and a sweating room in the *tepidarium*. Furthermore, a large *natatio* and water tank/reservoir were built in suitable places considering the water supply and sewerage systems of the Bath (Akok, 1968:8-11) (Figure 3.10-3.13-3.14).
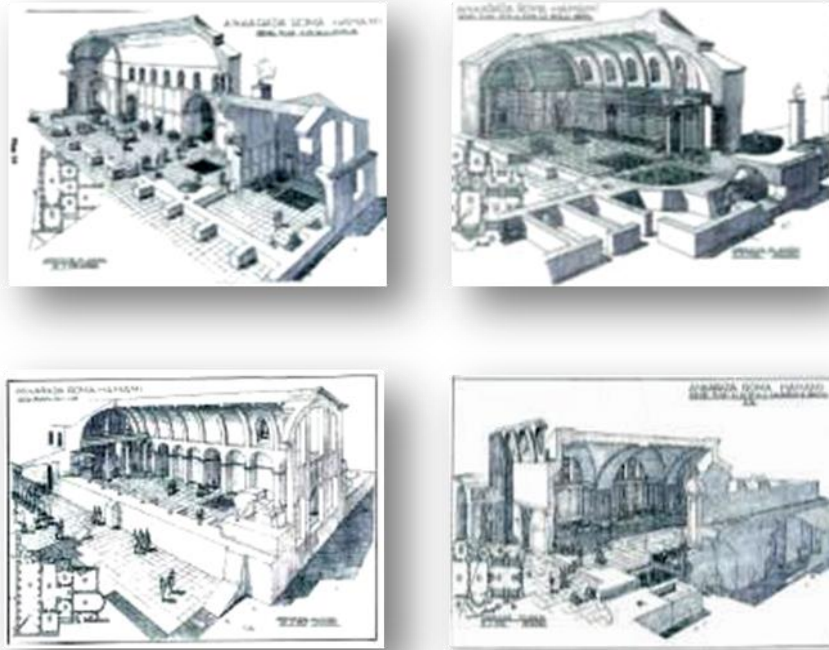
Figure 3.11 Drawings of perspectives of covered spaces of the Bath
(Akok, 1968:32-37; Bakar, 2008:135-140)

Heating for the entire bath building was supplied by 14 *praefurniums*, allowing the cold climatic conditions of Ancyra to be easily overcome, and the *apoditerium* part was also heated by *praefurnia* (Akok, 1955:311; Kadıoğlu et al., 2011:187) (Figure 3.14). Yegül says that the size of the Roman bath was determined by the number of furnaces, and because of its size, the Roman (Caracalla) Bath in Ankara had 14 furnaces and a big service corridor, covered with high, wide, stone vaults to be connected each other (Yegül, 2010:114).

The plan organization of the Bath has a clear asymmetric layout, and if the southern parts of the building were not left unfinished (Akok, 1955:311), the hot spaces of the building to the south would be less than half of the above-mentioned space. Yegül suggests that this Bath was in the category of "Bath-Gymnasium", and that the design of the building is incomprehensible when compared to the other Anatolian Baths (Yegül, 1992:279; Kadıoğlu et al., 2011:187). Besides, the final architectural projects at the site were carried out by the MK (Keskin, 2012); and Miyar (Nalbant, 2014) Architectural Office (Figure 3.12-3.13) (Drawing B.2-B.3 in Appendix B). As the visible architectural remains of the bath were below floor level, the building

survey project was developed based on the visible architectural remains, being the walls and components of the foundation and the hypocaust system. The remains in the site indicate that the Roman Bath was composed of two parts: bath building and *palaestra* as mentioned previously. The enclosed parts of the Roman Bath building include the *caldarium*, *tepidarium,* and *frigidarium (piscina and apoditerium)* (Figure 3.13-3.14). The open building part of the bath is the *palaestra,* although today only parts of the colonnade system can be seen (Figure 3.12-3.14). Although their layout can be assumed from the restitution plan which was drawn by Akok (1955), the east corner of the *palaestra* is not visible today, in that it now lies under the modern Çankırı Street. In the same way, the southern part of the stoa of the *palaestra* is not visible today, as it most probably extents under the garden of the adjacent school (Figure 3.12-3.15) (Drawing B.2 and Drawing B.7 in Appendix B).
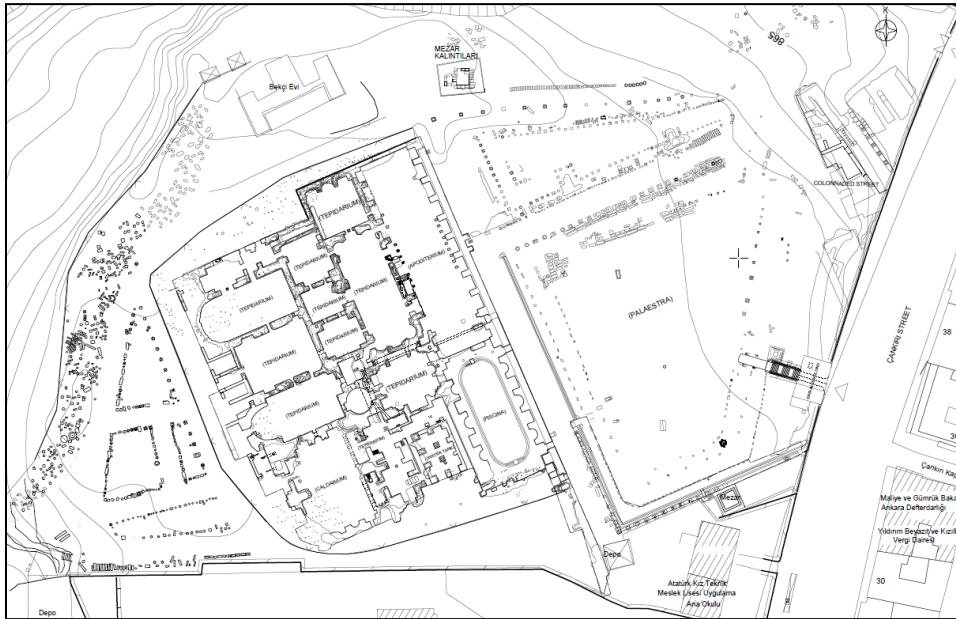
Figure 3.12 Location and plan of the Bath (Keskin, 2012; Nalbant, 2014)
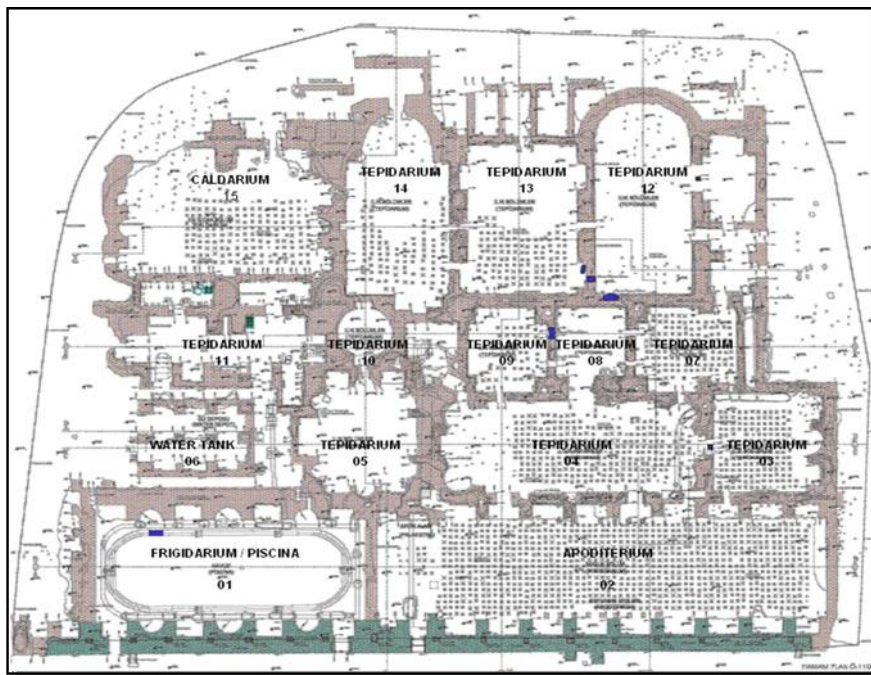
C-*Caldarium,* T-*Tepidarium,* F-*Frigidarium,* P- *Piscina,* A-*Apoditerium,* , WT-Water Tank

Figure 3.13 The plan of closed spaces of the Bath (Keskin, 2012; Nalbant, 2014)

Figure 3.14 (a) *Palaestra* (b) *Piscina* (c) *Apoditerium* (d) *Tepidarium* (e) *Caldarium* of the Bath (Akyol, 2012; photos: Zeynep Tanrıverdi, 2014)
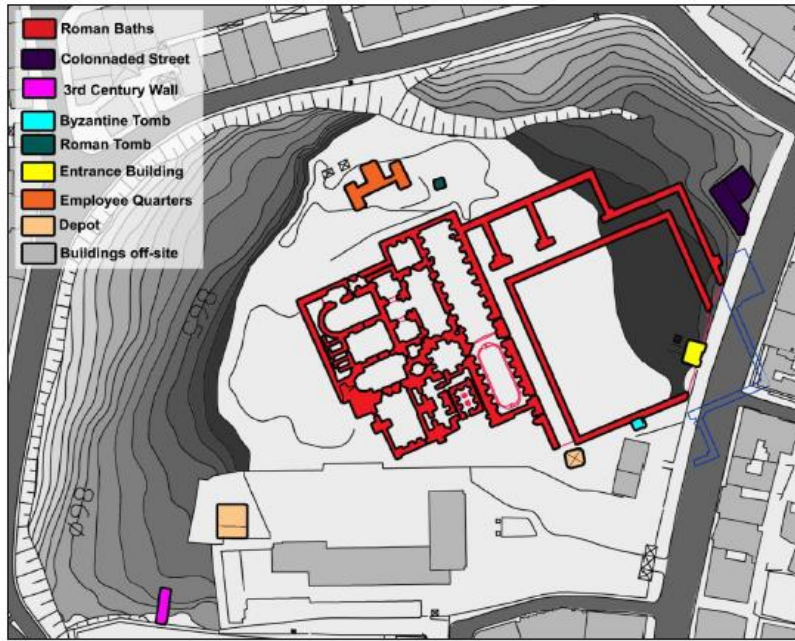
Figure 3.15 Components of the Roman Bath Open Air Museum (Mutlu, 2012:95)

Even though the site is known as the "Roman Baths Open Air Museum", it also contains the remains of a colonnaded street next to the *palaestra* of the Roman Baths to the northeastern, and part of a 3rd Century A.D fortification near the southwest corner of the site. The remains of the colonnaded street include the pavement, stylobat, postaments and stoa. According to experts the street likely continues towards the east beneath Çankırı Street (Figure 3.15-3.16) (Mutlu, 2012:94) (Drawing B.6 in Appendix B).

Figure 3.16 The remains of Colonnaded Street and the 3rd Century A.D Fortification
(photos: Zeynep Tanrıverdi, 2014)

The site also contains two tombs that were transferred from different sites in Ankara and relocated on the site. These two tombs are dating back to the Roman and Byzantine periods. The Roman tomb was discovered in 1998 in the Balgat district of Ankara during the construction of a building. The tomb has been dated to the first half of the 1st century A.D. It contains one small room (1.60m x 1.60m) and a larger main burial chamber (3m x 4m). The Byzantine tomb was found on the site of Ankara's central railway station during the construction of the station's administrative building in 1930. The tomb dates back to the 3rd–4th centuries A.D. The restoration work of the tomb was carried out by Directorate of the Museum of Anatolian Civilizations in 2012, after which it was opened for visitors. The tomb has again been closed to visitors and can be viewed only from the outside (Figure 3.15-3.17) Besides, some archaeological fragments are also exhibited on the site from different periods, and from other locations, including inscriptions, grave stones, stone carved tombs and parts of tombs, postaments and parts of different columns (Mutlu, 2012:98) (Figure 3.18).

Figure 3.17 Roman Tomb and Byzantine Tomb (photos: Zeynep Tanrıverdi, 2014)

Figure 3.18 Some archaeological fragments exhibited on the site (photos: Zeynep Tanrıverdi, 2014)

At the boundaries of the Roman Bath Open Air Museum, in addition to the archaeological remains, there are some later structures, including an entrance building and an excavation house. The entrance building was built in 1930 in the architectural style of the time and consists of two parts. The southern part is used for selling tickets, while the northern part contains such service rooms as toilets and employee offices. The other building is the excavation house, which is used by employees, and there are three small depot buildings on the site that are used for storage (Figure 3.15) (Mutlu, 2012:149), (Drawing B.2 in Appendix B).

3.4 Construction Techniques and Materials of Roman (Caracalla) Bath in Ankara

The ruins of the Bath building provide clues about the areas below floor level (the foundations and the hypocaust system), but very little information about the superstructure of the baths. The basic constructional components of the Bath are walls, columns, arches, vaults, installation components, etc., all of which are constructed using regional techniques and materials.

The foundation walls of the Bath vary depending on the workmanship arrangement. A double-faced constructional approach was applied for the foundation walls of the Bath, in which the core between walls was filled with rubble filling, while the outer surfaces were coated with facing materials.

Generally, stone materials were used on the walls as facing or as rubble filling materials. The stone materials used for facing are andesite and limestone. While the facing stones used were all similar in height, their widths differed. In order to face the masonry walls, largely andesite stones -sometimes called "Ankara Stone"- were used singularly or together with bricks as alternating four rows of brick interspersed with four rows of stone (Figure 3.19 (a)-(b)). On the other hand, tuff and sandstone were used in random sizes and shapes as backfill materials.

In contrast, the rubble wall remains which were found in the later excavations, where located on the road of the northwest end of the site, were constructed out of undressed stone. The stone material was also used in the channels of water installation system, which brought water to the Bath and distributed it therein (Figure 3.19 (c)-(d)).
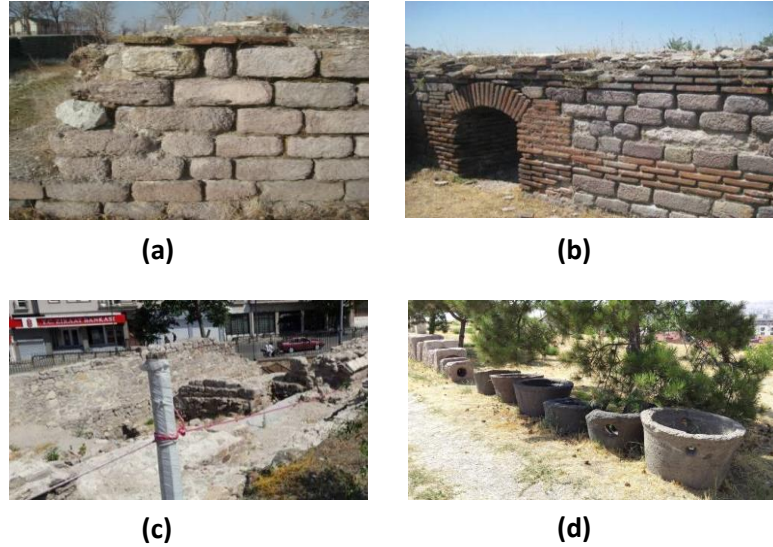
Figure 3.19 (a) The stone masonry wall (b) Masonry wall made from alternating layers stone and brick (c) The rubble stone wall (d) The perforated stone blocks for pipeline (photos: Zeynep Tanrıverdi, 2014)

Apart from andesite stones, the masonry, lintels, and thresholds of the gate and passage sections were built with thick marble and limestone blocks (Figure 3.20 (a)). Especially, decorative and construction fragments of the porticos of the Bath, including columns, *architraves*, and statues, were carved from marble blocks (Figure 3.21).

On the other hand, marble slabs were used to cover the floors or wall surfaces; it can be understood from traces of clamps were used to compress the marble. The fragments on the surfaces of the walls to the gallery on the ground floor were covered with flat, ornate marble up to a certain level. The gallery floors were covered with regular marble slabs, while the bathroom floors were coated with mosaics formed out of large pieces of marble. Similarly, the floor of the pool was covered with mosaics that were flat and white in color, and tessera measuring 1.5–2 cm (Figure 3.20 (b)) (Akok, 1968:8)

Figure 3.20 (a) Marble floor blocks (b) Mosaic of the pool

(photos: Zeynep Tanrıverdi, 2014)

Figure 3.21 Marble column and *architrave* fragments

(photos: Zeynep Tanrıverdi, 2014)

The arches, vaults, and *pilae* of the *hypocaust* system (Figure 3.22) and the walls of pool and bathroom were constructed out of brickwork. Besides, based on the excavation fragments, the superstructure elements of the vaults and domes which were used in time to cover the galleries and rooms were also constructed out of brickwork. While the brick shapes were rectangular and square in the arch, vault and walls, they were circular in the *pilae* of the *hypocaust* system. The brick material is red in color and it has a compact porosity (Figure 3.23).

Figure 3.22 The brickwork of arches and *pilae* (photo: Zeynep Tanrıverdi, 2014)

Figure 3.23 Rectangular, square and circular brick examples
(photos: Zeynep Tanrıverdi, 2014)

It can be further understood from the fragments of roof tiles found during the excavation that the roofs of some bath buildings were covered by tiles (Akok, 1968:11). Mortar and plaster materials used in the Bath served as both protection and decoration. The mortar was used between the stone, brick and the stone-brick, as a filler and binding material (Figure 3.24). The mortar joint material contains coarse sand, with lime as a binder (lime) and pieces of stone (aggregates) (Tanrıverdi et al., 2018:20-22). As can be understood from the existing ruins on the site, the walls, vaults, and arches of the Bath are coated with two layers of plaster, the first coat being a rough coat, which was then covered with two layers of the final render (Figure 3.25). Both layers contain various types of stone and brick aggregates and lime binding material (Şener, 2018:235; Tanrıverdi, et al., 2018:16).

Figure 3.24 Mortar examples in the Bath

(Şener, 2018:251; photos: Zeynep Tanrıverdi, 2014)
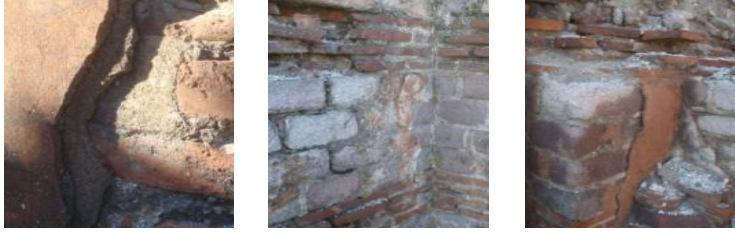
Figure 3.25 Plaster examples in the Bath

(Şener, 2018:250; photos: Zeynep Tanrıverdi, 2014)

An on-site investigation of the materials used for the bath reveals evidence of problems of deterioration. The typical examples of the deteriorations are efflorescence at the base of the walls, detachment and, loss of material, along with biological growth (Figure 3.26). Material losses and detachments are seen commonly in the stone masonry repaired with cement mortar in many areas.

Cement based repairing materials, atmospheric pollution, rising damp have introduced salt into the porous of building materials. Wetting-drying cycles and the subsequent dissolution and recrystallization of the salts in the walls and on the surface of the walls (as efflorescence) respectively are the main reasons for the disintegration and detachment of the materials.

Figure 3.26 Material lost, efflorescence and biological growth on materials of the Bath (photos: Zeynep Tanrıverdi, 2014)

3.5 Heating System of Roman (Caracalla) Bath in Ankara

The heating system of Roman baths was the key factor in the arrangement of the plan. The architectural plan of Roman Caracalla Bath in Ankara was no exception to this, being designed with the heating system built into the foundations. The furnaces, which are the main element of the "hypocaust system", heat the Bath from below. While the Bath's service areas were divided into adequate rooms for furnaces and storages, the connection between the center and outer service areas was via tunnels (Figure 3.28). There were 14 praefurniums in the various service areas demarcated on the foundation plan of the Bath (Figure 3.27). The furnaces of the bath were very special in terms of their constructional and architectural properties. The mouths of the furnaces were designed narrowly to allow them to be closed securely, and there were large chimneys in niches in the front service areas to allow the egress of smoke. The roofs of the service areas were left open to allow the smoke to escape (Akok, 1968:9).
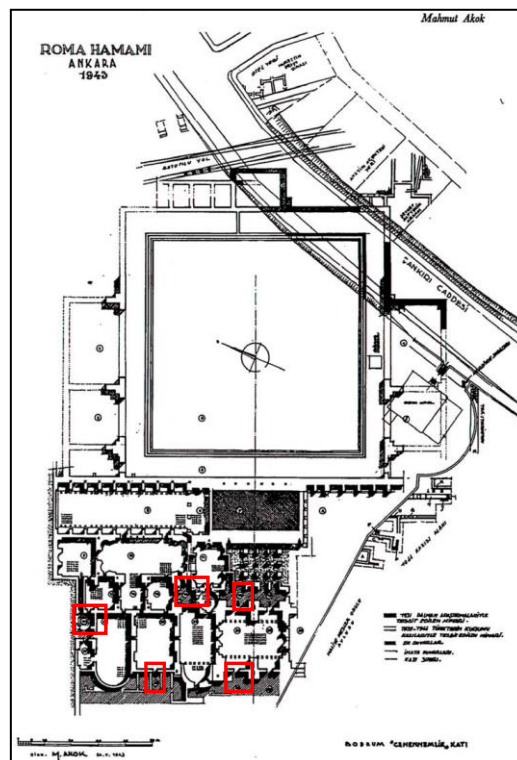
Figure 3.27 Location of the furnaces in foundation plan of the Bath (Akok, 1968:25)

The interiors of the firepans of the furnaces were built out of firebrick *pilae* and beams. The air heated in the furnaces spread beneath the floor of the gallery or through a vent between the marble coating and the walls. It means that the gallery parts of the Bath were heated from both the floor and the walls (Akok, 1968:9).

Figure 3.28 The tunnel passage in foundation of the Bath
(Akok, 1968:22; photo: Zeynep Tanrıverdi, 2014)

There were stoke holes below all of the enclosed building parts of the Bath, aside from the *piscina* (pool), measuring around 125 cm in height, allowing the service men to move around when they needed to. The floor of the gallery was supported by brick *pilae* that were circular in the middle and foursquare at the edge. The *pilae* were arranged in the form of a grid with 73 cm distance to each other and a square brick slab measuring 6x72x72 cm was placed on four *pilae* at each corner, after which, 10 cm of lime mortar was spread over the brick slab, and a further brick slab was placed on top of that. Then, 17 cm of mortar made with coarse sand was spread over the top, and 5 cm of adhesive mortar was applied with a thick marble slab to the floor, making an overall floor thickness in the gallery of 44–50 cm (Akok, 1968:9-10) (Figure 3.29).
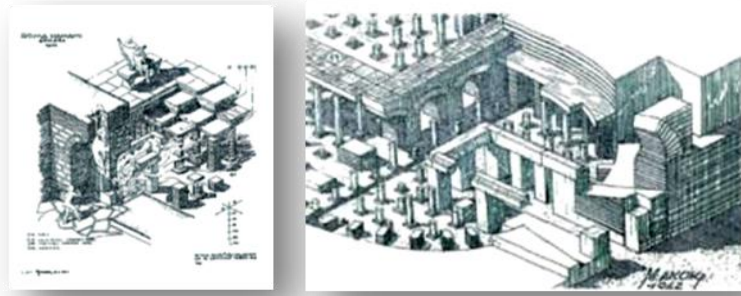
Figure 3.29 Drawings of furnace and *pilae* of the *hypocaust* system (Akok, 1968:19-20)

The circular brick *pilae*, used to carry the floor in central part of the gallery, is 23 cm in diameter and 5 cm thick, while the foursquare brick *pilae* that support the edge of the floor of the gallery measure 35x35x5 cm. The circular bricks making up the *pilae* each contained a 5 cm diameter hole through the center, providing a secure mortar connection (Akok, 1968:10) (Figure 3.30).

Figure 3.30 The circular *pilae* of *hypocaust* system of the Bath
(photos: Zeynep Tanrıverdi, 2014)

There are gutters and secondary ducts at the necessary points of the spaces in the stoke hole that carried the contaminated water from the upper galleries to the main channel. The floor of the stoke hole was covered with two layers of coarse blocks (blockage) (Akok, 1968:10).

3.5.1 Heating Energy Consumption of Roman (Caracalla) Bath in Ankara

The amount of wood required to heat the Roman Bath in Ankara was calculated by Başaran (2014) based on Tony Rook's calculations. Rook's (1978) study was carried out on the Welwyn Villa Bath, which has only 6 m² of warm and 6 m² of hot spaces

(total 12 m²). The temperatures of the hot, warm and cold rooms of the Bath were calculated as 70°C, 55°C and 25°C, respectively, for which an average of 114 tons of wood would be consumed per year. To meet this need 228 grown pine trees, weighing around 500 kg were cut. Başaran made the following calculation considering this information from Rook's study. Heating the *tepidarium* (warm room) and *caldarium* (hot room) sections of the Roman Bath in Ankara, which had an area of around 2000 m², required the burning of 38,000 grown pine trees each year, weighing around 500 kg. He claimed that Ankara's vast arid surroundings were due to this situation (Başaran, 2014:2-3). In other words, heating the bath for a year required the burning of 19,000 tons of wood, according to the calculation method of Başaran (2014) with the reference to Rook's work (1978). The heat value of wood is assumed to be 15,500 KJ/kg (Başaran, 1997:1013), meaning that the energy required to heat the bath was 70,340 kcal.

The data obtained within the scope of the thesis, however, shows that Başaran's calculation (2014) is far beyond the estimate, and this can be attributed to the architectural design, the components, and materials of the Bath, supported by its heating and insulation system. To begin with, in the architectural design of the Bath, spaces were arranged in a linear and adjacent compact plane to reduce heat loss. Moreover, the *Caldarium* section (hot rooms) of the Bath, as the hottest part, is oriented in a south-western direction so as to utilize the heat from the sun. Besides, the hypocaust system was constructed under the *apoditerium* (changing rooms) of the Bath, reducing heat loss between the rooms. Considering the cold winter climate in Ankara, this was an appropriate approach.

Secondly, when the architectural components of the bath are examined, the double-faced design of the walls of the bath (rubble fill to the core and coating materials on the two outer sides) provided insulation to the Bath and prevented the flow of heat out of the interior spaces. Aside from the design, as the bricks of the *pilae* (brick feet) in the hypocaust system are porous, they are able to absorb the hot air that circulated below the floor, contributing to the heating of the floor in all spaces.

Thirdly, a detailed material analysis conducted for the thesis showed that the material selection, material production, and material usage all contributed to the heating and insulation of the Bath. Among the reasons for the selection of the andesite material

for the double-faced walls of the bath include its abundance in the nearby region, its high durability against temperature differences and its high porosity, which prevents heat loss. Furthermore, the rubble fill to the cores of walls was also filled with highly porous sandstone and tuff, which are well suited for the storage of hot air and the insulation of the walls. The mortar used in the Bath was also produced for the specific purpose of use (structural mortar joints, mortar between the bricks of the *pilae*, rubble fill mortar) and specifically for the different sections of the bath (*Caldarium, Tepidarium*, Water Tank, etc.) to support different heat exchanges and heat insulation requirements. Accordingly, it can be understood that the Bath could be heated with less energy than defined in Başaran's calculation (2014).

Furthermore, the accuracy of the heating value calculated by Başaran (2014) is also doubtful, based on the following. Firstly, the Bath was used only during working hours, and so the *Caldarium* and *Tepidarium* sections were not at the same temperature at every hour of the day, meaning that energy consumption would vary throughout the day. Secondly, Rook's (1978) study was taken as reference for the calculation. In the study, the heating energy of the Welwyn Villa Bath was calculated according to 6 m² of *tepidarium* and 6 m² of *caldarium* spaces. Based on the assumption the *Caldarium* and *Tepidarium* sections had equal floor areas. However, these sections in the Roman Bath in Ankara had different floor area measurements (m²), and so the equal area assumption based on Rook's study are erroneous.

3.6 Water Supply System of Roman (Caracalla) Bath in Ankara

The water supply systems in Ankara's ancient buildings were examined in detail by Fıratlı, Özand and, Kaytan (Fıratlı, 1951; Özand, 1967; Kaytan, 2008). During the Roman period, the water was brought from Elmadağ via stone channels that split off into side branches in the city, from where it was distributed via terracotta pipes. The other water supply systems in Roman Ankara were the Roman dam built on the Hatipçayı (Bentderesi), the water wells and the drainage channels built between the limestone layers for water collection (Günel, Kılıcı, 2016:559). Similarly, in order to bring water to the higher points in the city, 20 km of channels which were bringing water from the Elmadağ springs that were located at an altitude of 1000 m were built by the Romans. (Figure 3.31) (Özand, 1967:1-3).
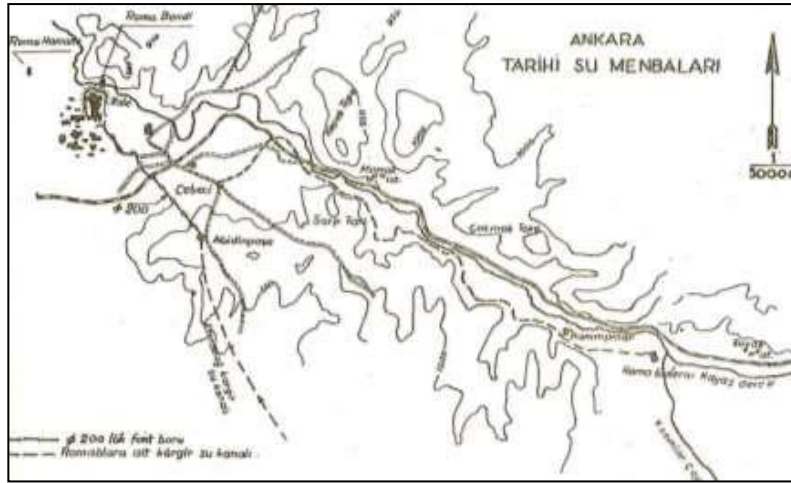
☐ Cast iron pipe-200Ø; - - - Masonry water channels of Romans

Figure 3.31 Historical waterways of Ankara (Özand, 1967:5)
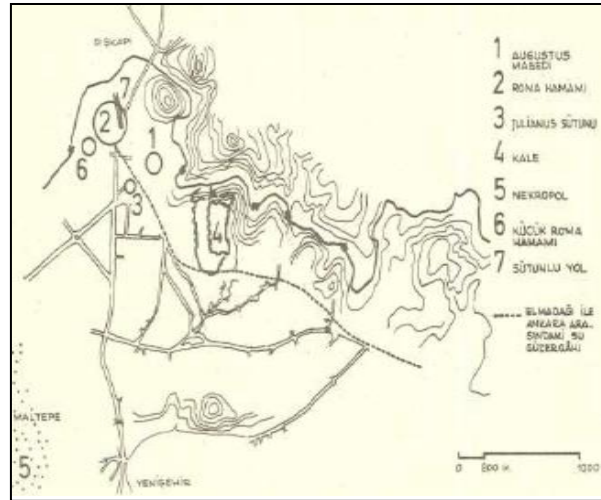
1- Augustus Roman Temple, 2- Great Roman Bath, 3- Column of Justinian 4- Ankara Castle;

5- Necropolis; 6- Small Roman Bath 7- Colonnaded Street

Figure 3.32 Ancient buildings and waterways in Ankara (Fıratlı, 1951:354)

According to Özand, water was brought to the Roman Bath in Ankara from Elmadağ via stone channels and then distributed through terracotta pipes around the Bath although the main route of waterways of bathing water was Cebeci, Hisarkapı, Çıkrıkçılar Hill and Çankırıkapı (Figure 3.32). The water needs of the Roman Bath in Ankara were satisfied by the water infiltration gallery built during the Roman period in Kayaş, 15 km away from the Bath, being brought to the city via the Hanım spring (Özand, 1967:1-3).

86

In fact, there is a lack of information on the supply of water and the internal distribution system of the Roman (Caracalla) Bath in Ankara due to the shortage of physical evidence and excavation reports (Fıratlı, 1951:352). However, the plan and topographic arrangement of the Bath may support some plausible guesses about the water supply of the building. According to Fıratlı, the water was supposed to enter the Bath building from the south-east or from the area that is now a secondary school (Atatürk Vocational and Technical Anatolian High School), based on the topographic status of the Bath site (Fıratlı, 1951:353; Kaytan, 2008:30). Other important evidence which shows that the water entered the Bath from the same direction was the discovery of the route composed of two perforated stone blocks which led towards the secondary school. Besides, the opinion was supported by more than one scattered perforated blocks which were found near the school (Fıratlı, 1951:353).

Another important indicator of the route of the supply and distribution of water in the Bath is the presence of two stone blocks with 16 cm diameter perforations between the footings, located behind the water tank reservoir (Figure 3.33) (Fıratlı, 1951:353; Kaytan, 2008:30).

Figure 3.33 The perforated stone near the foundation walls of the water tank reservoir (Kaytan, 2008:30-31)

Considering the perforated nature of these blocks, it is apparent that two of them belonging to the pipeline were used to bring water to the Bath, while the other two were used to distribute the water to the Bath. Fıratlı also suggested that the perforated stone blocks between the previously mentioned footings were part of the foundation of the water reservoir. The footings contain calcium carbonate incrustations due to spillages of water, supporting the existence of the tank reservoir (Fıratlı, 1951:353).

The results are supported by Akok, whose plans showed a water tank between the *caldarium* and *frigidarium* sections of the Bath (Figure 3.34). The base area of the water tank reservoir was 10 x 6 = 60 square meters, elevated on 12 footings from the *caldarium* and *frigidarium* sections to support the needed water in the bathing areas (Akok, 1968:10).
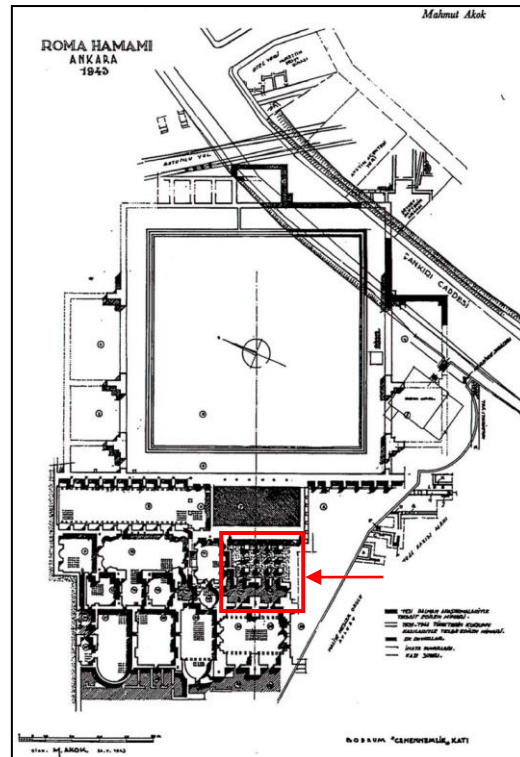
Figure 3.34 Location of the suggested water/tank reservoir in the foundation plan of the Bath (Akok, 1968:25)

Although the diameters of the pipe remains were different, Fıratlı suggests that two pipes found side-by-side in the foundations of the Municipality Building continued on to the tank reservoir that served the Bath. In other words, bathing water of the Bath was provided by city lines from the direction of the Municipality Building towards Çankırı Street which is in front of the Bath. The difference between diameters can be explained that the water need of the city was provided by these different pipelines (22 cm diameter in the foundations of the Municipality Building and 16 cm diameter at the Bath) which were settled between these two aforementioned points as the place of Municipality Building and Çankırıkapı Street

(Fıratlı, 1951:353). Fıratlı's opinion was supported with the finding of 6 and 16 cm diameter terracotta pipelines during the excavation of the foundations of the buildings at the intersection of Çankırı Street and Beşik Street (Fıratlı, 1951:353-354; Kaytan, 2008:32).

The very limited knowledge of the water supply of the Bath increased following the 2000 rescue excavation carried out to the south-west of the Bath to rediscover the early medieval fortification walls. The Roman Bath site was worked in 1947, 1985 and 1998 excavations (Temizsoy et al., 2002:146), while in 2001, 16 cm diameter terracotta pipeline traces, crossing the south-eastern part of the Bath, were discovered (Figure 3.35) (Temizsoy et al., 2002:147).

(a)   (b)
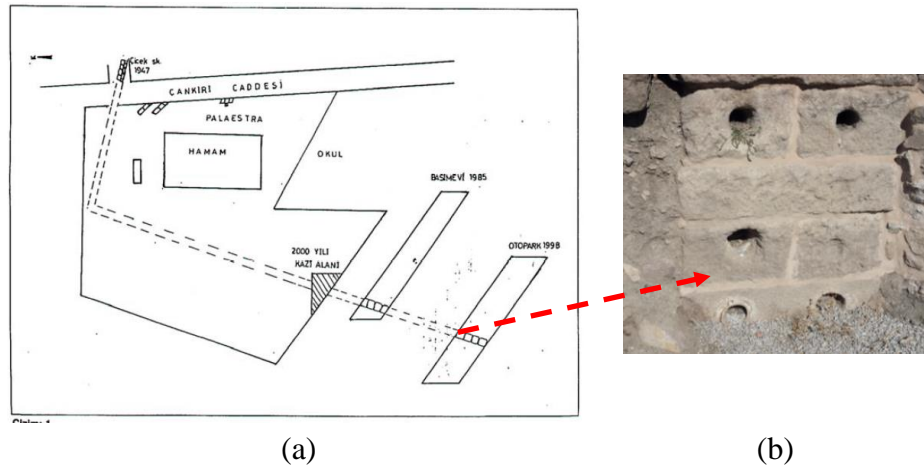
Figure 3.35 (a) Location of rescue excavations (Temizsoy et al., 2002:146) (b) terracotta pipes on the wall of water tank reservoir (photo: Zeynep Tanrıverdi, 2014)

Later, around 1.5 m below this level, four terracotta pipelines measuring 13 cm in diameter were found in the west of an area thought to be a *hypocaust* (Figure 3.36) (Temizsoy et al., 2002:148-149). It is not definite, but it is thought that this terra-cotta pipe was used to supply water to the private houses or the other buildings around the Bath (Temizsoy et al., 2002:148). Consequently, after the 2001 excavation, no further detailed research has been conducted on the introduction of water to Bath.
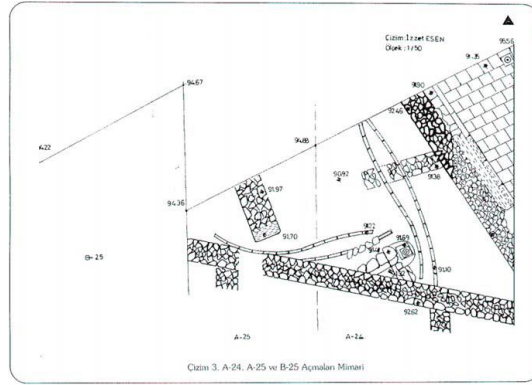
Figure 3.36 Plan of the excavated area and the found *terra-cotta* pipes
(Temizsoy et al., 2002:154)

Today, the Bath is an open-air museum and some of perforated stone aqueduct components are exhibited in the north of the site (Figure 3.37) (Esen, 2001:286-287; Kaytan, 2008:34-35).
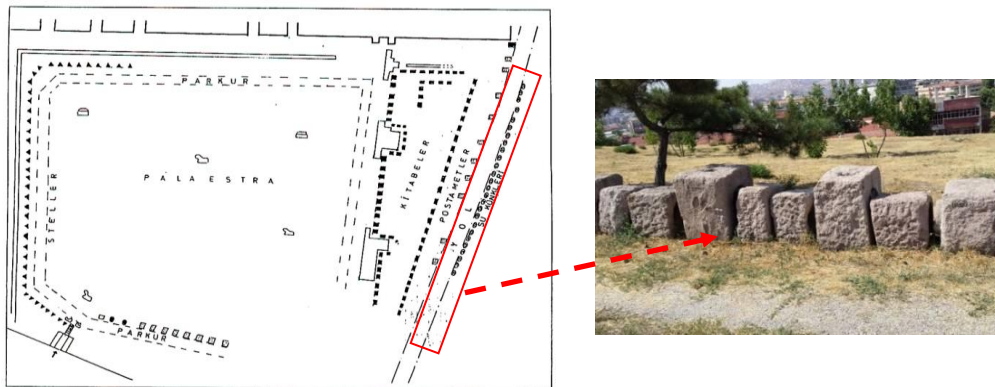
Figure 3.37 Location of the perforated stone blocks re-arranged on the north of the
Open Air Museum (Esen, 2001:289; photo: Zeynep Tanrıverdi, 2014)

CHAPTER 4

MATERIALS AND METHODS

This chapter concerns information about the materials studying and methodology of the experiments applied on the samples. The materials section was given in three subsections such as sampling, nomenclature, description, and documentation of the samples. The investigation methods of the analysis and test were explained in detail under subsections as analyses for basic physical and physicomechanical, compositional, chemical and mineralogical properties.

4.1 Materials

In the materials section, construction materials of the Roman (Caracalla) Bath in Ankara such as stones, stone tesserae, bricks, mortars, plasters, and calcerous layer were prepared for the laboratory analysis. Before the analyses, the studies were carried out as follows.

Field studies were performed first to collect the material samples and the samples were coded according to their location on the field, types and the numbers. The samples were then described on figures, tables, and drawings.

4.1.1 Sampling

Laboratory studies which include the basic physical, physicomechanical, compositional, mineralogical and chemical tests, and analyses were conducted in Historical Material Research and Conservation Laboratory (MAKLAB) at Gazi University and Laboratory at Ankara University Earth Sciences Application and Research Center (YEBİM). In the study, the samples - 13 stones, 3 stone tesserae, 29 bricks, 47 mortars, 4 plasters 1 calcerous layer - from that previous and new

collection (Table 4.1) were analyzed to determine characterization, provenance (source) of raw material, production technology, decay processes, compatibility and durability properties of the samples.

In the sampling process of the study, the groups of materials were first taken from the Roman (Caracalla) Bath in Ankara by field studies, and the samples were coded and the marked on the place of the ground plan. The points which samples are taken and the sample photographs were marked on the location plan in Figure A.1 - Figure A.6 in Appendix A. The photographs of each type of the samples were presented in Figure A.7 - Figure A.9 in Appendix A. Description of the samples were given in Table A.1 - Table A.5 in Appendix A.

Table 4.1 Type and number of the samples studied

Material Group Code	Material Explanation	Number of Main Samples
ARB-S	Stone/Rock Samples	13
ARB-Ts	Stone Tessera Samples	3
ARB-B	Brick Samples	29
ARB-M	Mortar Samples (Stone/Brick Joint and Rubble Filling)	47
ARB-P	Plaster/Plaster Layer Samples	4
ARB-Z	Calcerous Layer	1

4.1.2 Nomenclature of the Samples

In the nomenclature, first capital letters show the name of the origin region. ARB was used as the acronym for the "Ankara Roman Bath". The second capital letter showed the types of samples. Stone samples were named "S" code, while "Ts" code meant Stone Tessera and "B" code referred to Brick samples. While "M" showed Mortar samples, "P" and "Z" codes were used for Plaster and Calcerous layer of samples respectively. Sample number was shown at the end of the type of sample with corresponding numbers. For example, ARB-S1 was the first stone sample of the Roman Bath in Ankara.

4.1.3 Description and Documentation of the Samples

Stones: A total of thirteen stone samples were collected from the site. The stones were taken from different foundation walls of the Bath such as southeastern, western, and foundation walls of *piscina* (pool), *tepidarium* (warm room) and *caldarium* (hot room).

ARB-S1, ARB-S2 samples were from the corner of southeastern foundation walls. ARB-S3 was from the west wall of the *piscina* (P-1). The stone samples from ARB-S4 to ARB-S6 were from the southwest of *tepidarium* (T-11) foundation walls. The stone samples from ARB-S7 to ARB-S9 were from the nortwest of foundation walls of *caldarium* (C-15). ARB-S10 was from the northwestern foundation wall of the *tepidarium* (T-9). ARB-S11 was from structural component of the upper part. ARB-S12 and ARB-S13 were from corner of the exterior southwest wall of *caldarium* (C-15) (Table A.1 in Appendix A, and Figure A.3, Figure A.7 in Appendix A).

Stone Tesserae: There are three stone tessera samples taken from the *piscina*. Since ARB-Ts1 and ARB-Ts3 were from the base of east niche of the pool, ARB-Ts2 was from the base of the *piscina* (Table A.2 in Appendix A, and Figure A.6, Figure A.7 in Appendix A).

Bricks: Twenty-nine brick samples were collected from the site. The bricks were taken from the foundation walls of *piscina* (pool), *tepidarium* (warm room), *caldarium* (hot room), and the water tank, and heating and water supply system of the Bath. There are three types of bricks in the samples which are brick (structural), *pilae* and pipe (Table A.4 in Appendix A, and Figure A.4a, Figure A.4b, Figure A.8 in Appendix A).

Mortars: Forty-six mortar samples were collected from the different architectural parts of the Bath. Some of them were repairing mortars (Table A.5 in Appendix A, and Figure A.5a, Figure A.5b, Figure A.5c, Figure A.9 in Appendix A).

Plasters: There are four plaster samples. Three original of them were taken from the west wall of the *tepidarium* (T-5). The other repairing plaster was taken from the *piscina* (P-1) (Table A.3 in Appendix A, and Figure A.6, Figure A.7 in Appendix A).

4.2 Methods of Analysis

In this section, the experimental methods of the study, the preparation, and

application of the related tests and analyses on the samples were described. The tests and analyses were given in the following subsections.

4.2.1 Chromametric Analysis

Chromametric analysis was conducted for the assessment of colored samples. It was carried out by using ColorQAPocketSPEC device with Pro System III software (Figure 4.1). The colors were identified by using the Commission Internationaled'Éclairiage (CIE) L*a*b* system. In this system, (L) value defines the color in terms of its lightness, (a+) the intensity of red, (-a) intensity of green, (+b) intensity of yellow, and (-b) intensity of blue in that color (Akyol, 2009). In this study, measurements were done directly on the surface of brick samples.
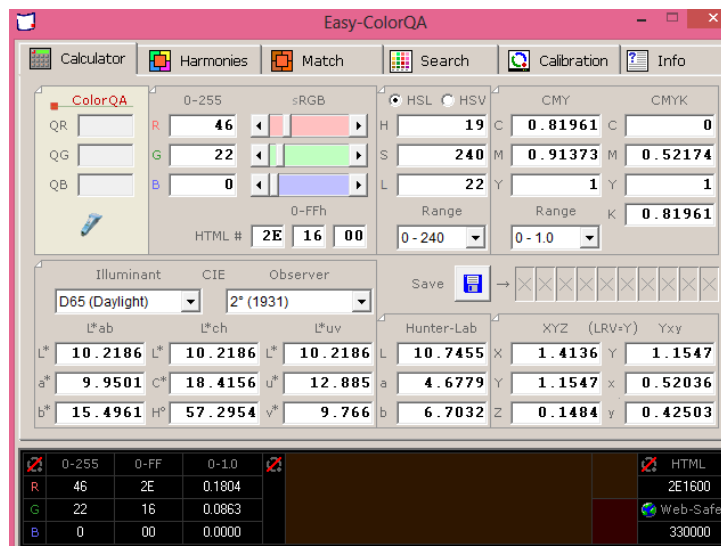
Figure 4.1 Screenshot of ColorQA Pro System Chromametry Software

4.2.2 Analyses for Basic Physical and Physicomechanical Properties

Physical and physicomechanical properties rely on technical statements of the characteristics of the construction materials (particularly stones and bricks) that can be defined within the determined standard limits (and consequently conveys data about competency/incompetency). The basic physical and physicomechanical properties of the samples were identified by bulk density, effective porosity, water absorption capacity, ultrasonic pulse velocity measurements and hardness test (Schmidt Hammer). By means of the analyses, the durability of the materials was identified.

4.2.2.1 Bulk Density, Effective Porosity and Water Absorption Capacity

Basic physical properties of construction materials of the Roman (Caracalla) Bath in Ankara were determined by the measurements of bulk density, effective porosity, and water absorption capacity using standard a test method RILEM test methods (RILEM, 1980; Teutonico, 1988; TS 699, 2009).

Bulk density (d) is the ratio of the mass to bulk volume of the sample. Its unit is g/cm³. Porosity (P) is the ratio of the pore volume to the total volume of the sample. Water absorption capacity (WAC) is the amount of water, which can be absorbed by samples (Borrelli, 1999).

The calculations of the bulk density, porosity and water absorption capacity of the samples were carried out by the measurement of their dry, wet and Archimedes weight. To obtain the wet weight of the samples, the samples were entirely submerged in distilled water for 48 hours and then placed in the vacuum (100 torr pressure) for one hour in order to remove the remaining air inside the pores. After being saturated with water, the samples were weighed in the air and the measurements were recorded as saturated weight "M_{sat}". To measure the Archimedes weights of the samples, each water saturated piece was measured in distilled water and recorded as Archimedes weight "M_{arc}". In order to obtain the dry weight of the samples, the samples were dried in an oven at 60°C for at least 24 hours, then the samples were weighed in the analytical balance and the results were recorded as the dry weight of the sample, "M_{dry}".

All weights were measured with a balanced sensitivity of 0.0001 g and using of all weights, bulk density (d), porosity (P) and water absorption capacity (WAC) of the samples were calculated using the following formula.

$$d \text{ (g/cm}^3\text{)} = (M_{dry}) / (M_{sat}-M_{arc}) \tag{4.1}$$

$$P \text{ (\% volume)} = [(M_{sat}-M_{dry}) / (M_{sat}-M_{arc})] \times 100 \tag{4.2}$$

$$WAC \text{ (\%weight)} = 100 \times (M_{sat}-M_{dry}) / M_{dry} \tag{4.3}$$

Where;

M_{dry}: Dry weight (g)

M_{sat}: Saturated weight (g)

M_{arc}: Archimedes weight (g)

$M_{sat}- M_{dry}$: Pore Volume

$M_{sat}- M_{arc}$: Bulk Volume

4.2.2.2 Ultrasonic Pulse Velocity Measurements

Ultrasonic Pulse Velocity (UPV) test is applied on the rock samples to determine their dynamic properties. Dynamic elasticity coefficients of rocks are calculated by analysis of ultrasonic measurement values of the prepared cylindrical or cubic test samples. The test is increasingly used in constructional technology for its ease of application and non-destructive nature. UPV measurement is carried out in three ways: direct, semi-direct and indirect transmission. The healthiest results are taken through the direct transmission measurement.

In this study, Matest C372N Model High Performance Ultrasonic Tester instrument was used for the measurements with the direct transmission process as follows:

The UPV instrument was turned on and the calibration of the measurement was done by placing a transmitter between the seismic analyzer.

The representative sample was taken from the material.

The transmitter and receiver of UPV instrument were placed in opposite sides (direct transmission) of the samples. A thin vaseline film was used on the surface of transmitter and the receiver to provide the good contact with the samples. At least one transit time measurement was taken.

The length between transmitter and receiver was measured by the caliper. The mesurement value was used for the calculation of the UPV.

Wave velocities were calculated using the following formula (RILEM, 1980).

In the formula, the impulsive penetration time value and the path length of the wave, which was defined as the thickness of the sample's value are used.

$$V = I/T \qquad\qquad (4.4)$$

Where;

V = P and S wave velocity (m/s)

I = Distance traversed by the wave (m)

T = Travel time (s)

To obtain the wave velocities of the samples, the impulse was given on the sample using the seismic velocity measuring instrument, and then the impulsive penetration time of the ultrasonic waves was recorded. The penetration time can be affected by many factors such as type, texture, grain size and shape, porosity, density, water content, temperature and anisotropy of the stone samples. Especially, the degree of

fissuring and pores of the samples significantly affect the penetration time of the ultrasonic waves (Brown, 1981).

4.2.2.3 Hardness Test (Schmidt Hammer)

Hardness test is performed to determine the strength of the samples. In order to measure the sample's hardness, a Schmidt (Rebound) hammer is utilized. The hardness values of rocks are used to predict the uniaxial compressive strength of the rocks. The test is preferred due to the non-destructive and practical method. The usage of Schmidt hammer is as the following;

- The plunger of Schmidt hammer is placed on against the surface of the samples
- A spring-loaded weight is released
- The amount the plunger rebounds is measured
- This rebound number is shown on a scale (in between 10-100)

The number can be affected by many factors as smoothness of the surface, size, shape, and internal moisture of the samples etc.

The rebound (strength) numbers of the aggregates in concretes are 40, 37, 32, 31 for river rock, granite, limestone, lightweight respectively (Luke, Snell, 2012).

In the study, a digital Schmidt hammer which is Digischmidt 2000 Proceq Testing instrument was used (Figure 4.2).

Figure 4.2 Schmidt hammer test device

97

4.2.3 Analyses for Compositional, Mineralogical and Chemical Properties

Compositional, mineralogical and chemical analyses of the samples were carried out to determine the characteristic, provenance (source), and technology of raw material properties of the samples. These were binder/aggregate ratio, particle size distribution, gravimetric analyses (Loss on Ignition – LOI), quantitative analyses of salt soluble (conductivity measurements and spot tests for anions), petrographical thin section optical microscopy, confocal Raman spectroscopy, scanning electron microscopy coupled with energy dispersive (SEM-EDX), and X-ray fluorescence (PED-XRF) analyses.

4.2.3.1 Analysis for Determination Binder / Aggregate Ratio

Mortar and plaster samples are generally composed of the binder and aggregate components. While acid-soluble parts of these samples are "binder", acid-insoluble parts are "aggregate".

Binder is a substance which is used to bind inorganic and organic particles and fibers to form strong components. It is produced by the chemical reactions which take place when heated, then mixed with water and/or other materials or just exposed to air. The main binder groups which are containing inorganic (mineral) particles are air hardening/non-hydraulic binders and hydraulic binders. The air hardening/non-hydraulic binders can only harden in the presence of air and also, they are not durable under humid conditions. Most common air hardening binders are clay which is present in most soils and lime which is high calcium or magnesium lime. Lime is the high-temperature product of the calcination of limestone. It used in different forms as burnt lime or quicklime (CaO) and as hydrated lime $Ca(OH)_2$. The hydraulic binders require water to harden and develop strength and also they are durable in humid conditions. Hydraulic and semi-hydraulic limes are derived from burning limestone which contains a large or moderate amount of clay. The most common hydraulic and semi-hydraulic limes are pozzolan and cement. Pozzolan is a natural siliceous or siliceous and aluminous material which is not cementitious itself. When it reacts with lime in the presence of water at room temperature, it will be hardened (Sičáková, 2015).

Aggregate or building aggregate is a construction material which is defined as an

inorganic, granular, loose, natural or artificial grains with grain size max 125 mm. The aggregate can be categorized according to different criteria as size, origin or production, apparent density. It can be used alone or with cementing materials as pozzolan, lime, cement etc (Sičáková, 2015).

In the study, as determining the percentages of aggregate and binder parts, the oven-dried samples (Msamp) were treated with 5% HCl acid to dissolve the binder (Middendorf, 1990; Jedrzejevska, 1981).

$$CO_3{}^{2-} (aq) + 2\ HCL\ (aq) \rightarrow CO_2\ (g) + 2Cl^-(aq) + H_2O\ (s)$$
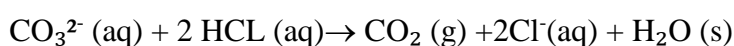
Then, the acid insoluble parts were filtered and the residue was washed with distilled water until it was free from all chloride ions. After that, the samples were dried in an oven at about 40°C and weighted (M_{agg}) with the sensitivity of 0.0001 g. The differences between the initial weight (M_{samp}) and acid insoluble weight (M_{agg}) were used for the calculation of the percentage of the acid soluble and insoluble parts. It was formulated as follows,

Insoluble % = [(M_{sam} - M_{agg})/M_{samp}] x 100   (4.5)

Acid Soluble % = 100 - Insoluble %   (4.6)

M_{samp}: Weight of the sample

M_{agg}: Weight of the aggregates

However, some aggregates which are present in mortar or plaster samples may be acid soluble. Because the aggregates are calculated with dissolved carbonated lime ($CaCO_3$), the acid soluble (lime) ratio in that samples does not give the exact result. To better evaluate acid soluble the binder/aggregate ratio, the lime must be calculated with respect to the lime ($Ca(OH)_2$) which had been used in the mortar and plasters (Akyol, 2009:57).

Therefore, the results of the binder/aggregate ratio are used to produce the new repairing samples as the original one.

4.2.3.2 Analysis for Determination of Particle Size Distribution of Aggregate

Particle size distribution represents the proportion of the varied size particles in the samples. The proportion is related to the number or weight of particles within stated size classes. By means of particle size distribution of aggregate, the proportion of the

varied size particles are identified and the new repairing samples are produced according to these results. In this study, to determine the particle size distribution of insoluble parts (aggregates) of mortar and plaster samples, the sieving method was used (Black, et at., 1965). In this method; the acid insoluble parts of the samples were filtered by a set of sieves as in the following process;

Sieves with different mesh sizes 2000, 1000, 500, 250, 125, and 63 μm were initially arranged in the sequence from top to bottom (TS EN 933-1/2012 take the place of TS3530 EN 933-1/April 1999; TS3530 EN 933-1/A1, 2007; Means, 1963).

The weighed sample was put on the mesh of the top sieve and the cover of the sieve was closed and then all superimposed sieves were shaken together.

The particles of the sample were transferred one at a time through the top to bottom sieves and then mass particles retained on each sieve were separated.

The remaining particles on each sieve were weighed and recorded. Finally, the percentage of the all particle size results was indicated in the graph.

In this process, there were some acid-soluble aggregates in mortar and plaster samples. To better evaluate the particle size distribution of these samples, the acid-soluble aggregates should be investigated by thin section and SEM-EDX analyses in terms of their sizes and approximate amounts.

4.2.3.3 Gravimetric Analysis (Loss on Ignition - LOI)

Gravimetric analysis (Loss on Ignition- LOI) is carried out to determine the amount of the water content, organic carbon and inorganic carbonate in material samples by measuring weight loss after being heated at the selected temperature (950°C for 24 hours). This analysis is rapid and low-cost. Based on the analysis, it is possible to identify a general sense of sediments properties of the samples (Vereş, 2002; Walter, Dean, 1974).

In the study, the gravimetric analysis was applied on mortar and stone samples containing carbonate as the following process;

Firstly, powdered sample (grain size <63 μm) was weighed about one gram accuracy with a balanced sensitivity of 0.0001 g, and then it was put in a pre-weighed porcelain crucible, which is not affected by a change in temperature. The sample in the porcelain crucible was then dried in an oven at 100-110°C for about several hours

and waited in the oven to cool completely. After that, the dried sample in the porcelain crucible was placed in a desiccator so that they would not absorb atmospheric water. Finally, the crucible and sample were weighed. The difference between the original and dry weight of the sample is the water amount of the sample. Secondly, the dry sample and crucible were put in a muffle furnace and heated to 450°C for about one hour. Then, the sample was cooled in room temperature and weighed again. The heating process was repeated at least two times. The difference in between this weight (after the heating processes) and the dry weight is the amount of the organic carbon ignited.

Thirdly, the sample again was placed in the muffle and heated to 950°C for one hour. Then, the sample was cooled in room temperature and weighed again. The difference of weight between at 450°C and 950°C gave the amount of CO_2 evolved from carbonate minerals. The heating process was repeated at least two times.

$$CaCO_3 \ (s) \rightarrow CaO \ (s) + CO_2 \ (g) \hspace{3cm} (\Delta H° = +176 \ J) \ (4.7)$$

The evolution process from $CaCO_3$ to CO_2 starts at about 800°C and it proceeds quickly. Most of the CO_2 evolves from calcium carbonate when the furnace is reached at 850°C temperature. Therefore, in the third process, the heating temperature was at 950°C.

4.2.3.4 Qantitative Analysis and Tests of Soluble Salts

Quantitative analysis and tests of soluble salts are applied on the samples during in situ sampling or in the laboratory. The aim of these studies is to determine the salt content which causes deterioration in the materials.

In this study, the experiments were applied on the stone and brick samples in the laboratory. While the salt amounts of the samples were determined by conductivity measurements, the salt types in the samples were identified with chemical spot tests in general and SEM-EDX analysis in detailed with microphotographies of the samples.

4.2.3.4.1 Conductivity Measurements (Calculation of Total Soluble Salts)

The quantitative analysis of soluble salts is examined by the measurement of the electrical conductivity of the samples. With the help of the analysis, the salt amounts of the samples are calculated.

In the study, the experiment was conducted as follows; approximately 5 gram of dried and powdered sample was mixed with 25 ml distilled water, and 1 drop of 0.1% sodium hexametaphosphate [$(NaPO_3)_6$] solution was added. The mixture was shaken strongly about four times in 30 minute intervals. Then, the solution was separated by a filter paper. The electrical conductivity (EC) of the filtrate was measured by using NeukumSerie 3001 conductometer/pHmeter. The electrode of the conductometer was immersed into the filtrate, and the conductivity was measured. The salt content of the samples was calculated using the following formula (Black, 1965):

$$EC = (0.0014118 \times R_{std}) / R_{ext} \qquad (4.8)$$

$$A = EC \times 640 \times 1000 \text{ mmho/cm} \qquad (4.9)$$

$$S \% = A \times (ml\ sol'n/1000) \times (1 / Ws) \times 100$$

where;

EC= Equivalence conductivity

R_{std}= Cell Resistance for Standart (0.01 M KCl)

R_{ext}= Cell Resistance for Extract Solution

A= Salt Concentration

Ws= Weight of Sample dissolved (mg)

S %= Percent Soluble Salt Content.

In the EC equation, 0.0014118 value expresses the electrical conductivity of the standard 0.01 M KCl solution in mhos per cm at 25°C. In the A equation, 640 value is the coefficient which expresses electrical conductivity in mmho/cm to salt concentration in mg/L and 1000 value is used to obtain mmhos per cm from the mhos per cm at 25°C.

4.2.3.4.2 Spot Test for Anions

The type of soluble salts is examined by means of the spot tests. In these tests, the types of salts are determined by detecting the anions in the sample solution. In this

study, the identification of the anions was performed using the Standard Merck Spot Test Kits (Feigl, 1989).

The Merck Spot Tests were applied for detection of the salts such as sulfates, phosphates, nitrates, nitrites, chlorides and carbonates which are dissolved in water and transported into the pores of building materials.

The process of the tests in the study is as follows;

1 gram of powdered sample was mixed with 100 ml distilled water and the mixture was shaken strongly and left to wait for 24 hours. Then, some amount of the aliquot was analyzed using the Merck Tests Procedure. This procedure was conducted for detection of anions for salts such as SO_4^{2-}, PO_4^{3-}, NO_3^-, NO_2^-, Cl^-, and CO_3^{2-}. For every salt anion, the detection procedure varies. The detection limits for the anions can be seen in Table 4.2.

Table 4.2. Detection limit of anions using of the Merck Spot Tests

Anion	Merck Code	Detection Limit (mg/L)
Carbonate (CO_3^{2-})	110046	4
Chloride (Cl^-)	114753	3
Nitrate (NO_3^-)	111170	10
Nitrite (NO_2^-)	108025	0.025
Phosphates (PO_4^{3-})	114846	0.050
Sulphates (SO_4^{2-})	110019	20

4.2.3.5 Petrographical Thin Section Optical Microscopy Analysis

Thin section analysis is important for the determination of the microstructure and mineral phases of the material samples. However, the morphological properties of the samples can be examined using thin section analyses separately.

Thin section analysis which can be studied for identification of the substance and minerals of the sample is correlated with the other compositional, chemical, and mineralogical analyses. For example, based on the thin section analysis it is possible to make a prediction about the chemical composition of the rock from the mineralogical composition, likewise, it is possible to obtain information on the mineralogical composition of the rocks with the results of chemical analysis.

Therefore, various petrochemical calculation methods (such as CIPW, Niggli, Rittman calculation methods) have been developed to measure the chemical and mineralogical compositions of the rocks (Kadıoğlu, 2001; Deniz, n.d). Besides, some of the physical and physico mechanical tests results can be supported by thin section analyses (Kerr, 1977; Rapp, 2002; Black, 1965).

The thin section is a slice of material/rock which is 30 µm (=0.03 mm) thickness placed on the glass slide to be examined under the optical polarized microscopy. It is possible to prepare thin sections for each sample. The processes of the thin section preparation are carried out by experts as cutting, grinding, polishing, mounting and finishing respectively (Hodges, 1964).

In the study, if the sample was durable, thin section processes were applied on directly. However, if it was fragile, it was first placed in a plastic molding box (1.5x3x1 cm) and epoxy resin was impregnated into the samples to fill the pores and to provide the durability of the samples. Then, the epoxy saturated hardened sample was removed from the plastic molding box to use of the thin section processes.

The durable sample was cut into 1 mm slice and approximately rectangular shape (30 mm x 20 mm) by slap saw, and then it was washed and dried respectively to avoid the dirt. After that, the rough surface of the 1 mm slice sample was grinded by a horizontal diamond grinder to reduce its thickness and during the application, water was used to avoid the dusting.

In the next step, the surface of the sample was polished by lapidary wheel machine with help of water and 320 grit, 400 grit, and 600 grit carborundum respectively, until getting the perfectly flat and mirror-smooth surface. At the end of the polishing process, the sample became a chip, and it was washed and dried on the hot plate.

After that, the mounting process was carried out. In this process, the polished side of the warmed chip was glued on the glass slide by epoxy and waited for 24 hours. After that, the chip was nearly cut and separated from the slide by a cut-off slab. After that, a vertical diamond grinder was applied to reduce the thickness of the chip. Then, grinding wheel machine was carefully used to achieve the required thickness of the chip (0.03 mm). Eventually, the chip was ready for the microscopic examination. As the thickness of the slip was 0.03 mm, the mineral colors on the chip could be confirmed by Michel Levy Interference Color Chart (Levy, 1888).

In the finishing process, different layers of the chip were checked under the optical polarized microscope to identify textural distribution and shape of the grains, types of the rock fragments and the other minerals etc. In the study, thin section analyses were performed with a LEICA Research Polarized Microscope DMLP Research model with the objectives of 40X.

4.2.3.6 Raman Spectroscopy

Raman spectroscopy is one of the spectroscopic techniques, concerned with inelastic scattering of monochromatic light, usually from a laser source. This technique is used to provide information on chemical structure, phase, polymorphism, crystallinity, and molecular interactions. Photons of the laser light are absorbed by the sample and then re-emitted. The frequency of the re-emitted photons is mostly the same as the incident photons. This process is known as Rayleigh scattering. However, a small part of photons (approximately one in a million photons) is shifted up or down in comparison with original monochromatic frequency, which is called the Raman effect. This shift provides information about vibrational and rotational transitions in molecules. The important condition for a molecule to be Raman active is to have anisotropic polarizability. In other words, the distortion induced in the electron distribution in the molecule by an electric field must be dependent on the orientation of the molecule in the field. All atoms are isotropically polarized and they are not Raman active, but molecules have anisotropic polarizability, so they are Raman active (Vandenabeele, 2013).

Raman spectroscopy provides both qualitative and quantitative information about the sample due to all of the molecules having own unique Raman spectrum and the intensity of the scattered light being proportional to the amount of material present. Raman spectroscopy is a very fast technique. Typically, Raman spectra are acquired quickly within seconds. Raman can be performed using range from UV to NIR. This makes Raman ideal for the study of inorganic materials that have vibrational frequencies in the far-infrared that are otherwise difficult to reach (Thermo Scientific, n.d.).

Raman spectroscopy is a non-destructive method. It can characterize the chemical composition and structure of objects of archaeological and historical importance in order

to determine their authenticity, provenance, and technology. The technique brings together studies from different areas and so the importance of the technique can be increased day by day (Edwards, Chalmers, 2005).

Raman technique is suitable for many organic and inorganic archaeological materials in the form of solids, liquids, polymers or vapors. Raman studies are applied directly to the samples because there is no need for sample preparation processes such as dissolution, grinding, or pressing that can cause changes in physical or chemical structure and this situation minimizes the possibility of cross-contamination. Glass and plastic packaging have weak Raman spectra, therefore, samples can be analyzed directly inside a glass bottle or plastic bag without having any contamination risk. Because water has also weak Raman spectra, aqueous samples are analyzed without having to remove water. Besides, there is no need to purge the instrument due to ambient humidity (Edwards, Chalmers, 2005).

In the analysis, Horiba Jobin-Yvon Lab Ram Confocal Raman Spectrograph with an Olympus BX41 microscope and Peltier cooling CCD (1024 x 256 pixels) detector was used to acquire Raman spectra. The 632.8 nm laser line of a He/Ne laser was used for Raman excitation.

4.2.3.7 Scanning Electron Microscopy Coupled with Energy Dispersive X-Ray Analyzer (SEM-EDX)

Scanning electron microscope (SEM-EDX) is a type of an electron microscope that creates high resolution and high magnification image of the material samples with enhanced depth of field for trace evidence.

In the SEM analysis process, a finely focused beam of electrons is sent on the samples and the beam interacts with atoms of the samples. Depending on the interactions, a series of measurable electron energies are produced. The energies are examined by means of a scanning electron microscope to create a three-dimensional image. The image result provides the complementary information about morphology and microstructure (size, shape, etc.) of the materials such as stone, brick, mortar, and plaster etc (Goldstein et al., 2012; Gossman Forensics, n.d.).

The scanning electron microscopy (SEM) works together with energy dispersive X-ray (EDX) spectroscopy. The energy dispersive X-ray (EDX) spectroscopy is used

for the elemental analysis or chemical composition of the material. In the EDX analysis process, the bombardment of the finely focused beam causes the emission of "X-rays" from the sample. After that, the X-rays are collected and converted to useful information by EDX instrument. The output from the EDX instrument is a spectrum. The spectrum displays peaks according to the energy levels (unique to individual atom) of the atoms. The higher peak of the spectrum shows the higher concentration of that element. The characterization of each element is capable of its own electromagnetic emission spectrum. The overlapping peaks on the spectrum are deconvolved with using special computer software (Goldstein et al., 2012; Gossman Forensics, n.d.).

In the study, the selected samples which are about 3 cm with a flat surface are coated with carbon to provide a conductive surface. After that, SEM analysis is conducted using JEOL JSM-6400 Scanning Microscope and NORAN System 6 programmed EDX instrument is used for EDX analysis.

4.2.3.8 X-Ray Fluorescence Analysis (PED-XRF)

In X-Ray Fluorescence analysis, the elements of the materials are excited by bombarding with high-energy X-rays or gamma rays and the atoms of the elements emit their own characteristic "secondary" X-ray fluorescence. By determining the energy (wavelength) of X-ray fluorescence emitted from a specific element, it is possible to identify the element.

The X-Ray Fluorescence (PED-XRF) analysis is widely used for quantitative and qualitative determination of elemental and chemical properties of the materials. While qualitative estimation is carried out by qualitative identification of elements having atomic numbers greater than of oxygen (>8) or; quantitative estimation is conducted on the all but lightest elements. As opposed to other elemental analysis, this analysis is preferred due to its many advantages such as being non-destructive, fast, cheap, safe, sensitive and specific (Hodges, 1964; Salmon, 1970; Skoog, et al., 2007).

The XRF instrument can be configured either to excite the sample or to detect the characteristic fluorescence. The correct combination of excitation and detection methods are determined by the specific application. The source of the X-ray can be

an X-ray tube or radioactive isotope (iron-55, curium-244, cadmium-109, or americium-241). The detection can be executed either by wavelength-dispersive X-ray fluorescence (WDXRF) or by energy-dispersive X-ray fluorescence (EDXRF) instruments. Working principles of these instruments are shown in Figure 4.3.

In the WDXRF instrument, the X-ray energies are separated depending on specific wavelengths by diffracting crystals. The related intensities are then measured by proportional counters. The excitation of the sample is provided by the X-ray tube. This technique has many advantages such as providing the best resolution, the shortest analysis time, and the highest sensitivity.

It is also used for the most demanding tasks. For example, neighbouring elements with large differences in concentrations are analyzed with WDXRF technique (Liptak, 2003).
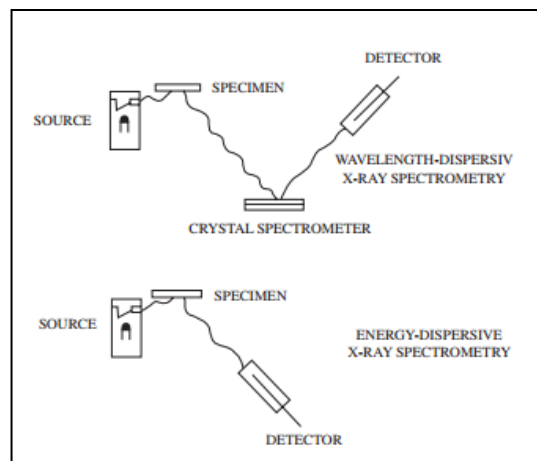
Figure 4.3 X-ray fluorescence spectrometers (Liptak, 2003)

With the EDXRF instrument, the characteristic fluorescence of the samples is determined. The detection of fluorescence is provided by a low-temperature, solid-state detector or a gas-filled proportional counter. The fluorescence is sorted electronically to produce an XRF spectrum of X-ray intensity energy. The excitation of the sample is provided by a low-level radioisotope source. While EDXRF technique provides excellent sensitivity with good resolution, especially for light element analysis, it is also useful for quality control and troubleshooting problems. Apart from these, it is compact and economic (Liptak, 2003).

There are two types of EDXRF configuration; "polarized" and "unpolarized".

Polarized energy dispersive (PED-XRF) is different from the unpolarized energy dispersive (XRF) due to providing significant background reduction in the fluorescence spectrum by excitation with polarized X-ray radiation based on the anisotropy of the atomic scattering cross section. In the polarized X-ray radiation, the sample is excited by linear polarized X-ray and only the fluorescence radiation is emitted from the sample. In other words, not any primary radiation is scattered from the sample. The fluorescence radiation reaches suitably to the detector. The components of polarized energy dispersive (PED-XRF) are designed with the beam, scattered beam and fluorescent beam at all orthogonal angles with each other (Stephens, Calder, 2004). In the study, PED-XRF spectrometer was used to determine the multi-element concentration of the samples. The instrument is Spectro XLAB 2000 PED-XRF, which has an Rh anode X-ray tube, 0.5 mm with window and Si (Li) by liquid N2 cooled with the resolution of <150eV at Mn K 5000 cps detector. With the help of the spectrometer, the elements from sodium (Na) to uranium (U) with atom number 11 and 92 numbers can analyze respectively. Besides, it measures heavy element up to 0.5 pmm and light elements up to 10 ppm (Shackley, 2011)

CHAPTER 5

RESULT AND DISCUSSION

In this study, the total 97 samples (13 stones, 3 stone tesserae, 29 bricks, 47 mortars, 4 plasters, and a calcerous layer) that were collected from Roman (Caracalla) Bath in Ankara were analyzed (Table A.1 - A.5 and Figures A.1 - A.9 in Appendix A). The results of the tests and analyses were explained in detail under subsections as chromametric, basic physical and physicomechanical, compositional, mineralogical and, chemical properties of the samples of Roman Bath in Ankara.

5.1 Chromametric Properties of the Samples

Chromametric analysis was conducted on the brick samples. The measurements were given in Table A.6 and Figure A.10 in Appendix A. According to the results, brick samples have brown, light brown, reddish and light reddish colors (Figure A.10 in Appendix A).

In the brick samples, the color code (L) values range between 19.02 and 46.56; the color code (a) values range between 8.56 and 24.02; and the color code (b) values range between 14.14 and 26.96 (Table A.6 in Appendix A).

5.2 Basic Physical and Physicomechanical Properties of the Samples

As basic physical and physicomechanical properties; bulk density, effective porosity, water absorption capacity, ultrasonic pulse velocity measurement and hardness of construction materials of the Ankara Roman (Caracalla) Bath samples (stones, stone tesserae, and bricks) were determined. Results are given in Table A.7-A.8 in Appendix A.

5.2.1 Bulk Density, Effective Porosity, Water Absorption Capacity Tests of the Samples

Stone Samples: Examining the results of the bulk density, porosity, and water absorption capacity of stone samples, the durability of the stone types can be predicted. While the wet bulk densities of stone samples of the Roman Bath are ranging between 2.41 and 2.73 g/cm³, the dry bulk densities of stone samples of the Roman Bath are between 2.23 and 2.72 g/cm³. As the total water absorption capacities of the stone samples vary between 0.16 and 4.24%, the total porosities of the stone samples are between 0.43 and 9.93% (Table A.7 in Appendix A).

Wet bulk densities of andesite samples which are the most commonly used material types in the field vary from 2.41 to 2.71 g/cm³ (av. 2.55%) and dry bulk densities of andesite samples vary from 2.23 to 2.68 g/cm³ (av. 2.38 g/cm³). The total water absorption capacities of the andesite stone samples change between 0.38 and 4.24% (av. 2.94%) and the total porosities of the andesite samples change between 1.03 and 9.67% (av. 6.83%) (Table A.7 in Appendix A). When the average dry bulk density value of the andesite stone samples (av. 2.55 g/cm³) is also compared with the average value of the andesite stones obtained by Kadıoğlu's study (av. 2.61 g/cm³) (Table A.9 in Appendix) (Kadıoğlu, 2001), it is seen that the andesite stone samples have low durability. The wet density, dry density, total absorption capacity and porosity of the sandstone sample are 2.48 g/cm³, 2.25 g/ cm³, 4.14% and 9.32% respectively (Table A.7 in Appendix A). The dry bulk density value of the sandstone sample (2.25 g/ cm³) is compared with the average value of the sandstones obtained by the study of Kadıoğlu (2.35 g/cm³) (Table A.9 in Appendix) (Kadıoğlu, 2001), so it is verified that the sandstone sample has low durability.

While wet bulk densities of limestone samples vary from 2.69 to 2.72 g/cm³ (av. 2.70 g/cm³) the dry bulk densities of the limestone samples are between 2.58 to 2.70 g/cm³ (av. 2.64 g/cm³). The total water absorption capacities of the limestone stone samples change between 0.26 and 1.48% (av. 0.87%) and the total porosities of the limestone samples change between 0.71 and 3.83% (av. 2.27%). The average dry bulk density value of limestone (2.64 g/cm³) is compared with the average value of the same type stone (2.55 g/cm³) obtained by Kadıoğlu's study (Table A.9 in Appendix) (Kadıoğlu, 2001) and it is seen that limestone is very durable.

Besides, as the wet and dry bulk densities of marble sample (ARB-S7) are 2.73 g/cm³ and 2.72 g/cm³, the water absorption capacity and porosity of the marble sample are 0.16% and 0.43% (Table A.7 in Appendix). In the same way, the dry bulk density value of the marble (2.72 g/cm³) is compared with the value of the marble (2.71 g/cm³) is obtained from the marble density table (Marble Density Aqua-Cal, n.d.), it is revealed that the marble is moderate strength.

Lastly, the wet bulk density, dry bulk density, water absorption capacity and porosity of the vitrifying tuff sample are 2.61 g/cm³, 2.35 g/cm³, 4.22%, and 9.93% respectively. The average dry bulk density value of the tuff (2.35 g/cm³) is compared with the dry bulk density values of the tuff stones (2.36-2.57 g/cm³) taken from the study of Dobson and Nakagawa (2005). It can be shown that vitrify tuff has low durability. However, radiolarite rock samples which have 2.69 g/cm³ wet bulk density, 2.63 g/cm³ dry bulk density, 0.90% water absorption capacity and 2.35% porosity average values are highly durable material. It is revealed that their average dry bulk density result (2.63 g/cm³) is compared with the average result of the same type stone (2.52 g/cm³) obtained by Kadıoğlu's study (Table A.9 in Appendix) (Kadıoğlu, 2001).

Brick Samples: While the wet bulk densities of the brick, *pilae* and pipe samples belonging to the Roman Bath are between 1.83-2.59 g/cm³, 2.04-2.33 g/cm³ and 2.50- 2.58 g/cm³, the dry bulk densities of the brick, *pilae* and pipe samples are between 1.39-1.72 g/cm³, 1.31-1.57 g/cm³ and 1.68 and 1.77 g/cm³. Besides, the total water absorption capacities of the brick, *pilae* and pipe samples vary between 6.25-33.10%, 18.23-30.15%, and 16.45-20.91% and total porosity values of them vary between 10.28-45.97%, 27.07-40.53% and, 29.15-35.05% respectively (Table A.8 in Appendix A).

The results of the brick indicated that ARB-B10 sample has different physical properties in terms of wet, dry bulk density, water absorption capacity and porosity results from the other samples. Especially, the dry bulk density result (2.07 g/cm³) of the sample is very high when compared with the results of the other bricks. Therefore, it is thought that the ARB-B10 sample is a repairing brick, used in restoration work in 1990 (Table A.8 in Appendix A).

According to Özışık (2000), the samples have low strength if their dry bulk density value is below 1.80 g/cm³ and their porosity value is above 30%. The results show that the average values of dry bulk density of brick, *pilae*, and pipe are 1.55 g/cm³, 145 g/cm³, and 1.72 g/cm³ and the average porosity values of them are 31.08%, 34.80%, and 32.10% respectively (Table A.8 in Appendix A). Therefore, all brick samples have low strength.

The similar study was applied on the Roman bricks used in Serapis Temple in the city of Pergamon (Aslan, Böke, 2009) and the similar physical results were obtained. The bricks have low density (1.65 g/cm³) and high porosity (35%), so they are of low strength. In the same way, the Roman bricks, from the ruins of Red Courtyard (Serapeum) monumental temple of in Pergamon and from several different buildings in ancient cities of Aigai and Nysa were examined by Sağın (2017). The similar physical results -low density and high porosity- were also obtained from these bricks. Finally, when all these results are interpreted together, it is possible to say that the brick materials are likely to be exposed to some environmental deterioration factors.

5.2.2 Ultrasonic Pulse Velocity Tests of the Samples

Ultrasonic pulse velocity measurements on the stone samples vary from 37 (µs) to 42.41 (µs). While the results of andesite stones change between 36.30 (µs) and 42.40 (µs), the ARB-S9 andesite sample which is from the northwest wall of the *caldarium* (C-15) has the lowest (36.30 µs) competency. The result is in parallel with its highly porous structure (Figure A.3 in Appendix A) so it can be interpreted that the sample has weak resistance. On the other hand, the limestone, sandstone and marble samples have similar ultrasonic pulse velocity values (Table A.10 in Appendix A).

5.2.3 Hardness Test (Schmidt Hammer) of the Samples

Hardness test was applied on only two stones because of the limited amount of the samples. The result values were used to predict the uniaxial compressive strength of the rock samples (Table A.11 in Appendix A). The average rebound (strength) numbers of ARB-S12 and ARB-S13 are 31.4 and 30.2 respectively. When these results were evaluated in the study of Luke and Snell (2012), it can be seen that the ARB-S12 and ARB-S13 stones are in the lightweight group. Therefore, ARB-S12 is

tuff and ARB-S13 is an andesite type. Besides, the data was supported by the other analysis as XRF, thin section analysis.

5.3 Compositional, Mineralogical and Chemical Properties of the Samples

Compositional, mineralogical, and chemical properties of the samples of Roman Bath in Ankara were investigated in detail in order to determine their material characteristics, sources (provenance), techniques and decay processes. The analyses which were applied on the samples are acidic aggregate/binder analysis, sieve (granulometric) analysis, gravimetric analysis, quantitative analyses of soluble salts, petrographic thin section, confocal Raman, SEM-EDX, and XRF analyses.

5.3.1 Determination Binder/Aggregate Ratio of the Samples

Binder/aggregate ratio of the mortar and plaster samples were measured with acidic aggregate/binder analysis so the ratio of the binder (calcium carbonate) and aggregate (silicates and silicon dioxide) components in the samples were determined. The results of the study were used to the complementary results of thin section analysis.

Mortar and plaster samples of the Roman Bath were treated with acid. After the analysis, the aggregates not containing carbonate were evaluated in order to determine the total aggregate/binding ratios (TA% & TB%) (Table A.12 and Figure A.11 in Appendix A). While the binder and aggregate ratio of the mortar samples are between 4.33-96.36% (av. 27.01%) and 3.64-95.67% (av. 72.99%), the binder and aggregate ratio of the plasters are between 8.63-42.88% (av. 25.75%) and 57.12-91.37% (av. 74.25%). (Table A.12 in Appendix A). These results show that the aggregates in the mortars and plasters are composed of coarse or very coarse sand. On the other hand, the binder/aggregate ratios of the original mortar and plaster samples of the Bath are quite close to the traditional 2:1 (aggregate:binder) ratio proposed by Vitruvius (1914, 1990) and Torraco (1988).

5.3.2 Determination of Particle Size Distribution of Aggregate of the Samples

Particle size and distribution of aggregates was determined by the sieve analysis (TS EN 933-1/2012). The aim of the analysis is to identify the percentage of the size and

amount of all particles in the mortar and plaster samples.

According to the results, the particle size distribution of aggregates of the mortar and plaster samples consists of the mixed aggregate of small, medium and coarse sand; and all of them are distributed homogeneously. Especially, the mortar and plaster samples have coarse or very coarse sand aggregates (>1000 µm; mortar av. 49.73% and plaster av. 35.03%) (Wentwort, 1922) (Table A.13 and Figure A.12 in Appendix A). In addition, in all aggregates, the amounts of angular coarse aggregates are more dominant than the rounded ones from the bank of the river and almost all of the aggregates in all original samples have the brick fragments (Figure A.13 in Appendix A). According to Stefanidou et al. (2014) the angular particles were used in the aggregates to provide a strong bond with the binder. Because these particles have high surfaces, they create large contact zones between the aggregate and binder. Therefore, it is considered that large amounts of the angular aggregates were used in mortar and plaster of the Bath.

5.3.3 Gravimetric Analysis (Loss on Ignition–LOI) of the Samples

Based on this analysis, water, organic carbon, and carbonate contents of the mortar and plaster samples are determined. The results of gravimetric analysis support the results of acidic aggregate and binder analysis.

The water contents (at 105ºC) of the different groups of the mortar and plaster samples vary from 0.16% to 0.73% and from 0.21% to 2.53% respectively. The organic carbon contents (at 450ºC) of the mortar and plaster samples vary from 1.47% to 6.21% and from 3.54% to 9.61% respectively. The carbonate contents (at 950ºC) of these samples vary from 11.29-40.88% for mortars and 33.18-48.22% for plasters. The results show that plasters have higher organic content than the mortars (Table A.14 in Appendix A).

5.3.4 Quantitative Analyses of Soluble Salts of the Samples

Quantitative analyses were applied on the samples to determine the amount of total soluble salt (conductivity measurements) and salt types (spot test for anions).

5.3.4.1 Conductivity Measurements (Calculation of Total Soluble Salts) of the Samples

The total soluble salt content of the samples was measured by conductometric analysis. This analysis was applied on the stone, stone tessera, brick, *pilae*, and pipe samples.

According to the test results, the salt content of the stone samples and stone tessera are ranging from 0.38 to 2.39% and 0.47 to 0.67% respectively. While the total salt content of the brick samples is between 0.40 and 3.67% (Av. 1.56%), the total salt content of the *pilae* samples is between 0.58 and 1.43% (Av. 1.02%). Lastly, the total soluble salt content of pipe samples is ranging from 1.49-2.45%. The average salt content of the stone samples is 1.11% except for tessera stone samples. The general average of all types of bricks is 1.35% except for the ARB-B10 repair brick (Table A.15 in Appendix A).

According to Dursun et al. (2008), if the amount of the salt in the soil is greater than 0.15%, it shows higher salinity. Therefore, salination is quite high in all samples as stone, stone tessera, brick, *pilae*, and, pipe. In the samples, the main sources of salinization are environmental impacts as climatic and atmospheric effects and salts of cement-based repair mortars.

Climatic and atmospheric effects especially cause high salinity for the stone samples taken from different places of the Roman Bath. As the long-term (between 1927-2017) meteorological data obtained from the bath sampling is evaluated, it is seen that the average rainfall amount was 11.5, the average temperature of the city center in the same month was 23.4°C, and the daily sunshine duration was 10.8 hours (Table A.16 in Appendix A) (MGM, n.d.). Particularly in rainy years, crystal salts in the pore space of stones undergo dissolution (Bland, Rolls, 1998). In the process, while the salts parts of the stone shrink because the salts in the pore of stone absorb water, the other salt-free parts of the stone expand (Al-Naddaf, 2009). Thus, due to different movement of the different parts of the stone, the deteriorations and dissolutions of the stone start from the inside to outside. Thus, as Torraco (1988) mentioned, it is observed that the structure of the stone is attenuated due to repeated wetting and drying cycles over the years. In the same way, the chemical effects of the salts caused the dissolution of some constituents of the stone (Magee et al., 1988) by

thermal expansion process with temperature fluctuation (Al-Naddaf, 2009). In the process, dissolved salts in the pore of the stone are recrystallized in the hot weather so it caused the internal pressure in the stone. Therefore, the most destructive effects (up to the loss of parts) were seen on the samples of the Bath at the beginning of the summer months (from June) (Table A.16 in Appendix A).

The other deterioration problems on the stone samples are caused by biological factors as plants, molds, algae, lichens (Feilden, 1981). Especially, water and moisture in the soils are the most critical components for biological weathering process. Therefore, the biological formations can often be seen on the stone blocks which are directly connected to the soil (Pidwirny, 2006)

When all samples of the Roman Bath are taken into consideration, the brick, *pilae*, and pipe samples have more damaging effects in their structure due to their higher porosity properties (Table A.15 in Appendix A). Similarly, in the rock types of the stones, andesites have more salting and deterioration problems in their structure because of their highly porous character (>6.5%) (Table A.7 in Appendix A). Besides, visual observations in the field and laboratory show that biological deteriorations have an important effect on all samples. Particularly, lichen formation can frequently be seen on the surface of the materials at the foundation part of the Bath.

5.3.4.2 Spot Test for Anions of the Samples

The standard (Merck) spot salt tests (such as nitrite, nitrate, phosphate, sulphate, and carbonate) were applied on the stone and brick samples of the Bath. The results of the tests were given in Table A.17a-17b in Appendix A.

pH Distribution in the Samples: The pH values of stone and stone tessera samples vary between 7.12-8.40 (av. 7.93) regardless of rock type. The pH values of brick, *pilae* and pipe samples vary between 6.73-8.35 (av. 7.75), 7.46-8.14 (av. 7.96), and 8.36-8.37 (av. 8.37) respectively. The general average pH of all is 7.88. Nearly all samples have weak basic properties (pH≥7) (except ARB-B19) (Table A.17a, A.17b in Appendix A).

Sulphate Test (SO_4^{2-}): The test was applied to determine the gypsum-containing binders or the black layer formation on the rocks, due to air pollution caused by

exhaust or flue gas (Borrelli, 1999). Besides, sulphate salts come from the dissolving of cement containing repair mortars. In the majority of the samples, there is a low amount (20, 40 mg/L) of sulphation (Table A.17a, A.17b in Appendix A).

Phosphate Test (PO_4^{3-}): This test was used to determine the effects of agricultural activities (phosphate fertilization), animal (fecal) or vegetal residues, sewage or household waste. In addition, the phosphate salts can be seen in the rock structures or organic additives in (plant-straw) the mortars or plasters depending on high moisture content (Borrelli, 1999). Thus, the samples at the southern part of the Bath have a low amount of the phosphate salts due to the low moisture content (Table A.17a, A.17b in Appendix A).

Carbonate Test (CO_3^{2-}): This test is used to identify lime-containing binder species in mortar and plaster as well as carbonate-content in stones (marble, travertine, limestone, etc.) (Borrelli, 1999). The results indicated that the samples have average and high values of carbonate, but especially brick samples contain higher carbanote content (Table A.17a in Appendix A).

Finally, stone, stone tessera and brick samples belonging to the Roman Bath were evaluated in terms of types of the water-soluble salts. It can be seen that all of them contain carbonate, phosphate, and sulphate type salts and they are weak basic properties (pH$\geq$7).

5.3.5 Petrographic Examination of Thin Section of the Samples

Petrographic examinations were carried out to identify microstructure and mineral phases (textural distribution of the grains, shape of the grains, types of rock fragments and other minerals etc.), source (provenance) and technology of the raw materials of all Bath's samples. In the analysis, the different layers of the sample chips were viewed under optical polarized microscopy and results were given below.

Stone Samples: As a result of the thin section optical microscope analysis, the stones were classified into five rock groups; andesite, limestone (biosparitic, dolomitic and meta) sandstone, marble and vitrify tuff (Table A.18 and Figure A.14 in Appendix). The original stones in the Bath (andesite, sandstone, and limestone) are used as a block or rubble filling material. The building block stones in the Bath are mostly andesite. The different deterioration stages are seen in some of these

andesite blocks. Besides, the provenances of all the stone types were identified in the scope of geological studies. The results show that the provenance of andesite, limestone, sandstone, vitrify tuff and marble samples are from Hüseyingazi Kale, Haymana, Memluk Yuva Village, Afyon Quarry (antique marble quarry), respectively (Kadıoğlu, et al., 2018) (Figure 5.1).
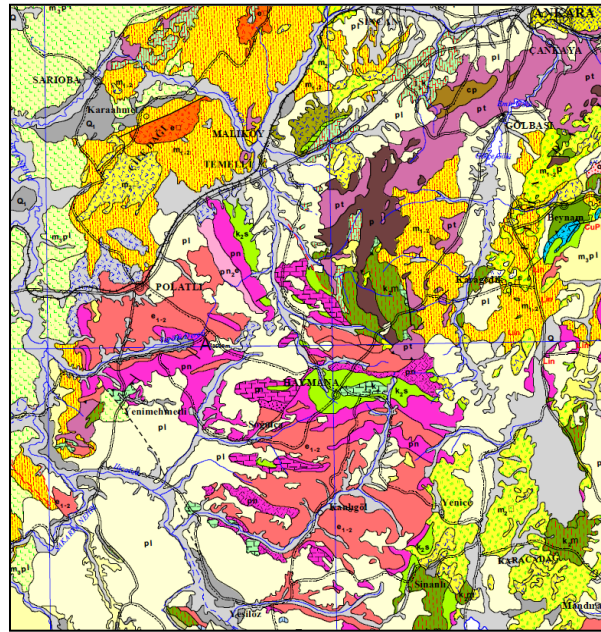
Figure 5.1 Geological map of nearby region of Ankara (MTA, 2002)
The more detailed geological map in Figure A.27a-A.27b in Appendix A

Stone Tessera Samples: The stone tesserae and related upper tessera mortar layers (setting bed and tesellatum) sampled from the mosaics in the *piscina* (pool) of the Bath were examined by thin section analysis. The sampled tesserae are in the radiolarite rock group (Table A.19 and Figure A.15 in Appendix A) and the provenance of them is from Elmadağ, Irmak Village Formation near Ankara (Figure 5.1). In addition, ancient mosaic consists of mainly four different layers: rudus, nucleus, setting bed, and tesellatum respectively. In the microphotographs of stone tesserae, the rudus mortar, which is collected from the pool in the Bath, is not obvious; on the other hand, the mosaic section is clearly distinguished from the nucleus and setting bed layers (Figure 5.2).
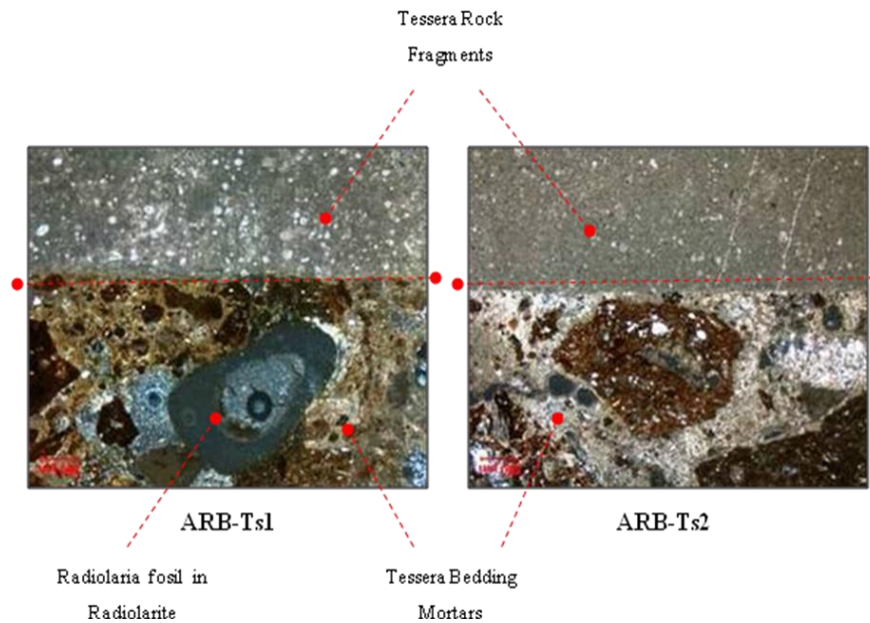
Figure 5.2 Thin section microphotographs of ARB-Ts1- Ts2 samples

Brick Samples: All of the original brick samples (brick, *pilae* and pipe samples) were studied petrographically except ARB-B10 which is the repair sample from the recent restoration work in the 1990's (Table A.20 and Figure A.16 in Appendix A). All bricks were divided into three subgroups in terms of their functions; brick (structural), *pilae* and pipe (Figure 5.3). When all bricks were examined together in terms of their matrix, aggregate structure, aggregate type, and their distribution in the matrix, mineral phase, porosity, and firing properties, all bricks are 8 groups. On the other hand, as the samples were examined separately in terms of petrographic structures, the bricks (structural), *pilae*, and pipes are 6 groups, 5 groups, and 2 groups respectively (Table A.20 in Appendix A).

Brick/*pilae*/pipe samples in porous construction (5-12% of the matrix) were fired at about 900°C. They are rich in mineral and rock type content (7-42% of the matrix). The rock aggregates of the brick groups are andesite, granite, andesite/basalt and metagrovac (Table A.20 in Appendix A). The provenance of the rock aggregates in the brick groups is as the following. Andesite originated brick groups (5 groups out of 8) are from the locality Hüseyingazi-Kale, granite originated brick group (Brick Gr5) is from Bala-Köprüköy, and metagrovac originated brick group (Brick Gr7) is from the local formation of south part of Ankara (round shaped particles originating

from the of river banks).

The clay type of the bricks is mainly illite and smectite from local sources of Ankara. The clay sources of the brick groups are as follows. Brick Gr1, Brick Gr2, Brick Gr4, and Brick Gr7 are from METU Forest or/and Cevizlidere District. The clay sources of Brick Gr3, Brick Gr5, and Brick Gr6 are from Yenidoğan region. The clay source of Brick Gr8 is from Tandoğan (Figure 5.1).

Figure 5.3 Brick, *pilae* and pipe at Roman Bath in Ankara

In addition, the brick fragments, which were found in the majority of the aggregate structure of the brick samples except for Brick Gr4 and Brick Gr5, are ranging from 1% to 2.5% of the total aggregate (Table A.20 and Figure A.16 in Appendix A). The additions of brick fragments in the bricks during the production process have some technological advances such as decreasing fire loss and water absorption % values and increasing firing shrinkage and compressive strength (Emrullahoğlu et al., 2004). In this way, the brick fragments contribute to the Bath's brick production technology. In the structural brick samples, the amount of clay in the matrix is larger and the grain size is fine. On the other hand, in the *pilae*, the silt-sized particles in the matrix are coarser and irregular and the matrix is more porous. The distribution of aggregates in the matrix of the structural brick is more homogeneous than the brick of *pilae*. According to these results, it is assumed that the structural bricks were produced in a higher quality compared to the *pilae*. In addition, the formation of secondary minerals and amorphous silicates and decay/deformation zone around grains (chilled margin) can be seen inside and around the pore of the matrix of the bricks of the *pilae* because of the direct effect of hot water vapor (hydro-temperature pressure) (Figure 5.4) and there are dissolutions and recrystallizations in the fissures at the matrix. These effects can not be seen in the pipes because they convey the cold

water. Besides, there are oriented aggregates in the matrix of the pipe samples due to ceramic production by turning machine (Figure A.16 in Appendix A).
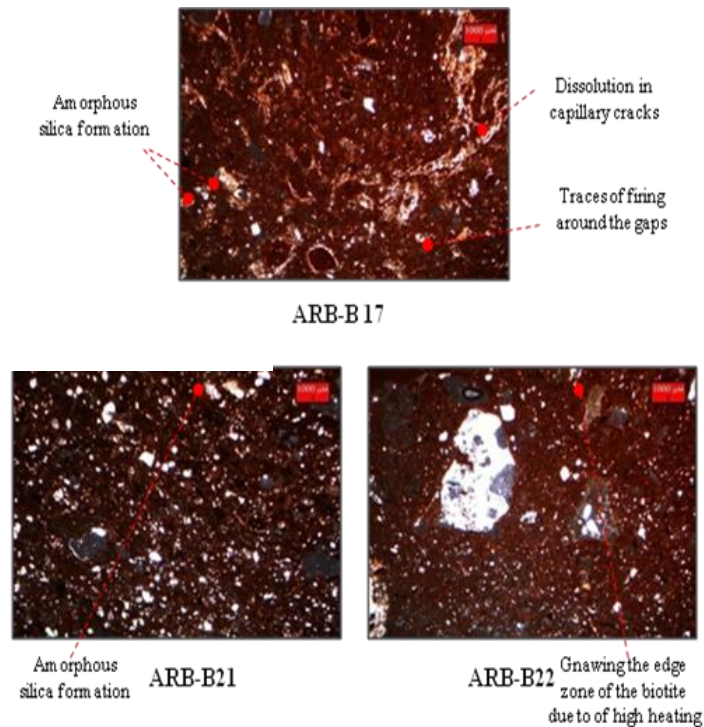
Figure 5.4 Hot water vapor effect on *pilae* type bricks (ARB-B17, ARB-B21, and ARB-B22)

Mortar and Plaster Samples: The mortar and plaster samples used in functions such as jointing, rubble filling, and decoration were examined petrographically.

While the mortar samples are classified into 8 groups, the plaster samples are into 2 groups. 3 mortar groups out of 8 (Mortar Gr1, Mortar Gr3, and Mortar Gr6) and one of the plasters (Plaster Gr1) are repairing (Table A.21 in Appendix A). The total aggregate content of the mortar and plaster groups varies between 25-45%. The binder structure of the mortars comprises of lime (structural or originals), lime/cement (in repair) and lime/clay/cement (in repair) binders (Table A.21 in Appendix A). Samples with cement-containing binders belong to the near-term repairs. Although all mortar samples contain lime type binder, some of them have the brick fragment which is around 5-15% of total aggregate (Table A.21 and Figure A.17 in Appendix) (Figure 5.5). On the contrary, all plaster samples contain lime

type binder, and brick fragments (about 10% and 15% of total aggregate) (Table A.21 and Figure A.18 in Appendix). It is known that brick-lime mortar and plasters have been used in the cisterns, aqueducts, and bridges even from ancient times because of their waterproof properties. According to Uğurlu, Böke (2009) and Böke et al. (2006), brick-lime mortars and plasters used in the hot and humid condition of the Ottoman Bath have hydraulic characters due to porous structure and brick fragments in their content. The brick fragments have good pozzolanicity because they contain high amount of calcium and the poor clay mineral in their raw materials and fired low temperature. Stefanidou et al. (2014) conducted a similar study on the hydraulic mortars of the ancient cisterns and baths in Greece. According to the study results, the structural mortars and plasters of ancient cistern and baths have good durability and cohesion properties because the hydrated lime connected with brick dust or natural puzzolans by forming the micro-crystalline matrix. On the other hand, the porous structure of mortars provided the area forming of the secondary crystallization of calcite. The crystallization created a more compact structure between the lime and brick fragments. In this context, lime and brick fragments in all plasters have good pozzolanicity and waterproof properties.

According to thin section observations, the *pilae* joint mortars (representative sample ARB-M22) (Figure 5.6) were prepared in a high quality when compared with those used in bath structural walls. The matrix of *pilae* consists of highly durable igneous volcanic particles (quartz, granite, basalt) and brick particles. These particles are distributed homogeneously as well as less than 1 mm in size. The shape of the particles is angular and round together in the matrix apart from structural mortars. In general, the dissolution is seen in the matrix because of the effect of hot vapor. Depending on all these results, the *pilae* mortar samples are most probably manufactured in the similar technology and in the same workshop.

Caldarium mortars (representative sample ARB-M40) (Figure 5.7) are more compact structure. The mortars include a variety of minerals and rock fragments like claystone, chert, sandstone, limestone etc. While the grains in the matrix of these mortars have rounded shape (nearby river banks), the grain size is coarser (>3 mm). *Tepidarium* mortars (representative samples ARB-M21 and ARB-M30) (Figure 5.6-Figure 5.7) composed of variously sized and shaped particles besides brick fragments

distributed heterogeneously in the matrix. These results indicated that the mortars were produced casually. Therefore, in the mortar sets, the structural mortars in *tepidarium* have low quality compared with the structural mortars in *caldarium.*
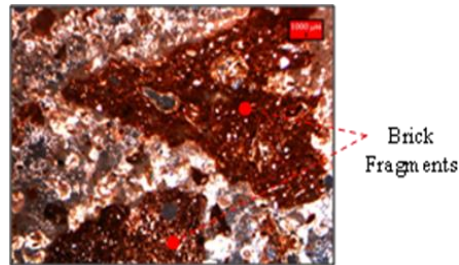
Figure 5.5 Coarse angular brick fragments in mortar sample (ARB-M5) in thin section microphotograph
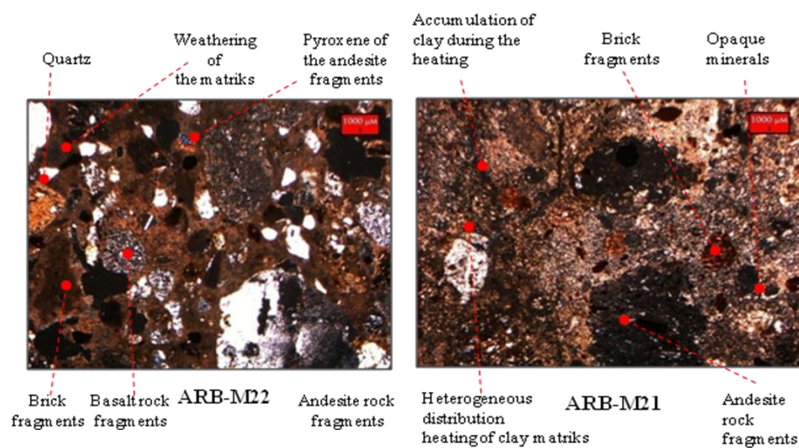
Figure 5.6 Comparison of *pilae* mortar (ARB-M22) and structural mortar (ARB-M21) in terms of production technology in thin section microphotographs
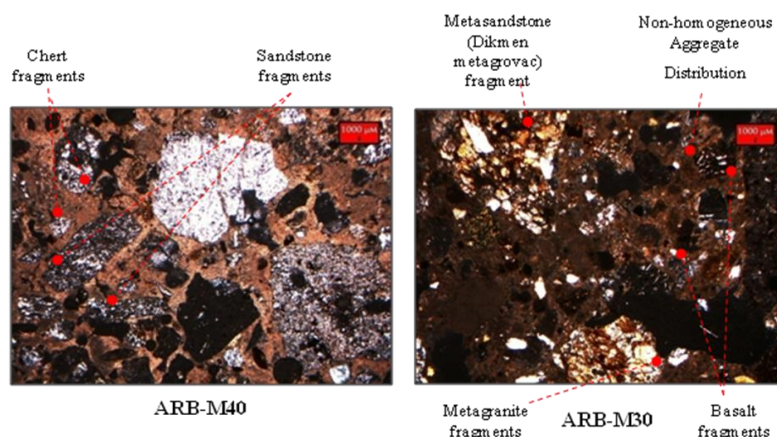
Figure 5.7 Comparison of structural *caldarium* mortar (ARB-M40) and structural *tepidarium* mortar (ARB-M30) in terms of construction technology in thin section microphotographs

5.3.6 Raman Confocal Spectroscopic Analysis of the Samples

Raman spectroscopy, which is used to determine the natural bond composition of the material, has nondestructive features during the analyses. In this study, Raman Analysis identified the mineral composition of the brick and their chemical bonding during the firing processes. Carbonate contents of the materials affect the migration of the CO_2 during the firing processes:

$$CaCO_3 \text{ (s)} \rightarrow CaO \text{ (s)} + CO_2 \text{ (g)}$$

Raman Spectroscopy is the best method for detecting the results of this process. A new chemical bonding can also be appearing during the firing processes of the brick production. It can be seen that the presence of iron-rich clay minerals of high temperature (above 900 ℃) may indicate the neoformation of minerals in the entire matrix and may also indicate that the production of ceramic or brick is at a high temperature. These spectra may reform a new formation of the minerals during the firing above 900℃ (Figure A.19 and A.20 in Appendix A).

Carbonate within the bricks may indicate that the production of these bricks is carried out in low firing temperature (<850℃) (Figure A.19 and A.20 in Appendix A). The Raman spectroscopy also shows that the bricks, which are produced at low firing temperature, have calcite and carbonate-bearing matrix (Edwards, 2005). Furthermore, based on Raman analysis, the main mineral compositions of the bricks in the Bath are biotite and hematite (Figure A.16 in Appendix A).

5.3.7 Scanning Electron Microscopy Coupled with Energy Dispersive X-Ray Analyser (SEM-EDX) of the Samples

Three samples (ARB-S6, ARB-B7, and ARB-Z1) were subjected to elemental analysis, particularly in terms of their black-colored pollution layers. According to the results, the presence of carbon and oxygen mass weights in ARB-S6 and ARB-B7 samples implies a form of organic pollution and a form of pollution that is related with the salt formation (such as aluminum silicate). In the case of ARB-Z1, the formation of salt is associated with both the presence of calcium and the environmental conditions (Table A.22 and Figure A.21 in Appendix). These analyses were performed with SEM-EDX, but different analytical methods were suggested to support the results.

5.3.8 X-Ray Fluorescence Analysis (PED-XRF) of the Samples

Chemical compositions of original and repair samples (stone, brick, mortar, plaster and calcareous layer) of the Bath were obtained by XRF analysis. Especially, trace element compositions are important in order to determine the raw material sources of the samples (Table A.23 - A.26 and Figure A.22 - A.26 in Appendix A).

These analyses show that the stone samples belonging to different rock groups (sedimentary, metamorphic and volcanic) reflect the chemical properties of those groups.

The andesite samples have a similar ratio of the content of their rock sources as SiO_2 (av. 62.91%) and Al_2O_3 (av. 12.03%) (Table A.23 in Appendix A). While the average value of CaO which is the basic oxide composition of the limestone, is 59.99%, CaO value of the marble sample (ARB-S10) is 59.19%. As the average value of carbonate (LOI: Loss on Ignition), which is another basic oxide composition of the limestone, is 37.80%, the carbonate (LOI: Loss on Ignition) value of the marble sample is 39.43% (Table A.23 in Appendix A). On the other hand, the basic oxide compositions of the tuff (ARB-S12) are SiO_2 (av. 62.08%) and Al_2O_3 (av. 12.27%), the basic oxide compositions of the sandstone (ARB-S8) are SiO_2 (av. 57.16%) and Al_2O_3 (av. 11.04%) (Table A.23 in Appendix A). When the basic oxide composition results of the XRF analysis is considered in terms of the andesite and the limestone samples, it can be seen that the andesite is in three groups and the limestone is in one group at triangle plotting (Figure A.22 in Appendix A). With XRF analysis, the trace element compositions of all types of stones were determined in ppm. Identified trace elements can be seen in (Table A.23 in Appendix A). The results supported their chemical rock group constitutions.

When the brick samples belonging to different parts of the bath were examined separately as original brick, *pilae*, and pipe, it was found that their basic oxide compositions are SiO_2, Al_2O_3, Fe_2O_3, K_2O, CaO, MgO LOI. While the basic oxide compositions of soil sources are SiO_2, Al_2O_3, Fe_2O_3, K_2O, MgO in all brick types studied separately in triangle plotting, it could be seen that they are in a similar group. Also, when the soil sources in all bricks studied together in triangle plotting; the similar results are also seen in one group. Besides, the trace element compositions of soil sources of all types of bricks (brick, *pilae*, and pipe) were

determined in ppm. Thus, the identified trace element results have similar values according to their types (Table A.24a, A.24b, and A.24c in Appendix A). Particularly trace element compositions give information about the raw material resources in which the bricks are produced (Mommsen, 2001) because the trace elements and the amounts cannot be changed during the firing process. Therefore, the trace elements in the raw material source and the bricks are the same (Finlay et. al, 2012).

Both the basic oxide compositions and trace elements results of the soil sources of all types of original bricks (brick, *pilae*, and pipe) in the Bath have similar chemical composition values, and the results are supported by triangle plotting results (Figure A.23 in Appendix A). Therefore, it was interpreted that all types of bricks were produced from the same raw material sources in the same workshops and on the same date. However, the sample of repair ARB-B10 clearly is differentiated from their original samples due to lower SiO_2 and CaO and higher Al_2O_3 and LOI contents, respectively (Table A.24a in Appendix A).

The similar XRF study was conducted on Roman bricks from Red Courtyard (Serapeum) in Pergamon and several different buildings from ancient cities of Aigai and Nysa. The results indicated that the bricks were composed of SiO_2, Al_2O_3, CaO, Fe_2O_3, MgO, and Na_2O. Especially, CaO shows that the bricks were produced using calcium-rich clay sources (Sağın, 2017). It is known that the carbonate sources have positive structural changes in brick production at low temperatures (X<900°C) (Elert et al, 2003). Carbonates reduce shrinkage during the firing process, provide higher vitrification and increase the pressure resistance of the bricks (Tite, Maniatis, 1975). In this context, using calcium-rich clay as a raw material for brick production in the low-temperature brick kiln was a conscious choice in the Roman period (Sağın, 2017). Therefore, the brick, *pilae*, and pipe of the Bath were produced in this way to take advantage of the carbonates.

The chemical composition data of the mortar sample from the XRF analysis show that the chemical content of the mortars is composed of SiO_2, Al_2O_3, Fe_2O_3, MgO, and K_2O oxide compositions. The main elements of the mortar are Si and Ca with as $SiO_2\%$, CaO% and LOI% values which are av. 28.90%, av. 28.74%, and av. 31.18% respectively. The other elements in these samples are Al, Fe, Mg and K with as an average of $Al_2O_3\%$, $Fe_2O_3\%$, $K_2O\%$ and MgO% values which are 5.11%, 2.66%,

1.24%, and 1.01% respectively (Table A.26 in Appendix A). When the oxide compositions result of mortars from different functions and sections of the Bath are analyzed separately, it can be seen that the soil/clay raw material source of the original joint mortars (SiO_2, Al_2O_3, Fe_2O_3, MgO and K_2O) used between the bricks of *pilae* was in a single group at triangle plotting (Figure A.25 in Appendix A). While the XRF analysis results of the mortars taken from different points in the *caldarium* were examined in triangle plotting, it was seen that they were in three groups, the XRF analysis results of the mortars taken from different points in the *tepidarium* show that they are in two groups at triangle plotting. Besides, the XRF analysis results of the mortars taken from different points of water tank indicated that they are grouped into three (Table A.26 and Figure A.25, A.26 in Appendix A). According to Oğuz et al. (2014), the mortars of Roman Era Bath in Myra consist of calcite and quartz minerals. While calcite minerals show that the binder material is lime, the existence of quartz minerals shows that aggregates consist mainly of silicon (SiO_2). In the same way, the original mortars of the Roman Bath in Ankara is mostly composed of lime binder (CaO) and silicon (SiO_2) aggregates (Table A.26 in Appendix A). However, the repair mortar sample ARB-M11 is clearly marked by the XRF Analysis. While CaO 19.58% and LOI 20.47% ratios are very low, SiO_2 43.51%, Al_2O_3 6.08%, and MgO 4.61% ratios are very high in these samples. The reason is that, the repairing sample has high cement and coarse aggregate ratios (Table A26 in Appendix A).

Similar to original mortar samples, the basic oxide compositions of original plaster samples (ARB-P2a, ARB-P2b, and ARB-P3) are SiO_2 (av. 21.76%), CaO (av. 24.09%) and LOI (av. 32.92%). The other oxide compositions in the plasters are Al_2O_3 (av. 5.11%), Fe_2O_3 (av. 2.66%), K_2O (av. 2.69%) and MgO (av. 1.44%) respectively. All oxide composition results of the raw material source of soil/clay in plasters (SiO_2, Al_2O_3, Fe_2O_3, MgO and K_2O) are similar and in one group at triangle plotting. In the same way, the trace element results of all original plasters are similar too (Table A.25 and Figure A.24 in Appendix A). Finally, all original plaster samples of the Roman Bath in Ankara have similar chemical compositions and are prepared with the same raw material sources.

5.3.9 Cementation Index Data of the Samples

The relationship between the aggregate and its competency properties of the mortar and plaster samples were assessed with the help of Cementation Index Data which is obtained with chemical composition properties of the mortars and plasters (Boynton, 1980). Cementation Index (CI) is the ratio of the part dissolved in acids to the part dissolved in bases. The mortars containing lime are divided as fat mortar (FL) and hydraulic mortar (WHL, MHL, and EHL). Among the mortars, the ones that have less than 5% aggregate content are the fat mortars with the high lime ratio, in other words, high CaO ratio. Among the mortars, the ones having an aggregate ratio higher than 5% have hydraulicity with low CaO ratio. In the composition of this type of mortars, silicon dioxide (SiO_2), calcium oxide (CaO), aluminum oxide (Al_2O_3) and iron oxide (Fe_2O_3) ratios are high (Lawrence, 2006).

The CI values of the mortar samples from the Roman Bath vary from 0.14-6.55 (av. 3.36). The CI values of the plaster samples from the Roman Bath vary between 1.88-2.69 (av. 2.51). These results indicate that the lime types of these samples are in cement or natural cement (C /NC) category which is highly stable. Therefore, because of their high CI data values, the mortar and plaster samples have high stability (Table A.27, A.28 in Appendix A).

5.4 Overall Results of the Tests and Analyses

In this thesis, the materials from the Archaeological area of Roman Bath in Ankara have been examined. Total 97 samples -13 stones, 3 stone tesserae, 29 bricks, 47 mortars, 4 plasters, and a calcerous layer- were collected from different parts of the Bath. Samples were examined to identify their raw material characteristics, provenance (source), production technologies; decay processes, durability and compatibility properties. The analyses and the tests applied on the materials are basic physical and physicomechanical tests (bulk density, effective porosity, water absorption capacity, ultrasonic pulse velocity and hardness tests), compositional, mineralogical, and chemical analyses (acidic aggregate/binder and sieve or granulometric analyses, gravimetric analysis, soluble salt test and analysis – spot salt test and conductometric analysis - petrographical thin section optical microscopy, Confocal Raman, SEM-EDX and XRF, analyses).

Stone and Stone Tessera Samples

It was found that the bulk density, porosity and water absorption capacity of the stone samples are changing according to their stone types (Table A.7 in Appendix A). All stone types results are compared with the similar stone types which were taken from previous studies (Table A.9 in Appendix A) (Kadıoğlu, 2001; Dobson, Nakagawa, 2005; Marble Density Aqua-Cal, n.d.). It can be seen that the andesite, sandstone and, tuff have low durability, but the marble sample has moderate strength. On the other hand, the durability of the limestone samples is high, similar to those of the radiolarite samples. In addition, the ultrasonic pulse velocity results show that the andesite samples have different UCS values, but the limestone marble and sandstone samples have similar UCS value (Table A.10 in Appendix A). Hardness results of the two stone samples show that ARB-S12 and ARB-S13 stones are in the lightweight group (Table A.11 in Appendix). The results are parallel with other analysis as XRF, thin section. Thus, ARB-S12 and ARB-S13 are in the vitrifying tuff and andesite rock groups, respectively.

The soluble salt content of the stone samples is ranging from 0.38 to 2.39% (Table A.15 in Appendix). According to Dursun et. al. (2008), if the amount of the salt in the soil is greater than 0.15%, it has high salinity. Therefore, all stone samples have high salinity. The spot tests on the stone and stone tessera samples show that the samples have average amount of phosphate and low amount of sulphate salts but considerable amount of carbonate salt. Regardless of the stone type, all stones have weak basic properties (Av.7.93) (pH$\geq$7) (Table A.17a in Appendix A).

The results of the petrographical thin section analysis of the stone samples show that rock types are andesite, limestone, sandstone, tuff, and marble (Table A.18 and Figure A.14 in Appendix A). Andesites have 3 subgroups. The source of the andesite samples is from Hüseyingazi Kale. Limestones have 3 subgroups; biosparitic limestone, dolomitic limestone and meta limestone, and the provenance of the limestone samples is from Haymana. As the provenance of the sandstone and tuff is from Memluk Yuva Village, the marble is from Afyon (antique marble quarry), and all of them are in one group (Kadıoğlu, et al., 2018) (Figure 5.1).

The thin section result of the stone tesserae shows that the sampled tesserae are in the radiolarite rock type (Table A.19 and Figure A.15 in Appendix A). The provenance

of the stone tesserae is from Elmadağ, Irmak Village Formation near Ankara (Figure 5.1).

Results of the XRF analysis show that stone samples have different rock groups (sedimentary, metamorphic and volcanic) reflecting the chemical properties of their groups. There are five groups of stones as andesite, limestone, sandstone, tuff, and marble. The andesite samples have the similar value of the content of their rock sources as SiO_2% and Al_2O_3%. In the same way, the tuff sample has SiO_2% and Al_2O_3% which is compatible with its rock group. In the limestone and marble samples, CaO% and LOI% amounts are high according to their rock sources. The trace element compositions of all types of stones were supported with their chemical rock groups. (Table A.23 in Appendix A). According to triangle plotting results, the andesite samples are in three groups and the limestone samples are in one group (Figure A.22 in Appendix A). SEM-EDX Analysis was conducted on only the stone sample ARB-S6. According to the presence of carbon and oxygen mass weights in the sample, there is a form of organic pollution and a form of pollution that is related with Al_2SiO_5 salt formation (Table A.22 and Figure A.21 in Appendix A). Finally, overall results of all analyses and tests on all stone samples can be seen in Table 5.1

Table 5.1 Overall results of all analyses and tests on all stone samples

Physical & Physicomechanical Tests		Soluble Salt Tests		Petrographical Thin Section Analysis			XRF Analysis
Durability		Salinity		Provenance		Group	Group
Andesite Sandstone Tuff	low	All Stone Types	high	Andesite	Hüseyingazi Kale	3	Andesite 3
		Salt Types		Limestone	Haymana	3	Limestone 1
Marble: Moderate		Phosphates(PO_4^{-3})	Ave	Sandstone Tuff	Memlük Yuva Village	1	**SEM-EDX Analysis**
Limestone Radiolarite	high	Sulphates (SO_4^{-2})	Low	Marble	Afyon (Antique Mable Quarry)	1	Organic pollution C (Carbon) O (Oxygen)
		Carbonates(CO_3^{-2})	Hig				
		pH (weak basic) Av 7.93		Stone Tessera	Elmadağ-Irmak Village	1	Salt Al_2SiO_5

Brick Samples

The colors of the bricks were found out to be brown, light brown, reddish and light reddish by Chromametric analysis (Table A.6 and Figure A.10 in Appendix A).

The average dry bulk density values of brick, *pilae* and pipe samples are 1.55 g/cm³, 145 g/cm³, and 1.72 g/cm³, respectively. The porosity values of brick, *pilae* and pipe samples are 31.08%, 34.80% and 32.10%, respectively (Table A.8 in Appendix A). These results were compared to the study of Özışık (2000), in which the samples have low durability if their dry bulk density value is below 1.80 g/cm³ and their porosity value is above 30%. It can be seen that all brick samples have low strength (Table A.8 in Appendix A).

Total soluble salt content of brick, *pilae* and pipe samples were determined by Conductometric Analysis. The general average of all types of bricks is 1.35% (Table A.15 in Appendix A). The results were compared to the salinity value (0.15%) of Dursun's study (2008). It can be seen that all brick samples have high salinity.

The salt types in the brick samples were determined by spot test. According to the test results, the brick samples have high phosphate and carbonate salts, but low sulphate salt. Besides, pH distribution in all brick samples has weak basic (av.7.88) (pH≥7) (Table A.17b in Appendix A).

According to thin section analysis, all types of original brick samples (brick, *pilae*, and pipe) are in 8 brick groups. The samples were analyzed separately in terms of petrographic structures in which bricks (structural) have 6 groups, *pilae* and pipe have 5 and 2 groups (Table A.20 and Figure A.16 in Appendix A). The firing temperature of all bricks (brick, *pilae*, and pipe) is about 900°C. The porosity in all bricks is about 5-12% of the matrix (brick 5-12%, *pilae* 4-12%, pipe 5-8% of the matrix). All types of bricks are rich in mineral and rock type which is about 7-42% of the matrix (brick 7-38%, *pilae* 15-42%, pipe 18-22% of the matrix). The rock types of aggregates in brick are andesite, granite, and metagrovac from different volcanic rock sources (Table A.20 in Appendix A). The provenance of the rock aggregates in the brick groups is as follows: Andesite originated brick groups are from the locality Hüseyingazi-Kale. Granite originated brick group is from Bala-Köprüköy and Metarovac originated brick group is from local formation south part of Ankara (round shaped particles originating from the of river banks). The clay sources of brick groups Brick Gr1, Brick Gr2, Brick Gr4, and Brick Gr7 are from METU Forest or/and Cevizlidere District. While the clay sources of Brick Gr3, Brick Gr5, and Brick Gr6 are from Yenidoğan region, the clay source of Brick Gr8 is from Tandoğan (Figure 5.1).

Moreover, some of the brick groups (except Brick Gr4 and Brick Gr5) have brick fragments ranging from 1% to 2.5% of the total aggregate (Table A.20 and Figure A.16 in Appendix A).

The general thin section examinations on all bricks of the Bath show that the amount of clay in the structural brick samples is larger and grain size is fine. However, the matrix of the *pilae* has more porous properties. The aggregate distribution of the *pilae* is not as homogeneous as (structural) bricks, and the bricks are more qualified than the *pilae* bricks. Besides, there are the formation of secondary minerals and decay/deformation zone (dissolutions and recrystallizations) around grains (chilled margin) inside and around the pore of the *pilae* bricks due to the direct effect of hot

water vapor (hydro-temperature pressure) (Figure 5.4). However, the pipe samples have not this effect, because these pipes were used to carry cold water. On the other hand, the pipe samples have oriented aggregates in their matrix because of ceramic production by turning machine (Figure A.16 in Appendix A).

The XRF results show that all type brick samples (brick, *pilae*, and, pipe) (Table A.24a, A.24b, A.24c in Appendix A) mainly have basic oxide compositions as SiO_2, Al_2O_3, LOI, CaO, Fe_2O_3, K_2O, MgO except for the ARB-B9 *pilae* brick sample. When the XRF results of the clay/soil sources of all type bricks (SiO_2, Al_2O_3, Fe_2O_3, K_2O, MgO) are evaluated by triangle plotting separately and together, it can be seen that all of them are in one group (Figure A.23 in Appendix A). In the same way, the values of trace element results are similar for all types of bricks (Table A.24a, A.24b, and A.24c in Appendix A). Therefore, it is thought that the production of all types of original bricks (brick, *pilae*, and, pipe) of the Bath was carried out from the same raw material sources (clay/soil) in the same workshops and on the same date.

The Raman analysis results of the bricks show that the formal mineral compositions of the bricks are biotite and hematite (Figure A.19 and A.20 in Appendix A).

SEM-EDX Analysis was conducted on only the brick sample ARB-B7. According to the presence of carbon and oxygen mass weights in ARB-B7, there is a form of organic pollution and a form of pollution related to the salt formation (such as aluminum silicate) (Table A.22 and Figure A.21 in Appendix A).

Lastly, overall results of all analyses and tests on all types of bricks can be seen in Table 5.2.

Table 5.2 Overall results of all analyses and tests on all types of bricks

Physical & Physicomechanical Tests	Soluble Salt Tests		Petrographical Thin Section Analysis				XRF Analysis
Durability	**Salinity**		**Provenance**		**Group**	T(°C)* P(%)* MTA(%)*	**Group**
Brick	All t Brick Types	high	**Rock in Aggregate**		Brick 6	~ 900 5-12 7-38	All type Bricks 1
	Salt Types		Andesite	Hüseyingazi Kale	*Pilae* 5	~ 900 4-12 15-42	
Pilae	Phosphates (PO_4^{-3})	high	Granite	Bala Köprüköy			**Raman Analysis**
			Metagrovac	Local formation of south part of Ankara	Pipe 2	~ 900 5-8 18-22	Biotite Hematite
	Sulphates (SO_4^{-2})	low	**Clay in Aggregate**		**Technology of Bricks**		**SEM-EDX Analysis**
Pipe	Carbonates (CO_3^{-2})	High	Brick Gr1 Brick Gr2 Brick Gr4 Brick Gr7	Metu Forest and Cevizlidere	**Ouality** Structural Bricks > *Pilae* Bricks		Organic pollution C (Carbon) O (Oxygen)
	pH (weak basic) 7.88		Brick Gr3 Brick Gr5 Brick Gr6	Yenidoğan			Salt Al_2SiO_5
			Brick Gr8	Tandoğan			

(*) T: Firing Temperature, P: Porosity, MTA: Matrix Total Aggregate Ratio

Mortar Samples

The results of the aggregate/binding analysis of mortar samples of the Roman Bath show that all of the mortars have high amount of aggregate content not containing carbonate (av. 27.01-72.99%) (Table A.12 and Figure A.11 in Appendix A) and they had similar binder-aggregate ratios. The ratios are quite close to the traditional aggregate:binder, 2:1 (Vitruvius, 1914, 1990; Torraco, 1988). The sieve analysis results of the mortars indicate that all samples have rich particles distribution (small,

medium and coarse sand) and homogeneity, but especially the amount of coarse particle sands (>1000 µm) (av. mortar 49.73%) are very high (Table A.13 and Figure A.12 in Appendix A). The aggregates which are rounded shape (from a nearby waterway) and angular were used together in the mortars, but the amount of angular aggregates are more than rounded ones of the bank of the river, and brick fragments are found almost all original natured samples (Figure A.13 in Appendix A).

Based on the gravimetric analysis, the amount of water content, organic carbon, and carbonate contents in the mortar samples was determined. The ratio of average water content of the mortar is 0.39% at 105°C. The ratio of average carbon content of the mortar is 3.47% at 450°C. The ratio of average carbonate content of the mortar is 22.97% (Table A.14 in Appendix A).

The thin section analysis results of the mortars indicate that there are 8 mortar groups. 3 groups out of 8 (Mortar Gr1, Mortar Gr3, and Mortar Gr6) are repairing.

While the total aggregate content of the mortar samples varies in between 25-45%, the total binder content varies in between 55-75%. Brick dust fragments in the aggregate of the original mortar is 5-15% of total aggregate. The binder structure of the mortars composed of lime (structural or originals), lime/cement (in repair) and lime/clay/cement (in repair) binders (Table A.21 and Figure A.17 in Appendix A) (Figure 5.5).

The thin section examination also revealed that the *pilae* mortars (representative sample ARB-M22) were prepared in a high quality when compared with structural mortars used in bath structural walls. The brick particles and igneous volcanic particles (quartz, granite, basalt) used in the matrix of *pilae* are distributed homogeneously. Also the angular and round particles were used together in the matrix of *pilae*. According to these results, the *pilae* samples most probably were produced in the similar technology and same ateliers (Figure 5.6).

Caldarium mortars (representative sample ARB-M40) are more compact constitution and they include a variety of minerals and rock fragments like claystone, chert, sandstone, limestone etc. As the size of the grain is coarser (>3 mm), the shape of grains is rounded (nearby river banks) and angular (Figure 5.7).

However, *tepidarium* mortars (representative samples ARB-M21 and ARB-M30) consist of various sized and shaped particles besides brick fragments distributed

heterogeneously in the matrix. It reveals that the mortars are casual production (Figure 5.6- Figure 5.7). Thus, structural mortars in *tepidarium* have low quality compared with the structural mortars in *caldarium*.

The XRF analysis results of the mortars show that their basic oxide compositions are SiO_2 (av. 28.90%), CaO (av. 28.74%) and LOI% (av. 31.18%). The other oxide compositions in these samples are Al_2O_3 (av. 5.94%), Fe_2O_3 (av. 2.66%), K_2O (av. 1.24%), MgO (av.1.01%) (Table A.26 and Figure A.24 in Appendix A). Original mortars used in different functions and sections of the Bath were analyzed separately; it was seen that the raw material source of the soil/clay (SiO_2, Al_2O_3, Fe_2O_3, MgO and K_2O) in original joint mortars used between the bricks of *pilae* was a single group at triangle plotting. In the same way, the mortars taken from the different points of the *caldarium*, *tepidarium* and water tank sections of the Bath were studied at triangle plotting, it was seen that *caldarium* mortars are in three groups, *tepidarium* mortars are in two groups, and water tank mortars in three groups (Table A.26 and Figure A.25, A.26 in Appendix A). Therefore, it was seen that the original mortars used in different functions and sections of the Bath were prepared according to their functions and places they were used. Besides, the average Cementation Index (CI) value of the mortar samples of the Bath is 3.36 (Table A.27 in Appendix A). The result shows that the lime type of the mortars is in natural cement or natural cement (C /NC) category and they are very strong samples.

Eventually, overall results of all analyses on all type of mortars can be seen in Table 5.3.

Table 5.3 Overall results of all analyses on all type of mortars

Acidic Aggregate/Binder Analysis		Sieve Granulometric Analysis	Gravimeric Analysis	Petrographical Thin Section Analysis				XRF Analysis
Ave. Mortar		Aggregate in Mortar %	Ratio WC(105°C %) Carbon(450°C %) Carbonate(%)	Matrix Binder Content (100%)	Matrix Aggregate Content (100%)		Group	Group
TB (%)*	TA (%)*	(>1000µm) Ave. 49.73		55-75	25-45		Total 8 Original 5 Repair 3	*Pilae* 1 *Caldarium* 3 *Tepidarium* 2 Water Tank 3
27.01	72.99	mostly very coarse sand homonegenus distriubution in all size (small, medium and coarse) sand	Ave. Mortar 0.39 (WC) 3.47 (Carbon) 22.97 (Carbonate)	Lime Lime/cement Lime/clay/ cement	Rock/ Mineral 85-100	BF* 5-15		
				Technology of Mortars Ouality				Cementation Index Data (CI)
		Angular aggregates > Round aggregates		*Pilae* Mortars > Structural Mortars *Caldarium* Structural Mortars > *Tepidarium* Structural Mortars				Natural Cement. &Cement (C /NC) 3.36 High

(*) T: Firing Temperature, P: Porosity, MTA: Matrix Total Aggregate Ratio

Plaster Samples

The results of the aggregate/binding analysis of plaster samples of the Roman Bath indicate that original (ARB-P3) and repairing (ARB-P1) plasters have a fairly high aggregate content (TA/TB%: 57.12/42.88% and 91.37/8.63%) (Table A.12 in Appendix A). According to the sieve analysis results, the particle size distribution of aggregates of the plaster samples consist of the mixed aggregate of small, medium and coarse sand; and all of them are distributed homogeneously. All type plasters have very coarse sand (>1000 µm) aggregates as original plaster is 33.16% and

repairing plaster is 36.91% (Table A.13 in Appendix A). In addition, in all types of plasters, angular coarse aggregates were mostly used compared to the rounded ones the bank of river and almost all plasters (original and repairing) contain brick fragments (Figure A.13 in Appendix A).

The gravimetric analysis was performed to determine the amount of water, organic carbon and carbonate contents in the plaster samples. According to the analysis results of original plaster (ARB-P3), the ratio of water content is 2.53% at 105°C, the ratio of carbon is 9.61% at 450°C and the ratio of carbonate content is 33.18% respectively. In the same way, the analysis results of repairing plaster (ARB-P1) show that the ratio of water content is 0.21% at 105°C, the ratio of carbon is 3.54% at 450°C, and the ratio of carbonate content is 48.22% respectively (Table A.14 in Appendix A).

According to the thin section analysis results, there are 2 groups of plaster (Plaster Gr1, Plaster Gr2), one (Plaster Gr1) of them is repairing (Table A.21 in Appendix A). While the total aggregate content of original and repairing plasters is 25% and 24%, the total binder content of them is 75% and 76% respectively. The binder structure of all type plasters is lime and all of them have brick fragments (10% in repairing and 15% in original plasters) (Table A.21 and Figure A.18 in Appendix A). Thus, it is accepted that the brick-lime plaster has been used due to its waterproof properties.

The XRF results indicated that the basic oxide compositions of original plaster samples (ARB-P2a, ARB-P2b, and ARB-P3) are SiO_2 (av. 21.76%), CaO (av. 24.09%) and LOI (av. 32.92%). The other oxide compositions are Al_2O_3 (av. 5.11%), Fe_2O_3 (av. 2.66%), K_2O (av. 2.69%) and MgO (av. 1.44%) respectively. The oxide composition results of the raw material source of soil/clay in all plasters (SiO_2, Al_2O_3, Fe_2O_3, MgO and K_2O) are similar and all of them are in one group at triangle plotting. Similarly, the trace element results of all plasters have similar chemical compositions (Table A.25 and Figure A.24 in Appendix A). For that reason, the plaster samples of the Roman Bath in Ankara were probably prepared with same raw material sources. Besides, the average Cementation Index (CI) value of the plaster samples is 2.51. The result show that binder type of these samples is in natural cement or natural cement (C /NC) category and all type plasters are more durable (Table A.28 in Appendix A).

In the end, overall results of all analyses on all type of plasters can be seen in Table 5.4.

Table 5.4 Overall results of all analyses on all type of plasters

Acidic Aggregate/Binder Analysis		Seive Granulometric Analysis	Gravimeric Analysis	Petrographical Thin Section Analysis			XRF Analysis
Original Plaster (ARB-P3)		**Aggregate in Plasters (%) (>1000μm)**	**Ratio WC(105°C %) Carbon(450°C %) Carbonate(%)**	**Matrix Binder Content (100%)**	**Matrix Aggregate Content (100%)**	**Group**	**Group**
TB (%)* 42.88	**TA (%)*** 57.12	**Original Plaster** Ave. 33.16	**Original Plaster (ARB-P3)** 2.53 (WC) 9.61 (Carbon) 33.18 (Carbonate)	75 Original Plaster	25 Original Plaster	Total 2 Original 1 Repair 1	All plasters 1
				76 Repairing Plaster	24 Repairing Plaster		
Repairing Plaster (ARB-P1)		**Repairing Plaster** Ave. 36.91 mostly very coarse sand	**Repairing Plaster (ARB-P1)** 0.21 (WC) 3.54 (Carbon) 48.22 (Carbonate) **Lime 100**	**BF*** 15 Original Plaster			**Cementation Index Data (CI)**
TB (%)* 8.63	**TA (%)*** 91.37	Angular aggregates > Round aggregates		**BF*** 10 Repairing Plaster			Natural Cement. &Cement (C /NC) 2.51 High

(*)TA: Total Aggregate Ratio, TB: Total Binder Ratio, BF: Brick Dust Fragmennts

141

CHAPTER 6

CONCLUSION

Roman (Caracalla) Bath in Ankara, a symbol of our distinct cultural heritage, bears the local properties of Anatolian baths in the Roman period as regards its archeological region, unique architecture, construction technique, heating and water supply system, and material properties. Along with having these characteristic values, the overall area reflects the spirit of Ankara in the Roman period with its social, cultural, economic, and political place in history. An in-depth analysis of all these values based on sound evidence was carried out within the scope of the study, and it was hoped that the novel findings about the material properties in particular would provide a foundation for the restoration and conservation activities preserving the uniqueness of the bath and transferring it to the future generations. Another significance of the study is that it will hopefully contribute to the material work towards the preservation of other unique Roman baths throughout Anatolia, which has a rich cultural heritage.

A multidisciplinary group of experts from natural sciences and social sciences cooperated in this large-scale archeomaterial study focusing on the construction materials of Roman (Caracalla) Bath in Ankara. The study ultimately reevaluated the existing knowledge about the Bath as to its history, archaeology, architecture, construction technique, and heating and water supply system, as well as revealing important information on social, cultural, economic, and political status of Roman period's Ankara.

Having reached new data on the physical, physicomechanical, compositional, mineralogical, and chemical properties of the construction materials used in Roman (Caracalla) Bath in Ankara, the study has contributed to the field of material. The data obtained was used to determine the characteristics, production technologies,

sources (provenance), durability, compatibility, current conditions, and decay factors of the Bath materials. Then, this data was interpreted by experts from natural sciences (chemists, geologists, mining engineers, civil engineers, chemical engineers) as regards the production, selection, and use of materials used in different parts of the Bath for various functions, the relation between them, and thereby their contribution to the Bath's architecture, construction technique, and functional systems (water supply, heating system). Similarly, the data was interpreted by experts from social sciences (historian, archeologist, architectural historian, restoration architect) in relation with the historical process, which led to conclusions about the particular period.

A total of 97 samples - 13 stones, 3 stone tesserae, 29 bricks, 47 mortars, 4 plasters and a calcareous layer – which were collected from various sections of the Bath were analyzed on the site and in the laboratory by means of archaeometric methods entailing a multidisciplinary approach.

At the initial analysis of stone and stone tessera samples, physical and physicomechanical test (bulk density, effective porosity, water absorption capacity, ultrasonic pulse velocity and hardness tests) results showed that andesite, sandstone, and tuff types of rocks have lower resistance, while limestone and radiolarite type stone, which is basically tessera, have higher resistance. Marble, on the other hand, has medium resistance. The strength of materials is affected by their inherent properties and environmental factors. Andesite, sandstone, and tuff stones have low resistance because they have a highly porous structure. An increase in porosity not only reduces bulk density but only exposes the material to environmental deformation. It emerged that the sources of environmental deterioration are moisture, water, salt, and biological factors. Particularly on ground level, where water and moisture are more effective, biological deformation augments the vegetation effect (moulds, lichen, algae, etc.). In situ salt tests and tests performed in the laboratory showed that another major cause of material deformation is salination. Conductivity measurement of soluble salt revealed that significant salination occurs in all materials. Its causes are different kinds of salt carried from the soil reservoir through ground moisture and cement based mortars recently used in joints of stone walls in restoration works. Results of the spot salt test revealed carbonate and phosphate in

144

high amounts and salination in the form of sulphate in smaller amounts. Carbonate forms as a result of the natural content of the material and decomposition of different salts on the stone material and crystallizes again creating calcareous layers on the surface. It was concluded that phosphate is caused by biologic and animal related factors in the environment and sulphate salt is caused by air pollution and cement based mortar used in restorations. All materials were observed to have weak basic properties. Following the thin section analyses applied to the materials, stone and stone tessera samples were first grouped petrographically, and then the rock sources were identified. In this grouping, andesite and limestones were classified into three, while sandstone, marble, and tuff were considered as one group. The main source of andesite type of stones, which were mainly used as the constructional stone in the Bath, is Hüseyingazi-Kale, while limestone is from Haymana (Kadıoğlu et al., 2018). The source of sandstone and tuff was speculated to be Memluk Yuva Village, and that of marble Afyon marble quarry (Antique Marble Quarry). Stone tessera (bedding mortar) samples, which used the Bath's mosaics, were regarded in the radiolarite rock group, and their place of origin is Elmadağ-Irmak Village. SEM-EDX analysis performed on the ARB-S6 stone sample showed that the black layer of pollution is due to organic pollution and sulphate salts. The element compositions of the materials were evaluated as a result of PED-XRF analysis, and it was found that different types of stones display the chemical properties of rock groups (sediment, metamorphic, volcanic etc.), from which they originate. Results of XRF analyses applied to the samples of the Baths' stones are in compliance with those of the thin section analysis. The analysis determined composition of major (>1%), minor (<1%), and trace (ppm) elements. Triangle plotting demonstrated that andesites fall into three groups; although two groups displayed relatively similar values, Stone Gr1b (andesite) sample containing ARB-S5 appeared to be markedly different. Results of the physical test applied to this stone confirmed that it is different from the others. This might be indicative of that this stone was used in the restoration work that was carried out in later periods. XRF element results of limestone were studied at triangle plotting and classified the material in one group depending on the rock origins (SiO_2, CaO, LOI) it belongs to. Results of XRF analysis of sandstone, marble, and tuff stones confirmed the elemental properties of rock sources these materials originate from.

An overall evaluation of the results pertaining to stone and stone tessera materials used during the construction of the Bath suggests that they were obtained from the present center of Ankara and its environs for low-cost and accessibility reasons. Similarly, all stone and stone tessera construction materials used in different sections of the Bath for different functions, e.g. for load bearing, coating, decorating, were observed to have been selected purposefully according to their properties and place of use in the Bath. Foundation walls of the Bath were mostly blocks of the local material, andesite, also called "Ankara stone". Andesite stones were used as coating material in the internal and external facades of the Bath walls having external casing, and the core between the coatings (stone and mortar) is rubble fill. It was concluded that andesite was particularly preferred in the construction of the Bath, wherein thermal differences occur frequently, because it is abundant in the close environment, durable, resistant to decay, able to prevent heat loss, and relatively less prone to the effects of heat variations. The secondary load bearing construction material in the Bath is limestone, which is commonly seen in its floors and doorways. It was probably preferred since it belongs to the main rock group of local formation. The material of marble, which is observed in only a few samples of stone blocks of walls today, was mostly used for decorative purposes, secondary load bearing element, and for coating in palaestra and pool sections, in the form of blocks and plaques. The marble blocks were used in the 95x95 m palaestra section of the Bath: 128 columns (32 in a row), column caps, stylobate, architrave, statue adornment. The fact that marble was transported in blocks from the antique marble quarries around Afyon and then treated is evidence to the importance of the Bath for the governors of the time to show off their political power. Furthermore, this probably meant the empire allocated a remarkable budget to this Bath considering that mining marble from the marble quarries then, transporting and treating it were all very costly. The traces of clamps over the walls in the pool section provide clue that the Bath walls were marble coated. Marble was a favored material in Roman period baths because it was hygienic, heat resistant, and aesthetic. Roman Bath in Ankara seems to have continued this tradition. Stones like tuff and sandstone, together with mortars, were used as rubble filling material in the core of foundation walls that had external casings (core and coating). Because tuff and sandstone materials are not durable

against external weather conditions, they were preferred in the internal core section of the bath particularly owing to their high porosity. Thus, these porous materials keep inside the hot air reaching certain temperatures in the bathing rooms, preventing its escape from inside. Indeed, design of bath walls with external casing and construction of them with appropriate materials contributed significantly to the heating and isolation of the Bath. In addition, the main material in the aggregate composition of brick and mortar materials is volcanic rocks (andesite, granite, basalt etc). These aggregates were preferred as they were easily and economically available at the local sources and capable of increasing durability with the binder material.

Moreover, it was presumed that stone tessera bedding mortar samples from the radiolarite rock group, which were used in the floor of *piscina* (pool) and which were highly durable and resistant to water, were preferred because of their physical and petrographical properties. Today stone and tessera materials are observed to have been partially distorted as the Bath area is exhibited openly or has gone through some interventions not compatible with its original form; still, it should be accepted that the experts and the craftsmen of the time made sound choices considering all the properties of the materials and used them wisely at proper sections of the Bath for appropriate functions.

The results of the analysis showed that bricks were used in three ways: structurally, in *pilae*, and in pipes. Chromametric Analysis results showed that the bricks were brown, light brown, reddish, and light reddish in color. According to the physical and physicomechanical tests, these three types of bricks have different properties in terms of durability. Dry bulk density and porosity of the three were analyzed, which yielded that they all have low durability. Structural bricks are relatively the most durable of the three, and those used in the *pilae* are the least durable. This can be attributed to the degree of porosity and environmental factors. Very similar porosity as they have, bricks used in the *pilae* are relatively more porous. On the other hand, being in direct contact with the ground, *pilae* are more prone to soil based moisture, salt, or biological decay, and thus more likely to go through rapid deterioration. Results of salt test performed both in situ and laboratory environment were in agreement with these results. Conductivity measurements in soluble salts pointed to high levels of salination in the materials. Spot salt test results revealed high levels of

carbonate and phosphate salts, and small quantity of sulphate salt in bricks. It was discovered that all bricks have weak basic properties. As a result of the thin section analysis, bricks were categorized into eight. Structural bricks were grouped into six, *pilae* into five, and pipe materials into two. All brick sample groups display authentic characteristics, except for Brick Gr5 (ARB-B10). It was determined that the original bricks have a firing temperature of around 900°C, a porous texture, and a rich composition as to minerals and rock type. Moreover, it was found that there are brick dust fragments in most brick samples (1.5-2.5% of the total aggregates). The aggregates used in the production of the brick materials were determined to be basically andesite, granite, and metagrovac, which originate from the local formations of Hüseyingazi Kale, Bala Köprüköy, and southern Ankara, respectively. The source of the clay material used was found to be METU forest and environs of Cevizlidere for Brick Gr1, Brick Gr2, Brick Gr4 and Brick Gr7, Yenidoğan for Brick Gr3, Brick Gr5, and Brick Gr6, Tandoğan for Brick Gr8. This study shows that the clay used in the production of brick was obtained from the present center of Ankara. Results of thin section analyses of structural brick, bricks in the *pilae* and pipes were comparatively analyzed, and differences in production technologies were found. The amount of clay in structural bricks is higher, particle sizes are thinner, and their distribution is more homogeneous. The clay particles used in the *pilae* is larger, their distribution is more heterogeneous, and porosity is higher. In addition, as a direct result of hot water vapor effect (hydro-temperature pressure), formation of secondary minerals and amorphous silicate, and deformation zones around the particles can be seen in these bricks inside and outside of the pores of the matrix. Thus, cracks and consequent dissolution occur in the matrix. As regards the pipe bricks, the distribution of particles displays traces of orientation, which signals that turning machine was used in making these pipes. Unlike in the *pilae* bricks, no decay or dissolution due to the effect hot water vapor was traced. This is expected since pipes convey cold water. Raman analysis, which was only applied to ARB-B22 *pilae* brick sample and ARB-B29 structural brick sample, demonstrated that biotite and hematite minerals are formal mineral compositions. Black layer pollution discovered in ARB-B7 sample by SEM-EDX analysis was considered to be caused by organic pollution and sulphate salts. This appears to be in agreement with spot salt test results.

Elemental composition of each of the three types of brick materials was analyzed by PED-XRF analyses. The triangle plotting results of SiO_2, Al_2O_3, MgO, K_2O, and, Fe_2O_3 percentages of bricks, the primary material of which is clay, revealed that they bear similar properties within themselves and tend to cluster into one single group. When SiO_2, Al_2O_3, MgO, K_2O, and, Fe_2O_3 percentages of all bricks were evaluated by triangle plotting, a similar single group emerged. Thus, it was concluded that raw material sources of clay in the three types of bricks, which are visible to the thin section analysis in more than one group, are all the same and of local formation. This led to the conclusion that the bricks were produced in the same mills, ateliers and in the same period.

An overall evaluation of the results pertaining to all bricks used in the construction of the bath led to the conclusion that they were produced from materials obtained from the center of Ankara today and the environs because clay and aggregate sources were easily and economically accessed. Thin section analysis of brick production technologies provided evidence that the craftsmen of the time prepared the bricks selecting the contents with varying ratios, particle sizes, and distribution depending on where they would be used. Grains of *pilae* in the hypocaust system, for example, are coarser, with heterogeneous distribution and high porosity. Presumably, they were prepared like this so that hot air would be captured by the pores of the *pilae* and be transferred to the bath floor and the bath floor would remain hot for a long time. In contrast, the structural bricks were made to have thin grains, with homogeneous distribution and low porosity to increase the strength of bricks carrying the load of the structure. Addition of brick fragments to bricks, thus achieving such technological advances such as decreasing fire loss and water absorption % values and increasing firing shrinkage and compressive strength (Emrullahoğlu et all, 2004), is also indicative of the fact that the craftsmen of that period possess such competence. Similarly, the orientation in the particles revealed by the thin section analysis of the pipe materials shows that turning machine was then known and used. According to the binder/aggregate analysis of mortar samples, aggregates not containing carbonate were widely used and all mortars had similar binder-aggregate ratios. They are quite close to the 2:1 (aggregate:binder) ratio (Vitruvius, 1914, 1990; Torraco, 1988) commonly used in traditional/standard applications. Granulometric

analysis (systematic elimination) was performed on the aggregates (those not containing carbonate) to determine the particle size of aggregates in the samples; it was found that all samples have rich particle distribution and homogeneity and most grains were composed of aggregates that are of the size of coarse or very coarse sand (500-1000 µm and > 1000 µm) (Wentwort, 1922). Rounded shape (from a nearby waterway) and angular aggregates were used together in the mortars, yet the latter was observed to have been used more. Brick fragments were also identified among some particles. Gravimetric analyses pointed to varying amounts of water, carbon, and carbonate in the composition of the mortars. These are in agreement with the loss of carbonate content (lime) determined by the acid loss test applied for the binder/aggregate. The thin section analysis revealed a total of eight groups of mortars, three of which are repair mortars. The total aggregate content of the mortars varied from 25-45%. While all mortars had lime binder, some contained brick fragments by 5-10%. Mortar binder compositions were lime, lime/gypsum, lime/clay/cement, and lime/cement mixtures. Mortars with cement containing binders are believed to have been used in the repairs. The technology used in the mortar joints taken from the foundation walls and the brickwork of the *pilae* was analyzed by thin section; it was found that mortar joints used in the *pilae* were composed of highly durable volcanic particles (quartz, granite, basalt) when compared to structural mortars. Aggregate particles have round and angular shapes and homogeneous distribution, with their sizes not exceeding 1 mm. Dissolution occurs around particles in these mortars, which is a direct effect of hot water vapor. The structural mortars (joint mortars used in walls) used in the hottest room (*caldarium*) and the warm room (*tepidarium*) were analyzed in terms of their technologies, and some differences were found out. Mortars with *caldarium* are more compact, having coarser grains (>3 mm). They are composed of various minerals and rock particles (like claystone, chert, sandstone, limestone etc.). The added aggregates are angular shaped or round shaped from nearby waterways. The mortars used in the *tepidarium* walls have heterogeneously distributed particles, which are of varying sizes and shapes. Moreover, mortars extracted from the pipes of the water tank (ARB-M42 and ARB-M43) and from the joints of stone channels carrying water to the bath (ARB-M46) were analyzed by means of thin section; they were found to

belong to the same class. Results of PED-XRF analysis applied to mortar samples taken from the Bath are in concordance with those of thin section analysis. The chemical content of the mortars is SiO_2, CaO, LOI, Al_2O_3, Fe_2O_3, MgO, and K_2O oxide compositions. XRF analysis of compositional specification of mortars used in several sections of the bath was conducted, and the triangle plotting indicated that the clay raw material sources (SiO_2, Al_2O_3, Fe_2O_3, MgO, and K_2O oxide compositions) of the original mortars used in the *pilae* bricks fall into one group. However, the mortars used in the various parts (structural joint mortars and rubble fill mortars in the walls and joint mortars used in *pilae* bricks) of *caldarium* section fall into three according to the raw material sources of clay. Those used in the *tepidarium* were found to fall into two in the XRF analysis triangle plotting. Mortar samples were taken from different parts of the water tank and subjected to XRF analysis; triangle plotting revealed three different groups of mortar. With its durability characteristics, the lime type used in the Bath belongs to the cement/natural cements (C/NC) category, which is quite durable. Mortars collected from joints of stone water channels and pipes were also subjected to XRF analysis, and similar chemical properties were detected; cementation index (CI) values of the mortars appeared to be far below the average values of all mortars. For the mortars between pipes and the mortar sample collected from stone water channels, cementation index (CI) values in fat lime (FL) category.

Overall, the results of analyses applied to mortars yielded the following results. According to the binder/aggregate analysis, the Bath mortars exhibit the traditional 2:1 ratio, and having the necessary competence, the experts of the time continue the tradition. Considerable use of coarse and very coarse aggregates (500-1000 µm and > 1000 µm) in the mortars, shown by granulometric analyses, is to augment the strength of the material. Lime binder in the mortars, when exposed to acid, water, moisture, and heat based external factors, is eroded almost by half, whereas these aggregates were largely preserved in the mortar. It is reckoned that intensive use of angular particles in aggregates is preferred because it expands the surface area between aggregates and binders and the contact region, thus strengthening the bond between the two materials. Sieve analysis detected addition of brick fragments. Although this may first be associated with their pozzolanic property, this addition

was only observed in some samples from the Bath, confirming that the main binder in the mortars is actually "lime", which exists in all materials. Mortar production technologies identified by thin section analysis showed that mortars used during the construction of the Bath were exclusively prepared to fit in which section and for which function they will be used. One evidence to the purposeful and careful use of mortars is that joint mortars used in *pilae* bricks contain aggregates that are composed of more durable rock/minerals when compared with those used in bath structural walls and they are distributed homogeneously. Indeed, these mortars are subject to greater exposure to hotter temperature, and thus heat effect is greater than in mortars used in structural walls. The production technologies of structural mortars (joint mortars and rubble fill mortars in the walls) used in different temperatures in different bath sections (*caldarium*, *tepidarium*, water tank etc.) were analyzed separately, and it was once again found that mortars were prepared with different contents and technologies according to the place of use and function. For example, mortars used in the walls of the *caldarium* (hot rooms) were prepared to have numerous minerals and rock particles (claystone, chert, sandstone, limestone etc.) that are smaller than 1 mm and homogeneously distributed; this was presumably done so purposefully to reinforce the materials considering the external factors such as high temperature, moisture, and vapor they will be exposed to. The fact that rock particles and minerals in mortars used in the *tepidarium* (warmth room) walls were prepared randomly as regards particle size and distribution was attributed to relatively limited exposure to external factors (heat, moisture, and vapor). Not surprisingly, the production technologies of mortars used in the hot room were decided to be more advanced than those used in the warmth room. Results of XRF chemical analysis and triangle plotting of mortars used for different purposes in different parts of the Bath were separately analyzed, and they were found parallel to thin section analysis. Triangle plotting performed in relation with the XRF chemical analysis of mortars in *pilae* indicated that clay/soil raw material source (SiO_2, Al_2O_3, Fe_2O_3, MgO, and K_2O oxide compositions) belongs to one single group, which suggested that these materials could have been produced in the same ateliers and around the same dates. Triangle plotting of mortars (joint mortars and rubble fill mortars) taken from varying parts of the *caldarium* walls is in compliance with thin

152

section results: they approximately fall into three groups. One explanation for this is that original structural mortars and rubble fill mortars are placed in two separate groups just as expected, whereas the repair mortars added to the walls much later are in the third group. This once again confirmed that the antique age craftsmen prepared the original mortars uniquely according to the requirements of the place of use. Triangle plotting result of wall mortars (ARB-M9, ARB-M11, ARB-M14) taken from the *tepidarium* revealed two groups, which is parallel to the thin section results. Two different groups emerged although they were used in similar spaces (*tepidarium*) for the same functions (rubble fill mortars) because the mortars used in *tepidarium* were prepared arbitrarily. When XRF chemical compositions of all mortars were evaluated together by triangle plotting, results were not incidentally multifold. This is attributed to the fact that mortars were prepared with different contents and production technologies depending on the function and place of use. Cementation index (CI) results demonstrated that the lime used in the Bath as binder is in the cement/natural cement(C/NC) category, which suggested that the experts of the period chose to use this binder on purpose to reinforce the material quality and strength. On the other hand, cementation index (CI) results pertaining to mortars taken from the joints of stone water channels (ARB-M46) and from the pipes (ARB-M42 and ARB-M43) showed that these sample are in fat lime category, (FL) which seems to be a purposeful choice as these materials are continually in contact with cold water.

The analysis results applied to plasters were inspected, and the binder/aggregate analysis showed considerable use of aggregates that were not containing carbonate. Granulometric analysis results showed that coarse and very coarse aggregates (500-1000 µm and > 1000 µm) were intensively used (Wentwort, 1922). The aggregates used in the samples are of round or angular shape, and brick fragments were found in all of them. Gravimetric analyses performed on the samples showed varying amounts of water, carbon, and carbonate in organic plasters. It was found that the amount of lime used in original and repair plasters are higher than that used in mortars. Following the thin section analysis, two groups of plasters were discovered: original and repair. While total aggregate content of the plasters varied from 24-25%, the binder of plasters is lime, and about 10-15% of aggregates were found to be brick

fragments in all samples. All original samples were evaluated as regards production techniques by petrographical thin section optical microscopy, and it was found that they have similar contents, particles, shapes, and distributions. Results of PED-XRF analysis run on plaster samples from the Bath are in compliance with the thin section findings. When chemical oxide compositions of clay/soil raw material of plasters were considered to be SiO_2, Al_2O_3, Fe_2O_3, MgO, and K_2O two groups of plasters emerged: original and repair. Cementation index (CI) results of plasters exhibited that lime used as binder is in the category of cement/natural cement (C/NC).

An overall evaluation of all analyses on plaster samples revealed the following results. Large amount of coarse and very coarse aggregates in mortars, which was identified by granulometric analysis, increased the resistance of plaster materials to acid, water, moisture, heat, etc. The use of round grains from nearby waterways in aggregates and angular particles together was explained twofold: local sources were utilized, and angular particles provide effective adherence having large surface area (Stefanidou et al, 2014). In gravimetric analysis applied only to finish plaster used for leveling the surface, more lime (organic, carbon, carbonate) than mortar was found; this is to increase the flexibility of plaster materials and the ease of application to surface. In addition, lime binder was used in plasters because of the physical composition of lime based plasters and its capability of balancing internal humidity change by its water vapor permeable characteristic (i.e., if humidity is high, it absorbs water vapor, or if humidity is low, it emits water vapor inside the space). Therefore, not only a comfortable and healthy atmosphere is ensured but also the biological degradation caused by moisture and condensation was prevented (EuLA, 2008). Both sieve and thin section analysis results led to the conclusion that brick fragments present in all plasters were added because of their pozzolanic properties. It was also concluded that brick fragments, which had long been known, were also preferred here because their raw material source contains calcium in high levels and clay mineral in moderate levels, thus they act as an effective pozzolanic and water repellent (Böke et al., 2006; Uğurlu, Böke, 2009). Thin section and XRF analysis of original plasters cluster in the same group, and they display local and similar properties as regards clay/soil raw material sources and aggregate-mineral contents and production technologies. These increase the probability that they were produced

in local ateliers and around the same time. The cementation index (CI) results of plasters demonstrated that, as lime type, in the category of cement/natural cement (C/NC), which has considerably high compressive strength, was used, which in turn showed that the craftsmen of the time produced the plaster materials deliberately to increase material quality.

These archaeometric studies conducted on the materials within the scope of the thesis were evaluated in terms of the historical and archeological characteristics of the Bath, and the following conclusions were derived. Findings of the past excavations, and coins and inscriptions of the latest period's (belonging to Caracalla and her mother Julia Domna) provide evidence that the Bath was built during the period of the Caracalla (Dolunay, 1941; Erzen, 1946; Bosch, 1967; Kadıoğlu et. al, 2011). Mention of the Megala Asklepia Soteria games organized in honor of Caracalla's recovery from illness on the inscriptions and remains of Asklepios' statue discovered during the excavations also point to the period of Caracalla (Bosch, 1967; Kadıoğlu et. al., 2011). Nevertheless, colonnaded street excavations carried out in the direction of the Bath entrance on Çankırı Street revealed some inscribed architrave blocks.

Researchers estimated that they were a part of the Bath paleastra, and based on the periodic characteristics of the inscriptions, the paleastra was built in the Hadrian period (Dalman, 1933; Bosch, 1967; Cooke, 1998; Bennett, 2003; Bennett, 2006; Kadıoğlu et. al., 2011). However, Cooke (1998) asserted that the bricks used in the construction may have been produced within the scope of a single project and the standard sized bricks (according to the measurement of Dodge category) may date back to Hadrian or Caracalla period (Kadıoğlu et. al., 2011). The chemical elemental analysis of all bricks (structural bricks, *pilae* and pipe) used within the scope of the study showed that the clay raw material sources of them are in the same category. That is, they were probably produced in the same ateliers and around the same time. This also confirms Cooke's claim that bricks used indoors were produced within the scope of a single project in Hadrian or Caracalla period. Still, two inscriptions handled by Bosch (1967) in Ankara suggested that the construction might have been built earlier (Bosch, 1967; Kadıoğlu et. al, 2011). These two inscriptions refer to the Polyeidos Gymnasium in the city. The fact that the Roman Bath of Ankara has a palaestra section in the form of a very large gymnasium character led Bosch and

some other researchers to believe that location of the bath might have been the location of Polyeidos Gymnasium (Bosch, 1967; Foss, 1977; Görkay, 2006). In other words, with an ongoing project, the Polyeidos Gymnasium was converted into the Ankara Roman Bath-Gymnasium complex with the addition of bath buildings (Görkay, 2006; Kadıoğlu et. al, 2011). Though this claim remains unproved, the existence of bath-gymnasium complexes in most Anatolian Roman baths somewhat promotes its likelihood. In addition, the ruins (andesite seat blocks) piled on the edge of the slope to the west of the Roman Bath of Ankara signaled that they might be the remains of the stadium structure. This conjures up the idea that these two constructions (Stadium-Bath) are related (Görkay, 2006; Kadıoğlu et. al, 2011). The studies carried out indicate that the stadium may have been located in the south of the Bath. According to the researchers, during the Caracalla period Megala Asklepia Soteria agonistic games, the crowd which gathered in the palaestra passes to the stadium through a gate to the south of palaestra. In Anatolia, there are other examples wherein stadium and bath are associated. Thus, the location of Ankyra Stadium is uncertain, yet it is conceived to be related with the Bath. This somewhat proves that the stadium, which was estimated to have been built in the 1st century A.D, was very close to and related with the Polyeidos Gymnasium, which is assumed to have been in the present place of the Bath (Görkay, 2006; Kadıoğlu et. al, 2011).

All these results suggested that two scenarios could apply to the construction of the baths. First, the palaestra, the open section of the Bath, is a part of the gymnasium and related with stadium that had been previously built, and as suggested by the similarity in the indoor bricks of the Bath; they (palaestra, gymnasium and bath buildings) were constructed within a single construction project. Second, the indoor spaces of palaestra, gymnasium, stadium, and bath buildings were planned in an interconnected design within the scope of an ongoing project and were built throughout history by means of additions. Thus, it was concluded that the similarity observed in brick materials must have originated from the knowledge production conveyed over the centuries from skilled craftsmen through written or spoken records.

The thesis intends to extensively present data about the architecture of the Roman Bath in Ankara based on field and literature research. Because the last walls of the

Bath were destroyed by dynamites in 1926 during some city planning works, (Dolunay, 1948; Akok, 1968) which were terminated immediately because of the remains found, the initial projects of the bath were designed by Akok in 1955 based on the remains of foundation walls and their traces. Later, the final version of the projects (building survey, restitution, restoration and landscaping) prepared by various architecture offices (Keskin, 2012; Nalbant 2014) were analyzed and concluded that the Bath bears features of bath-gymnasium synthesis, which is an authentic Anatolian contribution, as first claim by Yegül (2006). That is, the Greek gymnasium possessing palaestra with wide columns and Roman bath buildings with vaulted large halls coexist in the Ankara Roman Bath (Yegül, 2006). The excavations carried out in the past to identify whether the Bath is symmetrical or not ended up with the conclusion that the Bath is not symmetrical, or maybe it was meant to be, yet left incomplete (Akok, 1955; Kadıoğlu et al., 2011).

In this thesis, the restitution project (Drawing B.7-B.8-B.9 in Appendix B) designed based on the existing data on the Bath (Keskin, 2012; Nalbant 2014) displayed that the Bath has similar features with the plan scheme of the Gymnasium Bath in Magnesia ad Meandrum (Yegül, 2006), which is seen as a typical example of symmetric planning in Anatolia. Consequently, it was assumed that the bath-gymnasium complex of Roman Bath in Ankara, just like other great empire baths in Anatolia, was designed based on symmetrical and axial composition, yet left incomplete due to economic, political, or other causes.

Still, Yegül (2010) asserted that tendency to linear and orthogonal planning typically seen in other Anatolian baths is also dominant in the Roman Bath in Ankara and avoidance of circular features quite common in the baths of the West (Rome) is evident. Yegül (2010) explained this by the replacement of highly flexible materials like the Roman concrete produced in Rome with lime based rubble fill mortars serving the same purpose in Anatolia. Because the "lime" added to this mortar as binder is not as effective as the strong binder "pozzolan" added to the Roman concrete, the use of curvilinear forms in architecture was limited (Yegül, 2010). That is why; curvilinear forms can only be seen in niches in the Roman (Caracalla) Bath in Ankara. However, based on the results of cementation index (CI), it can be claimed that lime type in cement/natural cement category, which is rather strong, in

the structural mortars contributed remarkably to the durability of the Roman Bath in Ankara. Furthermore, the construction of the barrel vaults, which have been designed as the top roof system of the Bath (Akok, 1968) and exceed large open spaces, testify to the durability of this material. In brief, the thesis aimed to analyze the physical, physicomechanical, compositional, mineralogical, and chemical properties of the construction materials of the bath, which has survived up until now with its unique values. To this end, raw material characteristics, sources (provenance), production technologies, durability, compatibility, current state and reasons for deterioration of these materials were identified. It is hoped that these findings will be a springboard for the future restoration and conservation works for the protection of the unique value of the Bath and will pave the way for filling the gap in the literature concerning material analysis in other Roman baths in Anatolia. The study, which was geared towards material analysis, reevaluated the history, archeology, architecture, construction and functional systems of the Bath, as well as enabling the reformulation of views on social, cultural, economic, and political life in Roman Period's Ankara. Thus, specifically focusing on Roman (Caracalla) Bath in Ankara, it will shed light onto the path of researchers (archaeologists, architectural historians, art historians) who seek answers to numerous questions to the end of understanding the main subject of archaeometry, the history of civilization and culture.

REFERENCES

Abu-Jaber, N., Al-Saad, Z., Shiyyab A., Degryse, P., "Provenance of White Marbles from the Nabatean Sites of Qasr Bint and The Collonaded Street Baths at Petra, Jordan", MAA -Mediterranean Archaeology and Archaeometry-, Vol. 12, Iss. 1, pp. 21-29, 2012.

Adam, J.P., Roman Building: Materials and Techniques, (translated by Mathews, A.), London and New York, 1994.

Akşit, İ., Anatolian Civilizations and Historical Sites, Republic of Turkey Ministry of Culture and Tourism Publications, Ankara, 2009.

Akok, M., "Ankara Şehri İçinde Rastlanan İlk Çağ Yerleşmelerinden Bazı İzler ve Üç Araştırma Merkezi", Türk Tarih Kurumu, Belleten, Sayı: 75, Cilt: 19, s. 309-329, 1955.

Akok, M., "Ankara Şehrindeki Roma Hamamı" Türk Arkeoloji Dergisi, Sayı: 17, Cilt: 1, s. 5-37, 1968.

Akurgal, E., Ancient Civilizations and Ruins of Turkey, Türk Tarih Kurumu Basımevi, Ankara, 1970.

Akyol, A.A., Material Characterization of Ancient Mural Paintings and Related Base Materials: A case Study of Zeugma Archaeological Area, Archaeometry Department of METU, PhD Thesis, Supervisor: Prof. Dr. Şahinde Demirci, Ankara, Turkey, 2009.

Akyol, A.A., Ankara Roma (Caracalla) Hamamı Yapı Malzeme Analizi Raporu, Yayınlanmamış Rapor, Ankara Üniversitesi Yer Bilimleri Uygulama ve Araştırma Merkezi (YEBİM) ve Ankara Üniversitesi Başkent M.Y.O. Malzeme Araştırma ve Koruma Laboratuvarı (MAKLAB), 2012.

Al-Naddaf, M., "The effect of Salts on Thermal and Hydric Dilatation of Porous Building Stone", Archaeometry, Vol. 51, Iss. 3, pp.495-505, 2009.

Anabolu, M.U., Yunan ve Roma Mimarlığı, Dragon Yayınları, İstanbul, 1996.

Anabolu, M., İstanbul ve Anadolu'daki Roma İmparatorluk Dönemi Mimarlık Yapıtları, Arkeoloji ve Sanat Yayınları, İstanbul, 2001.

Anders, G.J.P.A., Jorg, C.J.A., Stern, W.B., Anders-Bucher, N., "On some physical characteristics of Chinese and European red wares", Archaeometry, Vol. 34, Iss. 1, pp. 43–52, 1992.

Arık, R.O., "Les résultats de fouilles faites á Ankara par la Société d'Histoire Turquie", La Turquie Kemaliste 20-26, pp. 47-57, 1937.

Arslan, M., Galatya Krallığı ve Roma Dönemi Ankara Şehir Sikkeleri/The Coins of Galatian Kingdom and the Roman Coinage of Ancyra in Galatia, Ankara Ticaret Odası Yayınevi, s. 150, 2004.

Aru, K.A., Türk Hamamları Etüdü, İstanbul Teknik Üniversitesi Mimarlık Fakültesi Doçentlik Tezi, İTÜ Yayınları, İstanbul, 1949.

Aslan Ö., Böke, H., "Properties of Roman bricks and mortars used in Serapis Temple in the city of Pergamon", Material Charecterization, Vol. 60, Iss.9, pp. 995-1000, 2009.

Bakar, N., Ankara Roma Hamamı ve Hamamda Ele Geçen Sütun Başlıkları, Selçuk Üniversitesi Sosyal Bilimler Enstitüsü Arkeoloji Anabilim Dalı, Klasik Arkeoloji Bilim Dalı Yüksek Lisans Tezi, Danışman: Prof. Dr. Ahmet Tırpan, Konya, 2008.

Başaran, T., "Roma Döneminde Hypokaust Sisteminin Isıl Analiz Yönünden Günümüz Yerden Isıtma Sistemi İle Karşılaştırılması", III. Tesisat Mühendisliği Kongresi ve Sergisi, Ek Bildiriler, MMO -Makine Mühendisleri Odası- Yayını, s. 1008-1018, 1997.

Bennett, J., "Ancyra, Metropolis Provinciae Galatiae", in P.R. Wilson (ed), The Archaeology of Roman Towns: Studies in homour of John S. Wacher, Oxford, pp. 1-12, 2003.

Bennett, J., "The Political and Physical Topography of Early Imperial Graeco-Roman Ancyra", Anatolica 32, pp.189-227, 2006.

Bingöl, O., Menderes Magnesiası, Magnesia ad Maeandrum, Basım: Aydın Valiliği, Ankara, 1998

Black, C.A., Evans, D.D., Ensminger, L.E., White, J.L., Clark, F.E., Methods of Soil Analysis, No. 9 in the Series Agronomy, American Society of Agronomy:Crop Science Society of America : Soil Science Society of America, Wisconsin, 1965

Bland W., Rolls, D., Weathering: An Introduction to the Scientific Principles, Arnold, London, pp.271, 1998

Borrelli, E., Conservation of Architectural Heritage, Historic Structures and Materials, Introduction, Arc Laboratory Handbook, Vol. 1, Iss. 99, ICCROM, UNESCO, WHC, Italy, 1999.

Bosch, E., Quellen zur Geschichte der Stadt Ankara im Altertum, Ser.7, No.46, Türk Tarih Kurumu Yayınları, Ankara, 1967.

Boynton, R.S., Chemistry and Technology of Lime and Limestone, 2nd Edition, John Wiley & Sons, New York, 1980.

Böke, H., Akkurt, S., "Ettringite formation in historic bath brick–lime plasters", Cement and Conrete Research, Vol. 33, Iss. 9, pp. 1457-1464, 2003.

Böke, H., Akkurt, S., İpekoğlu, B., Uğurlu E., "Characteristics of brick used as aggregate in historic brick-lime mortars and plasters", Cement and Conrete Research, Vol. 36, Iss. 6, pp.1115-1122, 2006.

Böke, H., Uğurlu, E., "The use of brick-lime plasters and their relevance to climatic conditions of historic bath buildings", Construction and Building Materials, Vol.23, Iss.6, pp. 2442-2450, 2009.

Bradley, R., Meredith, P., Smith, J., Edmonds, M., "Rock physics and the Neolithic axe trade", Archaeometry, Vol. 34, Iss. 2, pp. 223–233, 1992.

Brown, E.T, Rock Characterization, Testing and Monitoring: I.S.R.M. International Society for Rock Mechanics Suggested Methods, Pergamon Press, Oxford, New York, 1981.

Brown, K.A., Pluciennik, M., "Archaeology and human genetics: lessons for both" Antiquity, Vol. 75, Iss. 287, pp. 101-106, 2001.

Brödner, E., Die römischen Thermen und das Antike Badewesen, Eine Kulturhistorische, Wissenschaftliche Buchgesellschaft, Darmstadt, 1983.

Columella, L.J.M., Columella on Agriculture, Vol. 1, (Books 1-4), (translated by Harrison Boyd Ash), The Loeb Classical Library, Harvard University Press. 1941.

Conti, C., Martines, G., Sinopoli, A., "Construction Techniques of Roman Vaults: *Opus caementicum* and the octagonal dome of the Domus Aurea", Proceedings of the Third International Congress on Construction History, Cottbus, Berlin, Vol.1, pp. 401-408, 2009.

Cooke, S.D., The Monuments of Roman Ancyra Reviewed, Archaeology and History of Art Department, Bilkent University, MA Thesis, Supervisor: Dr. Jacques Morin, Ankara, Turkey, 1998.

Coşkun, A., Salamis Antik Kenti Roma Hamamı, Ankara Üniversitesi Sosyal Bilimler Enstitüsü, Arkeoloji Bölümü Yüksek Lisans Tezi, Danışman: Prof. Dr. Çoşkun Özgünel, Ankara, 2004.

Cotterell, B., Kamminga, J., Mechanics of pre-industrial technology: an introduction to the mechanics of ancient and traditional materials culture, Cambridge University Press, Cambridge, 1990.

Çördük, A., Yunan ve Roma Mimarisindeki Yapı Teknikleri, Ege Üniversitesi, Klasik Arkeoloji Bölümü, Yüksek Lisans Tezi, Danışman: Doç. Dr. Gül Gürtekin Demir, İzmir, 2006.

Dalman, K.O., Bittel K., Schneider, A., M., "Archäologische Funde in Ankara, 1932", AA -Archäologischer Anzeiger- 47, pp. 233-261, 1932.

Dalman, K.O., "1931'de Ankara'da Meydana Çıkarılan Asarı Atika" Türk Tarih Arkeologya ve Etnografya Dergisi 1, s. 121-133, 1933.

Daşbacak, C., "Antikçağda Buldan ve Temizlik Kültürü" Buldan Sempozyumu, Denizli, Türkiye, s. 957-966, 2006.

De Jerphanion G., S.J, Mélanges D'Archaéologie Anatolienne: Monuments Préhelléniques Gréco-Romains, Byzantins et Musulmans de pont, de Cappadoce et de Galatie, Beyrouth Imprimerie Catholique, 1928.

Degryse, P., Muchez, P., Loots L.L., Vandeput, L., Waelkens, K., and M., "The Building Stones of Roman Sagalassos (SW Turkey): Facies Analysis and Provenance", Facies, Vol. 48, pp. 9-22, 2002.

DeLaine, J., Design and Construction in Roman Imperial Architecture the Baths of Caracalla in Rome, Department of Classics, The University of Adelaide, PhD Thesis, Supervisor: Frank Sear, Adelaide, South Australia, May, 1992.

Dinç R., Tralleis Rehber/Guide, (Çeviren: Stephen Peterson), Arkeoloji ve Sanat Yayınları, İstanbul, 2003.

Dirlik, N., "Antik Dönemde Kemer ve Tonoz", TOD -Tarih Okulu Dergisi-, Yıl 10, Sayı XXXII, s. 815-846, Aralık 2017.

Dobson, P., Nakagawa, S., Summary of Rock Property Measuremens for Hong Kong Tuff Samples, Earth Sciences Division, Ernest Orlando Lawrence Berkeley National Laboratory, University of California, pp. 1-7, 2005.

Dolunay, N., "Haberler, Çankırı Kapı Hafriyatı", Belleten, Sayı 2, s.495-496, 1938.

Dolunay, N., "Türk Tarih Kurumu Adına Yapılan Çankırıkapı Hafriyatı", Belleten, Sayı: 19, Cilt: 5, s. 261-266, 1941.

Dolunay, N., "Çankırı Kapı Hafriyatı", III. Türk Tarih Kongresi 1943, Türk Tarih Kurumu Yayınları, s.212-218, 1948.

Dunbabin, K.M.D., "Baiarum Grata Voluptas - Pleasures and Dangers of the Bath", Papers of British School at Rome, Vol. 57, pp. 6-56, 1989.

Dunnel, R.C., "Why archaeolosits don't care about archaeometry, Archeomaterials, Vol.7, pp. 5-161, 1993.

Dursun, H., Dizdar, M.Y., Kırıştıoğlu, Ş., Özcan, İ., Hamurkar, Y., Toprak ve Arazi Sınıflaması Standartları Teknik Talimatı ve İlgili Mevzuat, Tarım ve Köyişleri Bakanlığı Tarımsal Üretim ve Geliştirme Genel Müdürlüğü Yayını, Ankara, s. 70, 2008.

Edmonson, M., Science technology and society from science fiction: scientism, technicism and archaeology, Scottish Archaeological Review, Vol. 7, pp. 23-31, 1990.

Edwards, H.G.M, Chalmers J.M., Raman Spectroscopy in Archaeology and Art History, RSC Chemistry Spectroscopy Monographs Series, Royal Society of Chemistry, Publishing, Cambridge, UK, 2005.

Ekinci, S., Deniz, Ö.Ş., Gür, N.V., "Yapı Kültürü ve Tasarım Verileri Işığında "Kargir Yığma Dış Duvarların Tarihsel Gelişimi", 6. Ulusal Çatı Sempozyumu, Bursa, Türkiye, s.105-114, 2012.

El-Gohary, M.A, Al-Naddaf M.M., "Characterization of Bricks used in the External Casing of Roman Bath Walls "Gadara Jordan"; MAA -Mediterranean Archaeology and Archaeometry-, Vol. 9, No. 2, pp. 29-46, 2009.

Elert, K., Cultrone, G., Novarro, C.R., Pardo, E.S., "Durability of bricks used in the conservation of historic buildings - influence of composition and microstructure", Journal of Cultural Heritage, Vol. 4, Iss. 2, pp. 91-99, 2003.

Eliav, Y.Z., "The Roman Bath As A Jewish Institution Another Look At The Encounter Between Judaish and Greco-Romen Culture", Journal for the Study of Judaism, Vol. 31, No. 4, pp. 416-454, 2000.

Emrullahoğlu, C.B., Karademir, H., Emrullahoğlu, Ö.F, "Tuğla Kırıklarının Tuğla Üretimimde Kullanımı", 5. Endüstriyel Hammadde Sempozyumu, İzmir, Türkiye, s.199-203, 2004.

Erim, K.T., Aphrodisias, Net Turistik Yayınları, İstanbul, 2002.

Ertuğrul, A., "Hamam Yapıları ve Literatürü", Türkiye Araştırmaları Literatür Dergisi, Cilt: 7, Sayı: 13, s. 241-266, 2009.

Erzen, A., İlkçağda Ankara, Türk Tarih Kurumu, Ankara, 1946.

Esen, İ., "Ankara Roma Hamamı 2000 Yılı Çalışmaları" 12. Müze Çalışmaları ve Kurtarma Kazıları Sempozyumu, Kuşadası, Türkiye, Kültür Bakanlığı Anıtlar ve Müzeler Genel Müdürlüğü Yayınları, Ankara, s. 285-292, 2001.

Eyice, S., "Hamam", Türkiye Diyanet Vakfı İslam Ansiklopedisi, Türkiye Diyanet Vakfı Yayınları, İstanbul, Cilt. 15, s. 402-430, 1997.

Fagan, G.G., "Sergius Orata Inventor of the Hypokaust?", Classical Association of Canada, Vol. 50, No. 1, pp. 56-66, 1997.

Fagan, G.G., Bathing in Public in the Roman World, University of Michigan Press, USA, 1999.

Fagan, G.G., "The Genesis of the Roman Public Bath: Recent Approaches and Future Directions", American Journal of Archaeology, Vol. 105, No.3, pp. 403-426, 2001.

Farrington, A., The Roman Baths of Lycia: an Architectural Study, The British Institute of Archeology at Ankara, Monograph 20, p. 23, 1995.

Feigl, F., Spot Tests in Organic Analysis, 7th Edition, Elsevier Publishing Company, Amsterdam, 1989.

Feilden, M.B., "Conservation of Materials and Practical Applications of Scientific Research in Restoration Work", 6th ICOMOS General Assembly and International Symposium, Roma, Italy, pp. 267-302, 1981.

Fıratlı, N., "Ankara'nın İlk Çağdaki Su Tesisatı", Belleten, Sayı: 57, Cilt:15, s. 349-359, 1951.

Finlay A.J., McComish J.M., Ottley C.J., Bates C.R., Selby D., "Trace element fingerprinting of ceramic building material from Corpow and York Roman fortresses manufactured by the VI Legion", The Journal of Archaeological Science, Vol. 39, No. 7, pp. 2385-2391, 2012.

Fletcher, S.B., A History of Architecture on the Comparative Method, Charles Scribner's Sons Book Publishing Company, New York, 1961.

Foss, C., "Late Antique and Byzantine Ankara", DOP -Dumbarton Oaks Papers-, No. 31, pp. 27-87, 1977

Frontinus, S.I., Sextus Iulius Frontinus De Aquaductu Urbis Romae, "Liber primus", (translated by Krohn), De Aquaductu Urbis Romae, Leipzig, 1922.

Gagniers, J.D., Devambez, P., Kahil, L., Ginouvés, R., Laodicée du Lycos, Le Nymphée campagnes 1961-1963, Presses de l'Université Laval, Quebec City, Canada, pp. 293-294, 1969.

Goldstein, J., Newbury D.E., Echlin, P., Joy, D.C., Fiori, C., Lifshin, E., Scanning Electron Microscopy and X-Ray Microanalysis: A text for Biologists, Material Scientists, and Geologists, Springer Science Business Media, New York, 2012.

Görkay, K., "Ankyra's Unknown Stadium", Istanbuler Mitteilungen 56, pp. 247-271, 2006.

Güleç, A., Ersen A., "Characterization of Ancient Mortars: Evaluation of Simple and Sophisticated Methods", Journal of Architectural Conservation, Vol. 4, Iss. 1, pp. 56-67, 1998.

Gültekin E., Bahçe ve Peyzaj Sanatları Tarihi, Türk İslam Bahçeleri, Çukurova Üniversitesi Ziraat Fakültesi Yayınları, Adana, 1998.

Günel, G., Kılıcı, A., "Ankara Altındağ Osmanlı Dönemi Hamamlarında Suyolları Üzerine Bir Araştırma", Akademik Sosyal Araştırmalar Dergisi, Yıl:4, Sayı:35, s. 557-580, 2016.

Güven, S., "Res Gestae Divi Augusti Yazıtı ve Ankara'nın Roma Dünyasındaki Yeri", Ankara Ankara, (Editor: Enis Batur), Yapı Kredi Yayınları, İstanbul, 1994.

Henderson, J., The Science and Archaeology of Materials, An investigation of inorganic materials, Routledge Publisher, London, 2000.

Hodges, H., Artifacts: An Introduction to Primitive Technology, Praeger Press, New York, 1964.

Hodgkinson, P., "Los Jardines de Catalunga Barcelano-Spain, Taler De Arquitectura", An Encyclopedia of Modern Architecture, (Editor:Yukio Futugawa), A.D.A. Edita Tokyo Co.Ltd., Tokyo, 1985.

Işık, Ö., Konya Şerafeddin Camisi Yakınındaki Türbenin Tuğla Duvar Malzemesinin Arkeometrik Yönden Araştırılması, Çukurova Üniversitesi Fen Bilimleri Enstitüsü Arkeometri Anabilim Dalı, Yüksek Lisans Tezi, Danışman: Prof. Dr. Selim Kapur, Adana, 2010.

Ivanov, S.A., Hülsen, C.C, Architektonische Studien: Aus den Thermen des Caracalla, Vol. 3, Reimer Publisher, Berlin, 1898.

Jedrzejevska, H., "Ancient Mortar as Criterion an Analysis of Old Architecture", Proceedings of Symposium on Mortars, Cements and Grouts Used in the Conservation of Historic Buildings, ICCROM, Rome, Italy, pp. 311-329, 1981.

Jones, A., "Archaeometry and Materiality: Materials-Based Analysis in Theory and Practice", Archaeometry, Vol. 46, Iss. 3, pp. 327-338, 2004.

Joria, A., "Sisteme di Riscaldamento Nelle Antiche Terme Pompeiane", Bulletino della Commissione archaeologica comunale di Roma, Vol. 86, pp. 167-189, 1978-1979.

Juvenal, The Sixteen Satires (translated by Peter Green), 9. Edition, Penguin Books, England, 1974.

Kadıoğlu, M., "Ankara Ulus *Opus Sectileri",* TAD -Türkiye Arkeoloji Dergisi- 31, pp. 351-391, 1997.

Kadıoğlu, M., Görkay, K., "Yeni Arkeolojik Araştırmalar Işığında Μητροπολιε Της Γαλατιας: Ankyra" , Anadolu/Anatolia 32, s. 21-148, 2007.

Kadıoğlu, M., Görkay, K., Mitchell S., Roma Dönemi'nde Ankyra, Yapı Kredi Yayınları, İstanbul, 2011.

Kadıoğlu, Y.K., Mafik ve Ultramafik Magmatik Kayaçların Ana-Eser REE Jeokimyasal Karakteristikleri ve Jeofiziksel Açıdan İncelenmeleri, Magmatik Petrojenez Lisans Üstü Yaz Okulu, Akçakoca-Düzce, TMMOB Yayınları No:61, s. 159-195, 2001.

Kadıoğlu, S.K., Kadıoğlu Y.K., Akyol A.A., "Ankara Roma Hamamı'nda Jeofizik ve Petrografik Çalışmalar", 39. Uluslararası Kazı, Araştırma ve Arkeometri Sempozumu, Bursa, Türkiye, Cilt: 2, s. 359-372, 2018.

Kaytan, E., An Investigation of Water Supply in Roman Ankara, History of Architectural Department of METU, MA Thesis, Supervisor: Prof. Dr. Suna Güven, Ankara, Turkey, pp. 29-36, 2008.

Keeley, L.H., Experimental Determination of Stone Tool Uses: A Microwear Analysis, Univerity of Chicago Press, U.S., 1980.

Kerr, P.F., Optical Mineralogy, Mc Graw-Hill Book Company, New York, 1977.

Keskin, M., Building Survey Drawings and Reports of Roman (Caracalla) Bath in Ankara, MK Architectural Office, Ankara, 2012.

Kilikoğlou, V., Vekkinis, G., Maniatis, Y., Day, P.M., "Mechanical Performance of Quartz Tempered Ceramics: Part 1, Strength and Toughness", Archaeometry, Vol. 40, Iss. 2, pp. 261–79, 1998.

Kingery, W.D., Learning from things: Method and Theory of Material Culture Studies (Editor: W. David Kingery), Smithsonian Institution Press, Washington, D.C., U.S., pp. 181–204, 1996.

Kinneir, J.M., Journey Through Asia Minor, Armenia and Koordistan, in the years 1813 and 1814; with remarks of the Marches of Alexander and retreat of the Ten Thousand, pp. 67-68, John Murray Publisher, London, 1818.

Kramar, S., Zalar, V., Urosevic, M., Körner, W., Mauko A., Mirtic, B., Lux J., Mladenovic A., "Mineralogical and microstructural studies of mortars from the bath complex of the Roman villa rustica near Mošnje (Slovenia)", Material Characterization, Vol. 62, Iss. 11, pp. 1042-1057, 2011.

Kretzschmer, F., Antik Roma'da Mimarlık ve Mühendislik, Arkeoloji Sanat Yayınları, İstanbul, 2000.

Kula Say, S., Erken Dönem Osmanlı Hamamlarında Eğrisel Örtüye Geçiş Sistemleri, İstanbul Teknik Üniversitesi Mimarlık Tarihi Bölümü Yüksek Lisans Tezi, Danışman: Prof. Dr. Afife Batur, İstanbul, 2007.

Lancaster, L.C., Concrete Vaulted Construction in Imperial Rome: Innovations in Contex, Cambridge University Press, Cambridge and New York, 2005.

Lancaster, L.C., Sottili, G., Marra, F., Ventura G., "Provenancing of Lightweight Volcanic Stones used in Ancient Roman Concrete Vaulting: Evidence from Turkey and Tunisia", Archaeometry, Vol. 52, Iss. 6, pp. 949-961, 2009.

Landels, J.G., Eski Yunan ve Roma'da Mühendislik, TÜBİTAK Yayınları, Ankara, 2000.

Lawrence, R.M., A Study of Carbonation in Non-Hydraulic Lime Mortars, Faculty of Engineering and Design Department of Architecture and Civil Engineering-University of Bath, PhD Thesis, Supervisors: Professor Pete Walker and Dr Dina D'Ayala, UK, 2006.

Levy, A.M., Lacroix, A., Les Mineraux Des Roches, Librarie Polytechnique, Baudry Et C. Editeurs, Paris, 1888.

Liptak, B.G., "Elemental Monitors", Instrument Engineers' Handbook, Process Measurement and Analysis, Volume 1, London, New York, Washinghton,, pp. 1344-1346, 2003.

Livius, T., Roma Tarihi Şehrin Kuruluşundan İtibaren, (Çeviren: Sabahat Şenbark), Arkeoloji ve Sanat Yayınları, İstanbul, 1994.

Luke, M., Snell P.E., "Using the Rebound Hammer" Western Technologies Inc., Poenix AZ, Proceedings of the 11th Annual Mongolian Concrete Conference, 2012.

MacDonald, W.L., The Architecture of the Roman Empire, Volume II, An Urban Appraisal, Yale University Press, New Haven and London, 1986.

Magee, A.W., Bull, P.A., Goudie, A.S., "Before rock decay: chemical weathering of constituent grains by salts", Engineering geology of ancient works, monuments and historical sites (Editors: Paul G. Marinos and George C. Koukis), Balkema Publishers, Rotterdam, pp. 779–786, 1988.

Magie, D., Roman Rule in Asia Minor, Volume 1, Princeton University Press, USA, 1948.

Magie, D., Anadolu'da Romalılar, (Çevirenler: Nezih Başgelen-Ömer Çapar), Arkeoloji ve Sanat Yayınları, İstanbul, 2001.

Mallwitz, A., Olympia and Seine Bouten, Wissenschaftliche Buchgesellschaft Publisher, Darmstadt, 1972.

Marey Mahmoud, H., Ali M.F., Pavlıdou E., Kantiranis, N., El-Badry, A., "Characterization of plasters from Ptolemaic Baths: New excavations near the Karnak Temple Complex, Upper Egypt", Archaeometry, Vol. 53, Iss. 4, pp. 693-706, 2011.

Martial, M.V., (translated by, Walter, C. A., Ker, M.A.), Martial Epigrams, London

Heinemann Collection, G. P. Putnam's Sons Publisher, New York, 1919.

Means, R.E., Parcher, J.V., Physical Properties of Soils, Charles E. Merrill Books, Columbus, Ohio, 1963.

Meiggs, R., Roman Ostia, 2nd Edition, Oxford University Press, UK, 1973.

Middendorf, B., Knöfel, D., "Use of Old and Modern Analytical Methods for the Determination of Ancient Mortars in Northern Germany", Proceedings of the 3rd Expert Meeting, Hamburg, NATA-CCMS Pilot Study on Conservation of Historic Brick Structures, Berlin, pp. 75-92, 1990.

Miller, D., Artefacts and the meaning of things, in The companion encyclopedia of anthropology, (Editor: Tim Ingold), Routledge, London, pp. 396–419, 1994.

Mitchell, S., "R.E.C.A.M. Notes and Studies No.1: Inscription of Ancyra", Anatolian Studies, Vol. 27, pp. 63-103, 1977.

Mitchell, S., "Imperial Building in the Eastern Roman Provinces", Harvard Studies in Classical Philology, Vol. 91, pp. 333-365, 1987.

Mitchell, S., Anatolia Land, Men, and Gods in Asia Minor, Volume I, The Celts And The Impact of Roman Rule, Clarendon Press, Oxford, UK, 1993.

Mommsen, H., "Provenance determination of pottery by trace element analysis: problems, solutions and applications", Journal of Radioanaltical and Nuclear Chemistry, Vol. 247, Iss. 3, pp. 657-662, 2001.

Mutlu, Ö., Integration of the Roman Remains in Ulus Ankara within in the Current Urban Contex, Restoration in Architecture Department of METU, MA Thesis, Supervisor: Prof. Dr. A. Güliz Bilgin Altınöz, Ankara, Turkey, 2012.

Nalbant, K., Conservation and Restoration Project Reports & Drawings of Roman Bath in Ankara, Miyar Architectural Office, Ankara, 2014.

Nielsen, I., Thermae et Balnea: The Architecture and Cultural History of Roman Public Baths, Volume 2, Aarhus University Press, Denmark, 1993.

Nielsen, I., "Early Provincial Baths and their Relations to Early Italic Baths", Journal of Roman Archaeology, Portsmouth, Rhode Island, USA, pp. 35-44, 1999.

O'Connor, T., Science, evidential archaeology and new scholasticism, Scottish Archaeological Review 8, pp. 1-7, 1991.

Oğuz, C., Turker, F., Kockal N.U.,"Construction Materials Used in the Historical Roman Era Bath in Myra", The Scientific World Journal, pp. 1-9, 2014.

Özand, E., Ankara Şehri Su Tesisleri, Ankara Sular İdaresi, Ankara, 1967.

Özışık, G., Yapı Mühendisliğinde Tuğla Elemanlar ve Yapı Sistemleri, Birsen Yayınevi, İstanbul, 2000.

Paulin, E., Restauration des monuments antique: Thermes de Diocletien, Firmin-Didot Publisher, Paris, 1890.

Peacock, D. P., "Neolithic Pottery Production in Cornwall", Antiquity, Vol. 43, Iss. 170, pp. 145–149, 1969a.

Peacock, D.P., "A Contribution to the Study of Glastonbury Ware from South-Western Britain", Antiquaries Journal, Vol. 49, Iss. 1, pp. 41–61, 1969b.

Peacock, D.P., Pottery in the Roman World: An Ethnoarchaeological Approach, (Longman Archaeology Series), Longman Publishing Group, London and New York, 1982.

Platon, Platon Yasalar I, II, (Çevirenler: Candan Şentuna-Saffet Babür), Kabalcı Yayınevi, İstanbul, 1998.

Pliny the Elder, The Natural History, (translated by John Bostock, H.T., Riley, Henry G., Bohm), Cambridge, Massachusetts, Harvard University Press, London, 1857.

Pollard, A.M., Heron, C., Archaeological Chemistry, Royal Society of Chemistry, Cambridge, UK, 1996.

Prioreschi P., Brief History of Medicine: Primitive and Ancient Medicine, Edwin Mellen Press, New York, 1991.

Prokopios, İstanbul'da Iustinianus Döneminde Yapılar, (Çeviren: Erendiz Özbayoğlu), Arkeoloji ve Sanat Yayınları, İstanbul, 1994.

Radt, W., Pergamon: Antik Bir Kentin Tarihi ve Yapıları, Yapı Kredi Yayınları, İstanbul, 2001.

Rapp, G., Archaeomineralogy (Natural Science in Archaeology), Springer, Berlin Heidelberg New York, 2002.

Rich A.B., A Dictionary of Roman and Greek Antiquities, Longmans, Green, Company, London, 1873.

RILEM, Tentative Recommendations, in: Commission-25-PEM, Recommended Test to Measure the Deterioration of Stone and to Assess the Effectiveness of Treatment Methods, Materials and Structures, Vol. 13, No. 73, pp. 173-253, 1980.

Ring, J.W.,"Windows, Baths, and Solar Energy in the Roman Empire", American Journal of Archaeology Vol. 100, No. 4, pp. 717-724, 1996.

Robert, L., "Inscription agonistique d'Ancyre, Concours d'Ancyre", Hellenica 11/12, pp. 350-368, 1960.

Rook, T., "The Development and Operation of Roman Hypokausted Baths", Journal of Archeological Science, Vol. 5, Iss. 3, pp. 269-282, 1978.

Roueché, C., Performers and Partisans at Aphrodisias in the Roman and Late Roman Periods, (Journal of Roman studies monograph VI), Society for the Promotion of Roman Studies, London, 1993.

Sağın E.U., "Anadolu'da Roma Dönemi Yapı Tuğlalarının Özellikleri", Mühendislik Mimarlık Fakültesi Dergisi, Journal of the Faculty of Engineering and Architecture of Gazi University, Cilt: 32, Sayı:1, s. 205-214, 2017.

Salmon, M.E., "An X-Ray Fluorescence Method for Micro-Samples", IIC American Group Technical Papers from 1968 through 1970, IIC-American Group, New York, pp. 31-46, 1970.

Scarborough, J., Roman Medicine, First Edition, Cornell University Press, New York, 1969.

Scherrer, P., Efes Rehberi, Avusturya Arkeoloji Enstitüsü ve Efes Müzesi İşbirliği, Ege Yayınları, İstanbul, 2000.

Schiffer, M.B., "Some Relationships between Behavioural an Evolutionary Archaeologies", American Antiquity, Vol. 61, Iss. 4, pp. 643-662, 1996.

Sevimli, Ş., Anadolu Uygarlıklarında Temizlik Kavramı ve Uygulamalarının Evrimi, Çukurova Üniversitesi Sağlık Bilimler Enstitüsü Deantoloji ve Tıp Tarihi Anabilim Dalı, Doktora Tezi, Danışman: Prof. Dr. İlter Uzel, Adana, 2005.

Shackley, M.S, (Ed.), "An Introduction to X-Ray Fluorescence (XRF) Analysis in Archaeology", X-Ray Fluorescence Spectrometry (XRF) in Geoarchaeology, Springer, New York, pp. 7-44, 2011.

Sherwood, A.N., Roman Architectural Influence in Provincia Asia: Augustus to Severus Alexander, Art and Archaeology Department of Princeton University, PhD Thesis, Supervisors: John W. Humphrey. Michael Walbank. Bob Schmiel, and Barry Baldwin, New Jersey, USA, pp. 178-194, 2000.

Sičáková, A., "Basics of Building Materials", Technická univerzita v Košiciach (Technical University of Kosice) Publications, Slovakia, 2015.

Skoog, D.A., Holler, F.J., Crouch, S.R., Principles of Instrumental Analysis, 6th Edition, Thomson Brooks/Cole, Belmont, California, pp. 317-325 , 2007.

Smith, W., ed., Dictionary of Greek and Roman Geography, Little, Brown Company, Boston, 1870.

Smolijaninovaitė, K., A, Study on Historic Hamams in Istanbul Changing Aspects of Cultural Use and Architecture, Arts in World Heritage Studies Department,

Brandenburg University of Cottbus, MA Thesis, Supervisors: Prof. Dr. phil. Habil Marie-Theres Albert (Brandenburgische Technische Universität Cottbus) and Dr. Zeynep Kuban (Istanbul Technical University), Brandenburg, Germany, 2007.

Staggs, H.J., Roman Baths at Antiochia Ad Cragum: A Preliminary Evaluation of Bath Architecture As Social Signals in the Ancient Mediterranean World, Anthropology Department, University of Nebraska – Lincoln, MA Thesis, Supervisor: Professor LuAnn Wandsnider, Lincoln, US, 2014.

Stefanidou, M., Pachta V., Konopissi S., Karkadelidou F., Papayianni I., "Analysis and characterization of hydraulic mortars from ancient cisterns and baths in Greece", Materials and Structures, Vol. 47, Iss. 4, pp. 571–580, 2014.

Stephens, W.E., Calder, A. "Analysis of Non-Organic Elements in Plant Foliage Using Polarised X-Ray Fluorescence Spectrometry", Analitica Chimica Acta 527, pp. 89-96, 2004.

Strabon, Geographika, Antik Anadolu Coğrafyası, Kitap: XII-XIII-XIV, (Çeviren: Adnan Pekman), Arkeoloji ve Sanat Yayınları, İstanbul, 2000.

Strickland, M.H., Roman Building Materials, Construction Methods and Architecture: The identity of an Empire, Art History Department, Graduate School of Clemson University, MA Thesis, Supervisors: Pamela Mack, Alan Grubb and Caroline Dunn, South Carolina, USA, pp. 41-43, 2010.

Şener, Y.S., "Ankara Roma Hamamı'nda Koruma Çalışmaları: Yapısal Malzeme Bozulmaları ve Öneriler", 39. Uluslararası Kazı, Araştırma ve Arkeometri Sempozyumu, Cilt: 2, s. 233-255, Bursa, Türkiye, 2018.

Şimşek, C., "İkici Sezon Hierapolis Roma Hamamı Kazı Çalışmaları", 5. Müze Kurtarma Kazıları Semineri, Didim, Türkiye, T.C. Kültür Bakanlığı Yayınları, Ankara, s. 243-264, 1996.

Tanrıverdi, Z., Akyol, A.A., Atalay, Ü., "Ankara Roma Hamamı Yapı Malzemelerinde Arkeometrik Çalışmalar", 39. Uluslararası Kazı, Araştırma ve Arkeometri Sempozumu, Cilt: 1, s. 13-37, Bursa, Türkiye, 2018.

Temizsoy, İ., Esen, İ., Ateşoğulları S., "Ankara Roma Hamamı 2001 Yılı Kurtarma Kazıları" Sempozyumu, 13. Müze Çalışmaları ve Kurtarma Kazıları Sempozyumu, Denizli, Türkiye, Kültür Bakanlığı Anıtlar ve Müzeler Genel Müdürlüğü Yayınları, Ankara, s. 145-158, 2002.

Teutonico, J.M., A Laboratory Manual for Architectural Conservators, ICCROM, Rome, Italy, pp: 32-122, 1988.

Thorpe, M., Roma Mimarlığı, (Çeviren: Rıfat Akbulut), Homer Yayınevi, İstanbul, 2002.

Tite, M.S., Methods of physical examination in archaeology (Studies in archaeological science), Seminar Press, London, 1972.

Tite, M.S., Maniatis, Y., "Examination of ancient pottery using the scanning electron microscope", Nature International Journal of Science, Vol. 257, pp. 122-123, 1975.

Tite, M.S., "Archaeological Science - Past Achievements and Future Prospects", Archaeometry, Vol. 33, Iss. 2, pp. 139-151, 1991.

Torraco, G., Porous Building Materials, Materials Science for Architectural Conservation, ICCROM, Rome, Italy, 1988.

Tournefort, J.P. de, Relaxion d'un voyage du Levant (1717), Tournefort Seyahatnamesi, (Çeviren: Ali Berktay), (Editor: Stefanos Yerasimos), Kitap Yayınevi, İstanbul, 2005.

TS 699, Natural Building Stones- Methods of Inspection and Laboratory Testing, Turkish Standards Institution, Ankara, 2009.

TS EN 933-1/2012, Tests for geometrical properties of aggregates- Part 1: Determination of particle size distribution – Sieving method, Turkish Standards Institution, Ankara, 2012.

Uğurlu, E., Böke, H., "The use of brick-lime plasters and their relevance to climatic conditions of historic bath buildings", Construction and Building Materials, Vol. 23, Iss. 6, pp. 2442-2450, 2009.

Umar, B., Pisidia, Akbank Yayınları, İstanbul, 1989.

Ürük, Z.F., "Medeniyetler içinde Hamamın Gelişimi ve Kültürel Olarak Mekan Analizleri", Akademik Sosyal Araştırmalar Dergisi, Yıl: 4, Sayı: 28, s. 185-209, 2016.

Vandenabeele, P., Practical Raman Spectroscopy: An introduction, First edition, John Wiley & Sons Publishing Company, US, 2013.

Vereş, D.Ş., "A Comparative Study Between Loss on Ignition and Total Carbon Analysis on Minerogenic Sediments", Studia Universitatis Babeş-Bolyai, Geologia XLVII, 1, Romania, pp. 171-182, 2002.

Vitruvius, P.M., Vitruvius The Ten Books on Architecture, (translated by Morris Hicky Morgan), Harvard University Press, Cambridge, 1914.

Vitruvius, P.M., Mimarlık Üzerine On Kitap, The Ten Books On Architectura, (Çeviren: Suna Güven), Şevki Vanlı Mimarlık Vakfı Yayınları, Yapı Endüstri Merkezi, Ankara, 1990.

Walter, E., Dean, J.R., "Determination of Carbonate and Organic Matter in Soils,

Calcareous Sediments and Sedimentary Rocks by Loss on Ignition", Journal of Sedimentary Petrology, Vol. 44, No. 1, pp. 242-248, 1974.

Wentwort, C.K., "A scale of Grade and Class Terms for Clastic Sediments", Journal of Geology Vol. 30, No. 5, pp. 377-392, 1922.

Wheeler, M., Roma Sanatı ve Mimarlığı, (Çeviren: Zeynep Koçel Erdem), Homer Kitabevi, İstanbul, 2004.

Whitmore, A.M., Small finds and the social environment of the Roman baths, Anthropology Department, University of Iowa, PhD Thesis, Supervisor: Associate Professor Glenn R. Storey, Iowa, U.S., 2013.

Yegül, F.K., The Bath-Gymnasium Complex at Sardis (Archaeological Exploration of Sardis Report 3), Harvard University Press, Cambridge, 1986.

Yegül, F.K., Baths and Bathing in Classical Antiquitiy, MIT Press Cambridge, or Architectural History Foundation, New York, 1992.

Yegül F., "Efes ve Sardis: Antik Çağda Kentleşme ve Anadolu Seçeneği", 1994 Yılı Anadolu Medeniyetleri Müzesi Konferansları, T.C. Kültür Bakanlığı Yayınları, Ankara, 1995.

Yegül, F.K., Antik Çağ'da Hamamlar ve Yıkanma, Homer Kitabevi ve Yayıncılık, İstanbul, 2006.

Yegül, F.K., Roma Dünyasında Yıkanma, Koç Üniversitesi Yayınları, İstanbul, 2010.

Zajac, N., "The Thermae: a Policy of Public Health or Personal Legitimation?", Journal of Roman Archaeology, Portsmouth, Rhode Island, USA, pp. 99-105, 1999.

Web

AAMM, Ankara Anadolu Medeniyetler Müzesi-1921, Ankara Roma Hamamı, (n.d.), http://www.anadolumedeniyetlerimuzesi.gov.tr., visited in August 12, 2017.

AİKVTM, Aydın İl Kültür ve Turizm Müdürlüğü, "Milet", (n.d.), http://www.aydinkulturturizm.gov.tr/TR,64428/milet.html, visited in May 8, 2018.

Başaran, T., "Tarih ve Arkeoloji Antik Roma Hamamlarında Ağaç Katliamı", 2014, https://tarihvearkeoloji.blogspot.com.tr/2014/12/antik-roma-hamamlarnda-agac-katliam.html, visited in May 10, 2018.

Crouch D.P., Ortloff, Ch.,"Ephesus Municipal Water System Analysis," Zeitschrift für klassische Archäologie 5 / XII / 1997, http://homepage.univie.ac.at/elisabeth.trinkl/forum/forum1297/05wass.htm, visited in May 8, 2018.

Deniz, K., Jem 419/Jem 459 Magmatik Petrografi Dersi, (n.d.), https://acikders.ankara.edu.tr/pluginfile.php/58483/mod_resource/content/1/JEM419-459_MagmatikPetrografiDersi_5.Hafta.pdf, visited in October 19, 2018.

DİKVTM, Denizli İl Kültür ve Turizm Müdürlüğü, "Pamukkale Hierapolis Ancient City", (n.d.), http://www.pamukkale.gov.tr/en/ancient-cities/pamukkale-hierapolis, visited in May 8, 2018.

EuLA-European Lime Association, Lime in Mortars, Benefits of using lime-based mortars, Brussels, Belgium, 2008, https://www.britishlime.org/documents/EuLA_Lime_in_Mortars.pdf, visited in June 9, 2018.

Gossman Forensics, A Division of Chem Right Laboratories, Inc. "How Does Scanning Electron Microscope/Energy Dispersive X-ray (SEM/EDX) Work? (n.d.), "http://www.gossmanforensics.com/pdf-library/pdf-analytical-methods/sem-edx.pdf, visited in Sep 26, 2017.

İİKVTM, İzmir İl Kültür ve Turizm Müdürlüğü, "Efes", (n.d.), http://www.izmirkulturturizm.gov.tr/TR,77418/efes-selcuk.htm, visited in May 8, 2018.

KVKBK - Kültür Varlıklarını Koruma Bölge Kurulu- Cultural inventory list of Ankara, 2005 Decree Date and No: 9.12.2005- 1110, http://www.korumakurullari.gov.tr/Eklenti/41321,ankara-envanter.pdf?, visited in April 17, 2018.

KVVMGM - Kültür Varlıkları ve Müzeler Genel Müdürlüğü, "Sardes Antik Kenti ve Bintepeler Lidya Tümülüsleri" (n.d.), http://www.kulturvarliklari.gov.tr/TR,51373/sardes-antik-kenti-ve-bintepeler-lidya-tumulusleri-mani-.html, visited in May 8, 2018.

Labate, V., Roman Walls, Article, Ancient History Encyclopedia, 31 August, 2016, https://www.ancient.eu/article/942/roman-walls/, visited in May 21, 2018.

Ladstatter, S., Zabrana, L., Efes Antik Kenti, (n.d.), http://www.aktuelarkeoloji.com.tr/efes-antik-kenti, visited in May 8, 2018.

Marble Density-Aqua-Cal, (n.d.), https://www.aqua-calc.com/page/density-table/substance/marble, visited in June 8, 2018.

MGM, Meteroloji Genel Müdürlüğü; İllerimize ait İstatistikî Veriler, (n.d.), https://www.mgm.gov.tr/veridegerlendirme/il-ve-ilceler-istatistik.aspx, visited in May 28, 2018.

MİKVTM - Manisa İl Kültür ve Turizm Müdürlüğü, "Sardes Antik Kenti (Salihli)" (n.d.),

http://www.manisakulturturizm.gov.tr/TR,73014/sardes-antik-kenti-salihli.html, visited in May 8, 2018.

Miszczak, I., Turkish Archaeological News, "Perge",2017, http://turkisharchaeonews.net/site/perge, visited in May 8, 2018.

MTA – Maden Tetkik Arama Genel Müdürlüğü, (Düzenleyen: Necati Turhan), 2002, http://www.mta.gov.tr/v2.0/dairebaskanliklari/jed/images/harita_basimi/1_500_olcek li_haritalar/ankara_b.jpg, visited in June 9, 2018.

Muench, S.T., "Ancient Roman Concrete", Brewminate A Bold Blend of News&Ideas, December 8, 2017,
https://brewminate.com/understanding-roman-concrete/ visited in November 19, 2018.

Nenova, S., Ancient World Alive, Ancient Greek and Roman Bathing, October 27, 2015, http://www.ancientworldalive.com/single-post/2015/10/27/Ancient-Greek-and-Roman-Bathing, visited in March 2, 2018.

Nicholls, M., "Aqueducts and drainage", (n.d.), https://www.futurelearn.com/courses/rome/0/steps/27623, visited in May 9, 2018.

Pidwirny, M., "Weathering", Fundamentals of Physical Geography, 2nd Edition. Date, 2006 viewed, http://www.physicalgeography.net/fundamentals/10r.html, visited in June 4, 2018.

Pinterest, Antik Mimari ile İlgili Bilgileri Keşfedin, (n.d.), www.pinterest.com, visited in May 11, 2017.

Sharo, C., Roman Architecture, Presentation on Prezi, 16 June 2016, https://prezi.com/q7cd5kiezjzw/roman-architecture/, visited in November 19, 2018.

Stilwell, R.; MacDonald, W. L.; McAlister, M. H., The Princeton Encyclopedia of Classical Sites, 1999,
http://www.perseus.tufts.edu/hopper/text?doc=Perseus:text:1999.04.0006:entry=mile tos, visited May 8, 2018.

Squires, N., Virtual reality goggles unlock splendour of huge ancient Roman baths complex, Rome 20 December, 2017,
https://www.telegraph.co.uk/news/2017/12/19/virtual-reality-goggles-unlock-splendour-huge-ancient-roman/, visited in May 21, 2018.

Thermo Scientific, "Introduction to Raman Spectroscopy" (n.d.), http://www.biotechprofiles.com.tr , visited in Oct 11, 2017.

UNESCO, Pergamon and its Multi-Layered Cultural Landscape (n.d.), https://whc.unesco.org/en/list/1457, visited in May 8, 2018.

www.googleearth.com. "Ankara Roma Hamamı" (n.d.), visited in January 10, 2017

Yegül, F., Roman Building Technology and Architecture, University of California, Santa Barbara, (n.d.), https://archserve.id.ucsb.edu/courses/arthistory/152k/, visited, May 22, 2018.

Yıldız, M., Roma İmparatorluğunda Yıkanma Kültürü, Word Arkeoloji, 2017, http://worldarkeoloji.blogspot.com/2017/11/roma-imparatorlugunda-hamamlar-ve.html, visited in May 19, 2018.

SAMPLE FIGURES OF THE THESIS
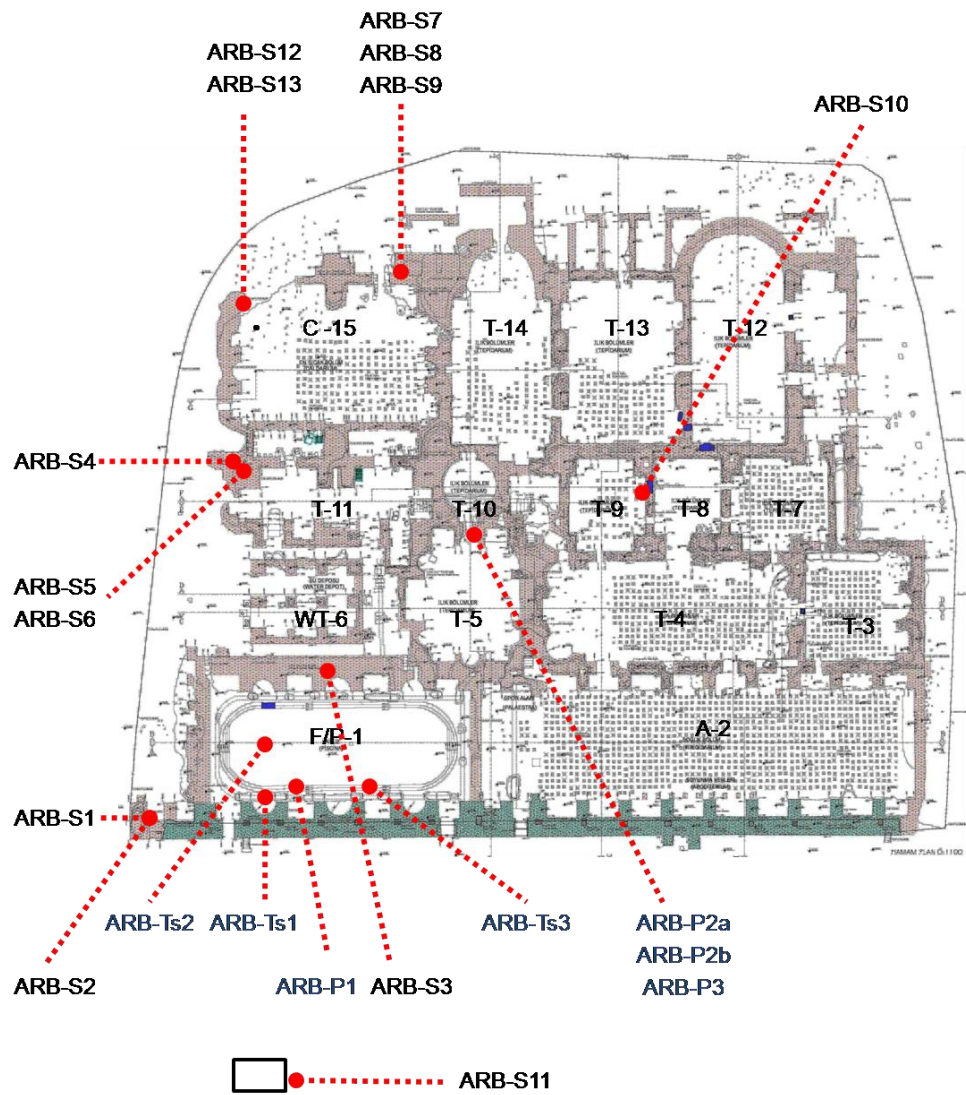
Figure A.1 The location of stone, stone tessera and plaster samples on the plan
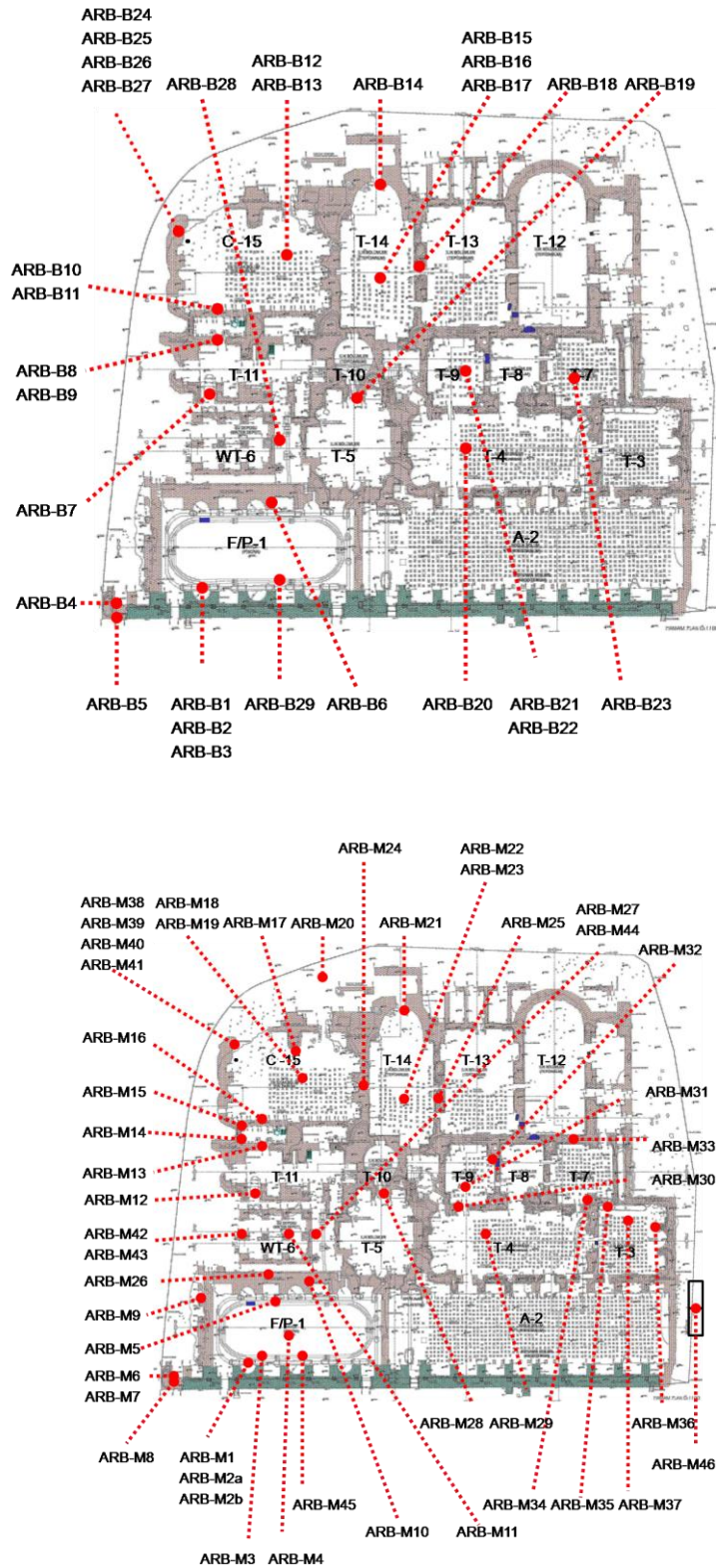
Figure A.2 The location of brick and mortar samples on the plan

178
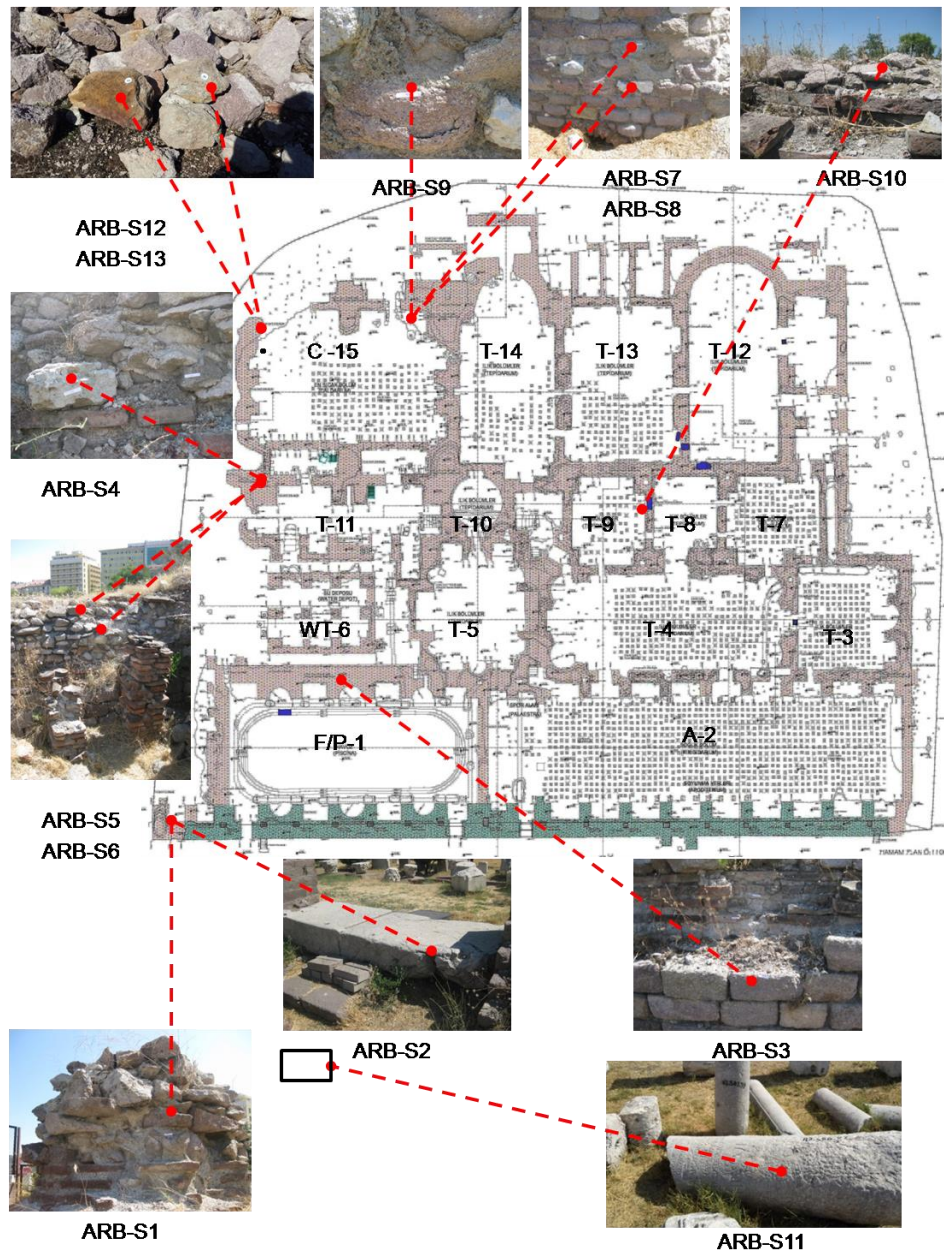
Figure A.3 Photographs of stone samples on the plan
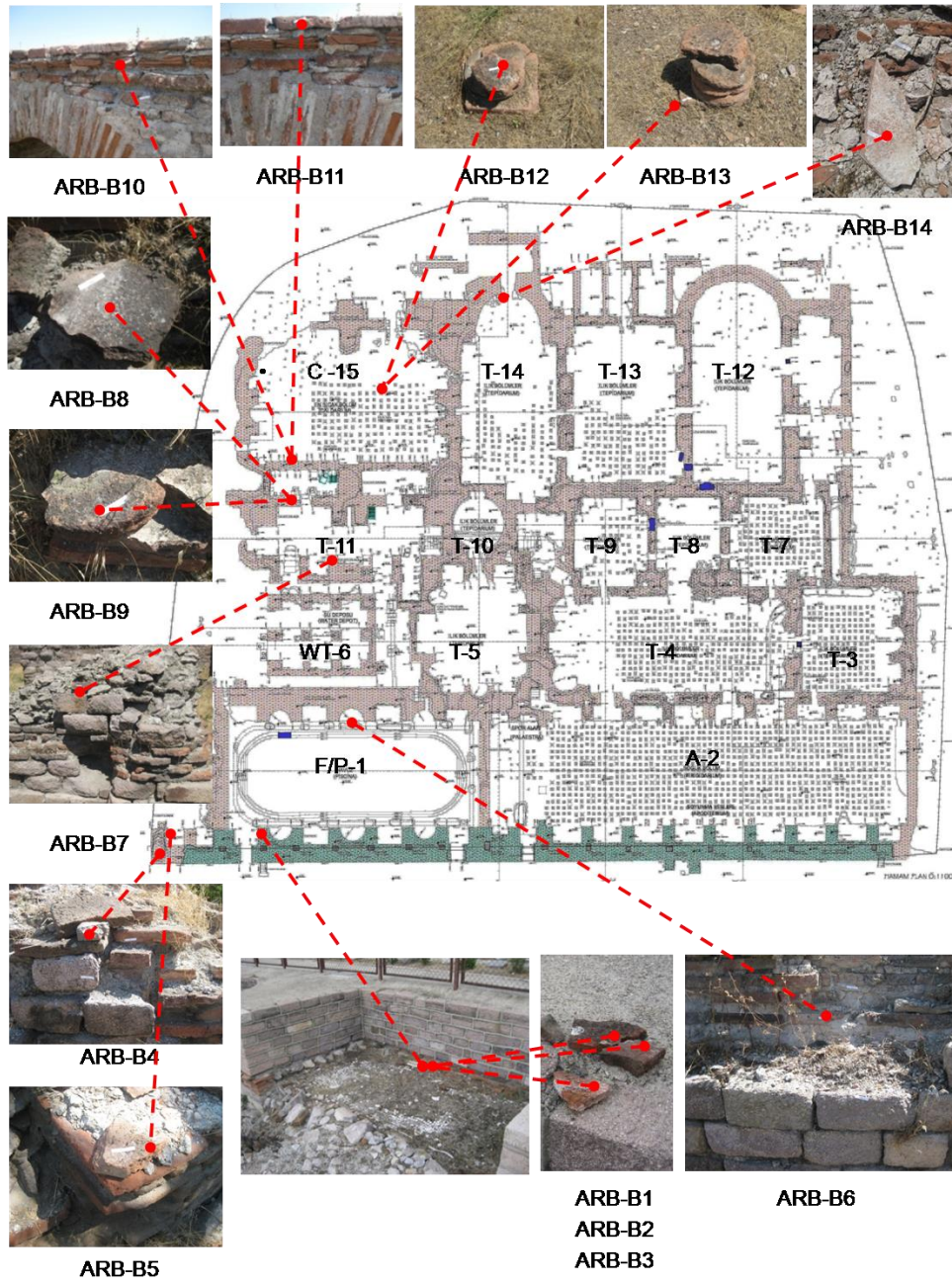
Figure A.4a Photographs of brick samples on the plan

180
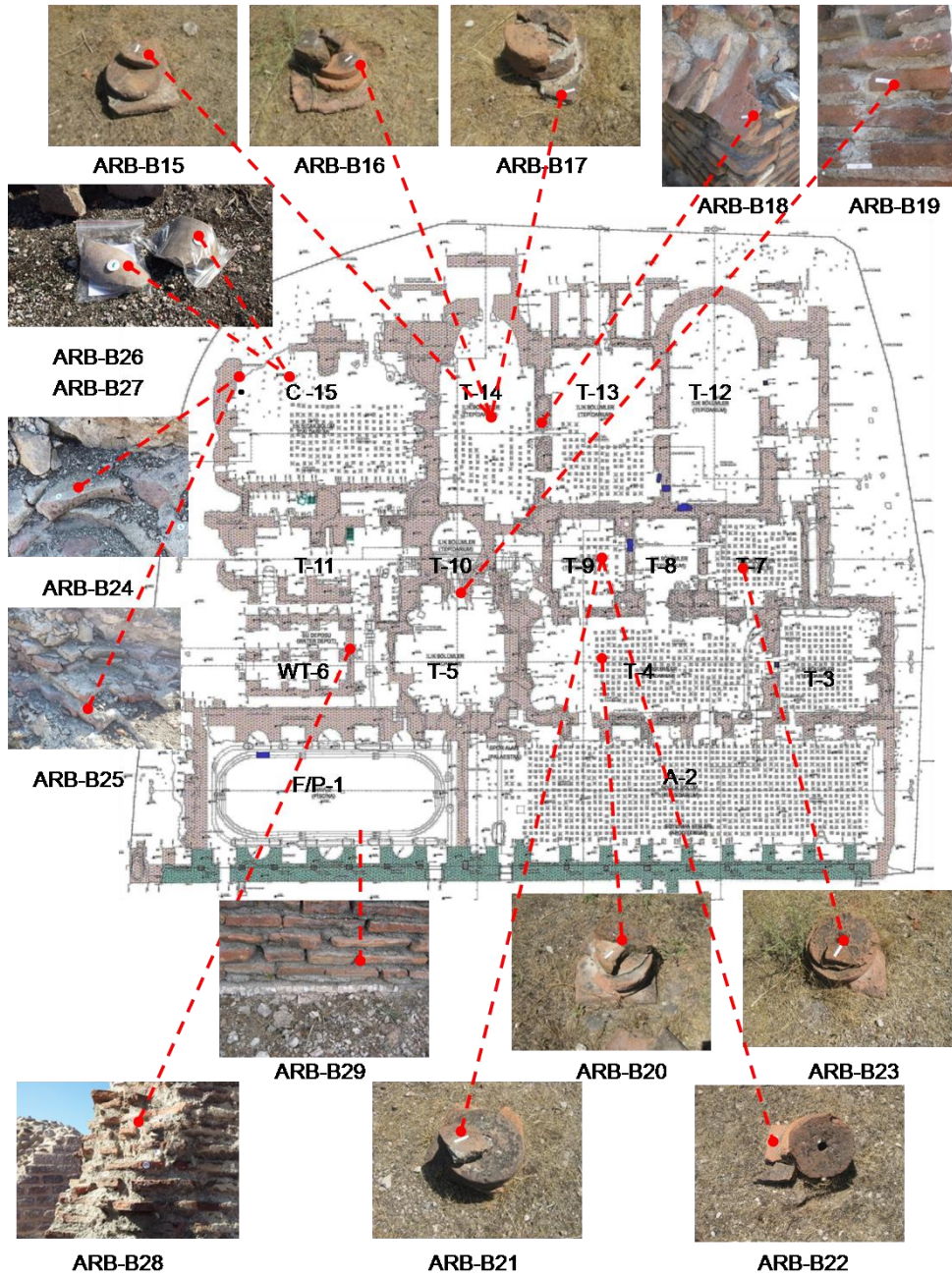
Figure A.4b Photographs of brick samples on the plan
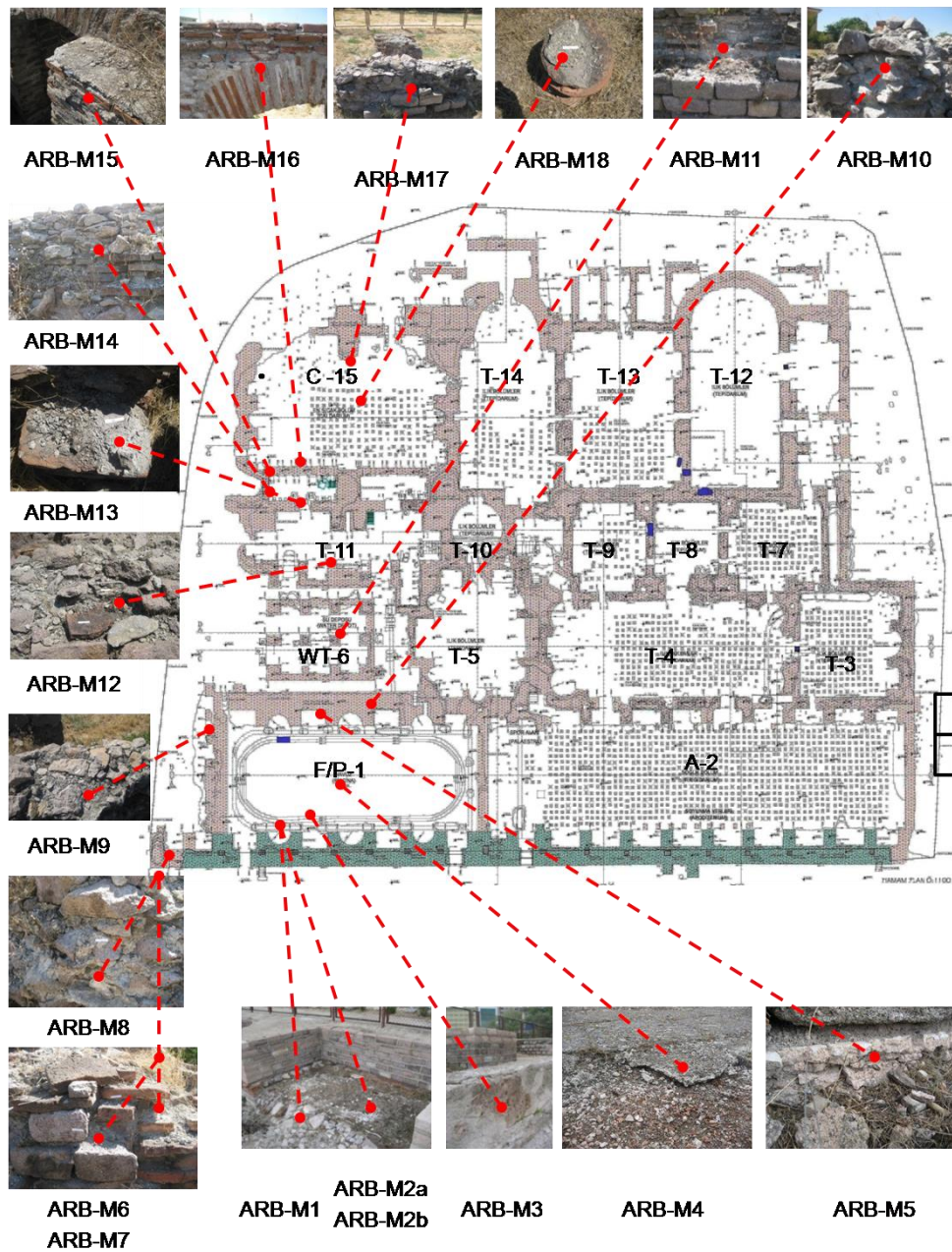
Figure A.5a Photographs of mortar samples on the plan

182
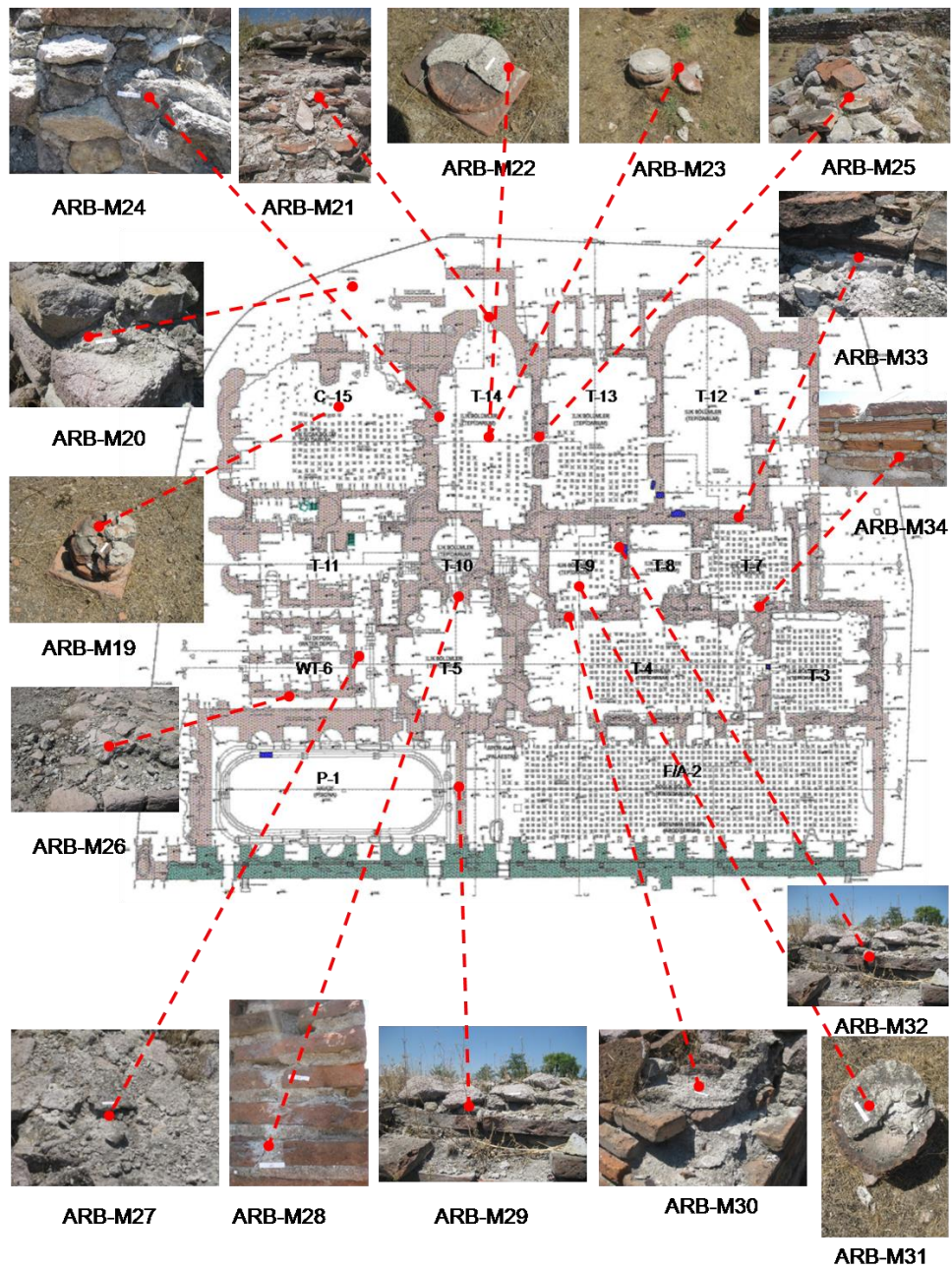
Figure A.5b Photographs of mortar samples on the plan
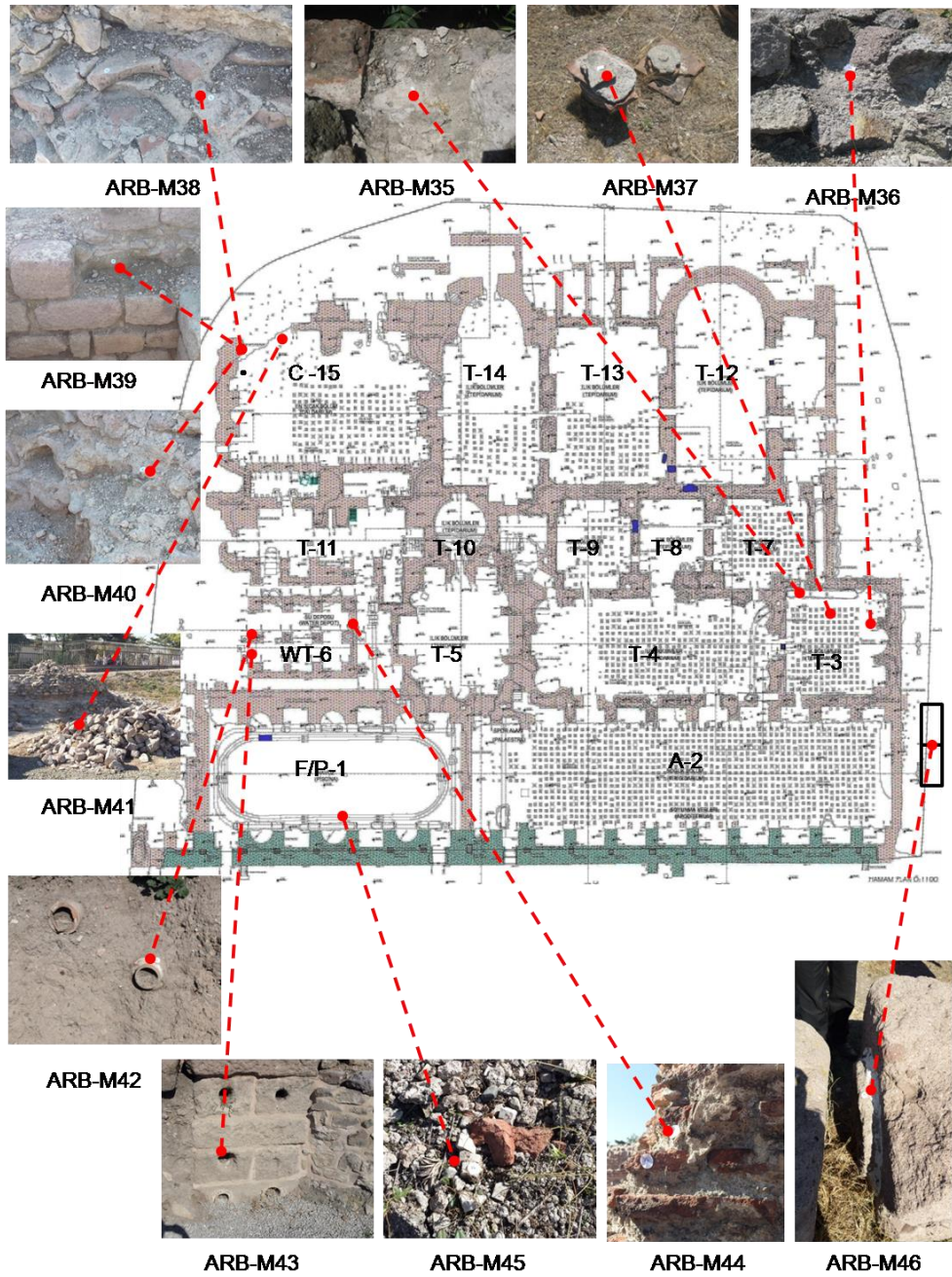
Figure A.5c Photographs of mortar samples on the plan
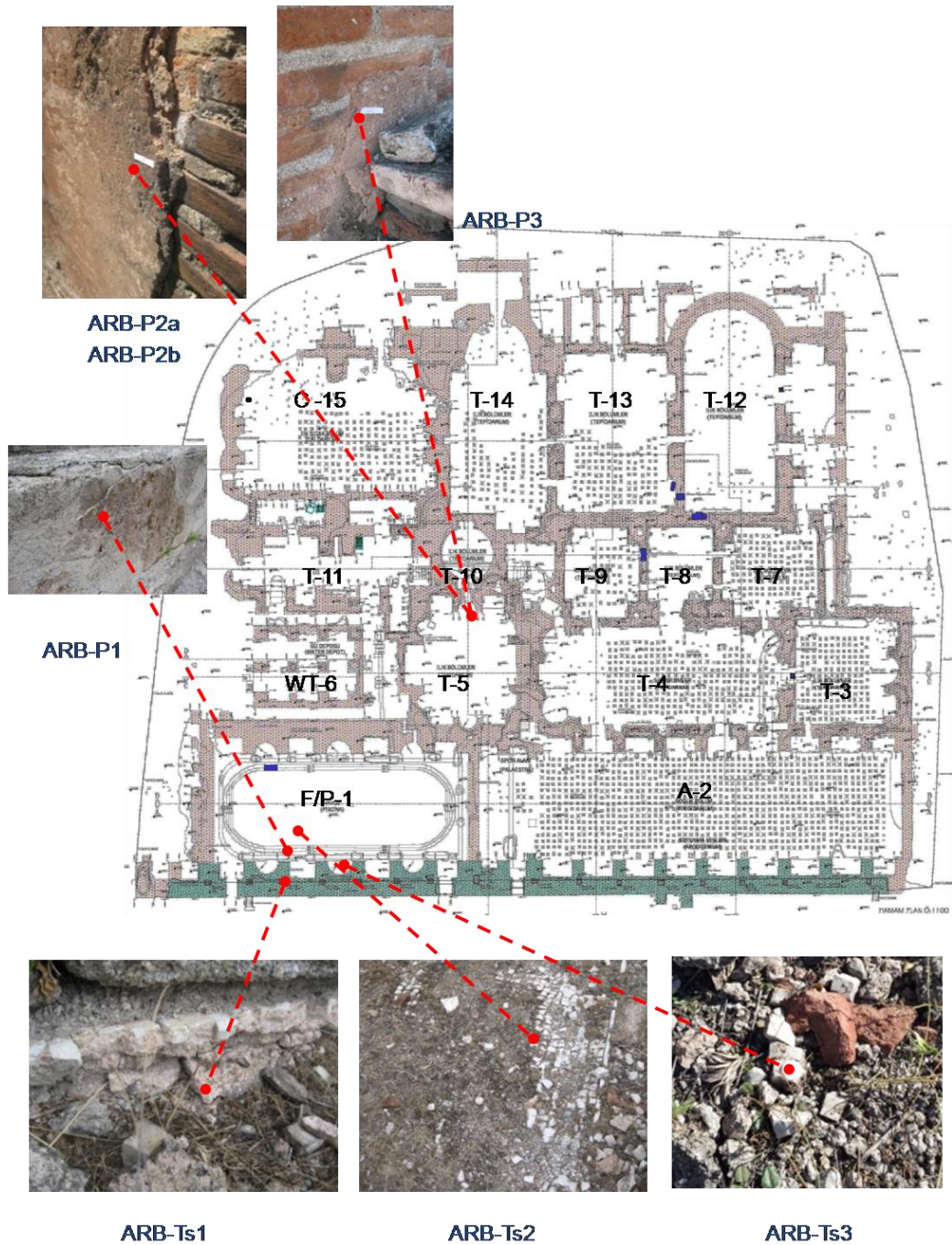
Figure A.6 Photographs of plaster and stone tessera samples on the plan

Table A.1 Descriptions of the stone samples collected from the Roman Bath

Samples	Section	Description
ARB-S1	F/P-1	Stone from corner of the southeast stone wall (13)*
ARB-S2	F/P-1	Stone from the base of southeast wall (16)
ARB-S3	P-1	Stone from the west wall of Piscina-1(20)
ARB-S4	T-11	Stone from rubble filled of southwest of Tepidarium-11 (28)
ARB-S5	T-11	Stone from rubble filled of southwest of Tepidarium-11 (29)
ARB-S6	T-11	Stone from rubble filled of southwest of Tepidarium-11 (30)
ARB-S7	C-15	Stone from the northwest wall of Caldarium-15 (41)
ARB-S8	C-15	Highly deteriorated stone from northwest wall of Caldarium-15 (42)
ARB-S9	C-15	Highly deteriorated stone from northwest wall of Caldarium-15 (43)
ARB-S10	T-9	Stone from over the arched of northwest wall of Tepidarium-9 (68)
ARB-S11	-	Structural component of the upper part (1)
ARB-S12	C-15	Stone from corner of the exterior southwest wall of Caldarium-15 (10)
ARB-S13	C-15	Stone from corner of the exterior southwest wall of Caldarium-15 (11)

Table A.2 Descriptions of stone tessera samples collected from the Bath

Samples	Section	Description
ARB-Ts1	P-1	Stone Tessera from base of the niche of the east of Piscina (1)*
ARB-Ts2	P-1	Stone Tessera from base of Piscina-1 (9)
ARB-Ts3	P-1	Stone Tessera from base of the niche of the east of Piscina-1 (18)

Table A.3 Descriptions of the plaster samples collected from the Roman Bath

Samples	Section	Description
ARB-P1	P-1	Plaster of the northeast façade of Piscina-1 (7)*
ARB-P2a	T-5	Upper plaster layer of the west wall of Tepidarium-5 (56)
ARB-P2b	T-5	Lower plaster layer of the west wall of Tepidarium-5 (56)
ARB-P3	T-5	Plaster from the west wall of Tepidarium-5 (57)

(*) Specified Numbers indicate the order of the sampling

Table A.4 Descriptions of brick, pilae and pipe samples collected from the Bath

Type	Samples	Section	Description
Brick	**ARB-B1**	**P-1**	Brick from base of the east niche of Piscina-1(3)*
	ARB-B2	**P-1**	Brick from base of the east niche of Piscina-1 (4)
	ARB-B3	**P-1**	Brick from base of the east niche of Piscina-1 (5)
	ARB-B4	**F/P-1**	Brick from the corner of the southeast wall (11)
	ARB-B5	**F/P-1**	Brick from console of the extansion of southeast wall (15)
	ARB-B6	**P-1**	Brick from the west wall of Piscina (19)
	ARB-B7	**T-11**	Brick from the northeast wall of Tepidarium-11 (22)
	ARB-B8	**T-11**	Brick from the of southwest of Tepidarium-11 (24)
	ARB-B11	**T-11**	Brick from the arched wall masonry, the southwest of Tepidarium-11 (34)
	ARB-B14	**T-14**	Brick from the southwest wall of Tepidarium-14 (45)
	ARB-B18	**T-14**	Brick from the arch of northwest wall of Tepidarium-14 (52)
	ARB-B19	**T-5**	Brick from the southwest wall of Tepidarium-5 (59)
	ARB-B24	**C-15**	Square brick from the corner of the exterior southwest wall of Caldarium-15 (2)
	ARB-B25	**C-15**	Brick from the corner of the exterior southwest wall of Caldarium-15 (4)
	ARB-B28	**WT-6**	Brick from the brickwork column neighboring of the northwest wall of Water Reservoir-6 (14)
	ARB-B29	**P-1**	Square brick from the seat of Piscina (Width-length: 39x39, height: 2,5-3 cm (17)
Brick	**ARB-B10**	**T-11**	Repair brick over the arched wall the east of southwest of Tepidarium-11 (32)
Pilae	**ARB-B9**	**T -11**	Round pilae fromTepidarium-11 (25)
	ARB-B12	**C-15**	Round pilae from Caldarium-15 (38)
	ARB-B13	**C-15**	Square pilae from Caldarium-15 (39)
	ARB-B15	**T-14**	Round pilae from Tepidarium-14 (48)
	ARB-B16	**T-14**	Round pilae from Tepidarium-14 (49)
	ARB-B17	**T-14**	Square pilae from Tepidarium-14 (50)
	ARB-B20	**T-4**	Round pilae from Tepidarium-4 (62)
	ARB-B21	**T-9**	Round pilae from Tepidarium-9 (64)
	ARB-B22	**T-9**	Square pilae from Tepidarium-9 (66)
	ARB-B23	**T-7**	Round pilae from Tepidarium-7 (69)
Pipe	**ARB-B26**	**C-15**	Pipe from the corner of the exterior southwest wall of Caldarium-15 (8)
	ARB-B27	**C-15**	Pipe from the corner of the exterior southwest wall of Caldarium-15 (9)

(*) Specified Numbers indicate the order of the sampling

Table A.5 Descriptions of the mortar samples collected from the Roman Bath

Samples	Section	Type	Explanation
ARB-M1	P-1	BMJ(**)	Mortar from base of the northeast niche of Piscina-1 (1)*
ARB-M2a	P-1	MM	Mosaic mortar layer from the base of the northeast niche of Piscina-1 (2)
ARB-M2b	P-1	MM	Mosaic mortar layer from the base of the northeast niche of Piscina-1 (2)
ARB-M3	P-1	LM	Levelling mortar from the northeast seat wall of Piscina-1 (6)
ARB-M4	P-1	LM	Levelling mortar from the base of Piscina-1 (8)
ARB-M5	P-1	TM	Tessera bedding mortar from the base of Piscina-1 (9)
ARB-M6	F/P-1	BRFM	Bedding mortar bonds brick from the wall southeast corner (10)
ARB-M7	F/P-1	SRFM	Rubble filled mortar from the wall southeast corner of the Bath (12)
ARB-M8	F/P-1	SRFM	Rubble filled mortar from the extension wall of the southeast corner of (14)
ARB-M9	P-1	SRFM	Rubble filled mortar from the south exterior wall of Piscina-1 (17)
ARB-M10	P-1	SMJ	Mortar joint bonds brick from the west niche wall of Piscina-1 (18)
ARB-M11	WT-6	SRFM	Rubble filled mortar from the middle wall of Water Reservoir (21)
ARB-M12	T-11	SRFM	Rubble filled mortar from the brickwork of northeast of Tepidarium-11 (23)
ARB-M13	T-11	BMJ	Mortar joint bonds bricks from the brickwork of southwest of Tepidarium-11 (26)
ARB-M14	T-11	BRFM	Rubble filled mortar from the brickwork of the southwest of Tepidarium-11 (27)
ARB-M15	T-11	BMJ	Mortar from the brickwork of the southwest of Tepidarium-11 (31)
ARB-M16	C-15	BMJ	Mortar from the arched wall of the northeast of Caldarium-15 (33)
ARB-M17	C-15	SRFM	Rubble filled mortar from the southwest wall of Caldarium-15 (35)
ARB-M18	C-15	PMJ	Mortar joint bonds the round pilaes of Caldarium-15(36)
ARB-M19	C-15	PMJ	Mortar joint bonds the round pilaes of Caldarium-15 (37)
ARB-M20	C-15	BRFM	Rubble filled mortar from the southwest exterior wall of Bath (40)
ARB-M21	T-14	BRFM	Rubble filled mortar from the west wall of Tepidarium-14 (44)
ARB-M22	T-14	PMJ	Mortar joint from the pilaes of Tepidarium-14 (46)
ARB-M23	T-14	PMJ	Mortar joint from the pilaes of Tepidarium-14 (47)
ARB-M24	T-14	BRFM	Rubble filled mortar from the southeast wall of Tepidarium-14 (51)
ARB-M25	T-14	BRFM	Rubble filled mortar from the northwest wall of Tepidarium-14(53)
ARB-M26	WT-6	BRFM	Rubble filled mortar from the northeast wall of Water Reservoir (54)
ARB-M27	WT-6	BRFM	Rubble filled mortar from the brickwork column neighboring of the northwest wall of Water Reservoir-6 (54)
ARB-M28	T-5	BMJ	Mortar joint from the southwest brickwork wall of Tepidarium-5 (60)
ARB-M29	P-1	BMJ	Mortar joint bonds bricks from the northwest wall of Piscina-1 (61)

(*) Specified Numbers indicate the order of the sampling
(**) Specified Types; BMJ: Brick Mortar Joint, MM: Mosaic Mortar, LM: Levelling Mortar, TM: Tessera Mortar, BRFM: Brick Rubble Filled Mortar, SRFM: Stone Rubble Filled Mortar, PMJ: Pilae Mortar Joint, pMJ: pipe Mortar Joint, SMJ: Stone Mortar Joint.

Table A.5 Continued

ARB-M30	T-4	BMJ(**)	Mortar joint bonds bricks from the southwest wall of Tepidarium-4 (63) *
ARB-M31	T-9	PMJ	Mortar joint bonds the pilaes of Tepidarium-9 (65)
ARB-M32	T-9	BRFM	Rubble filled mortar from the northwest wall of Tepidarium-9 (67)
ARB-M33	T-7	BMJ	Mortar joint from the southwest wall of Tepidarium-7 (70)
ARB-M34	T-7	BMJ	Mortar joint from the northeast wall of Tepidarium-7 (71)
ARB-M35	T-3	BMJ	Mortar joint through channel of the southwest wall of Tepidarium-3 (63)
ARB-M36	T-3	SRFM	Rubble filled mortar from the northwest wall of Tepidarium-3 (73)
ARB-M37	T-3	PMJ	Mortar joint bonds pilaes of Tepidarium-3 (74)
ARB-M38	C-15	SMJ	Mortar corner of the exterior southwest wall of Caldarium-15 (3)
ARB-M39	C-15	SMJ	Mortar from the level of the base of corner exterior southwest wall of Caldarium-15 (5)
ARB-M40	C-15	SRFM	Rubble filled mortar corner of the exterior southwest wall of Caldarium-15 (6)
ARB-M41	C-15	SRFM	Rubble filled mortar from the corner of the exterior southwest wall of Caldarium-15 (7)
ARB-M42	WT-6	pMJ	Mortar joint bonds pipes on the southeast wall of the Water Reservoir-6 (12)
ARB-M43	WT-6	pMJ	Mortar joint bonds pipes on the southeast wall of the Water Reservoir-6 (13)
ARB-M44	WT-6	BMJ	Mortar joint bonds square bricks from the brickwork column neighboring of the northwest wall of Water Reservoir-6 (15)
ARB-M45	P-1	TM	Tessera bedding mortar from base of Piscina-1 (16)
ARB-M46	-	SMJ	Mortar joint bonds stone channels which are placed on north of the Bath (18)

(*) Specified Numbers indicate the order of the sampling

(**) Specified Types; BMJ: Brick Mortar Joint, TM: Tessera Mortar, BRFM: Brick Rubble Filled Mortar, SRFM: Stone Rubble Filled Mortar, PMJ: Pilae Mortar Joint, pMJ: pipe Mortar Joint, SMJ: Stone Mortar Joint.
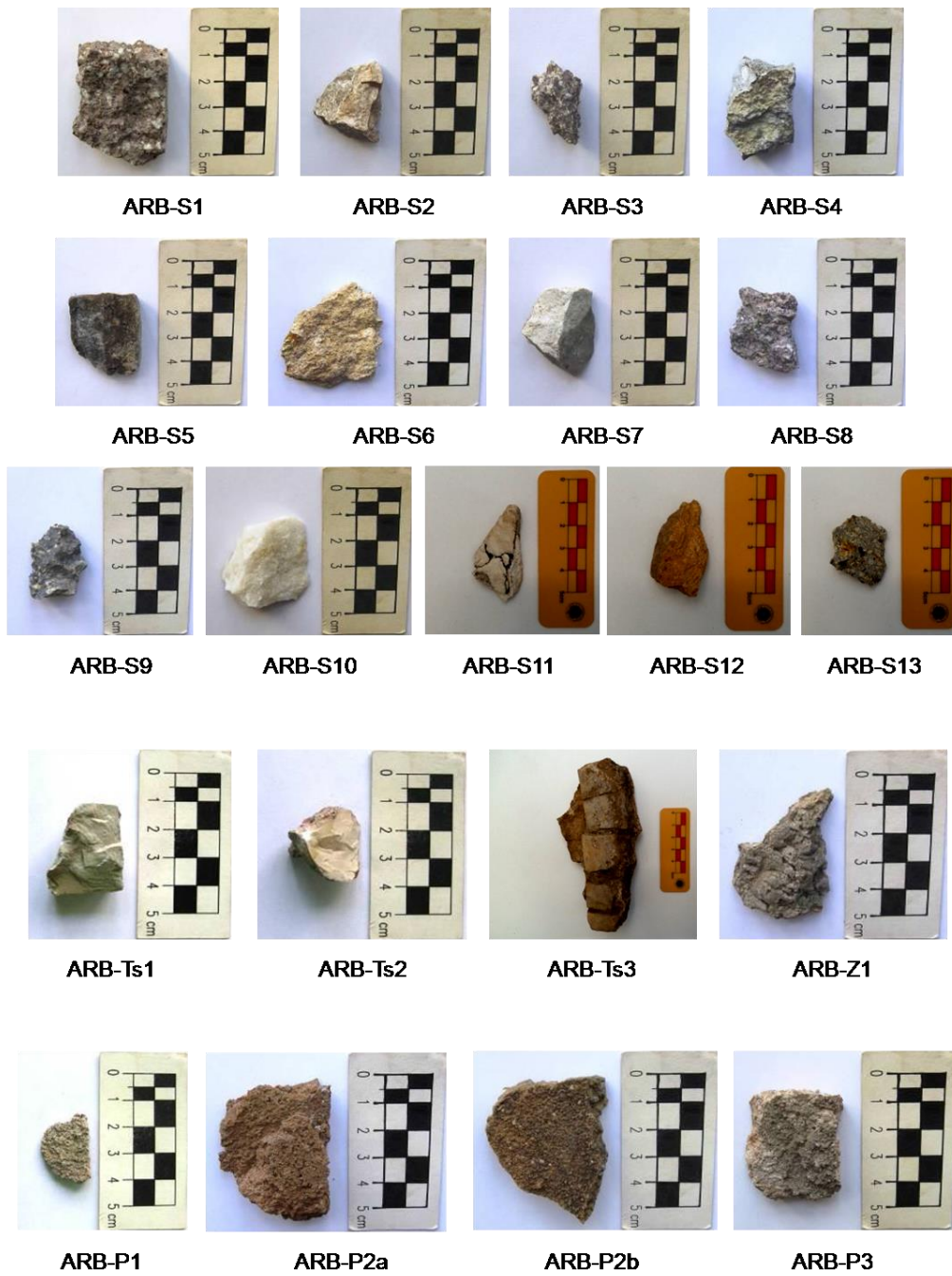
Figure A.7 Stone samples, stone tessera, plaster samples
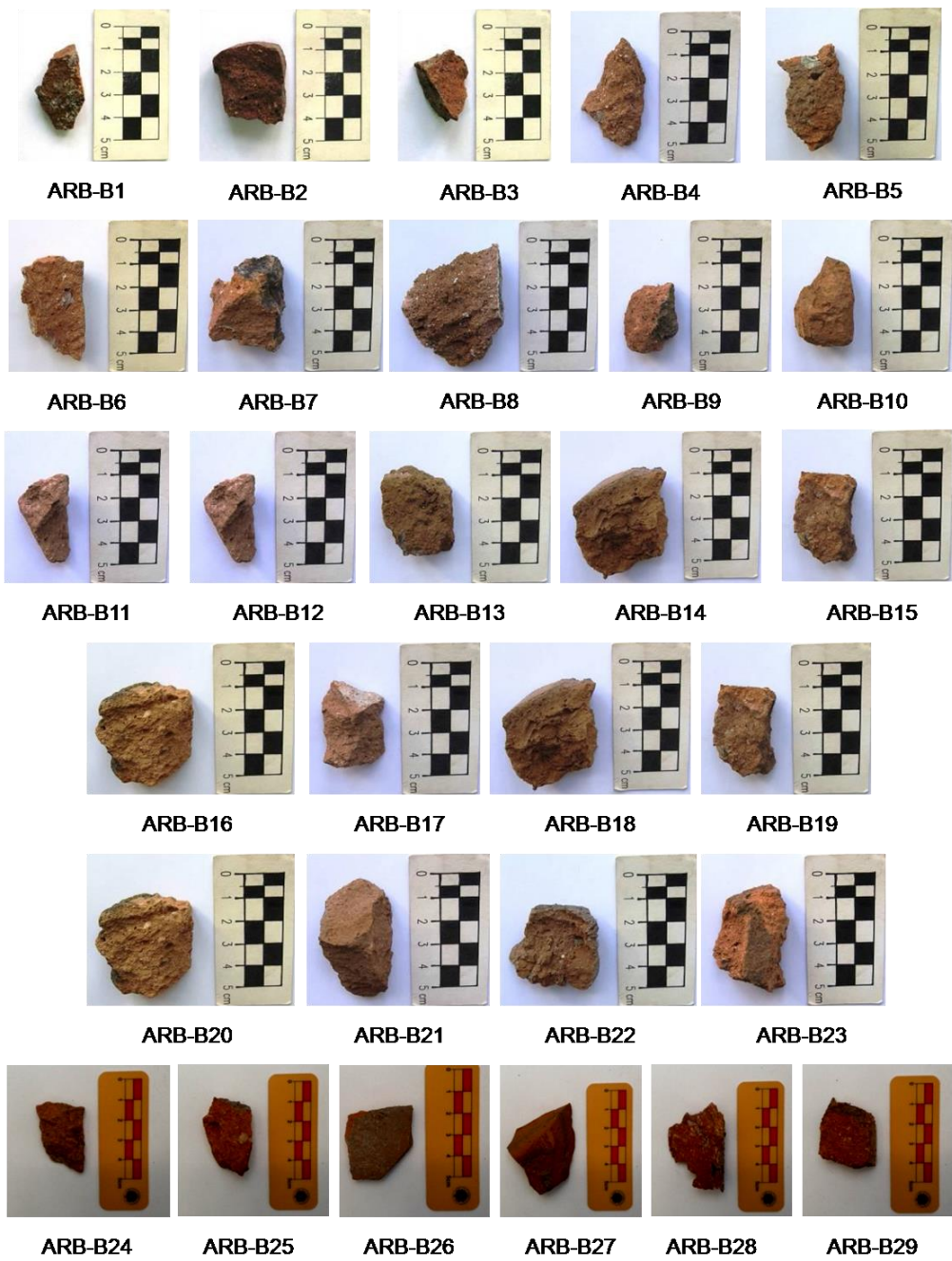
Figure A.8 Brick samples
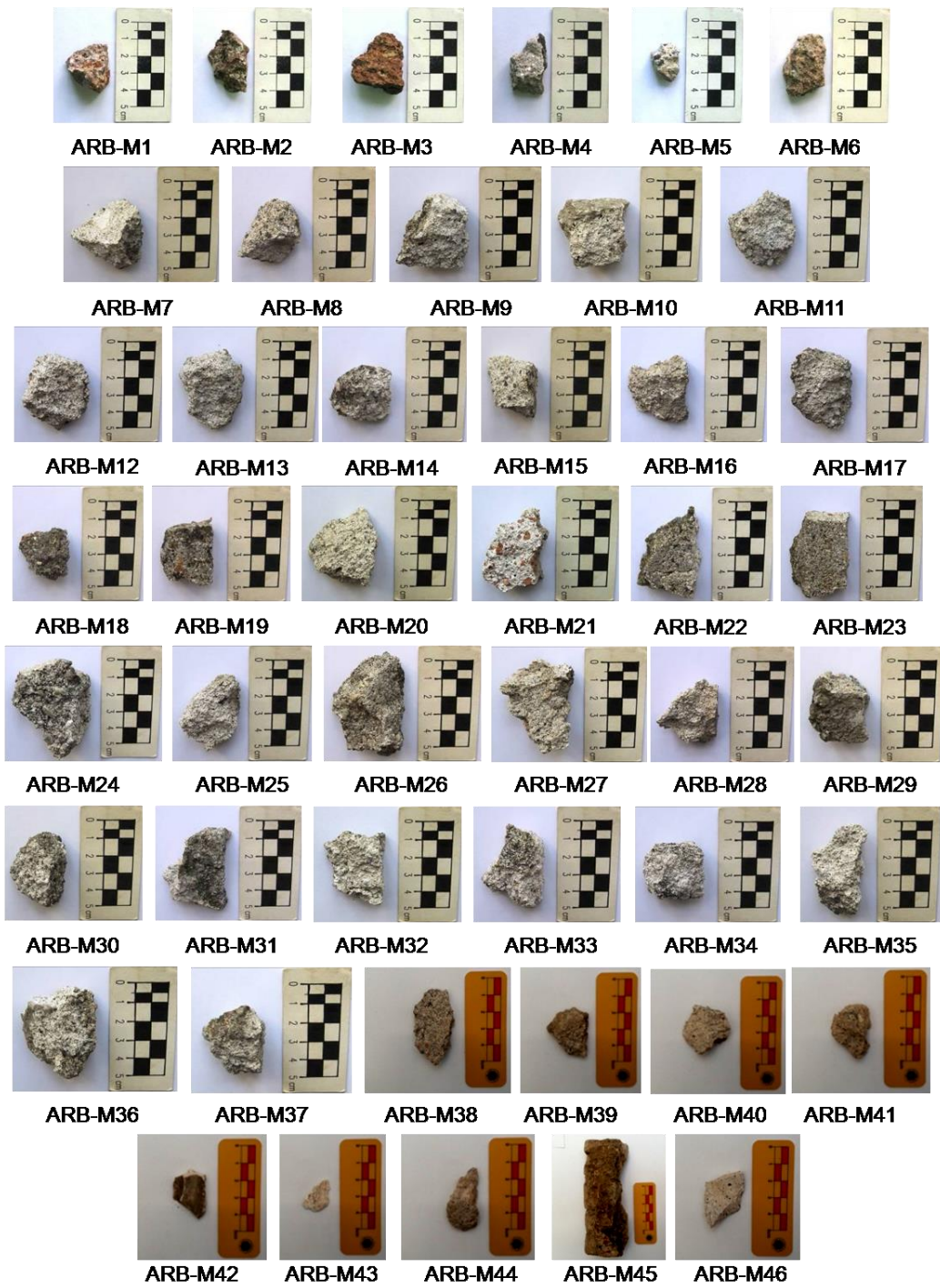
Figure A.9 Mortar samples

Table A.6 Chromametric data; colour codes of (CIE L"a"b) the brick samples

Samples	L	a	b	Color
ARB-B1	29.20	12.27	19.57	Light Brown
ARB-B2	27.13	11.36	17.36	Light Red
ARB-B3	19.27	9.52	15.84	Light Red
ARB-B4	29.30	14.04	21.63	Light Brown
ARB-B5	21.90	17.73	20.27	Light Brown
ARB-B6	30.52	16.74	19.63	Light Brown
ARB-B7	25.37	14.40	20.22	Light Brown
ARB-B8	19.02	8.72	14.14	Light Red
ARB-B9	27.96	12.63	18.54	Light Brown
ARB-B10	31.32	12.00	19.29	Light Brown
ARB-B11	31.42	13.83	20.74	Light Brown
ARB-B12	33.19	22.06	25.23	Reddish
ARB-B13	25.46	8.56	16.30	Light Red
ARB-B14	46.56	13.31	28.43	Light Brown
ARB-B15	32.90	18.49	25.89	Brown
ARB-B16	33.74	12.75	21.96	Light Brown
ARB-B17	31.69	13.21	21.07	Light Brown
ARB-B18	28.44	15.49	23.62	Brown
ARB-B19	39.87	13.12	26.51	Light Brown
ARB-B20	34.31	11.71	21.47	Light Brown
ARB-B21	25.41	9.96	17.56	Light Red
ARB-B22	27.67	18.59	25.18	Brown
ARB-B23	25.99	11.78	22.75	Light Brown
ARH-B24	31.19	11.53	19.10	Light Brown
ARH-B25	29.49	17.52	22.64	Brown
ARH-B26	33.13	13.53	24.20	Light Brown
ARH-B27	26.78	24.02	26.96	Reddish
ARH-B28	25.49	17.70	19.25	Brown
ARH-B29	26.50	19.23	21.90	Reddish

ARB-B1

ARB-B11

ARB-B21

ARB-B2

ARB-B12

ARB-B22

ARB-B3

ARB-B13

ARB-B23

ARB-B4

ARB-B14

ARB-B24

ARB-B5

ARB-B15

ARB-B25

ARB-B6

ARB-B16

ARB-B26

ARB-B7

ARB-B17

ARB-B27

ARB-B8

ARB-B18

ARB-B28

ARB-B9

ARB-B19

ARB-B29

ARB-B10

ARB-B20
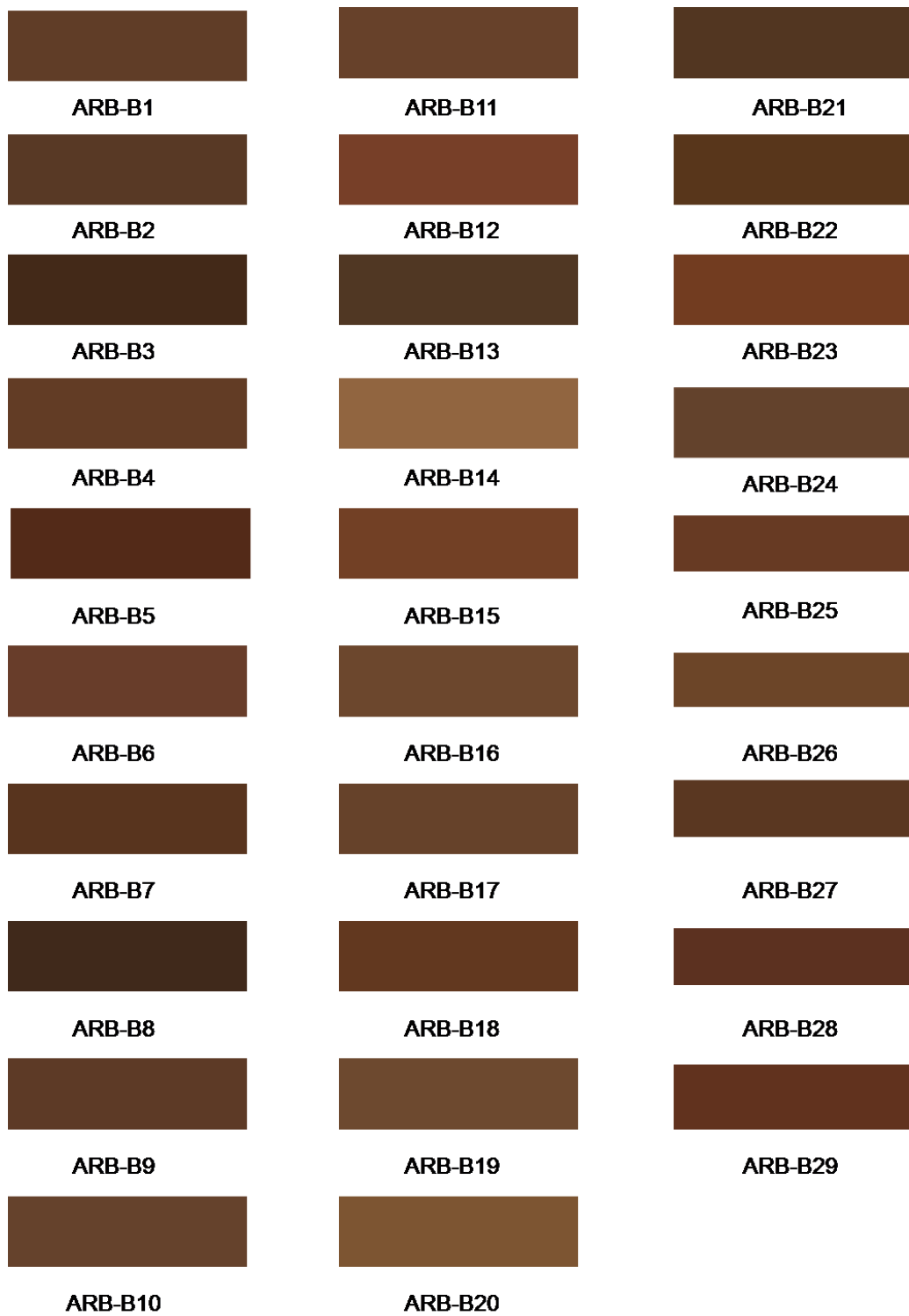
Figure A.10 Colors of brick samples by Chromametric Analysis

194

Table A.7 Bulk density, porosity and water absorption capacity of the stone samples

Örnekler	Bulk density-wet (g/cm3)	Bulk density-dry (g/cm3)	WAC (%)	P (%)	Type
ARB-S1	2.41	2.23	3.20	7.15	Andesite
ARB-S2	2.69	2.58	1.48	3.83	Limestone
ARB-S3	2.48	2.28	3.43	7.84	Andesite
ARB-S4	2.50	2.31	3.24	7.50	Andesite
ARB-S5	2.71	2.68	0.38	1.03	Andesite
ARB-S6	2.61	2.41	3.15	7.61	Andesite
ARB-S7	2.72	2.70	0.26	0.71	Limestone
ARB-S8	2.48	2.25	4.14	9.32	Sandstone
ARB-S9	2.61	2.43	2.90	7.03	Andesite
ARB-S10	2.73	2.72	0.16	0.43	Marble
ARB-S12	2.61	2.35	4.22	9.93	Tuff
ARB-S13	2.52	2.28	4.24	9.67	Andesite
ARB-Ts1	2.69	2.66	0.49	1.31	Radiolarite
ARB-Ts2	2.68	2.59	1.31	3.38	Radiolarite
Andesite Ave.	2.55	2.38	2.94	6.83	Andesite Ave.
Limestone Ave.	2.70	2.64	0.87	2.27	Limestone Ave.
Radiolarite Ave.	2.69	2.63	0.90	2.35	Radiolarite Ave.

Table A.8 Bulk density, porosity and water absorption capacity of the brick, pilae and pipe samples

Örnekler	Bulk density-wet (g/cm3)	Bulk density-dry (g/cm3)	WAC (%)	P (%)	Type
ARB-B1	2.14	1.69	12.46	21.04	Brick
ARB-B2	1.83	1.65	6.25	10.28	
ARB-B3	1.87	1.62	8.26	13.39	
ARB-B4	2.33	1.51	23.47	35.34	
ARB-B5	2.37	1.44	27.24	39.20	
ARB-B6	2.37	1.53	22.93	35.18	
ARB-B7	2.35	1.47	25.45	37.46	
ARB-B8	2.09	1.59	15.14	24.04	
ARB-B11	2.30	1.54	21.56	33.10	
ARB-B14	2.33	1.66	17.14	28.51	
ARB-B18	2.24	1.45	24.46	35.38	
ARB-B19	2.14	1.63	14.64	23.86	
ARB-B24	2.59	1.72	19.50	33.56	
ARB-B25	2.46	1.46	28.09	40.89	
ARB-B28	2.42	1.45	27.56	40.03	
ARB-B29	2.57	1.39	33.10	45.97	
ARB-B10	2.61	2.07	9.99	20.68	Repaired
ARB-B9	2.13	1.31	29.58	38.68	Pilae
ARB-B12	2.32	1.38	29.34	40.53	
ARB-B13	2.13	1.53	18.63	28.44	
ARB-B15	2.33	1.48	24.65	36.47	
ARB-B16	2.27	1.52	21.55	32.86	
ARB-B17	2.20	1.32	30.15	39.91	
ARB-B20	2.32	1.57	20.66	32.43	
ARB-B21	2.04	1.49	18.23	27.07	
ARB-B22	2.25	1.41	26.32	37.18	
ARB-B23	2.32	1.52	22.59	34.39	
ARB-B26	2.50	1.77	16.45	29.15	Pipe
ARB-B27	2.58	1.68	20.91	35.05	
Brick	**2.27**	**1.55**	**20.45**	**31.08**	**Brick**
Pilae	**2.23**	**1.45**	**24.17**	**34.80**	**Pilae**
Pipe	**2.54**	**1.72**	**18.68**	**32.10**	**Pipe**

Table A.9 Geochemical characteristic and geophysical properties of magmatic rocks, (Kadıoğlu, 2001)

Rock Name	Bulk Density (g/cm³)	Average Bulk Density
Sedimentary Rocks		
Alluvion	1.96-2.00	1.98
Clay	1.63-2.60	2.21
Aggregate	1.70-2.40	2.00
Silt	1.80-2.20	1.93
Soil	1.20-2.40	1.92
Sand	1.70-2.30	2.00
Sandstone	1.61-2.76	2.35
Shale	1.77-3.20	2.40
Limestone	1.93-2.90	2.55
Dolomite	2.28-2.90	2.70
Chalk	1.53-2.60	2.22
Halite	2.10-2.60	2.22
Magmatic Rocks		
Rhyolite	2.35-2.70	2.52
Granite	2.50-2.81	2.64
Andesite	2.40-2.80	2.61
Syenite	2.60-2.95	2.77
Basalt	2.70-3.30	2.99
Gabbro	2.70-3.50	3.03
Metamorphic Rocks		
Schist	2.39-2.90	2.64
Gneiss	2.59-3.00	2.80
Phyllite	2.68-2.80	2.74
Slate	2.70-2.90	2.79
Granulite	2.52-2.73	2.65
Amphibolite	2.90-3.04	2.96
Eclogite	3.20-3.54	3.37

Table A.10 Ultrasonic Pulse Velocity of the stone samples

Samples	SV (µs)	SV (Km/s)	Types of Rock
ARB-S1	42.40	1.95	Andesite
ARB-S2	37.00	2.41	Limestone
ARB-S3	41.60	2.00	Andesite
ARB-S4	39.60	2.16	Andesite
ARB-S5	37.80	2.33	Andesite
ARB-S6	38.00	2.31	Andesite
ARB-S7	38.20	2.29	Limestone
ARB-S8	38.80	2.23	Sandstone
ARB-S9	36.30	2.49	Andesite
ARB-S10	38.80	2.23	Marble

Table A.11 Hardness test results of the stone samples

Samples	Mesur. 1	Mesur. 2	Mesur. 3	Mesur. 4	Mesur. 5	Average	Type
ARB-S12	31.0	31.0	31.0	32.0	32.0	**31.4**	Tuff
ARB-S13	29.0	30.0	30.0	31.0	31.0	**30.2**	Andesite

Table A.12 The Binder-Aggregate Ratio of the mortar and plaster samples

Samples	Total Binder Ratio (%)	Total Aggregate Ratio (%)
ARB-M2a	17.02	82.98
ARB-M3	14.97	85.03
ARB-M5	10.21	89.79
ARB-M6	24.40	75.60
ARB-M7	32.36	67.64
ARB-M8	25.39	74.61
ARB-M9	23.77	76.23
ARB-M10	20.67	79.33
ARB-M11	14.68	85.32
ARB-M12	23.29	76.71
ARB-M13	16.45	83.55
ARB-M14	19.78	80.22
ARB-M17	24.49	75.51
ARB-M18	18.43	81.57
ARB-M20	24.96	75.04
ARB-M22	27.90	72.10
ARB-M23	35.95	64.05
ARB-M24	24.98	75.02
ARB-M25	24.67	75.33
ARB-M26	23.14	76.86
ARB-M27	20.35	79.65
ARB-M28	38.97	61.03
ARB-M30	23.76	76.24
ARB-M31	33.02	66.98
ARB-M32	23.63	76.37
ARB-M33	25.36	74.64
ARB-M34	24.24	75.76
ARB-M35	19.91	80.09
ARB-M36	27.23	72.77
ARB-M38	20.20	79.80
ARB-M39	24.58	75.42
ARB-M40	26.90	73.10
ARB-M41	21.88	78.12
ARB-M42	94.10	5.90
ARB-M43	96.36	3.64
ARB-M44	4.33	95.67
ARB-P1	8.63	91.37
ARB-P3	42.88	57.12
Mortar Ave.	**27.01**	**72.99**
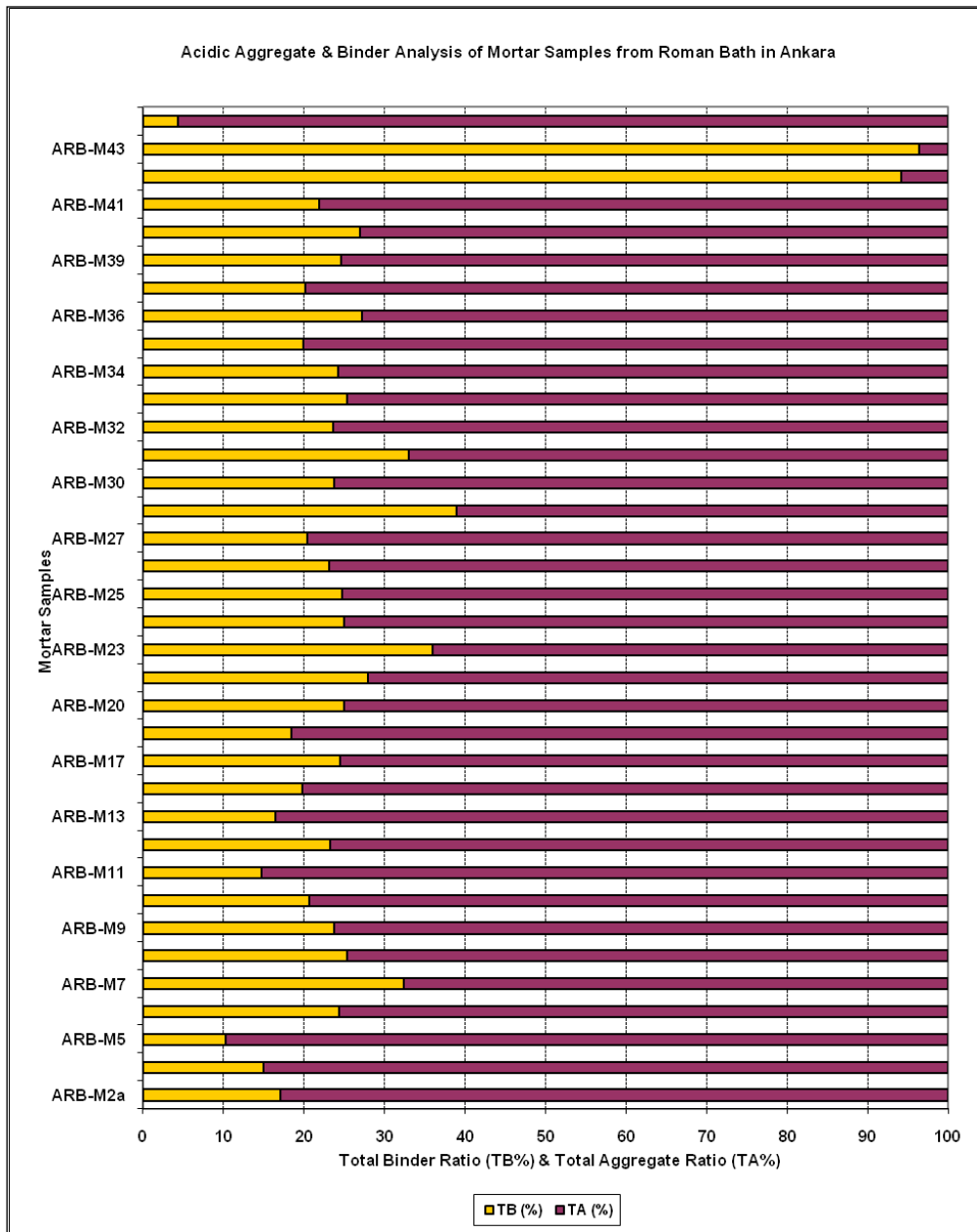
Figure A.11 The Binder-Aggregate Ratio of the mortar and plaster samples

Table A.13 The Particle Size Distribution of the mortar and plaster samples

Samples	<63 μm	>63 μm	>125 μm	>250 μm	>500 μm	>1000 μm
ARB-M2a	1.21	4.64	7.76	10.15	18.16	58.07
ARB-M3	1.82	4.63	9.42	13.34	22.54	48.25
ARB-M5	2.23	1.25	6.83	11.98	17.23	60.48
ARB-M6	1.24	1.02	3.63	12.41	20.87	60.84
ARB-M7	1.33	1.25	4.64	15.37	21.59	55.83
ARB-M8	1.22	1.45	4.26	14.62	22.95	55.50
ARB-M9	1.03	1.01	5.83	20.37	22.88	48.89
ARB-M10	2.27	1.66	4.28	14.15	26.93	50.71
ARB-M11	1.36	1.38	3.52	14.36	31.33	48.04
ARB-M12	0.94	0.69	1.86	6.76	23.31	66.45
ARB-M13	1.01	1.02	4.84	20.09	16.00	57.04
ARB-M14	0.82	0.97	3.05	13.43	23.14	58.59
ARB-M17	1.08	1.25	4.11	15.44	29.19	48.95
ARB-M18	1.72	1.77	4.77	14.79	22.54	54.42
ARB-M20	1.94	2.57	8.09	13.29	16.57	57.54
ARB-M22	1.62	1.75	5.35	22.51	31.40	37.38
ARB-M23	2.25	3.01	9.02	32.47	30.44	22.81
ARB-M24	0.92	0.84	2.98	13.43	27.00	54.83
ARB-M25	1.41	1.21	4.22	11.51	30.11	51.53
ARB-M26	1.38	1.72	4.48	14.39	29.37	48.66
ARB-M27	0.98	1.16	3.00	7.56	20.64	66.66
ARB-M28	1.08	1.14	4.80	19.38	29.66	43.93
ARB-M30	1.49	2.45	8.03	14.27	18.03	55.73
ARB-M31	1.80	2.08	7.76	27.64	25.98	34.73
ARB-M32	1.04	1.49	4.00	14.25	27.37	51.85
ARB-M33	1.02	1.23	2.80	8.80	28.17	57.98
ARB-M34	1.00	1.13	2.90	9.14	28.59	57.24
ARB-M35	1.23	1.23	2.96	10.14	24.68	59.76
ARB-M36	2.63	1.31	3.28	10.26	24.87	57.65
ARB-M38	1.36	2.41	4.38	9.15	29.41	53.28
ARB-M39	0.95	1.09	3.72	9.46	23.70	61.09
ARB-M40	0.59	1.28	4.42	14.39	27.25	52.07
ARB-M41	8.28	0.86	3.56	16.41	25.93	44.96
ARB-M42	85.80	1.91	2.69	4.73	2.19	2.69
ARB-M43	15.52	11.97	15.91	22.16	26.74	7.70
ARB-M44	2.24	6.50	13.47	19.30	20.33	38.16
ARB-P1	1.54	2.58	7.91	20.69	30.38	36.91
ARB-P3	9.20	7.97	11.36	15.40	22.92	33.16
Mortar Ave.	**4.33**	**2.07**	**5.30**	**14.50**	**24.08**	**49.73**
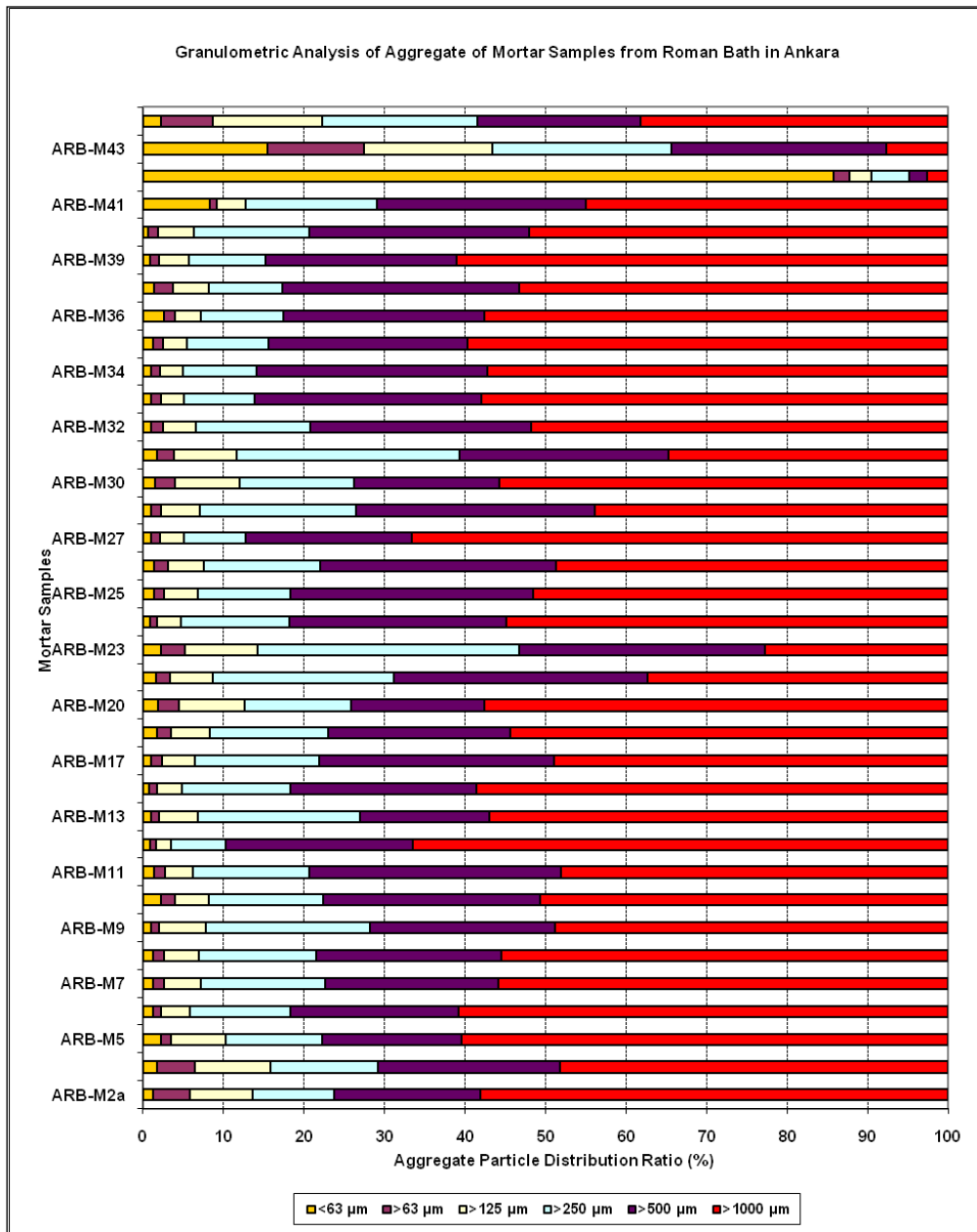
Figure A.12 The Particle Size Distribution of the mortar and plaster samples
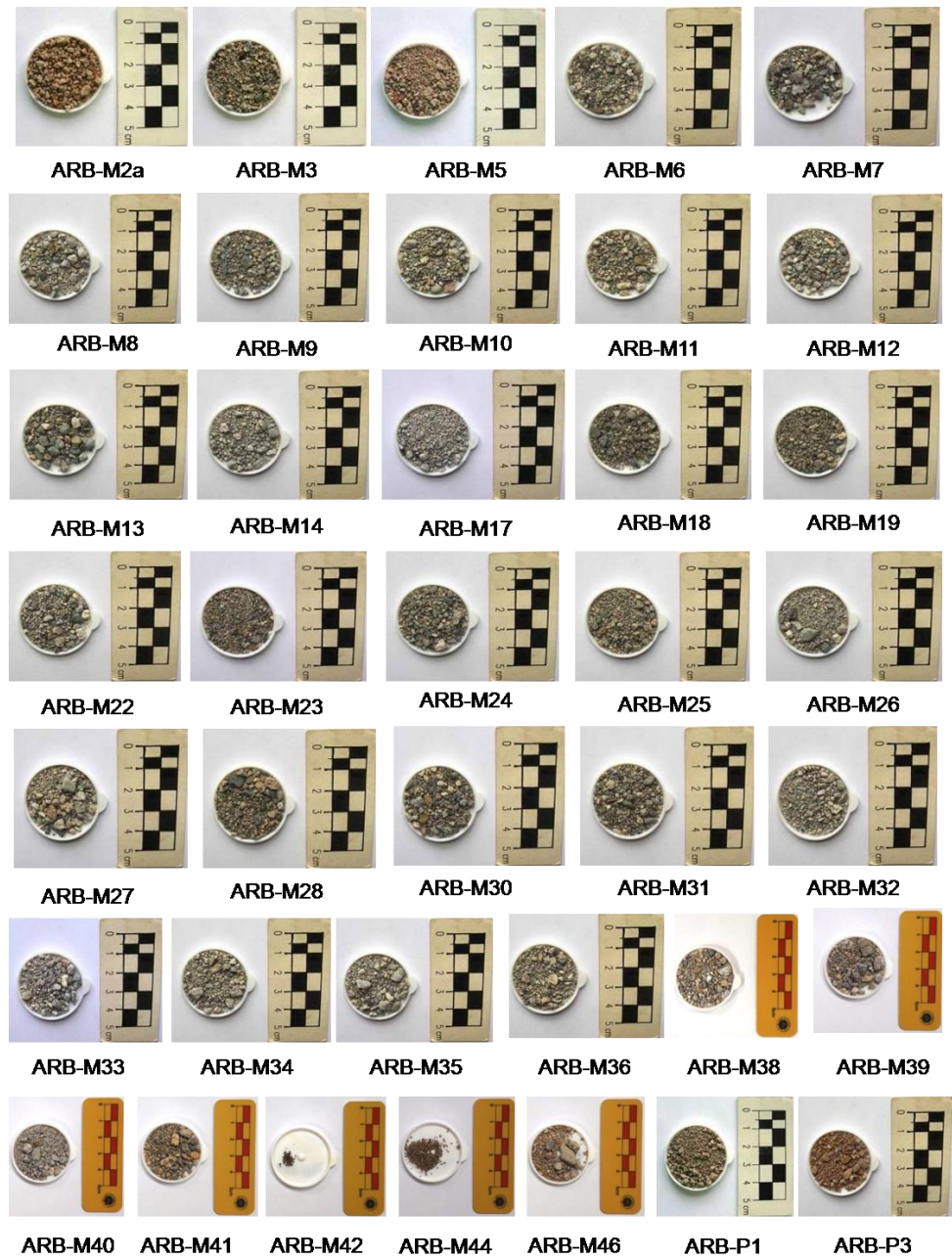
Figure A.13 Colors of brick samples by Chromametric Analysis

Table A.14 The results of the gravimetric analysis for different groups of mortar and plaster samples

Samples	Cru. Wt. (g)	Sample Wt. (g)	Total Wt. (105°C, g)	Sample Wt. (105°C, g)	Ratio WC (105°C, %)
ARB-M1	17.6605	1.1579	18.8138	1.1533	0.40
ARB-M4	13.4931	1.2460	14.7354	1.2423	0.30
ARB-M5	21.8664	1.1616	23.0200	1.1536	0.69
ARB-M12	18.2296	1.6066	19.8336	1.6040	0.16
ARB-M21	18.2325	1.0133	19.2384	1.0059	0.73
ARB-M29	17.9767	1.7849	19.7593	1.7826	0.13
ARB-M33	21.7302	1.0884	22.8139	1.0837	0.43
ARB-M37	22.8786	1.4937	24.3678	1.4892	0.30
ARB-P1	21.5986	1.2636	22.8596	1.2610	0.21
ARB-P3	17.6766	1.3500	18.9925	1.3159	2.53
Mortar Ave.					0.39

Örnekler	Total Wt. (450°C, g)	Ratio Carbon (450°C, %)	Total Wt. (950°C, g)	Sample Wt. (950°C, %)	Ratio Carbonate (%)
ARB-M1	18.7655	4.19	18.5888	19.51	34.84
ARB-M4	14.7019	2.70	14.6215	9.17	16.37
ARB-M5	22.9550	5.63	22.8045	18.68	33.36
ARB-M12	19.7993	2.14	19.7322	6.32	11.29
ARB-M21	19.1759	6.21	19.0081	22.89	40.88
ARB-M29	19.7331	1.47	19.6292	7.30	13.03
ARB-M33	22.7819	2.95	22.6925	11.20	20.00
ARB-M37	24.3305	2.50	24.2509	7.85	14.02
ARB-P1	22.8149	3.54	22.5191	27.00	48.22
ARB-P3	18.8661	9.61	18.7480	18.58	33.18
Mortar Ave.		3.47			22.97

Table A.15 Conductometric Analysis results of the stone, stone tessera, brick, pilae and pipe samples

Samples	SS (%)	Stone Type	Samples	SS (%)	Samples	SS (%)
ARB-S1	0.77	Andesite	ARB-B1	1.26	ARB-B9	0.59
ARB-S2	1.08	Limestone	ARB-B2	0.81	ARB-B12	0.89
ARB-S3	1.27	Andesite	ARB-B3	1.00	ARB-B13	0.58
ARB-S4	1.30	Andesite	ARB-B4	1,06	ARB-B15	0.58
ARB-S5	1.77	Andesite	ARB-B5	1.26	ARB-B16	1.43
ARB-S6	2.39	Andesite	ARB-B6	0.40	ARB-B17	1.23
ARB-S7	1.01	Limestone	ARB-B7	1.64	ARB-B20	1.23
ARB-S8	1.49	Sandstone	ARB-B8	0.68	ARB-B21	1.33
ARB-S9	1.59	Andesite	ARB-B11	0.44	ARB-B22	1.03
ARB-S10	0.38	Marble	ARB-B14	3.67	ARB-B23	1.30
ARB-S12	0.89	Tuff	ARB-B18	1.73	Pilae Ave.	1.02
ARB-S13	0.42	Andesite	ARB-B19	2.42		
ARB-Ts1*	0.47	Radiolarite	ARB-B24	2.36	ARB-B26	1.49
ARB-Ts2*	0.67	Radiolarite	ARB-B25	2.61	ARB-B27	2.45
Stone Ave.	1.11		ARB-B28	1.63		
			ARB-B29	1.96	ARB-B10**	1.44
			Brick Ave.	1.56	Gen. Ave.	1.35

(*) Except ARB-Ts1, ARB-Ts2

(**) ARB-B10

Table A.16 Historical Weather Data of Ankara (MGM, n.d.)

ANKARA	Ocak	Şubat	Mart	Nisan	Mayıs	Haziran	Temmuz	Ağustos	Eylül	Ekim	Kasım	Aralık	Yıllık
Ölçüm Periyodu (1927 - 2017)													
Ortalama Sıcaklık (°C)	0.2	1.6	5.7	11.3	16.1	20.1	23.5	23.4	18.8	12.9	7.1	2.4	11.9
Ortalama En Yüksek Sıcaklık (°C)	4.1	6.3	11.4	17.3	22.3	26.6	30.2	30.3	25.9	19.8	12.9	6.4	17.8
Ortalama En Düşük Sıcaklık (°C)	-3.3	-2.4	0.5	5.2	9.6	12.8	15.7	15.9	11.7	7.0	2.4	-0.8	6.2
Ortalama Güneşlenme Süresi (saat)	2.7	3.9	5.2	6.5	8.5	10.1	11.4	10.8	9.2	6.7	4.6	2.5	82.1
Ortalama Yağışlı Gün Sayısı	12.1	11.1	10.7	11.0	12.1	8.4	3.4	2.6	4.0	6.8	8.0	11.6	101.8
Aylık Toplam Yağış Miktarı Ortalaması (mm)	39.5	35.0	38.6	42.3	51.2	34.2	13.7	11.5	17.8	27.6	31.7	43.9	387.0
Ölçüm Periyodu (1927 - 2017)													
En Yüksek Sıcaklık (°C)	16.6	21.3	27.8	31.6	34.4	37.0	41.0	40.4	37.7	33.3	24.7	20.4	41.0
En Düşük Sıcaklık (°C)	-24.9	-24.2	-19.2	-7.2	-1.6	3.8	4.5	5.5	1.5	-9.8	-17.5	-24.2	-24.9

Table A.17a Spot Salt Tests of the stone samples

Samples	Phosphate (PO_4^{3-})	Sulphate (SO_4^{2-})	Carbonate (CO_3^{2-})**	pH
ARB-S1	0.20*	-*	112*	7.78**
ARB-S2	0.20	-	112	8.04
ARB-S3	0.20	-	112	7.80
ARB-S4	-	-	112	8.18
ARB-S5	-	20	112	8.24
ARB-S6	-	40	112	8.13
ARB-S7	0.20	-	192	8.05
ARB-S8	0.20	-	112	7.55
ARB-S9	0.20	-	192	7.66
ARB-S10	-	20	192	8.00
ARB-S12	0.20	20	192	8.38
ARB-S13	-	-	80	8.40
ARB-Ts1	-	-	112	7.66
ARB-Ts2	-	20	112	7.12
Average				7.93

Table A.17b Spot Salt Tests of the brick samples

Samples	(PO_4^{3-})	(SO_4^{2-})	(CO_3^{2-})	pH	Samples	(PO_4^{3-})	(SO_4^{2-})	(CO_3^{2-})	pH
ARB-B1	-*	-*	112*	7.43**	ARB-B9	0.20*	-*	192*	8.08**
ARB-B2	-	-	112	7.32	ARB-B12	-	20	192	7.95
ARB-B3	-	20	112	7.25	ARB-B13	-	20	112	8.06
ARB-B4	0.20	20	592	7.36	ARB-B15	0.20	-	192	7.89
ARB-B5	0.40	20	192	7.32	ARB-B16	-	-	112	8.08
ARB-B6	0.20	20	192	7.80	ARB-B17	0.20	-	112	8.08
ARB-B7	0.20	20	192	8.14	ARB-B20	-	20	592	7.46
ARB-B8	0.20	-	192	7.92	ARB-B21	-	20	112	8.03
ARB-B11	-	-	192	7.91	ARB-B22	-	20	192	8.09
ARB-B14	-	40	112	7.37	ARB-B23	-	-	112	8.14
ARB-B18	-	-	192	7.97	Pilae Ave.				7.96
ARB-B19	-	20	592	6.73					
ARB-B24	0.20		112	8.39	ARB-B26	0.20		112	8.37
ARB-B25	0.20		80	8.39	ARB-B27	-		80	8.36
ARB-B28	0.20		112	8.34					
ARB-B29	-		112	8.35	ARB-B10	-	40	112	7.97
Brick Ave.				7.75	Gen. Ave.				7.88

Except ARB-B10
(*) Sensitivity of Spot Tests; (SO_4^{2-}): 20 mg/L,(PO_4^{3-}): 0.20 mg/L, (CO_3^{2-}): 4 mg/L
(**) 100 mL in water

Table A.18 Petrography of the stone samples

Stone Groups	Rock Types	Hardness (Mohs)	Rock & Minerals*	Texture	Explanations
Stone Gr1a	Quartz Andesite	6 - 6.5	Pl,A,Am, By,Op,Mg,Py	Hyalopilitic Porphyric	
Stone Gr1b	Andesite	6 - 6.5	Q,Pl,Am,Ol	Hyalopilitic Porphyric	Opacified structure
Stone Gr1c	Andesite	6 - 6.5	Q,Pl,Am,By,Ol	Hyalopilitic	Opacified and clayey structure
Stone Gr2a	Biosparitic Limestone	2.5 - 3	C	Sparitic	Micro fractures/cracks filled with recrystallized calcites
Stone Gr2b	Dolomitic Limestone	2.5 - 3	C,D		Micro fractures/cracks filled with recrystallized calcites
Stone Gr2c	Meta Limestone	2.5-3	C,Q,Op,Ar		
Stone Gr3	Sandstone	4.5 - 5	Q,Pl,By,Op		Micro fractures/cracks filled with recrystallized calcites, amorphous silicates (such as chalsedony)
Stone Gr4	Marble	~3	C,Ms,Op	Granoblastic	Calcite twins with 0.3 mm grain size
Stone Gr5	Tuff	2 - 2.5	B,A,Qs,Pl,By, Cl,Am,Sr,C,Op	Hyalopilitic	Opacified biotite and amphiboles

(*) A: Andesite, Am: Amphibole, Ar: Aragonite, B: Basalt, By: Biotite, C: Calcite, Cl: Chlorite, D: Dolomite, G: Granite, Mg: Magnetite, Ms: Muscovite, Ol: Oligoclase Andesine, Op: Opaque Minerals, Pl: Plagioclase, Py: Pyroxene, Q: Quartz, Qs: Quartzite, R: Radiolarite, S: Sandstone, Sr: Sericite

Grouping of Stone Samples

Stone Gr1a: ARB-S1, ARB-S3, ARB-S13

Stone Gr1b: ARB-S5

Stone Gr1c: ARB-S4, ARB-S6, ARB-S9

Stone Gr2a: ARB-S2

Stone Gr2b: ARB-S7

Stone Gr2c: ARB-S11

Stone Gr3: ARB-S8

Stone Gr4: ARB-S10

Stone Gr5: ARB-S12

Table A.19 Petrography of the stone tessera and tessera mortar samples

Stone Tessera	Rock Types	Hardness (Mohs)	Explanations
ARB-Ts1 ARB-Ts2	Radiolarite	5.5 - 6	Epioceaonic (upper layer of oceanic) sediments is the origin of radiolarites. Radiolarites containing radiolaria fossils, which have been transported as a bedding product in the mortar are located. Amorphous silica mineral, very little chalcedony, calcite, opaque minerals can be seen.
Related Tessera Mortar	50% carbonate and marble dust matrix, 25% aggregate (limestone, basalt, andesite, quartz, chert, plagioclase and fossils-radiolaria) and 25% brick fagments.		

ARB-S1 ARB-S2 ARB-S3

ARB-S4 ARB-S5 ARB-S6

ARB-S7 ARB-S8 ARB-S9

ARB-S10 ARB-S11 ARB-S12

ARB-S13
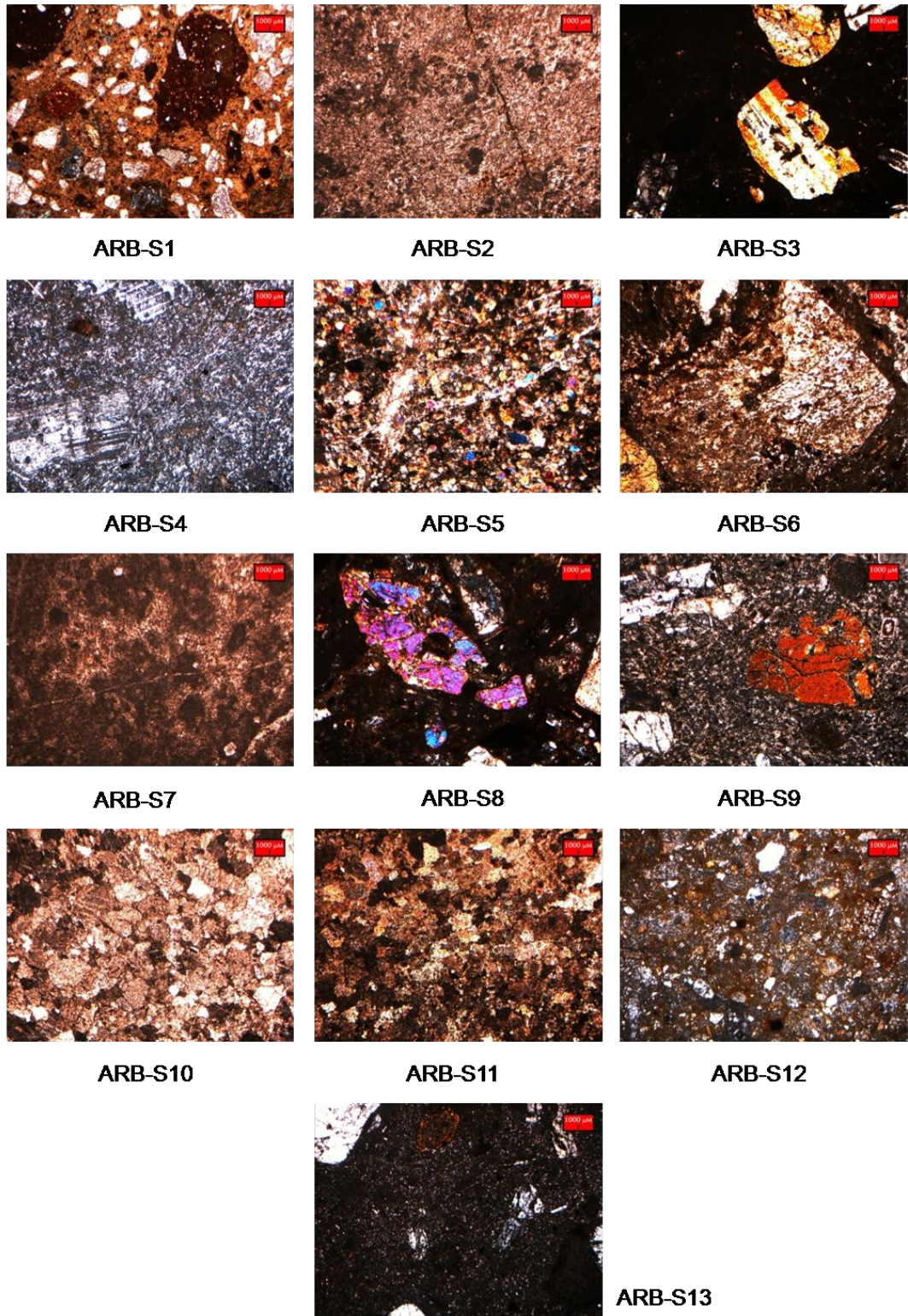
Figure A.14 Thin section microphotograps of stone samples
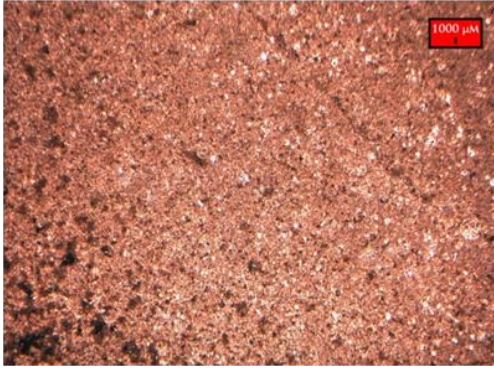
ARB-Ts1
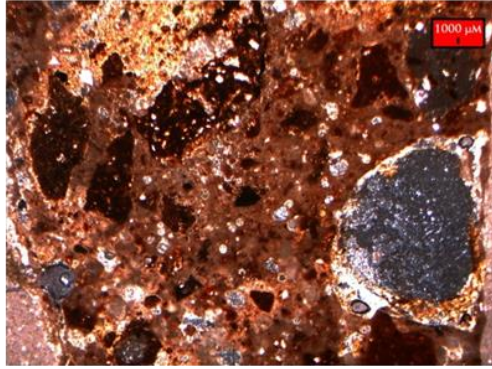
ARB-Ts1 -M
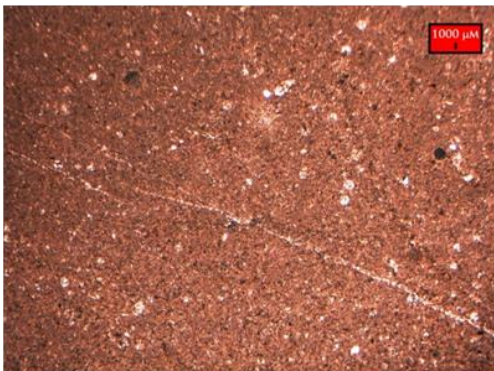
ARB-Ts2
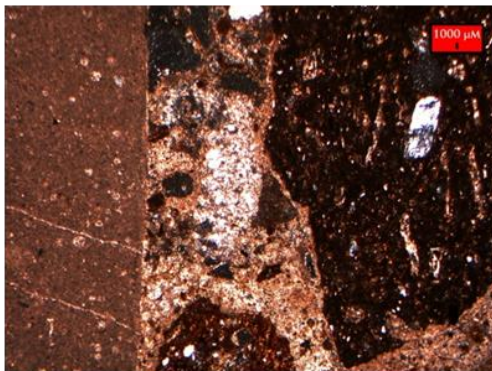
ARB-Ts2-M

ARB-Ts3
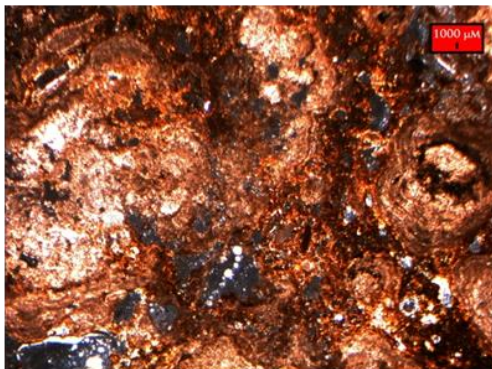
ARB-Z1

Figure A.15 Thin section microphotograps of stone tessera (ARB-Ts1 and ARB-Ts2), their mortars (ARB-Ts1-M and ARB-Ts2-M) and calcerous layer (ARB-Z1)

Table A.20 Petrography of the brick samples

Brick Groups	T(°C)*	P(%)*	MTA(%)*	Rock & Minerals**	Rock Origin
Brick Gr1	>900	12	25	Q,Ch,By,Am,Pl,Py, Ss,G,A,B,BF(2.5%)	Andesite
Brick Gr2	>900	7	15	Ss,A,Ch,Q, By, Pl,By,BF(2.5%)	Andesite
Brick Gr3	>900	8	38	Q,Ch,By,Pl,Py, G,A,B,Op,BF(1.5%)	Andesite
Brick Gr4	>900	5	22	Q,Ch,By,Am,Pl,Ss,A,B	Andesite
Brick Gr5	<900	4	33	G,Ch,S,Q,Pl,By,Tr	Granite
Brick Gr6	>900	7	42	A,Q,Pl,By,Py, Am,Op,BF(1%)	Andesite
Brick Gr7	<900	8	18	G,Ss,A,Q,Ch, B,Op,Am,BF(2%)	Metagrovac
Brick Gr8	<900	9	7	A,B,By,BF,Op,BF(1.5%)	Andesite and Basalt

(*) T: Firing Temperature, P: Porosity, MTA: Matrix Total Aggregate Ratio

(**) A: Andesite, Am: Amphibole, B: Basalt, BF: Brick Dust Fragments, By: Biotite, Ch: Chert, G: Granite, Op: Opaque Minerals, Pl: Plagioclase, Py: Pyroxene, Q: Quartz, Qs: Quartzite, R: Radiolarite, S: Schist, Ss: Sandstone, Tr: Trimonite

Grouping of Brick Samples

Brick Gr1: ARB-B1, ARB-B22, ARB-B28
Brick Gr2: ARB-B2, ARB-B14, ARB-B17
Brick Gr3: ARB-B3, ARB-B4, ARB-B5, ARB-B6, ARB-B7,
        ARB-B8, ARB-B11, ARB-B12, ARB-B16, ARB-B21
Brick Gr4: ARB-B9, ARB-B15, ARB-B18, ARB-B19, ARB-B23, ARB-B26
Brick Gr5: ARB-B10
Brick Gr6: ARB-B13, ARB-B20
Brick Gr7: ARB-B24, ARB-B25, ARB-B27
Brick Gr8: ARB-B29

* The specified samples with blue coloured are pilae, and red coloured ones are pipe

211

ARB-B1 ARB-B2 ARB-B3 ARB-B4 ARB-B5

ARB-B6 ARB-B7 ARB-B8 ARB-B9 ARB-B10

ARB-B11 ARB-B12 ARB-B13 ARB-B14 ARB-B15

ARB-B16 ARB-B17 ARB-B18 ARB-B19 ARB-B20

ARB-B21 ARB-B22 ARB-B23 ARB-B24 ARB-B25

ARB-B26 ARB-B27 ARB-B28 ARB-B29
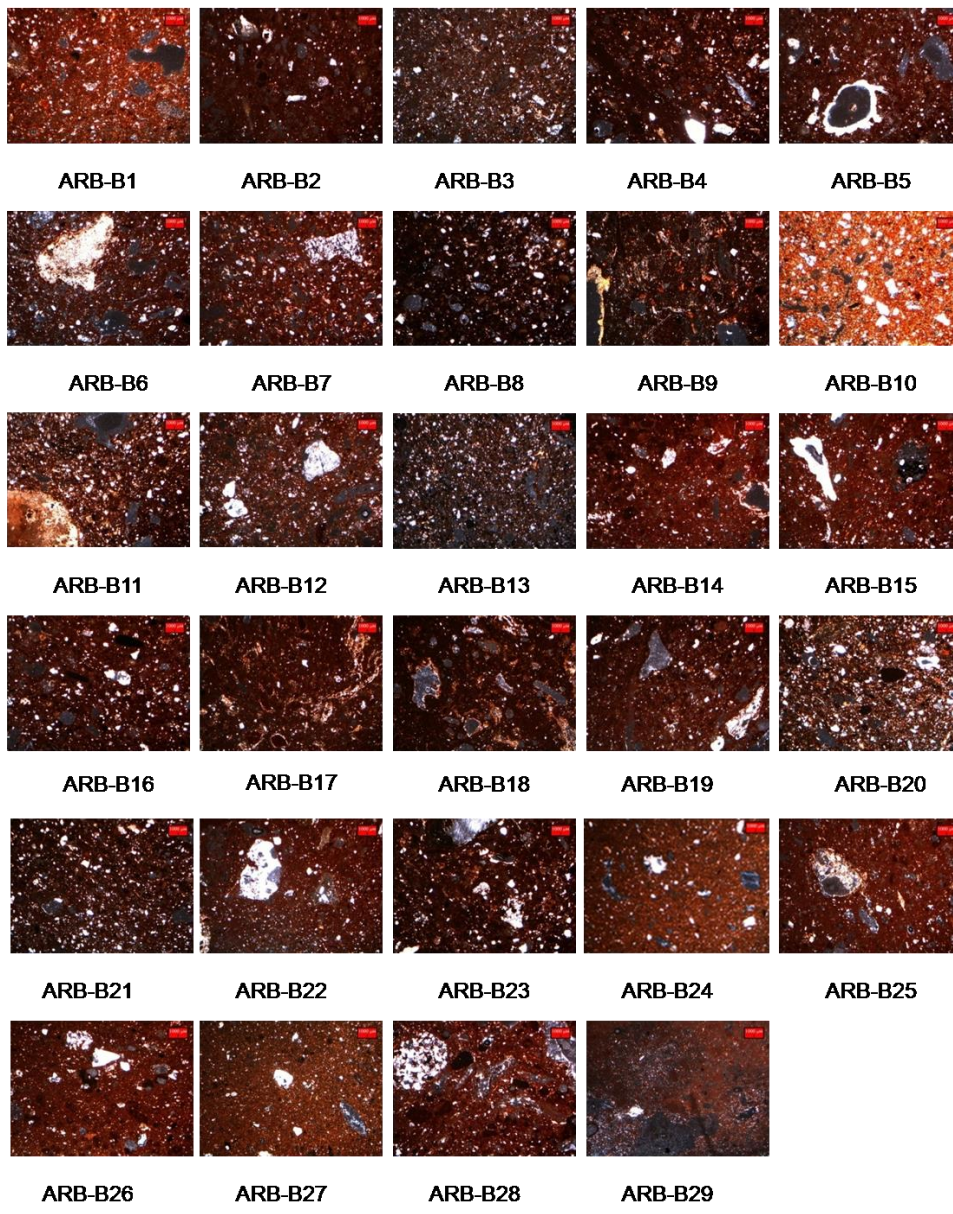
Figure A.16 Thin section microphotograps of brick samples

Table A.21 Petrography of the mortar and plaster samples

Mortar and Plaster Groups	MTB (%)	MTA (%)
Mortar Gr1	**74**	**26**
Mortar Gr2	60	40
Mortar Gr3	**68**	**32**
Mortar Gr4	55	45
Mortar Gr5	75	25
Mortar Gr6	**65**	**35**
Mortar Gr7	74	26
Mortar Gr8	55	45
Plaster Gr1	**74**	**26**
Plaster Gr2	75	25

Mortar & Plaster Groups	Matrix Binder Content (100%)					Matrix Aggregate Content (100%)		
	Lime	M	Cl	Cm	Gyp	Rock & Mineral*	BF	Org
Mortar Gr1	**100**	**-**	**-**	**-**	**-**	**85 (L,Op,B,A,R)**	**15**	**-**
Mortar Gr2	100	-	-	-	-	88 (L,Op,A,R)	12	-
Mortar Gr3	**70**	**-**	**-**	**30**	**-**	**90 (Qs,B,A,S)**	**10**	**-**
Mortar Gr4	100	-	-	-	-	100 (Q,L,Pl,B,A,Qs,Py,By)	-	-
Mortar Gr5	100	-	-	-	-	100 (Q,Ç,Qs,A,Pl,By)	-	-
Mortar Gr6	**60**	**-**	**20**	**20**	**-**	**100 (Q,Pl,Ç,A,Op,Qs,)**	**-**	**-**
Mortar Gr7	100	-	-	-	-	95 (O,Ç,Pl,G,A,Op)	5	-
Mortar Gr8	100	-	-	-	-	100 (B,A,Qs,Ç,L,Py,Op,Ss,R)	-	-
Plaster Gr1	**100**	**-**	**-**	**-**	**-**	**90 (L,Op,A,R)**	**10**	**-**
Plaster Gr2	100	-	-	-	-	85 (Q,Pl,By,A)	15	-

(*) A: Andesite, B: Basalt, By: Biotite, Ch: Chert, G: Granite, Cl: Clay, Cm: Cement, Gyp: Gypsum, L: Limestone, S: Sandstone, M: Marble Powder, MTA: Matrix Total Aggregate Ratio, MTB: Matrix Total Binder Ratio, Op: Opaque Minerals, Org: Organic Content, Pl: Plajiyoklas, Py: Pyroxene, Q: Quartz, Qs: Quartzite, R:Radiolarite, BF: Brick Dust Fragments

Grouping of the Mortar and Plaster Samples

Mortar Gr1: ARB-M1
Mortar Gr2: ARB-M2a, ARB-M2b, ARB-M5, ARB-M45
Mortar Gr3: ARB-M3, ARB-M4
Mortar Gr4: ARB-M6, ARB-M7, ARB-M8, ARB-M9, ARB-M10, ARB-M11, ARB-M12, ARB-M13, ARB-M14, ARB-M15, ARB-M16, ARB-M17, ARB-M19, ARB-M20, ARB-M22, ARB-M23, ARB-M24, ARB-M25, ARB-M28, ARB-M29, ARB-M30, ARB-M31, ARB-M32, ARB-M33, ARB-M34, ARB-M35, ARB-M36, ARB-M37
Mortar Gr5: ARB-M33, ARB-M42, ARB-M43, ARB-M44, ARB-M46
Mortar Gr6: ARB-M26, ARB-M27
Mortar Gr7: ARB-M18, ARB-M21
Mortar Gr8: ARB-M38, ARB-39, ARB-M40, ARB-M41

Plaster Gr1: ARB-P1
Plaster Gr2: ARB-P2a, ARB-P2b, ARB-P3

* The specified samples with red coloured ones are repaired

ARB-M1 ARB-M2a ARB-M2b ARB-M3 ARB-M4 ARB-M5

ARB-M6 ARB-M7 ARB-M8 ARB-M9 ARB-M10 ARB-M11

ARB-M12 ARB-M13 ARB-M14 ARB-M15 ARB-M16 ARB-M17

ARB-M18 ARB-M19 ARB-M20 ARB-M21 ARB-M22 ARB-M23

ARB-M24 ARB-M25 ARB-M26 ARB-M27 ARB-M28 ARB-M29

ARB-M30 ARB-M31 ARB-M32 ARB-M33 ARB-M34 ARB-M35

ARB-M36 ARB-M37 ARB-M38 ARB-M39 ARB-M40 ARB-M41

ARB-M42 ARB-M43 ARB-M44 ARB-M45 ARB-M46
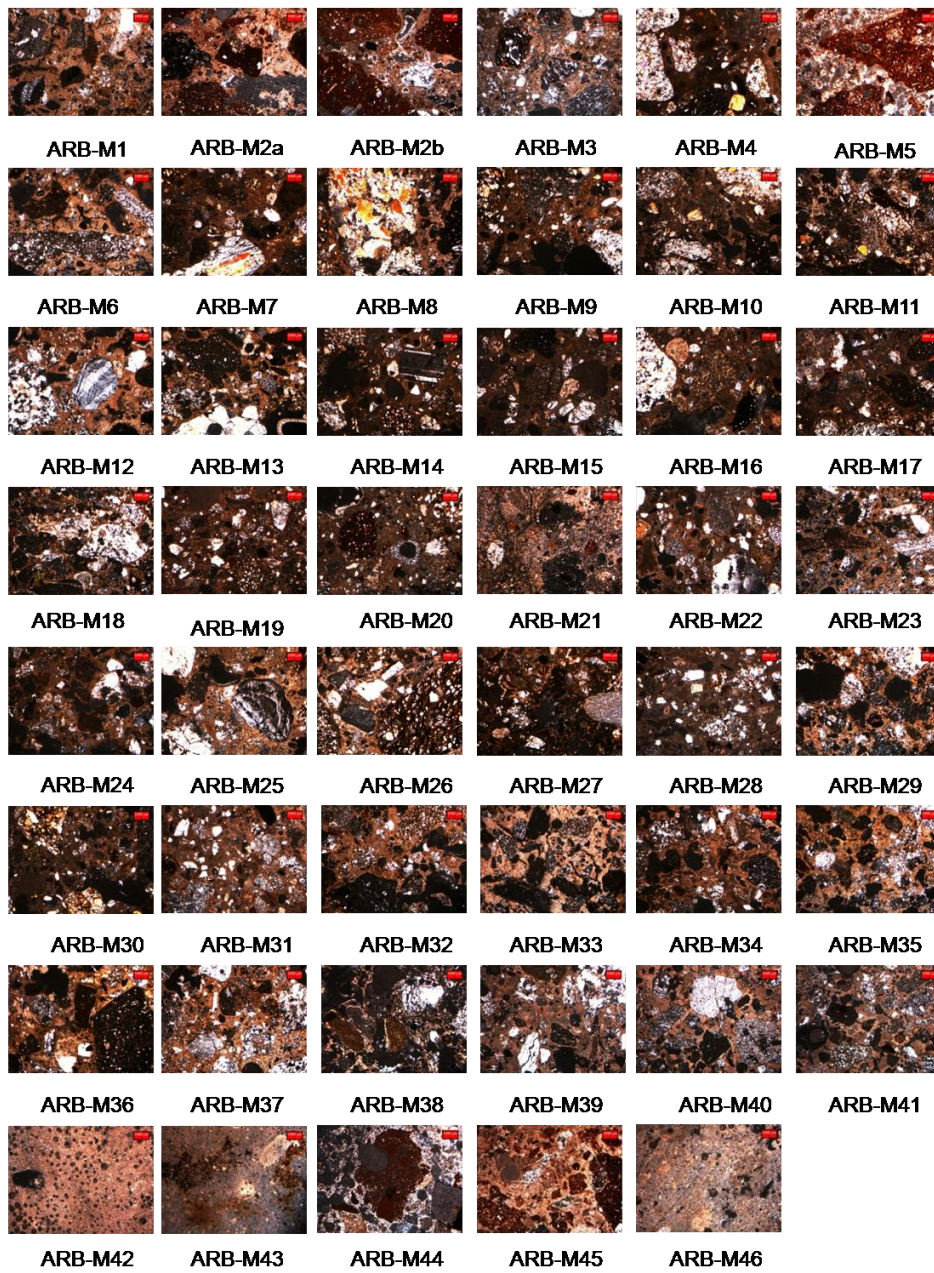
Figure A.17 Thin section microphotograps of mortar samples

214
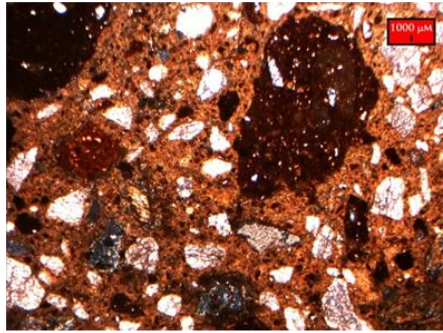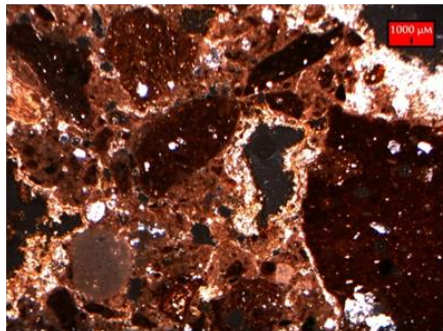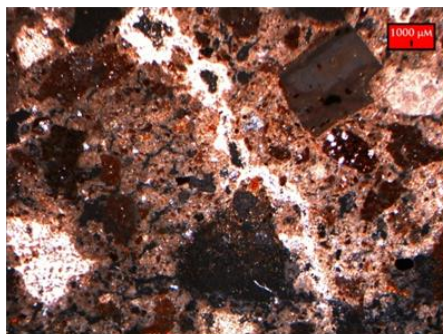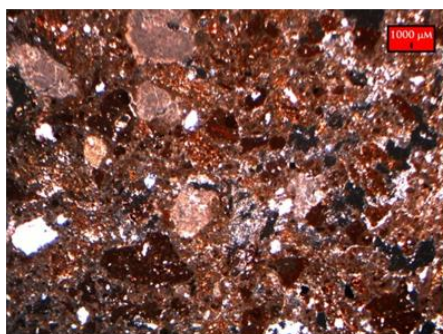
Figure A.18 Thin section microphotograps of plaster samples
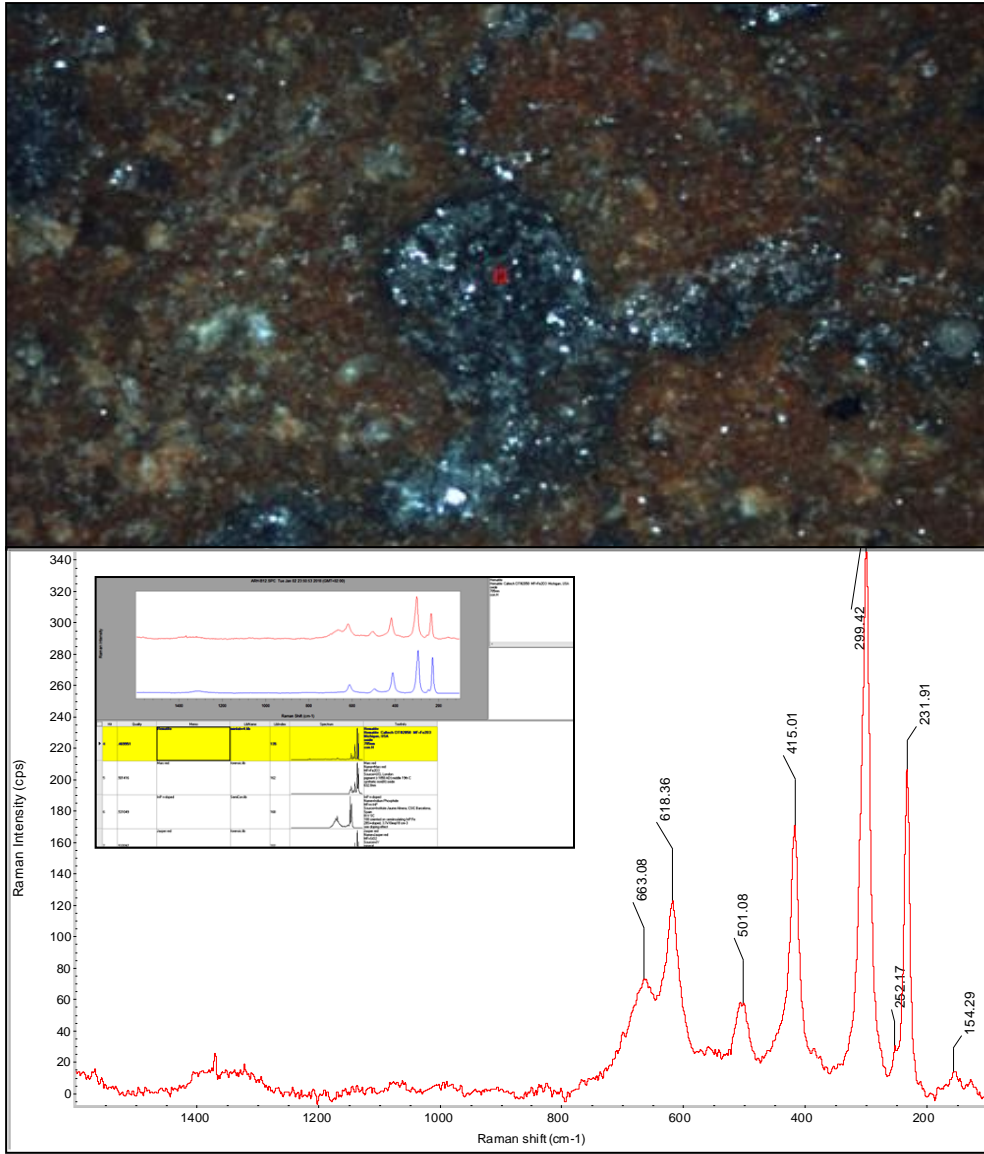
Figure A.19 Raman Analysis Results (sample ARB-B22)
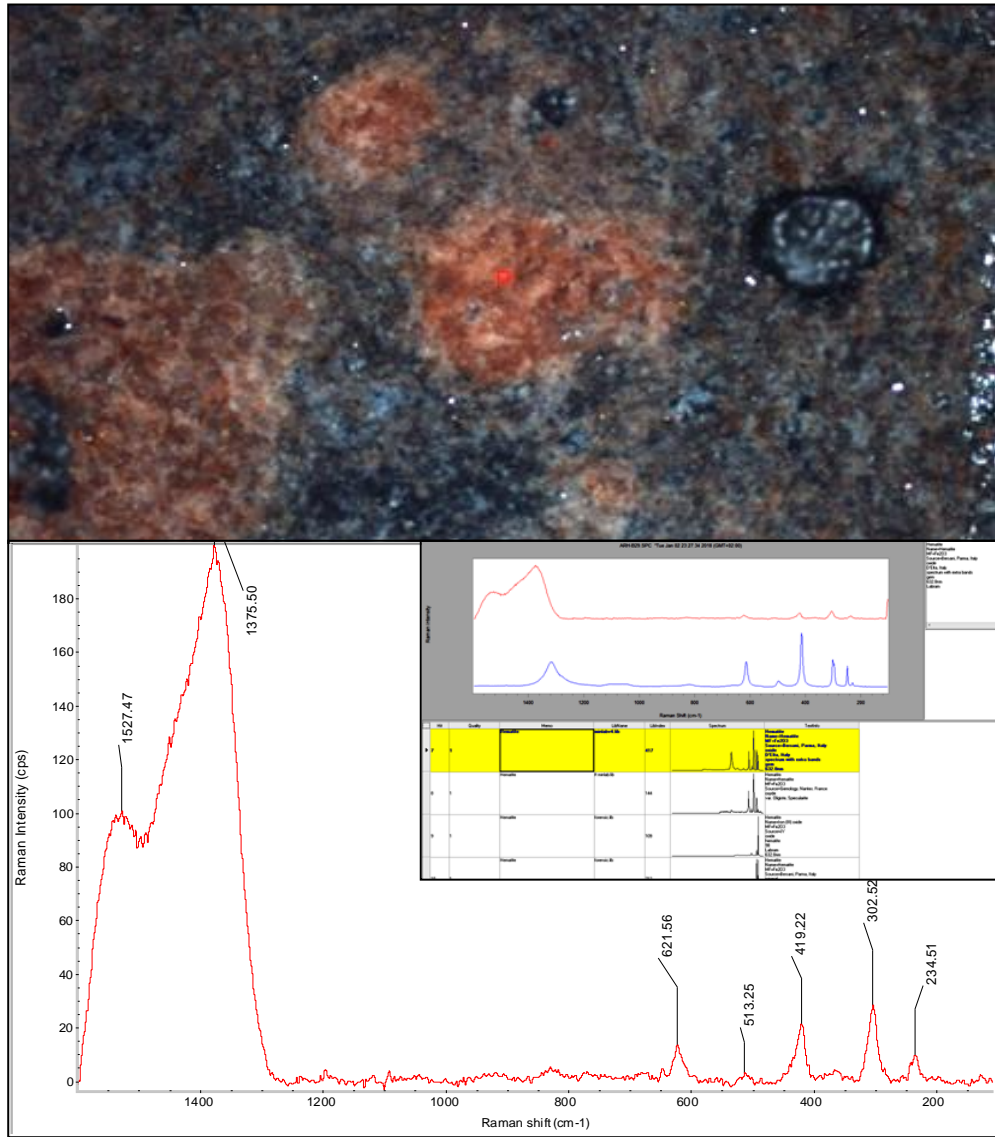
Figure A.20 Raman Analysis Results (Sample ARB-B29)

Table A.22 SEM-EDX Analysis Results of ARB-Z1, ARB-S6 and ARB-B7

Sample	Identified Elements and Mass Weights (%)											
Code	C	O	Na	Mg	Al	Si	S	Cl	K	Ca	Fe	Ti
ARB B7	23.64	55.82	0.48	1.00	3.02	12.16	0.36	-	0.59	1.49	1.44	-
ARB S6	31.43	50.96	1.01	0.82	3.81	7.28	0.08	0.03	0.71	2.85	0.93	0.08
ARB Z1	8.29	51.93	0.42	0.75	2.81	5.34	8.08	0.20	2.23	18.79	0.83	0.33
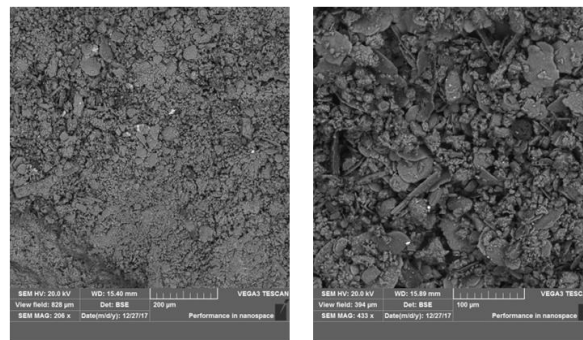
ARB-Z1
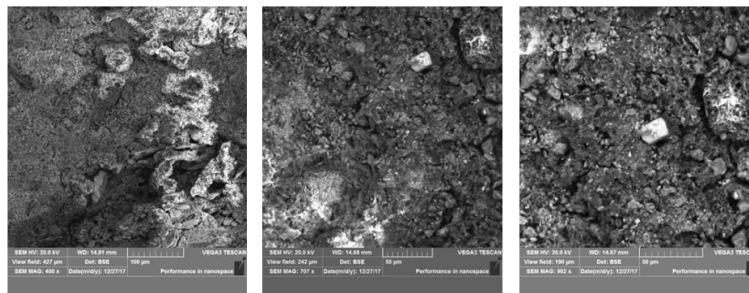
ARB-S6
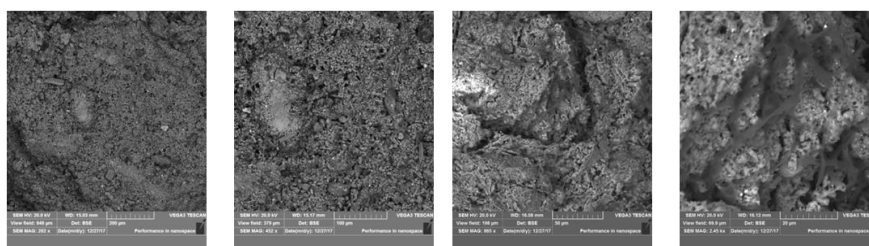
ARB-B7

Figure A.21 SEM microphographs of calcereous (ARB-Z1), stone (ARB-S6) and brick (ARB-B7) samples

Table A.23 X-ray Flourescence (PED-XRF) Analysis Results of Stone Samples

Element	Conc'n	ARB-S1	ARB-S3	ARB-S4	ARB-S5	ARB-S6	ARB-S9	ARB-S13	Ave.
Na_2O		2.64	2.82	2.78	1.61	3.69	3.02	2.01	**2.65**
MgO		1.22	1.12	0.993	2.07	0.781	0.768	1.51	**1.21**
Al_2O_3		11.63	12.75	12.99	6.44	14.45	12.81	13.12	**12.03**
SiO_2		58.27	61.57	63.84	65.62	65.14	61.06	64.86	**62.91**
P_2O_5		0.152	0.167	0.211	0.118	0.201	0.197	0.246	**0.185**
SO_3		0.300	0.570	0.920	0.774	0.211	0.936	0.060	**0.539**
Cl	%	0.000	0.025	0.018	0.018	0.0002	0.028	0.0002	**0.013**
K_2O		2.24	2.81	2.84	0.430	3.51	2.76	2.27	**2.41**
CaO		4.11	2.90	2.92	1.40	1.01	3.42	4.34	**2.87**
TiO_2		0.383	0.453	0.525	0.289	0.483	0.467	0.560	**0.451**
V_2O_5		0.008	0.013	0.014	0.016	0.017	0.015	0.014	**0.014**
Cr_2O_3		0.017	0.023	0.028	0.075	0.012	0.030	0.005	**0.027**
MnO		0.058	0.018	0.019	0.107	0.017	0.018	0.073	**0.044**
Fe_2O_3		3.08	3.23	1.80	4.86	3.05	2.40	3.66	**3.15**
LOI*		16.33	11.49	10.9	16.66	7.45	12.63	7.87	**11.90**
Co		29.9	10	16.8	36.6	17	18.2	24	**21.8**
Ni		44.7	42.9	45.4	40.8	6.4	37.5	14.1	**33.1**
Cu		12.2	11.1	16.1	8.2	9.3	13.4	13.9	**12.0**
Zn		33.5	44.5	55.8	44.3	45.3	37.8	41.5	**43.2**
Ga		16.2	16.8	17.4	7.1	16.6	18.1	18.9	**15.9**
Ge		0.9	0.9	1.2	1.8	1.3	0.7	0.8	**1.1**
As		2.5	0.5	2.1	7.7	21.6	0.9	2.9	**5.5**
Se		0.4	0.2	0.2	0.2	0.4	0.2	0.2	**0.3**
Br		0.5	0.2	0.4	0.2	0.7	0.2	0.2	**0.3**
Rb		62.2	77.9	81.5	9.9	100.8	74.3	60.2	**66.7**
Sr		390.9	320.1	332	79.4	277.2	357.3	368.5	**303.6**
Y		9.8	9.4	12	7.7	14.6	12.8	14.7	**11.6**
Zr		138.7	155.2	124.4	143	133.3	138.8	143.6	**139.6**
Nb		19.7	18.6	17.4	5.5	27.6	16.5	15.3	**17.2**
Mo		5.2	2.7	4.8	3	3.5	2.5	2.6	**3.5**
Cd		0.7	0.8	0.7	0.8	2.6	0.7	0.8	**1.0**
In	ppm	0.9	0.7	0.7	0.7	1	0.7	0.7	**0.8**
Sn		1.6	1.9	0.9	0.8	3.1	1.9	0.9	**1.6**
Sb		1	0.8	0.8	1.6	1.4	0.6	0.7	**1.0**
Te		1.3	1.1	1.1	1.1	1.3	1.2	1.8	**1.3**
I		2.3	2.1	2	2	2.4	2	2.1	**2.1**
Cs		3.4	3.6	3.5	3.6	7.5	3.6	3.7	**4.1**
Ba		488.9	526.9	517.7	98.5	640.3	542.5	527.8	**477.5**
La		26.3	23.1	28.3	7.5	18.1	24.9	16.8	**20.7**
Ce		43.3	43.8	48.4	26.8	35.6	51.7	39.1	**41.2**
Hf		5.4	6.1	5.3	3.8	4.9	4.8	3.7	**4.9**
Ta		4.7	2.4	4.1	2.2	3.5	2.4	2.5	**3.1**
W		3.5	2.1	2.1	2.1	3.1	2.6	2	**2.5**
Hg		0.7	0.5	0.6	0.6	1	0.6	0.6	**0.7**
Tl		1	0.7	0.7	0.6	1	0.7	0.7	**0.8**
Pb		17.3	22.9	17.3	12.6	9.7	18.8	14	**16.1**
Bi		0.8	0.5	0.5	0.4	0.8	0.5	0.5	**0.6**
Th		10.9	12.8	12.9	3.3	11.5	12.7	10.3	**10.6**
U		11.1	8.2	6.9	6.2	20.1	6.4	6.2	**9.3**
		Andesite							

(*) Loss on Ignition at 950°C

Table A.23 Continued

Element	Conc'n	ARB-S2	ARB-S7	ARB-S11	Ave.	ARB-S8	ARB-S10	ARB-S12	ARH-Z1
Na_2O		0.089	0.084	0.057	**0.077**	2.620	0.110	2.55	0.140
MgO		0.020	0.030	0.016	**0.021**	1.500	0.025	0.814	0.802
Al_2O_3		0.190	0.310	0.460	**0.318**	11.04	0.102	12.27	3.17
SiO_2		0.910	3.01	1.17	**1.70**	57.16	0.529	62.08	11.03
P_2O_5		0.004	0.004	0.018	**0.009**	0.171	0.004	0.179	0.207
SO_3		0.090	0.094	0.161	**0.115**	1.155	0.099	1.36	10.690
Cl	%	0.014	0.027	0.012	**0.017**	0.034	0.014	0.112	0.424
K_2O		0.010	0.010	0.085	**0.033**	2.470	0.007	3.46	1.47
CaO		60.90	58.76	60.30	**59.99**	5.690	59.19	2.32	38.72
TiO_2		0.003	0.015	0.027	**0.015**	0.412	0.003	0.492	0.239
V_2O_5		0.002	0.002	0.001	**0.002**	0.016	0.002	0.016	0.010
Cr_2O_3		0.004	0.009	0.002	**0.005**	0.042	0.003	0.008	0.006
MnO		0.038	0.013	0.004	**0.018**	0.013	0.009	0.021	0.048
Fe_2O_3		0.080	0.150	0.091	**0.109**	3.480	0.043	4.86	1.54
LOI*		37.83	37.83	37.75	**37.80**	14.34	39.43	9.85	31.45
Co		7.6	10.6	6.4	**8.2**	36.4	3.9	23.5	25.1
Ni		4.3	3.9	2.2	**3.5**	46.3	4.2	33.3	18.1
Cu		0.9	1.2	0.9	**1.0**	13.6	1.4	11.3	20.5
Zn		2.5	4.7	4.6	**3.9**	37.5	5.7	63.8	48.8
Ga		2.3	2.7	2.4	**2.5**	15.4	2.2	18.4	6.9
Ge		0.8	0.7	0.4	**0.6**	0.6	0.6	1.5	0.7
As		1.7	0.9	0.7	**1.1**	1.2	0.6	41.5	6.8
Se		0.6	0.5	0.3	**0.5**	0.4	0.5	0.3	0.5
Br		0.6	1.1	1	**0.9**	0.3	0.5	1.9	7.6
Rb		1.1	1.5	2.7	**1.8**	62.7	1.1	95.4	31.8
Sr		585.1	186.1	459.4	**410.2**	434.1	87.4	237.7	407
Y		0.8	0.7	0.5	**0.7**	11	0.7	14.2	2.9
Zr		8.8	6.3	15.5	**10.2**	145.1	5.5	157.8	34.6
Nb		3.5	3.9	4	**3.8**	19.3	3.8	23.2	3.6
Mo		3.3	3.7	3.8	**3.6**	3.6	3.6	3.7	7.1
Cd		0.9	0.8	1	**0.9**	1.7	1	0.9	1
In		0.9	0.7	1.1	**0.9**	1	1	0.8	0.9
Sn	ppm	1.1	1	0.5	**0.9**	1.5	1.1	1	6.4
Sb		1.8	1.1	1	**1.3**	1	1.7	2.8	1.3
Te		1.3	1.3	1.3	**1.3**	1.3	1.3	1.2	1.3
I		2.2	2	2.1	**2.1**	2.3	2.2	2.1	7.1
Cs		3.8	7.3	3.6	**4.9**	3.9	3.8	3.2	7.7
Ba		13.6	17.7	22.1	**17.8**	439.1	5.5	526.1	178.5
La		13.6	7.4	17.9	**13.0**	23.2	20.9	26.5	13.1
Ce		18.9	10	10	**13.0**	39.1	10	32.4	20.6
Hf		4.4	4.6	3.1	**4.0**	5.7	4.7	2.9	4.9
Ta		3.9	3.7	2.4	**3.3**	4.3	3.8	2.5	5.2
W		3	3.3	2	**2.8**	3.5	3.7	2.2	4
Hg		1.2	1.3	0.8	**1.1**	0.9	1.2	0.7	1.3
Tl		2.4	1.2	1.2	**1.6**	1.2	1.2	0.9	1.4
Pb		3.5	5.4	4.2	**4.4**	16.7	3.8	18.6	39.2
Bi		1.8	1.2	0.6	**1.2**	0.8	1	1	1.2
Th		1.7	1	1.8	**1.5**	11.2	0.7	14	4.1
U		14.6	28.8	11	**18.1**	31.1	9.2	18.8	9.4
		Limestone				Sandst.	Marble	Tuff	Calcerous Layer

(*) Loss on Ignition at 950°C

220

Table A.24a X-ray Flourescence (PED-XRF) Analysis Results of Brick Samples

Element	Conc'n	ARB-B1	ARB-B2	ARB-B3	ARB-B4	ARB-B5	ARB-B6
Na$_2$O		0.510	0.530	0.950	0.840	0.910	0.880
MgO		2.61	3.00	2.38	2.92	3.05	2.50
Al$_2$O$_3$		14.01	14.79	14.10	13.38	14.23	13.58
SiO$_2$		54.95	48.77	51.66	52.13	55.97	47.52
P$_2$O$_5$		0.476	0.692	0.421	1.02	1.163	0.548
SO$_3$		0.885	0.573	0.534	0.935	0.253	0.617
Cl	%	0.040	0.048	0.035	0.072	0.040	0.077
K$_2$O		2.99	3.66	2.73	3.03	3.23	2.94
CaO		8.75	8.53	6.31	6.89	6.71	9.89
TiO$_2$		0.783	0.746	0.873	0.783	0.820	0.774
V$_2$O$_5$		0.019	0.022	0.021	0.017	0.021	0.019
Cr$_2$O$_3$		0.022	0.019	0.018	0.022	0.015	0.024
MnO		0.111	0.126	0.127	0.124	0.141	0.116
Fe$_2$O$_3$		6.52	6.75	6.58	6.46	6.43	6.49
LOI*		7.83	11.48	13.93	11.83	7.83	14.63
Co		39.9	29.5	23.3	36.9	25.8	37.4
Ni		73.6	76.5	65.5	77.5	71.3	73.3
Cu		40.8	50.9	39.5	43.9	51.9	51.2
Zn		91.8	107.9	92.5	128.9	116.6	83.8
Ga		18.4	20.2	21	21.1	18.9	19.8
Ge		0.6	0.8	0.9	1.1	1.2	0.4
As		15.3	19.7	7.5	9.5	7.4	6.4
Se		0.3	0.4	0.3	0.3	0.5	0.3
Br		0.6	2	1.1	1.1	1.5	1.7
Rb		95.7	100	82.4	88.2	87	76.7
Sr		246.9	267.1	259.5	281.9	317.3	270.5
Y		23.6	25.3	24.6	23.7	24	23.4
Zr		202.3	181.8	209.6	213.1	205.2	220.5
Nb		16.3	13.8	19.8	16.8	21.8	17.6
Mo		3.4	4.3	3.9	3.8	3.2	3.4
Cd		0.9	1.4	0.8	0.8	0.9	0.8
In		0.9	1	0.8	0.8	0.8	0.9
Sn	ppm	4.7	4.4	3.5	2.6	3.2	5.1
Sb		1.9	0.8	0.9	1	0.9	0.9
Te		1.2	1.2	1.2	1.2	1.3	1.2
I		2.2	2.1	2.1	2.1	2.3	2.1
Cs		3.7	3.5	3.6	3.7	3.8	4.5
Ba		517.1	549.1	500.9	572.1	506.5	541
La		32.8	33.5	41.1	35.7	23.9	38.6
Ce		77.3	53.4	70.8	72.1	53.3	77.1
Hf		4.8	5.1	4.5	3.3	6.7	4.5
Ta		4	5.7	3.9	4	7.2	4.3
W		3	4.2	4.3	4.7	4.8	3.9
Hg		0.8	1.1	0.8	0.8	1.3	0.8
Tl		0.9	1.3	0.9	0.9	1.5	0.9
Pb		30.6	44	32.1	30.2	26.5	20.5
Bi		0.7	1	0.6	0.6	1.1	0.6
Th		13.4	13.6	12.5	11.2	12.4	11.6
U		8.5	19.1	7.9	8.2	8.3	8.8
Type		Brick					

(*) Loss on Ignition at 950°C

Table A.24a Continued

Element	Conc'n	ARB-B7	ARB-B8	ARB-B10	ARB-B11	ARB-B14	ARB-B17
Na$_2$O	%	0.700	1.08	0.074	1.020	0.054	0.460
MgO		2.90	2.83	2.85	2.90	3.01	3.18
Al$_2$O$_3$		14.75	14.11	16.54	14.80	12.88	15.21
SiO$_2$		52.03	51.96	49.24	52.08	57.36	54.19
P$_2$O$_5$		0.573	0.688	0.138	0.496	0.364	0.805
SO$_3$		0.439	0.462	0.202	0.364	0.453	0.344
Cl		0.049	0.056	0.000	0.010	0.536	0.061
K$_2$O		3.19	3.07	2.75	2.72	4.53	3.18
CaO		6.41	8.44	4.51	6.36	7.40	8.49
TiO$_2$		0.845	0.800	0.708	0.865	0.784	0.851
V$_2$O$_5$		0.024	0.025	0.016	0.021	0.018	0.026
Cr$_2$O$_3$		0.023	0.040	0.018	0.024	0.023	0.015
MnO		0.119	0.119	0.091	0.119	0.106	0.151
Fe$_2$O$_3$		6.78	6.65	6.74	6.71	5.96	7.36
LOI*		11.39	9.87	16.32	11.39	6.93	5.34
Co	ppm	15.6	48.8	49.5	29.4	41.2	28.3
Ni		88.2	74.3	75	75.3	69.3	80.8
Cu		42.1	41.4	36.4	40.7	38.7	54.6
Zn		100.8	94.2	86.1	93	84.4	105.4
Ga		20.4	19.2	22	22.2	17.4	24.2
Ge		0.5	2.2	1.4	1.9	0.5	1.6
As		9.8	15.7	33.2	10.7	11	16.2
Se		0.3	0.3	0.5	0.4	0.3	0.5
Br		2.1	0.3	0.4	1	2.9	5.9
Rb		100.3	99	107.3	95.2	102.1	96.3
Sr		248.7	310.3	194.5	228.4	187.8	286.4
Y		25.6	24	30.8	25.9	21.9	25.6
Zr		231.5	204.2	276.5	249.6	182.7	186.9
Nb		22.8	19.9	20	21.6	17.2	19.5
Mo		5.5	3.3	4.5	4.8	3.3	4.6
Cd		2.3	0.9	0.9	0.9	0.9	0.8
In		0.9	0.9	0.8	0.9	0.8	0.8
Sn		5.8	4.4	3.7	2.8	3.5	2.2
Sb		1	0.7	3.4	1	0.9	1
Te		1.3	1.2	1.3	1.3	1.2	1.2
I		2.2	2.1	2.3	2.4	2.1	2.3
Cs		3.7	3.7	9.1	6	3.7	8.4
Ba		539.8	526.2	518.8	524	537.3	611.7
La		31.2	37.4	34.9	42.4	36.3	42.9
Ce		57.1	70.1	80.1	89.9	81	80.4
Hf		5.7	6.6	4.7	7.1	3.1	6.2
Ta		4.1	6.6	6.2	6.6	3.9	7.6
W		3	2.9	4.7	4.8	2.8	5.2
Hg		0.8	0.8	1.3	1.4	0.7	1.4
Tl		1.1	1	1.5	1.5	0.8	1.7
Pb		33.7	24.6	22.2	28.6	29.5	22
Bi		0.6	0.6	0.8	0.7	0.6	0.9
Th		14	12.2	12.2	11.6	12.9	11.7
U		23.1	8.6	8.5	8.8	8.6	9.1
Type		Brick					

(*) Loss on Ignition at 950°C

222

Table A.24a Continued

Element	Conc'n	ARB-B18	ARB-B19	ARB-B24	ARB-B25	ARB-B28	ARB-B29	Ave.
Na_2O	%	0.870	1.21	0.090	0.160	0.100	0.560	**0.611**
MgO		2.93	3.01	3.11	2.77	2.59	2.95	**2.86**
Al_2O_3		16.22	12.68	14.99	13.90	13.51	15.48	**14.40**
SiO_2		52.86	43.93	59.37	58.85	54.21	53.76	**52.82**
P_2O_5		0.500	0.579	0.383	0.694	0.442	0.767	**0.597**
SO_3		0.843	1.97	0.095	0.125	0.218	0.190	**0.528**
Cl		0.024	1.346	0.007	0.016	0.027	0.064	**0.139**
K_2O		3.16	3.77	4.18	3.09	3.06	3.60	**3.27**
CaO		5.92	9.58	6.96	9.97	9.49	7.81	**7.69**
TiO_2		0.939	0.740	0.844	0.791	0.858	0.807	**0.812**
V_2O_5		0.030	0.020	0.020	0.025	0.025	0.028	**0.022**
Cr_2O_3		0.025	0.026	0.020	0.021	0.017	0.022	**0.022**
MnO		0.143	0.109	0.110	0.133	0.128	0.126	**0.122**
Fe_2O_3		7.58	6.04	6.21	6.84	6.30	7.03	**6.63**
LOI*		7.93	14.63	3.84	2.85	9.93	6.85	**9.71**
Co		24	37.9	39.2	31.7	29.4	43.9	**34.0**
Ni		84.7	71.8	77.2	77.7	73.3	85.2	**76.1**
Cu		53.5	43.5	38.2	44.2	43.8	45.3	**44.5**
Zn		156.2	76.6	84.9	93.3	84.3	104.1	**99.2**
Ga		21.5	17.4	16.9	19.8	18	22.5	**20.1**
Ge		0.5	0.4	2.1	0.9	1.5	1.4	**1.1**
As		7.3	7.5	11.2	17	19	17	**13.4**
Se		0.3	0.3	0.3	0.3	0.3	0.3	**0.3**
Br		1.9	8	0.7	0.9	2	2	**2.0**
Rb		101.4	87.2	95.9	97	69.7	106.8	**93.8**
Sr		212.6	351	223.2	257	290.4	276.8	**261.7**
Y		28.5	22.4	23.9	23.7	21.2	26.7	**24.7**
Zr		214.3	194.9	196.8	181.8	162	204.5	**206.6**
Nb		22.8	19.4	17.5	20	16.5	23.5	**19.3**
Mo		3.8	6	3.7	3.8	4.8	7.4	**4.3**
Cd		0.8	0.9	0.8	0.6	0.9	0.9	**1.0**
In	ppm	1	0.8	0.7	1	0.8	0.7	**0.9**
Sn		1.5	0.9	1	2.6	1	6.2	**3.3**
Sb		1	1	0.9	0.9	0.9	1	**1.1**
Te		1.3	1.2	1.2	1.2	1.2	1.3	**1.2**
I		2.2	2.1	2.2	2.1	2	2.2	**2.2**
Cs		4.6	3.7	3.7	3.6	3.5	3.8	**4.5**
Ba		550.6	512.9	641.9	539.6	463.4	700.6	**547.4**
La		40.6	39.2	26.8	31.8	35.9	34.3	**35.5**
Ce		81.3	49.1	73.8	72.3	59	72.6	**70.6**
Hf		10	4.4	3	7.1	5.1	4.5	**5.4**
Ta		4.4	4	3.8	4.1	4	4.1	**4.9**
W		3.1	2.8	2.9	3	2.8	3	**3.7**
Hg		1.3	0.7	0.8	0.9	0.8	0.8	**1.0**
Tl		1	0.9	0.8	1	0.7	0.8	**1.1**
Pb		28.8	14.6	24.7	27	23.3	43.7	**28.1**
Bi		0.6	0.6	0.6	0.6	0.9	0.7	**0.7**
Th		13.2	12.4	12	12.3	8.7	14.6	**12.4**
U		24.8	8.5	8.3	10.5	13.1	8.7	**11.2**
Type		Brick						

(*) Loss on Ignition at 950°C

Table A.24b X-ray Flourescence (PED-XRF) Analysis Results of Pilae Samples

Element	Conc'n	ARB-B9	ARB-B12	ARB-B13	ARB-B15	ARB-B16
Na$_2$O		0.380	0.370	1.110	0.930	0.960
MgO		3.29	2.79	2.61	3.18	2.88
Al$_2$O$_3$		13.38	14.78	11.28	15.87	14.79
SiO$_2$		48.01	61.16	54.03	54.66	62.80
P$_2$O$_5$		0.835	0.586	0.557	0.617	0.426
SO$_3$		0.510	0.759	1.450	0.323	0.527
Cl	%	0.021	0.049	0.000	0.007	0.027
K$_2$O		2.84	3.38	2.26	3.24	3.10
CaO		10.70	6.32	6.12	5.68	6.22
TiO$_2$		0.789	0.824	0.829	0.906	0.854
V$_2$O$_5$		0.020	0.021	0.023	0.026	0.024
Cr$_2$O$_3$		0.019	0.024	0.014	0.021	0.030
MnO		0.130	0.121	0.117	0.125	0.119
Fe$_2$O$_3$		6.57	6.66	5.73	7.08	6.60
LOI*		12.38	2.37	13.45	7.83	0.33
Co		34.3	30.3	37.3	57.2	32.1
Ni		75	80	55.4	78.9	79.6
Cu		52.2	45.4	36.3	43.6	200.5
Zn		122.7	96.3	106.5	100.1	92.6
Ga		18.8	20.1	16.1	22.7	18.8
Ge		1.3	2.1	1.7	2	2.3
As		17.5	10.9	8.2	14.9	15.6
Se		0.5	0.3	0.4	0.5	0.3
Br		8.9	1.4	2	1.4	2.4
Rb		89.5	99.6	65.2	107.6	97
Sr		296.7	241.9	328.1	225.3	241.3
Y		24.5	25.4	19.5	27.6	26.3
Zr		176.3	225.7	180.1	229.9	260.7
Nb		16.6	18	21.5	24.3	23.8
Mo		3.6	3.9	3.5	6.7	3.5
Cd		0.9	0.8	0.9	0.9	0.9
In	ppm	0.9	0.8	0.8	0.4	0.6
Sn		5.5	2.9	3.3	3.4	7.8
Sb		1	0.9	1	0.9	1
Te		1.3	1.1	1.3	1.4	1.2
I		3.5	2.1	2.3	2.4	2.2
Cs		12.1	3.6	4	4	3.7
Ba		539.4	535.5	521.5	536.5	537.2
La		43.3	33.9	33.7	34.3	34.5
Ce		71.4	73.8	55.2	83.5	62
Hf		8.4	5.5	7.6	6	5.9
Ta		7.4	4.1	6	6.9	7.4
W		5	2.8	4.7	5	3
Hg		1.4	0.9	1.2	1.3	0.8
Tl		1.6	0.9	0.9	1.6	0.9
Pb		35.2	32.3	24.5	30.6	53.3
Bi		1.2	0.6	1	1.1	0.7
Th		12.2	13.7	9.2	13	13
U		8.3	7.9	6.7	9	8.8
Type		Pilae				

(*) Loss on Ignition at 950°C

Element	Conc'n	ARB-B20	ARB-B21	ARB-B22	ARB-B23	Ave.
Na$_2$O		0.220	1.33	1.46	0.680	**0.827**
MgO		2.70	2.64	2.57	2.84	**2.83**
Al$_2$O$_3$		14.01	14.85	15.77	14.52	**14.36**
SiO$_2$		48.02	51.42	54.51	52.80	**54.16**
P$_2$O$_5$		0.393	0.342	0.522	0.491	**0.530**
SO$_3$		0.547	0.472	0.447	0.499	**0.615**
Cl	%	0.048	0.034	0.023	0.017	**0.025**
K$_2$O		2.87	2.87	2.92	2.88	**2.93**
CaO		6.08	4.41	5.84	5.62	**6.33**
TiO$_2$		0.787	0.843	0.936	0.845	**0.846**
V$_2$O$_5$		0.026	0.018	0.024	0.027	**0.023**
Cr$_2$O$_3$		0.019	0.026	0.021	0.022	**0.022**
MnO		0.110	0.112	0.145	0.121	**0.122**
Fe$_2$O$_3$		6.41	6.64	6.92	6.85	**6.61**
LOI*		17.73	14.84	7.73	11.38	**9.78**
Co		38	59.6	36.4	59.2	**42.7**
Ni		78.4	84.7	77.5	81.6	**76.8**
Cu		38.9	41.2	45.7	40.9	**60.5**
Zn		84.6	117.8	107.2	105.3	**103.7**
Ga		20.1	18.8	20.8	22	**19.8**
Ge		0.4	0.9	2.2	1	**1.5**
As		15.3	10.4	16.9	18.4	**14.2**
Se		0.4	0.3	0.3	0.5	**0.4**
Br		2.2	2.9	1.1	1.6	**2.7**
Rb		89.7	101.7	92.2	100	**93.6**
Sr		221.1	195.5	279	240	**252.1**
Y		24.1	24.3	27	26.9	**25.1**
Zr		211.6	235.1	215.4	231.8	**218.5**
Nb		18.6	18.4	24.8	23.9	**21.1**
Mo		5.4	4	2.8	6	**4.4**
Cd		0.8	0.9	1.1	0.9	**0.9**
In		0.8	0.8	1.7	0.9	**0.9**
Sn	ppm	2.1	2.5	5.7	2.9	**4.0**
Sb		0.7	0.8	0.9	1.1	**0.9**
Te		1.2	1.2	1.2	1.4	**1.3**
I		2.1	2.1	2.1	2.4	**2.4**
Cs		3.7	3.6	3.6	5.6	**4.9**
Ba		499.2	528.5	538.5	516	**528.0**
La		34.9	39.7	37.2	39.4	**36.8**
Ce		74.8	81.3	79.2	80.9	**73.6**
Hf		3.2	5.5	7.4	5.6	**6.1**
Ta		3.8	3.9	4	6.5	**5.6**
W		2.8	6	2.4	5	**4.1**
Hg		0.7	0.7	0.8	1.3	**1.0**
Tl		0.9	0.9	0.7	1.6	**1.1**
Pb		22	39.8	35.3	32.5	**33.9**
Bi		0.6	0.6	0.4	1.1	**0.8**
Th		12.3	12.1	11.8	11.4	**12.1**
U		7.8	6.8	18.1	9.6	**9.2**
Type				Pilae		

(*) Loss on Ignition at 950°C

Table A.24c X-ray Flourescence (PED-XRF) Analysis Results of Pipe Samples

Element	Conc'n	ARB-B26	ARB-B27	Ave.
Na_2O		0.360	0.390	**0.375**
MgO		2.23	2.84	**2.54**
Al_2O_3		14.76	16.22	**15.49**
SiO_2		58.60	59.28	**58.94**
P_2O_5		0.271	0.275	**0.273**
SO_3		0.141	0.130	**0.136**
Cl	%	0.026	0.020	**0.023**
K_2O		2.76	3.09	**2.93**
CaO		7.20	5.74	**6.47**
TiO_2		0.800	0.844	**0.822**
V_2O_5		0.022	0.026	**0.024**
Cr_2O_3		0.020	0.016	**0.018**
MnO		0.125	0.130	**0.127**
Fe_2O_3		6.60	7.38	**6.99**
LOI*		6.83	3.74	**5.29**
Co		63.3	30.9	**47.1**
Ni		62	71.8	**66.9**
Cu		34.3	39.3	**36.8**
Zn		85.5	94.8	**90.2**
Ga		21.5	23.3	**22.4**
Ge		0.8	1.1	**1.0**
As		13.5	9.7	**11.6**
Se		0.3	0.3	**0.3**
Br		1.2	1.3	**1.3**
Rb		90.1	100.2	**95.2**
Sr		266	221.2	**243.6**
Y		22.3	24.2	**23.3**
Zr		188.1	185.1	**186.6**
Nb		15.6	18	**16.8**
Mo		5	3.6	**4.3**
Cd		0.8	1	**0.9**
In		0.8	1	**0.9**
Sn	ppm	3.5	2.2	**2.9**
Sb		0.5	0.6	**0.6**
Te		1.2	1.2	**1.2**
I		2.1	2.1	**2.1**
Cs		3.7	4.2	**4.0**
Ba		527.7	488.7	**508.2**
La		26	32.5	**29.3**
Ce		68.2	66.7	**67.5**
Hf		3.7	5.4	**4.6**
Ta		3.6	3.9	**3.8**
W		2.7	3.6	**3.2**
Hg		0.8	0.8	**0.8**
Tl		0.9	1.4	**1.2**
Pb		30.4	24.1	**27.3**
Bi		0.4	0.6	**0.5**
Th		12.1	14.2	**13.2**
U		8.1	13.6	**10.9**
Type			Pipe	

(*) Loss on Ignition at 950°C

Table A.25 X-ray Flourescence (PED-XRF) Analysis Results of Plaster Samples

Element	Conc'n	ARB-P1	ARB-P2a	ARB-P2b	ARB-P3	Ave.
Na$_2$O		0.050	0.120	0.190	0.130	**0.147**
MgO		0.953	1.40	1.60	1.32	**1.44**
Al$_2$O$_3$		5.03	5.78	5.98	6.07	**5.94**
SiO$_2$		20.51	21.37	21.63	22.29	**21.76**
P$_2$O$_5$		0.253	0.285	0.296	0.253	**0.278**
SO$_3$		0.523	3.55	3.27	12.75	**6.52**
Cl	%	0.031	0.906	1.054	0.394	**0.785**
K$_2$O		1.31	2.92	3.01	2.16	**2.69**
CaO		33.88	23.41	23.76	25.10	**24.09**
TiO$_2$		0.399	0.476	0.478	0.473	**0.476**
V$_2$O$_5$		0.010	0.016	0.013	0.013	**0.014**
Cr$_2$O$_3$		0.011	0.017	0.015	0.008	**0.013**
MnO		0.065	0.068	0.066	0.072	**0.069**
Fe$_2$O$_3$		3.16	3.66	3.57	3.43	**3.55**
LOI*		33.98	36.99	35.83	25.93	**32.92**
Co		14.2	19.7	21	34.3	**25.0**
Ni		30	39.6	41.3	38.1	**39.7**
Cu		21.8	30.4	27.9	26.1	**28.1**
Zn		58.9	52.1	54.4	58.1	**54.9**
Ga		9.7	11.4	11.5	11.1	**11.3**
Ge		1	1	0.7	1.4	**1.0**
As		7.8	10.2	8.9	14.7	**11.3**
Se		0.3	0.4	0.5	0.5	**0.5**
Br		1.9	5.8	6.6	4.7	**5.7**
Rb		37.9	56.9	56.1	43.8	**52.3**
Sr		424	291	304.5	295.4	**297.0**
Y		9.7	12.8	12	11.9	**12.2**
Zr		85.3	122.3	116.2	107.7	**115.4**
Nb		10.6	10.3	11.2	13.8	**11.8**
Mo		3.5	3.7	3.2	3.9	**3.6**
Cd		0.9	1	0.9	0.9	**0.9**
In	ppm	0.9	1	0.9	0.9	**0.9**
Sn		2.1	2.8	1.6	2.1	**2.2**
Sb		1	1.1	1.1	1.5	**1.2**
Te		0.6	1.5	1.4	1.3	**1.4**
I		2.1	2.6	2.4	2.3	**2.4**
Cs		4.3	4.5	4.1	3.5	**4.0**
Ba		263.9	307.9	306.4	305.4	**306.6**
La		28.5	24.2	17.4	11.9	**17.8**
Ce		23.3	45.1	42	34.7	**40.6**
Hf		3	4.9	6.5	4.7	**5.4**
Ta		3.4	6.1	5.9	5.7	**5.9**
W		2.6	4.1	4.1	4	**4.1**
Hg		0.8	1.4	0.9	1.3	**1.2**
Tl		0.9	1.4	0.7	0.8	**1.0**
Pb		19.7	20	23	31.5	**24.8**
Bi		0.6	1.1	0.6	1.1	**0.9**
Th		6.3	6.7	7.5	7.4	**7.2**
U		9.1	11.6	12.1	10.3	**11.3**

(*) Loss on Ignition at 950°C

Table A.26 X-ray Flourescence (PED-XRF) Analysis Results of Mortar Samples

Element	Conc'n	ARB-M1	ARB-M3	ARB-M4	ARB-M5	ARB-M6	ARB-M7	ARB-M8
Na$_2$O	%	0.048	0.051	0.048	0.048	0.085	0.047	0.048
MgO		1.40	1.25	0.928	2.28	0.385	0.525	0.664
Al$_2$O$_3$		8.73	5.40	5.87	8.88	4.26	5.42	6.11
SiO$_2$		31.41	25.87	33.87	36.28	25.85	30.89	38.77
P$_2$O$_5$		0.266	0.117	0.132	0.332	0.152	0.142	0.146
SO$_3$		0.646	0.933	0.874	1.337	0.484	0.492	0.889
Cl		0.023	0.023	0.018	0.031	0.084	0.030	0.031
K$_2$O		2.20	0.93	0.929	3.02	1.11	1.14	1.40
CaO		24.01	28.72	20.55	22.99	32.89	24.16	23.71
TiO$_2$		0.569	0.416	0.371	0.538	0.321	0.356	0.337
V$_2$O$_5$		0.016	0.017	0.012	0.019	0.008	0.012	0.010
Cr$_2$O$_3$		0.012	0.039	0.006	0.011	0.017	0.020	0.005
MnO		0.081	0.064	0.110	0.087	0.061	0.043	0.064
Fe$_2$O$_3$		4.25	3.95	4.86	3.91	2.36	2.68	2.60
LOI*		26.62	32.83	31.83	20.72	31.43	34.82	25.91
Co	ppm	20.5	32	14.8	17.2	18	19.2	12.1
Ni		52.4	75.6	29.8	51.7	14.9	17.8	29.2
Cu		25.6	38.6	20.5	32.7	14.5	10.9	14.8
Zn		64.1	66.3	64.9	65.1	27.6	32	39.6
Ga		12.6	10.1	8.3	11.3	8.8	9.9	10.2
Ge		1.4	0.7	1.3	0.4	0.7	0.4	0.8
As		11.3	21.4	15.4	10.9	12.4	10.4	29
Se		0.3	0.3	0.3	0.3	0.5	0.3	0.3
Br		1.6	0.3	0.9	1.8	1.1	1.2	1.1
Rb		39.3	38.1	28	40.6	28.4	36.2	39
Sr		538.5	348.2	386.6	265.2	225.4	211.4	250.8
Y		13.9	12.3	9.5	16.3	10.3	9.2	8.8
Zr		140.1	255	83.5	106.6	96.6	102	84.5
Nb		17.1	9.1	12.6	9.4	14.5	13	12.8
Mo		3.3	4.6	3.1	3.4	3.6	6.3	3.4
Cd		0.9	0.8	0.8	0.8	0.9	0.8	1.5
In		0.9	0.8	0.8	0.8	1	0.8	0.9
Sn		2	0.8	2.6	1.9	2	0.9	1
Sb		0.9	0.9	1	0.9	1	0.9	0.9
Te		1.2	1.1	1.1	1.1	1.3	1.2	1.6
I		2	2	2.1	2	2.7	2	2
Cs		3.4	4.1	3.6	3.4	3.7	4.1	3.5
Ba		318.3	304.2	344.4	258.1	188.2	316	264.8
La		34.3	25.1	21.2	23.2	7.7	27.2	25.6
Ce		52.4	34	34.4	39.6	26.7	10	29.7
Hf		5	3.4	3.8	3.2	4.4	2.4	2.8
Ta		3.5	4.2	3.1	3.8	4.6	2.7	2.1
W		2.7	3.1	2.4	2.6	3.4	3	2.3
Hg		0.8	0.9	0.8	0.8	1.3	0.7	0.8
Tl		0.9	0.9	0.8	0.8	1.4	0.8	0.9
Pb		18.7	21.5	26.9	21.1	10	12.5	13.1
Bi		0.6	0.7	0.6	0.5	1.1	0.6	0.6
Th		8.1	4.4	5.8	6.5	5.6	6.6	7.2
U		12.7	8.1	10.3	8.2	17.2	8.2	24.6

(*) Loss on Ignition at 950°C

Table A.26 Continued

Element	Conc'n	ARB-M9	ARB-M10	ARB-M11	ARB-M12	ARB-M13	ARB-M14
Na_2O	%	0.051	0.050	0.074	0.048	0.054	0.050
MgO		0.431	0.541	4.619	0.609	0.748	0.705
Al_2O_3		4.63	5.74	6.08	5.91	5.00	5.23
SiO_2		25.19	34.21	43.51	34.18	27.56	35.11
P_2O_5		0.097	0.128	0.122	0.119	0.121	0.107
SO_3		0.387	0.656	0.833	0.599	1.24	0.482
Cl		0.033	0.038	0.006	0.032	0.255	0.027
K_2O		0.907	1.41	1.61	1.59	1.14	1.16
CaO		29.96	23.87	19.58	24.10	19.67	21.81
TiO_2		0.316	0.312	0.343	0.331	0.372	0.304
V_2O_5		0.012	0.011	0.015	0.011	0.012	0.015
Cr_2O_3		0.016	0.030	0.008	0.016	0.013	0.015
MnO		0.049	0.051	0.049	0.067	0.046	0.056
Fe_2O_3		2.61	2.54	2.69	2.26	2.64	3.10
LOI*		35.92	30.33	20.47	30.872	41.5	31.54
Co	ppm	21.9	15.8	22.7	30.1	19.9	31.5
Ni		21.6	21.3	25.3	24.4	18.2	22.8
Cu		12.4	11.3	20.1	10.6	9.1	16.8
Zn		36	29	32.3	26.4	31.3	32.9
Ga		8.8	9.6	9	9.7	10.4	9.4
Ge		0.4	0.4	0.7	0.4	0.3	1
As		11.8	12.7	13.4	12	10.6	23.9
Se		0.3	0.3	0.4	0.3	0.2	0.2
Br		0.9	0.9	2.6	0.6	4.1	0.8
Rb		29.6	33	33.8	37.8	36	33.7
Sr		273.2	201.5	275.9	239.5	252.5	227.3
Y		10.1	9.1	10.4	10.6	8.8	9.4
Zr		118	153.6	83.8	83.4	95.3	87.2
Nb		11.7	8.9	8.8	12.7	9.2	9.4
Mo		3.8	5	3.2	3.3	2.8	5.7
Cd		0.9	0.8	0.7	0.8	0.7	0.8
In		0.9	0.6	0.9	0.8	0.8	0.9
Sn		1.8	0.5	1.1	1.6	1.1	1
Sb		1.2	1.2	3.3	0.9	0.8	1.4
Te		1.2	1.2	1.1	1.2	1.1	1.2
I		2.1	2.6	2.3	2.1	2.1	1.4
Cs		3.6	3.5	3.9	3.5	3.6	3.8
Ba		248.7	220.8	191.9	258.5	342	264.1
La		17.2	24.1	13.6	27.5	7.5	21.1
Ce		23.8	20.2	35.5	26.8	38.4	25.9
Hf		2.7	1.9	4.2	1.8	2.4	1.8
Ta		2.8	2.6	4.9	2.6	2.3	2.8
W		2.3	2.1	3.6	2.1	2.1	2.2
Hg		0.8	0.7	1.2	0.7	1.5	0.8
Tl		0.8	0.8	1.4	0.8	0.7	0.8
Pb		8.9	11.5	9.6	11.2	9.4	12.3
Bi		0.6	0.5	0.9	0.6	0.6	0.6
Th		5.3	5.9	5.1	6.7	4.9	6.5
U		18.4	7.9	8.4	11.6	7.1	7.6

(*) Loss on Ignition at 950°C

Table A.26 Continued

Element	Conc'n	ARB-M15	ARB-M16	ARB-M17	ARB-M18	ARB-M19	ARB-M20
Na$_2$O	%	0.085	0.056	0.048	0.600	0.081	0.048
MgO		1.39	1.41	0.559	1.14	1.394	0.534
Al$_2$O$_3$		3.29	4.25	4.91	6.97	4.94	5.03
SiO$_2$		17.22	20.94	29.50	40.37	23.59	25.76
P$_2$O$_5$		0.052	0.077	0.123	0.222	0.123	0.131
SO$_3$		1.084	1.95	0.669	0.975	1.18	0.674
Cl		0.061	0.071	0.031	0.037	0.008	0.025
K$_2$O		0.65	1.46	1.12	1.62	0.91	1.17
CaO		39.71	30.07	24.05	14.89	30.73	27.51
TiO$_2$		0.258	0.240	0.303	0.443	0.373	0.366
V$_2$O$_5$		0.014	0.010	0.012	0.012	0.013	0.012
Cr$_2$O$_3$		0.019	0.025	0.016	0.021	0.012	0.009
MnO		0.071	0.068	0.049	0.077	0.058	0.056
Fe$_2$O$_3$		2.30	2.59	2.68	3.85	2.77	2.98
LOI*		33.89	36.4	35.69	28.83	34.29	35.73
Co	ppm	18	11	11.8	12	19	28.5
Ni		54.2	60.3	29.9	51.8	22	25
Cu		20.2	21.7	17.7	20.3	14.6	12.1
Zn		27.8	35.6	46.3	53.9	68.2	32.5
Ga		7.1	8.4	8.7	12.6	10.4	9.3
Ge		0.7	0.4	0.4	0.4	0.7	1.1
As		18	17.3	6.3	24.8	10.8	8.2
Se		0.5	0.3	0.3	0.3	0.5	0.3
Br		1.3	1.6	2.5	1	1.6	0.9
Rb		31.9	46	34.2	62.2	27.6	36.7
Sr		850.9	710.1	214.3	397.1	536.3	191.9
Y		6.6	7.1	8.7	14.8	9	10.9
Zr		87.9	88.7	88.9	156.6	152.1	169.7
Nb		12	3.6	9.9	19.2	11.4	8
Mo		4.1	5.2	3.2	6.4	4.1	3.4
Cd		2.5	0.9	0.8	0.8	0.7	0.9
In		1.1	0.7	0.9	0.9	1	0.9
Sn		1.2	1.1	0.8	2.4	1	1.7
Sb		1.1	1	1	1	1.7	0.7
Te		1.4	1.2	1.2	1.2	1.3	1.3
I		2.3	2.2	1.4	2.2	2.3	2.1
Cs		3.2	3.8	2.9	3.6	3.9	5.1
Ba		278.7	442	300.1	427.6	256.8	247.8
La		17.3	20.8	24.1	29	17.7	7.6
Ce		38.8	21	25.1	55.4	33.1	22.5
Hf		5.2	3	3.5	2.2	4	2.6
Ta		5.7	3.4	2.9	3.2	4.7	2.7
W		4.5	2.6	2.3	3.5	4.3	2.3
Hg		1.5	0.8	0.7	0.8	1.4	0.8
Tl		1.5	0.4	0.8	0.9	0.9	0.8
Pb		10.2	23.5	13.2	17.8	16.5	14.8
Bi		0.6	0.7	0.6	0.6	1.1	0.6
Th		6.1	6.8	5.4	9.7	5.5	6.3
U		19.7	15.2	11.7	20.8	16.8	8.2

(*) Loss on Ignition at 950°C

Table A.26 Continued

Element	Conc'n	ARB-M21	ARB-M22	ARB-M23	ARB-M24	ARB-M25	ARB-M26
Na_2O		0.078	0.047	0.081	0.047	0.052	0.048
MgO		1.86	0.897	0.958	0.536	0.583	0.916
Al_2O_3		6.35	4.48	4.64	5.42	5.45	6.12
SiO_2		40.66	22.47	23.76	30.73	31.14	35.46
P_2O_5		0.194	0.105	0.098	0.127	0.104	0.126
SO_3		0.737	1.52	1.66	0.617	0.496	0.927
Cl	%	0.045	0.021	0.020	0.025	0.027	0.028
K_2O		1.63	0.843	0.967	1.40	1.39	1.03
CaO		26.31	28.22	31.25	23.61	22.69	23.19
TiO_2		0.423	0.304	0.380	0.333	0.339	0.420
V_2O_5		0.014	0.008	0.008	0.010	0.012	0.013
Cr_2O_3		0.010	0.005	0.011	0.005	0.008	0.010
MnO		0.068	0.060	0.060	0.067	0.047	0.056
Fe_2O_3		3.00	2.42	2.88	2.70	3.02	2.88
LOI*		18.83	38.83	33.29	34.83	34.82	28.38
Co		18.6	12.9	22.3	27.8	21.6	12
Ni		28.4	25.1	19.3	20	22	24
Cu		18	14.5	11	12.3	17	13.6
Zn		39.7	78	59.8	37.2	39.8	44.6
Ga		10.1	8.2	8.7	10.8	9.5	10.5
Ge		1.5	0.4	0.7	0.4	0.4	1.1
As		12.7	13.8	10.3	21.1	10.5	9.1
Se		0.4	0.2	0.5	0.3	0.3	0.3
Br		2.1	3.4	1.2	3	1.5	0.2
Rb		32.3	25.1	27.3	38.7	39.5	30.5
Sr		244.6	439.9	522.5	241.6	203.1	285.3
Y		10	7.7	8.3	9.7	10.5	10.4
Zr		96.7	82.4	85.7	90.5	106.2	100.1
Nb		12.9	8.2	7.9	3.3	10.7	9
Mo		3.7	3.1	4.5	2.9	2.9	3.3
Cd		0.6	0.8	0.9	0.8	0.8	0.9
In	ppm	1	0.8	0.9	0.8	0.8	0.8
Sn		2.7	1	1.1	1.4	0.9	1.5
Sb		1	1	1.1	4.4	2.3	0.9
Te		1.8	1.2	1.4	1.1	1.2	1.2
I		2.1	1.5	2.3	2	2	2
Cs		5	3.6	3.8	3.4	5.2	3.6
Ba		193.2	288.3	252.1	358.8	285.1	246.2
La		18.8	23	23.8	21.6	24.7	21.4
Ce		36.3	24.1	34	22.7	19.5	32
Hf		4.4	3	4.4	1.8	2.6	1.8
Ta		5	2.8	4.4	2.7	2.7	2.7
W		3.8	2.7	4	1.7	2.2	2.3
Hg		1.3	0.8	1.3	0.7	0.7	0.7
Tl		1.4	0.8	1.5	0.8	0.7	0.8
Pb		12	14.9	14.8	11.8	9.9	10.9
Bi		1	0.6	1.1	0.6	0.6	0.5
Th		6.4	3.5	4.3	6.3	5.7	5.8
U		19.1	8.6	9.2	6.9	8.5	20

(*) Loss on Ignition at 950°C

Table A.26 Continued

Element	Conc'n	ARB-M27	ARB-M28	ARB-M29	ARB-M30	ARB-M31	ARB-M32	ARB-M33
Na_2O	%	0.076	0.380	0.053	0.050	0.050	0.047	0.075
MgO		0.677	0.865	1.35	0.693	0.742	0.567	0.309
Al_2O_3		5.82	4.44	6.33	5.26	3.90	5.06	4.72
SiO_2		37.80	20.82	34.37	30.13	19.99	30.38	29.02
P_2O_5		0.106	0.191	0.171	0.119	0.092	0.103	0.106
SO_3		0.501	0.828	1.23	0.815	1.21	0.813	0.437
Cl		0.013	1.58	0.029	0.028	0.036	0.020	0.008
K_2O		1.83	2.28	1.42	1.06	0.877	1.32	1.43
CaO		25.58	28.94	19.73	23.61	34.69	25.57	34.79
TiO_2		0.294	0.454	0.468	0.370	0.304	0.291	0.237
V_2O_5		0.007	0.013	0.015	0.012	0.008	0.011	0.005
Cr_2O_3		0.011	0.015	0.049	0.005	0.006	0.007	0.003
MnO		0.047	0.078	0.082	0.058	0.058	0.043	0.035
Fe_2O_3		2.08	2.36	4.13	2.91	2.57	2.20	1.48
LOI*		25.83	36.98	30.93	34.92	35.72	33.82	27.93
Co	ppm	23.2	23.9	26.2	21.3	24.6	13.7	16.7
Ni		14.6	19.7	65.8	23.1	22.8	18.3	5.6
Cu		14.2	10.3	48.9	12.7	14	10.6	6.3
Zn		36.4	31.7	59.1	46.6	54.2	29.9	19.3
Ga		8.5	9.8	11.4	11.6	8.2	9.2	7
Ge		0.9	0.4	1.6	0.4	0.5	0.4	0.5
As		13.1	9.6	25.7	38.9	10.8	9.6	12.2
Se		0.4	0.3	0.3	0.3	0.3	0.2	0.4
Br		2.3	7.6	0.9	0.5	1.2	0.8	1.4
Rb		27.9	30.9	50.4	37.2	26.3	31.1	21.3
Sr		222.9	354.8	403	247.5	351.7	267.3	219.7
Y		7.4	8.9	11.7	9.1	8.2	7	7.6
Zr		69.9	99.3	137.6	123.4	80.2	78.4	58.1
Nb		5.9	12.1	13	13	8.1	10.4	16.6
Mo		3.1	3	3.4	4.2	3.2	3.3	3.7
Cd		0.9	0.9	1.7	0.9	0.9	0.8	1.4
In		0.8	0.8	0.8	0.9	0.8	0.7	1
Sn		1.6	0.9	2.4	1	1.7	0.9	1.1
Sb		0.8	0.9	0.9	1	1.3	0.9	2.8
Te		0.8	1.2	0.8	1.2	1.1	1.1	1.3
I		2.2	2.1	2.1	2	1.3	2	3.2
Cs		4.5	3.6	3.6	3.6	3.5	3.4	3.7
Ba		223	313.8	382.7	303.7	223.7	269.8	144.9
La		20.3	7.5	23	21.2	17.4	22.5	9.8
Ce		17.7	23.9	49.9	20.7	17.7	24.9	30.1
Hf		4.3	6.5	3.3	2.2	2.7	1.7	3.6
Ta		4.5	2	4.1	2.8	3.1	2.4	3.9
W		3.4	2.1	2.6	2.2	2.6	2.1	3.5
Hg		1.1	0.7	0.8	0.7	0.8	0.7	1.2
Tl		1.3	0.8	0.9	1.2	0.8	0.8	0.8
Pb		21.2	12.8	19.9	16	11.7	10.1	9.9
Bi		1	1.1	0.6	0.7	0.6	0.6	0.9
Th		5.3	4.8	9.2	5.2	3.9	4.4	5
U		13.6	9.1	22.9	8	13.8	7.9	21.7

(*) Loss on Ignition at 950°C

Table A.26 Continued

Element	Conc'n	ARB-M34	ARB-M35	ARB-M36	ARB-M37	ARB-M38	ARB-M39	ARB-M40
Na_2O		0.077	0.062	0.046	0.560	0.046	0.045	0.042
MgO		0.192	0.702	1.12	1.36	1.04	0.385	0.354
Al_2O_3		3.99	6.64	5.21	7.39	6.01	3.89	3.64
SiO_2		22.08	38.63	33.36	39.36	54.29	26.19	26.49
P_2O_5		0.086	0.119	0.108	0.167	0.114	0.079	0.059
SO_3		0.498	1.13	0.717	1.11	0.382	0.284	0.129
Cl		0.017	0.042	0.027	0.029	0.000	0.007	0.008
K_2O	%	0.86	1.83	1.12	1.62	0.960	0.884	0.783
CaO		34.75	21.88	25.92	16.82	23.91	35.93	34.69
TiO_2		0.246	0.382	0.308	0.475	0.287	0.258	0.235
V_2O_5		0.009	0.014	0.011	0.014	0.020	0.012	0.006
Cr_2O_3		0.004	0.019	0.006	0.026	0.005	0.010	0.003
MnO		0.043	0.064	0.043	0.083	0.051	0.064	0.049
Fe_2O_3		1.74	2.72	2.07	4.35	2.11	2.33	1.92
LOI*		35.72	25.82	29.72	26.56	10.47	29.33	31.94
Co		14.1	22.8	9.5	24.2	12.9	31.7	20.4
Ni		14.2	17.3	14.4	57	21.1	18.6	16.4
Cu		11.1	7.2	10.6	45.2	14.6	11	11
Zn		30.1	27.6	29.8	52.4	32	27.2	24.6
Ga		8.2	9.3	9.7	12.6	9.8	7.7	7.6
Ge		0.7	0.4	1.2	1.1	1.2	0.4	0.4
As		16.1	13.2	10.6	26.1	16.7	8.2	7
Se		0.4	0.3	0.3	0.3	0.2	0.3	0.3
Br		1.7	0.7	2.5	1	1.9	2.3	1.2
Rb		24.5	41.1	28.7	56.6	29.4	29.5	22.7
Sr		210.7	291.1	316.1	395.4	221.1	239.5	216.4
Y		7.2	10	7.5	13.4	9.7	10	7.3
Zr		62.4	85.9	101	163.6	127.4	99.9	89.5
Nb		10.3	12	10.3	17.3	7	5.9	9.2
Mo		7.4	3.3	2.6	5.4	3	3.3	3
Cd		0.7	0.8	0.7	0.9	0.7	0.8	0.8
In	ppm	0.8	0.8	0.8	0.9	0.8	0.8	0.7
Sn		1.5	0.9	0.9	1	0.9	0.9	0.7
Sb		1	1.5	1.7	1	3.7	0.9	0.8
Te		1.3	1.2	0.9	1.3	1.1	1.6	1.1
I		2.3	1.8	1.3	2.2	2.3	2	1.9
Cs		3.7	3.6	3.6	3.9	3.4	3.6	4.4
Ba		237.2	302.5	249.4	436.8	145.4	229.6	206.5
La		7.5	7.4	19	26.6	23.9	12.4	21.6
Ce		22.6	27.4	18.1	63	22.4	30.2	26.4
Hf		4.3	2.3	4.8	7.9	2.5	2.6	2.7
Ta		4.4	2.6	2.6	4	2.7	2.8	2.8
W		3.9	2.2	2.3	2.5	2.1	2.5	2.2
Hg		1.3	0.7	0.7	0.8	0.7	0.8	0.5
Tl		1.5	0.8	0.8	0.9	0.8	0.5	0.8
Pb		12.3	10.4	10.9	20.7	13.5	9.7	8.7
Bi		0.4	0.6	0.6	0.6	0.8	0.6	0.6
Th		3.9	6.5	4.5	9.5	4.3	4.7	3.4
U		8.7	8.1	7	8.5	9.6	8.5	9.6

(*) Loss on Ignition at 950°C

233

Table A.26 Continued

Element	Conc'n	ARB-M41	ARB-M42	ARB-M43	ARB-M44	ARB-M45	ARB-M46	Ave.
Na_2O		0.048	0.043	0.050	0.047	0.047	0.045	**0.086**
MgO		0.456	0.037	0.015	0.675	2.07	0.118	**1.01**
Al_2O_3		3.66	0.913	0.466	5.71	7.08	0.677	**5.11**
SiO_2		26.08	3.60	2.36	31.92	25.24	4.10	**28.90**
P_2O_5		0.081	0.157	0.192	0.129	0.245	0.101	**0.133**
SO_3		0.229	0.190	0.188	0.409	0.230	0.307	**0.755**
Cl	%	0.010	0.019	0.021	0.005	0.014	0.016	**0.066**
K_2O		0.872	0.216	0.186	1.53	1.52	0.290	**1.24**
CaO		38.60	58.79	56.07	29.79	29.00	56.19	**28.74**
TiO_2		0.285	0.063	0.057	0.346	0.468	0.064	**0.332**
V_2O_5		0.007	0.006	0.002	0.013	0.014	0.002	**0.011**
Cr_2O_3		0.005	0.003	0.003	0.006	0.014	0.003	**0.012**
MnO		0.066	0.045	0.112	0.063	0.126	0.028	**0.062**
Fe_2O_3		2.20	0.357	0.475	2.79	3.70	0.506	**2.66**
LOI*		27.99	35.93	39.24	26.94	30.79	37.83	**31.18**
Co		20.6	17.6	20.6	15.5	21.2	21.3	**19.8**
Ni		17.3	2.1	4.3	25.3	41.2	2.6	**26.9**
Cu		8.6	12	25.3	19.1	30	4.3	**16.8**
Zn		25.3	10.8	23.7	37	49.8	17.9	**39.5**
Ga		7.4	2.3	2.1	10	9.9	1.8	**9.0**
Ge		0.4	0.4	0.5	1.1	1	0.4	**0.7**
As		22.1	2.4	2.5	11.3	11.4	6.6	**14.0**
Se		0.3	0.3	0.3	0.3	0.3	0.3	**0.3**
Br		1.6	4.6	6.5	0.3	1.4	3.1	**1.8**
Rb		31	4.6	3.7	33.6	38.9	4	**32.4**
Sr		265.1	259.6	351	226.5	327.8	238.7	**314.7**
Y		8.8	2.3	1.6	9.2	13.1	1.3	**9.2**
Zr		86.2	25.5	16.7	75.7	113.3	26.5	**100.3**
Nb		5.1	4.2	3.6	5.5	8.5	7.3	**10.0**
Mo		3.5	3.5	3.5	2.7	2.6	7.1	**3.8**
Cd		0.9	1.3	1	0.8	0.8	0.9	**0.9**
In	ppm	0.8	0.9	1	0.8	0.9	0.9	**0.8**
Sn		1	1.1	1.2	0.9	0.6	1.8	**1.3**
Sb		1	1	1.2	1	0.9	0.9	**1.3**
Te		1.2	1.2	1.5	0.5	1.2	1.1	**1.2**
I		2	2.2	8.2	1.5	2.2	3.4	**2.2**
Cs		3.6	3.5	4.7	3.5	4.7	3.4	**3.8**
Ba		225.4	115	161.8	209.9	404.7	54.8	**265.3**
La		18.9	14.5	27.2	15.7	22.6	16.7	**19.6**
Ce		20.6	10	14	29.2	29.4	9.8	**28.2**
Hf		2.7	3.1	3.7	2.8	3.2	2.8	**3.3**
Ta		2.3	3.1	3.8	3.1	3.6	2.6	**3.3**
W		2.4	2.5	2.8	2.4	2.7	2.9	**2.7**
Hg		0.8	0.9	0.8	0.9	0.8	0.7	**0.9**
Tl		0.5	0.8	0.9	0.8	0.9	0.8	**0.9**
Pb		7.4	6.8	53.8	13.8	14.3	5.2	**14.4**
Bi		0.7	0.7	0.8	0.6	0.6	0.7	**0.7**
Th		3.9	0.7	2.4	5.4	7.1	0.6	**5.4**
U		9.7	20.3	16.1	7.5	8.4	11	**12.1**

(*) Loss on Ignition at 950°C
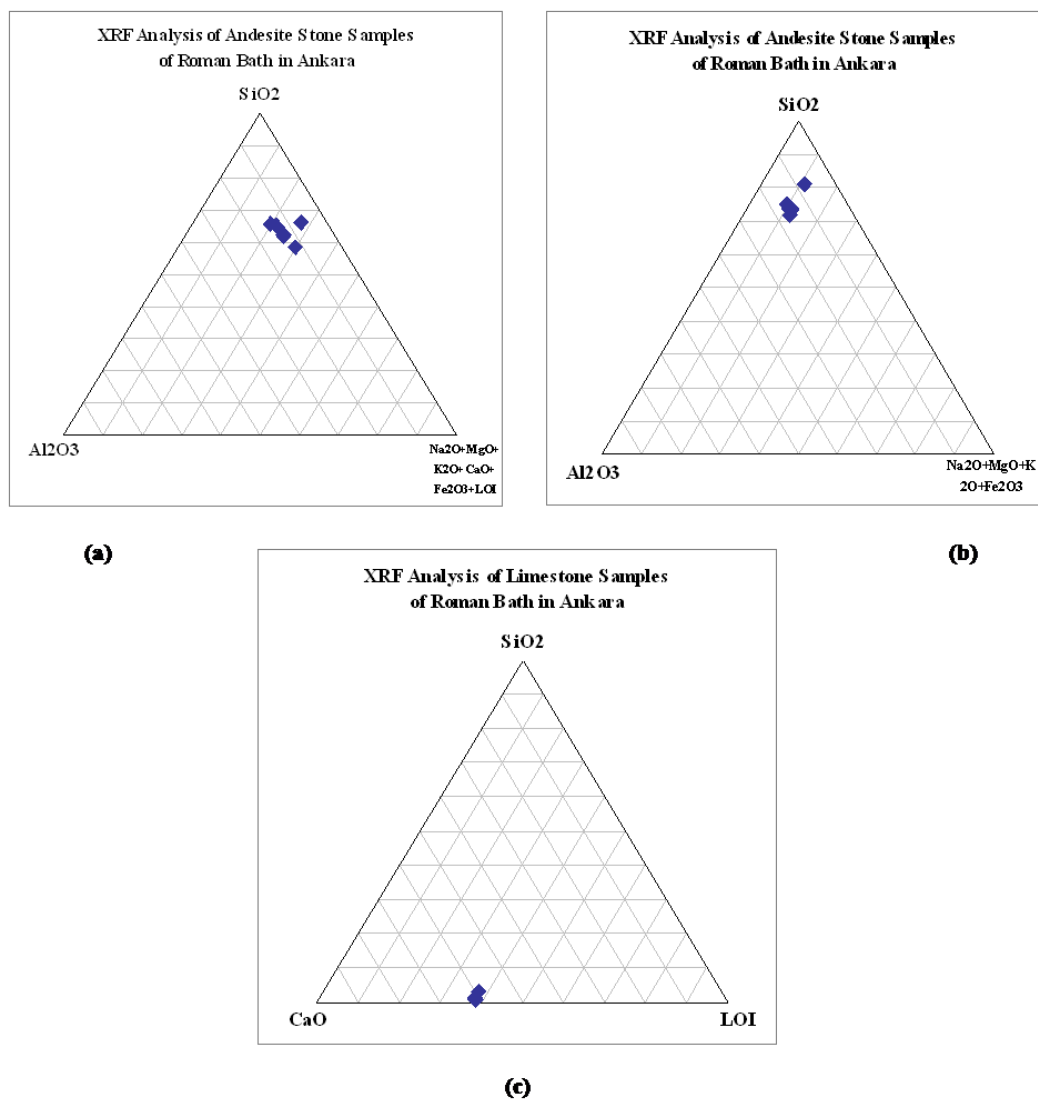
Figure A.22 XRF Analysis – Triangle Plotting of Andesite Stone Samples and Limestone Samples of Roman Bath in Ankara

a) XRF Analysis of Andesite Stone Samples of Roman Bath in Ankara – Triangle Plotting (SiO_2–Al_2O_3–Na_2O+MgO+K_2O+CaO+Fe_2O_3+LOI)

b) XRF Analysis of Andesite Stone Samples of Roman Bath in Ankara–Triangle Plotting (SiO_2–Al_2O_3–Na_2O+MgO+K_2O +Fe_2O_3)

c) XRF Analysis of Limestone Stone Samples of Roman Bath in Ankara–Triangle Plotting (SiO_2–CaO–LOI)
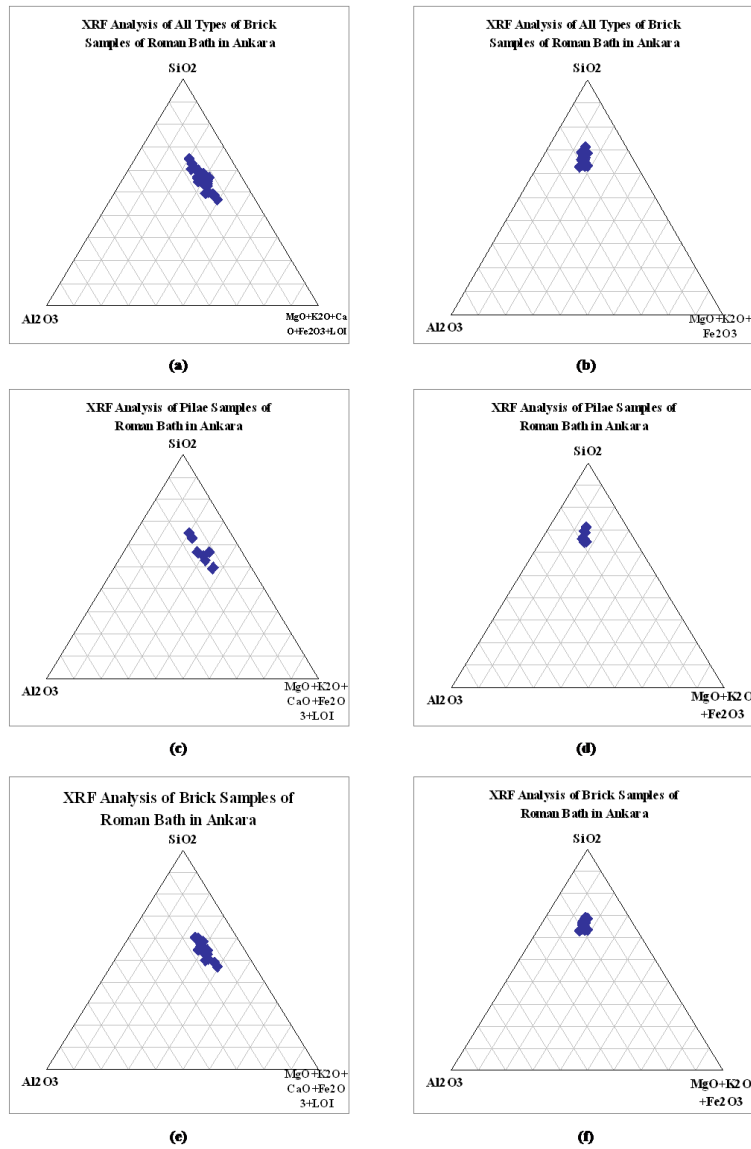
Figure A.23 XRF Analysis – Triangle Plotting of All Types of Brick, Pilae and
Brick (structural) Samples of Roman Bath in Ankara

a) XRF Analysis of All types of Brick Samples of Roman Bath in Ankara – Triangle Plotting (SiO_2–Al_2O_3–$MgO+K_2O+CaO+Fe_2O_3+LOI$)
b) XRF Analysis of All types of Brick Samples of Roman Bath in Ankara –Triangle Plotting (SiO_2–Al_2O_3–$MgO+K_2O+Fe_2O_3$)
c) XRF Analysis of Pilae Samples of Roman Bath in Ankara–Triangle Plotting (SiO_2–Al_2O_3–$MgO+K_2O+CaO+Fe_2O_3+LOI$)
d) XRF Analysis of Pilae Samples of Roman Bath in Ankara of Roman Bath in Ankara –Triangle Plotting (SiO_2–Al_2O_3–$MgO+K_2O+Fe_2O_3$)
e) XRF Analysis of Brick Samples of Roman Bath in Ankara–Triangle Plotting (SiO_2–Al_2O_3–$MgO+K_2O+CaO+Fe_2O_3+LOI$)
f) XRF Analysis of Brick Samples of Roman Bath in Ankara–Triangle Plotting (SiO_2–Al_2O_3–$MgO+K_2O+Fe_2O_3$)

236
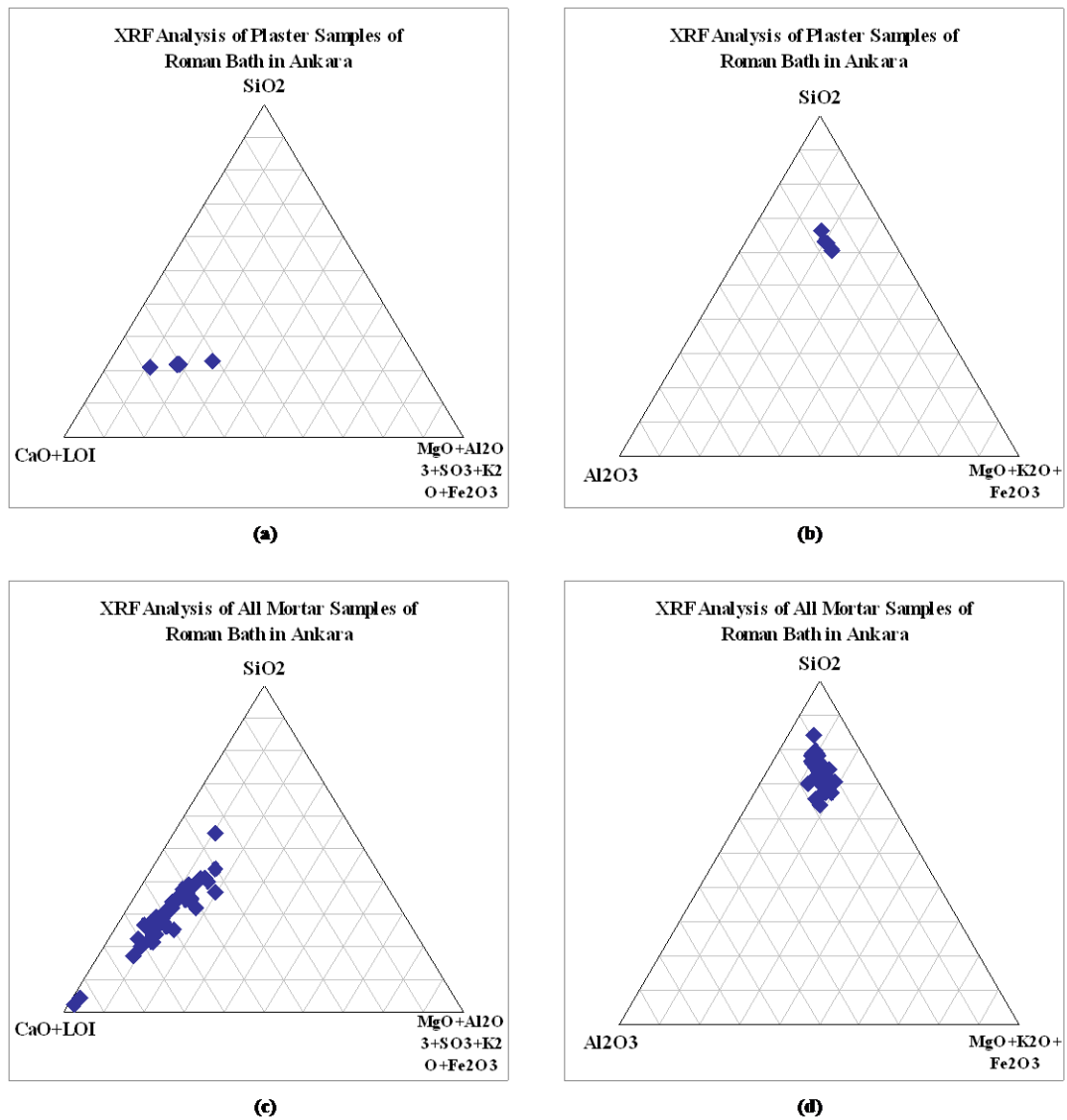
Figure A.24 XRF Analysis – Triangle Plotting of All Types of Plaster and Mortar Samples of Roman Bath in Ankara

a) XRF Analysis of Plaster Samples of Roman Bath in Ankara – Triangle Plotting (SiO_2–$CaO+LOI$–$MgO+Al_2O_3+SO_3+K_2O+Fe_2O_3$)

b) XRF Analysis of Plaster Samples of Roman Bath in Ankara – Triangle Plotting (SiO_2–Al_2O_3–$MgO+K_2O+Fe_2O_3$)

c) XRF Analysis of All Mortar Samples of Roman Bath in Ankara – Triangle Plotting (SiO_2–$CaO+LOI$–$MgO+Al_2O_3+SO_3+K_2O+Fe_2O_3$)

d) XRF Analysis of All Mortar Samples of Roman Bath in Ankara – Triangle Plotting (SiO_2–Al_2O_3–$MgO+K_2O+Fe_2O_3$)

Figure A.25 XRF Analysis – Triangle Plotting of Pilae Mortar Samples of Roman Bath in Ankara

a) XRF Analysis of Pilae Mortar Samples of Roman Bath in Ankara – Triangle Plotting (SiO_2–$CaO+LOI$–$MgO+Al_2O_3+SO_3+K_2O+Fe_2O_3$)

b) XRF Analysis of Pilae Mortar Samples Samples of Roman Bath in Ankara – Triangle Plotting (SiO_2–Al_2O_3–$MgO+K_2O+Fe_2O_3$)

c) XRF Analysis of Caldarium Mortar Samples of Roman Bath in Ankara – Triangle Plotting (SiO_2–$CaO+LOI$–$MgO+Al_2O_3+SO_3+K_2O+Fe_2O_3$)

d) XRF Analysis of Caldarium Mortar Samples of Roman Bath in Ankara – Triangle Plotting (SiO_2–Al_2O_3–$MgO+K_2O+Fe_2O_3$)

Figure A.26 XRF Analysis – Triangle Plotting of Pilae Mortar Samples of Roman Bath in Ankara

a) XRF Analysis of Tepidarium Mortar Samples of Roman Bath in Ankara – Triangle Plotting (SiO_2–$CaO+LOI$–$MgO+Al_2O_3+SO_3+K_2O+Fe_2O_3$)

b) XRF Analysis of Tepidarium Mortar Samples of Roman Bath in Ankara – Triangle Plotting (SiO_2–Al_2O_3–$MgO+K_2O+Fe_2O_3$)

c) XRF Analysis of Water Tank Mortar Samples of Roman Bath in Ankara – Triangle Plotting (SiO_2–$CaO+LOI$–$MgO+Al_2O_3+SO_3+K_2O+Fe_2O_3$)

d) XRF Analysis of Water Tank Mortar Samples of Roman Bath in Ankara – Triangle Plotting (SiO_2–Al_2O_3–$MgO+K_2O+Fe_2O_3$)

Table A.27 Cementation Index of Mortar Samples of Roman Bath in Ankara

Samples	MgO	Al₂O₃	SiO₂	CaO	Fe₂O₃	CI	Lime Type
ARB-M1	1.404	8.73	31.41	24.01	4.25	3.92	C/NC
ARB-M3	1.252	5.40	25.87	28.72	3.95	2.70	C/NC
ARB-M4	0.928	5.87	33.87	20.55	4.86	4.86	C/NC
ARB-M5	2.282	8.88	36.28	22.99	3.91	4.40	C/NC
ARB-M6	0.385	4.26	25.85	32.89	2.36	2.38	C/NC
ARB-M7	0.525	5.42	30.89	24.16	2.68	3.82	C/NC
ARB-M8	0.664	6.11	38.77	23.71	2.60	4.78	C/NC
ARB-M9	0.431	4.63	25.19	29.96	2.61	2.56	C/NC
ARB-M10	0.541	5.74	34.21	23.87	2.54	4.25	C/NC
ARB-M11	4.619	6.08	43.51	19.58	2.69	5.04	C/NC
ARB-M12	0.609	5.91	34.18	24.10	2.26	4.19	C/NC
ARB-M13	0.748	5.00	27.56	19.67	2.64	4.12	C/NC
ARB-M14	5.000	5.23	35.11	21.81	3.10	3.72	C/NC
ARB-M15	1.397	3.29	17.22	39.71	2.30	1.30	NC
ARB-M16	1.410	4.25	20.94	30.07	2.59	2.06	C/NC
ARB-M17	0.559	4.91	29.50	24.05	2.68	3.65	C/NC
ARB-M18	1.141	6.97	40.37	14.89	3.85	7.55	C/NC
ARB-M19	1.394	4.94	23.59	30.73	2.77	2.27	C/NC
ARB-M20	0.534	5.03	25.76	27.51	2.98	2.85	C/NC
ARB-M21	1.857	6.35	40.66	26.31	3.00	4.28	C/NC
ARB-M22	0.897	4.48	22.47	28.22	2.42	2.38	C/NC
ARB-M23	0.958	4.64	23.76	31.25	2.88	2.29	C/NC
ARB-M24	0.536	5.42	30.73	23.61	2.70	3.89	C/NC
ARB-M25	0.583	5.45	31.14	22.69	3.02	4.09	C/NC
ARB-M26	0.916	6.12	35.46	23.19	2.88	4.45	C/NC
ARB-M27	0.677	5.82	37.80	25.58	2.08	4.31	C/NC
ARB-M28	0.865	4.44	20.82	28.94	2.36	2.17	C/NC
ARB-M29	1.352	6.33	34.37	19.73	4.13	4.96	C/NC
ARB-M30	0.693	5.26	30.13	23.61	2.91	3.79	C/NC
ARB-M31	0.742	3.90	19.99	34.69	2.57	1.76	C/NC
ARB-M32	0.567	5.06	30.38	25.57	2.20	3.52	C/NC
ARB-M33	0.309	4.72	29.02	34.79	1.48	2.50	C/NC
ARB-M34	0.192	3.99	22.08	34.75	1.74	1.94	C/NC
ARB-M35	0.702	6.64	38.63	21.88	2.72	5.17	C/NC
ARB-M36	1.12	5.21	33.36	25.92	2.07	3.68	C/NC
ARB-M37	1.36	7.39	39.36	16.82	4.35	6.55	C/NC
ARB-M38	1.04	6.01	54.29	23.91	2.11	6.34	C/NC
ARB-M39	0.385	3.89	26.19	35.93	2.33	2.19	C/NC
ARB-M40	0.354	3.64	26.49	34.69	1.92	2.28	C/NC
ARB-M41	0.456	3.66	26.08	38.60	2.20	2.02	C/NC
ARB-M42	0.037	0.913	3.60	58.79	0.36	0.19	NC
ARB-M43	0.015	0.466	2.36	56.07	0.48	0.14	NC
ARB-M44	0.675	5.71	31.92	29.79	2.79	3.20	C/NC
ARB-M45	2.07	7.08	25.24	29.00	3.70	2.58	C/NC
ARB-M46	0.118	0.677	4.10	56.19	0.51	0.23	NC
Mortar Ave.	1.01	5.11	28.90	28.74	2.66	3.36	C/NC

Table A.28 Cementation Index of Plaster Samples of Roman Bath in Ankara

Samples	MgO	Al_2O_3	SiO_2	CaO	Fe_2O_3	CI	Lime Type
ARB-P1	0.95	5.03	20.51	33.88	3.16	1.88	C/NC
ARB-P2a	1.40	5.78	21.37	23.41	3.66	2.75	C/NC
ARB-P2b	1.60	5.98	21.63	23.76	3.57	2.72	C/NC
ARB-P3	1.32	6.07	22.29	25.10	3.43	2.69	C/NC
Plaster Ave.	1.32	5.72	21.45	26.54	3.46	2.51	C/NC

Lime Type	Lime Type	CI
Fat Lime	FL	<0.30
Weakly hydraulic Lime	WHL	0.30 – 0.50
Moderately hydraulic Lime	MHL	0.51 – 0.70
Eminently hydraulic Lime	EHL	0.71 – 1.10
Natural Cements	NC	1.11-1.70
Cement/Natural Cements	C/NC	1.70<

Figure A.27a Geological Map of Ankara S: 1/500 000

243

Figure A.27b Geological explanations of the map

244

APPENDIX B

DRAWINGS OF THE THESIS

Drawing B.1 Immediate Surroundings of Roman Bath in Ankara

Drawing B.2 Site Plan of the Bath S: 1/500

Drawing B.3 Building Survey Drawing of the Bath S: 1/100

Drawing B.4 Horizontal Sections of the Bath S: 1/50

Drawing B.5 Vertical Sections of the Bath S: 1/50

Drawing B.6 The Remains of Colonnaded Street,

        Location Plan S: 1/1000 and Site Plan S: 1/200

Drawing B.7 Restitution Site Plan of the Bath S: 1/500

Drawing B.8 Restitution Plan and Sections of the Bath S:1/200

Drawing B.9 Isometric Perspective of the Closed Spaces of the Bath S: 1/200
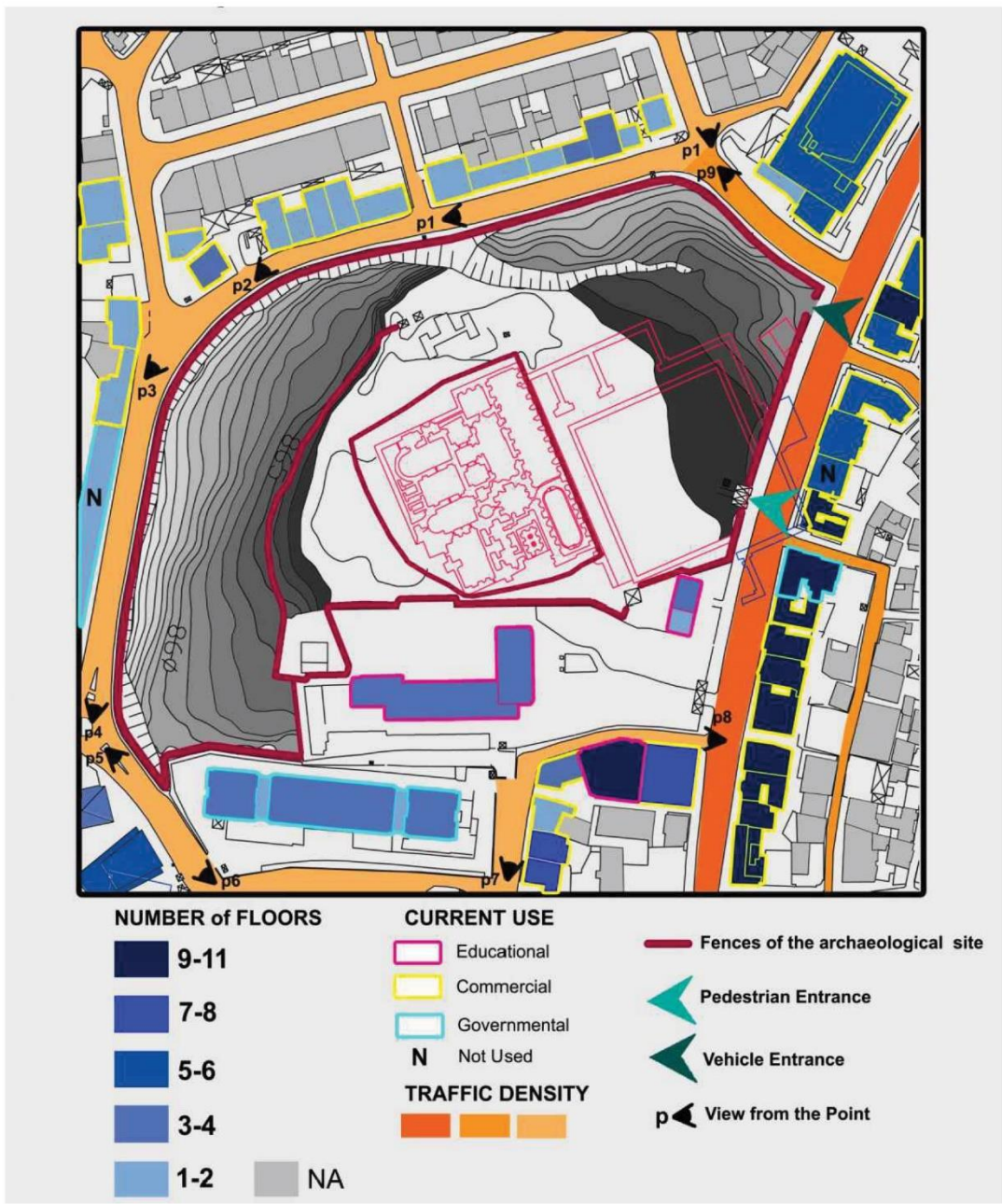
Drawing B.1 Immediate Surroundings of Roman Bath in Ankara
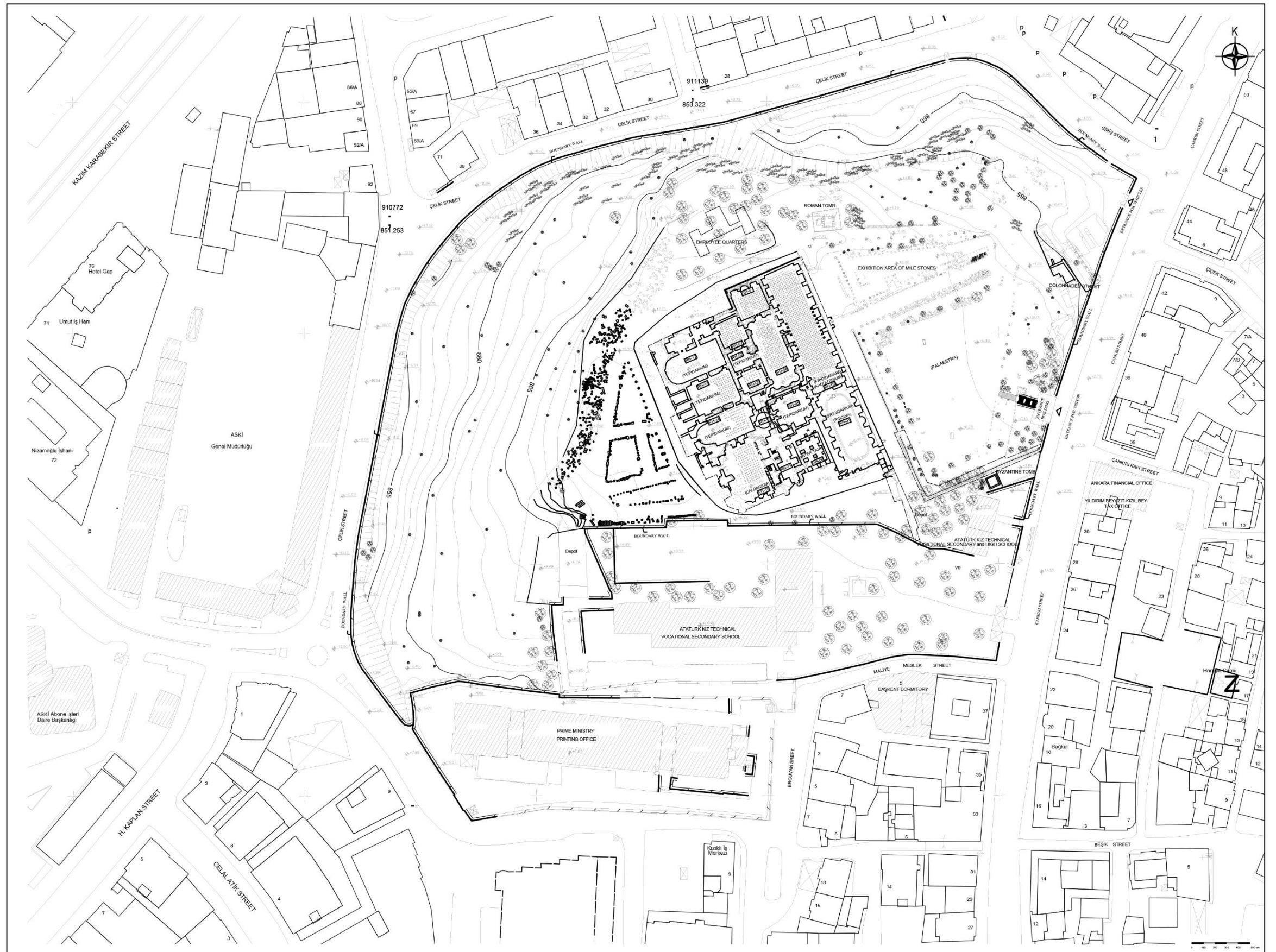
Drawing B.2 Site Plan of the Bath S:1/500
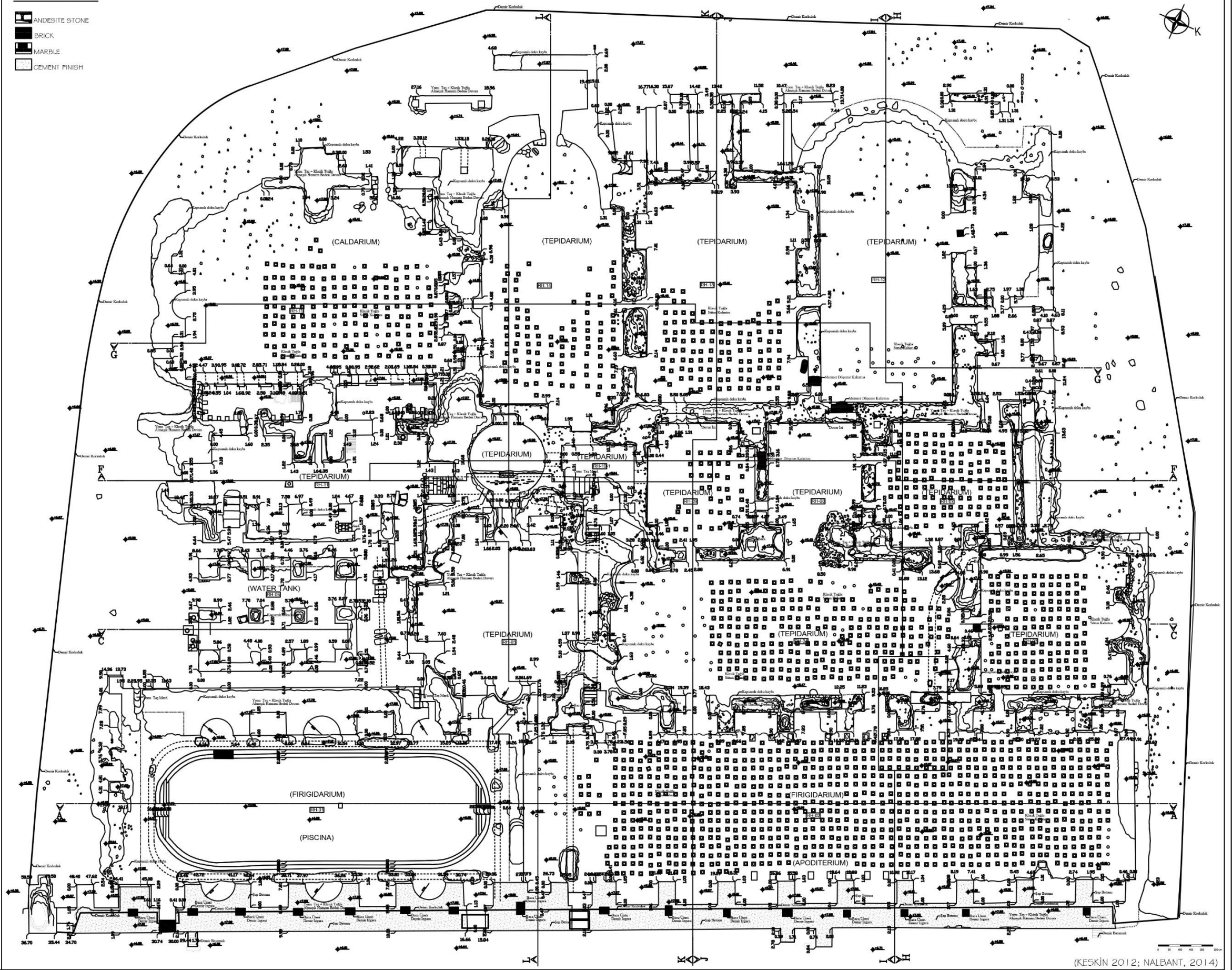
Drawing B.3 Building Survey Drawing of the Bath S: 1/100
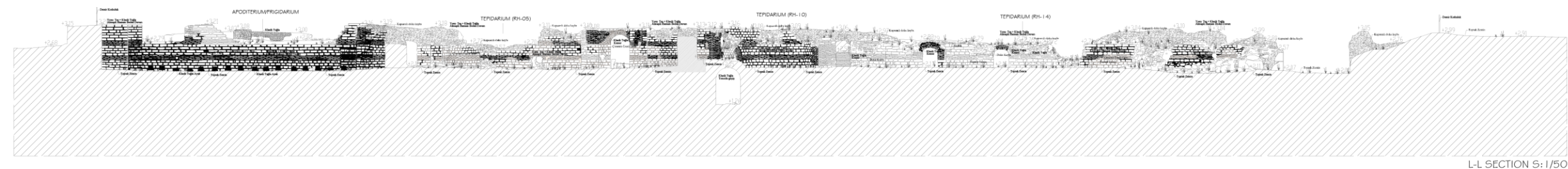
L-L SECTION S:1/50
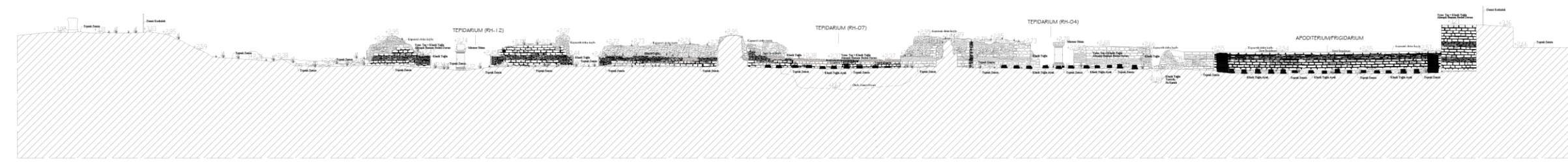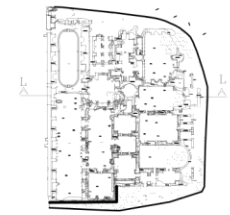
H-H SECTION S:1/50
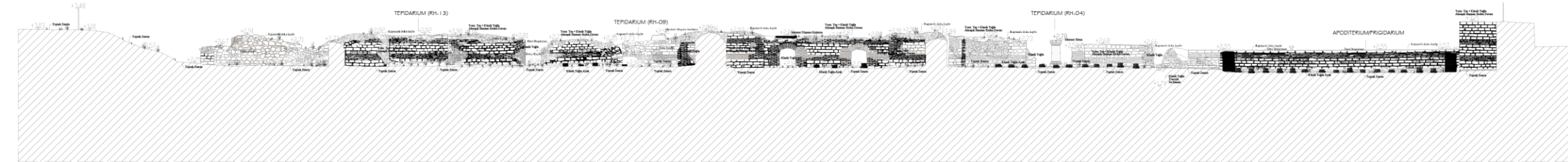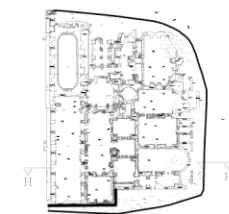
J-J SECTION S:1/50
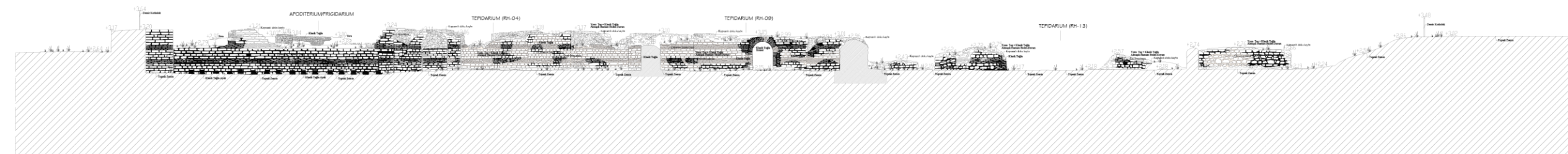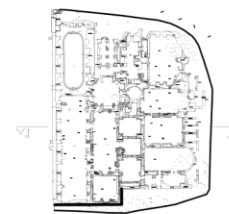
K-K SECTION S:1/50
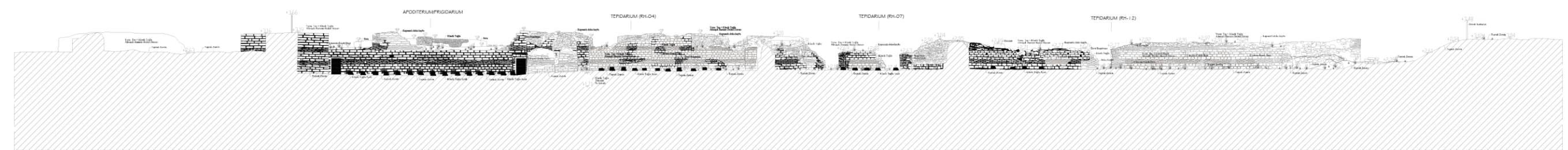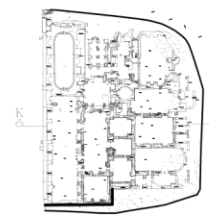
I-I SECTION S:1/50
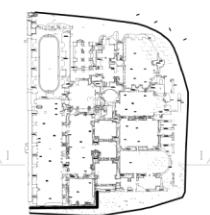
Drawing B.4 HORİZONTAL SECTIONS OF THE BATH S:1/50

MATERIAL ANALYSIS

ANDESITE STONE

BRICK

MARBLE

MORTAR

(KESKİN, 2012; NALBANT, 2014)

Drawing B.4 Horizontal Sections of the Bath S:1/50

249

A-A SECTION S:1/50

C-C SECTION S:1/50

F-F SECTION S:1/50

G-G SECTION S:1/50

Drawing B.5 VERTICAL SECTIONS OF THE BATH S:1/50

MATERIAL ANALYSIS

ANDESITE STONE

BRICK

MARBLE

MORTAR

(KESKİN, 2012; NALBANT, 2014)

Drawing B.5 Vertical Sections of the Bath S:1/50

Drawing B.6 THE REMAINS of COLONNADED STREET
THE LOCATION PLAN S:1/1000 and SITE PLAN S:1/200

EXHIBITION AREA OF MILE STONES

COLONNADED STREET

ÇANKIRI STREET

ÇİÇEK STREET

(PALAESTRA)

ENTRANCE FOR VEHICLES

ENTRANCE FOR VISITORS

ENTRANCE BUILDING

BOUNDARY WALL

(PISCINA)

FRONT VIEW S:1/20

1-1 SECTION S:1/20

COLUMN DETAIL S:1/20
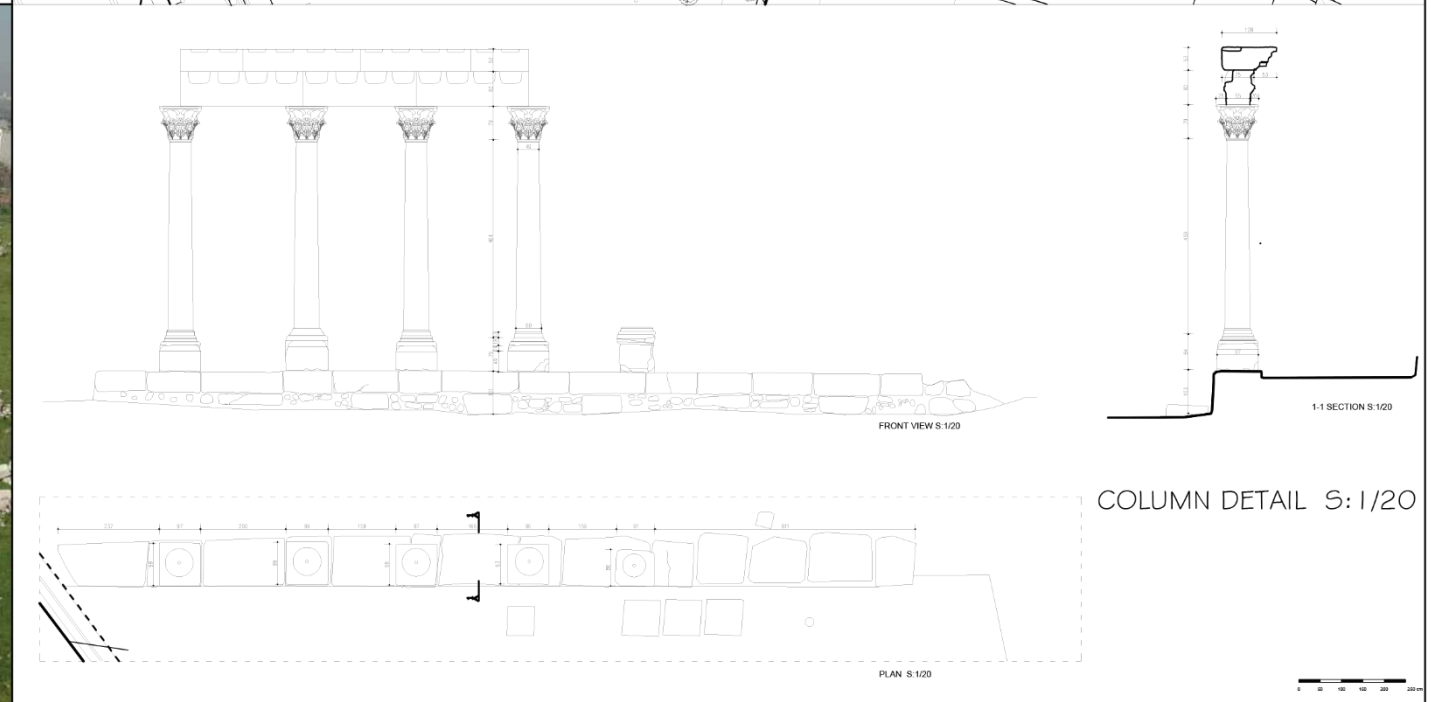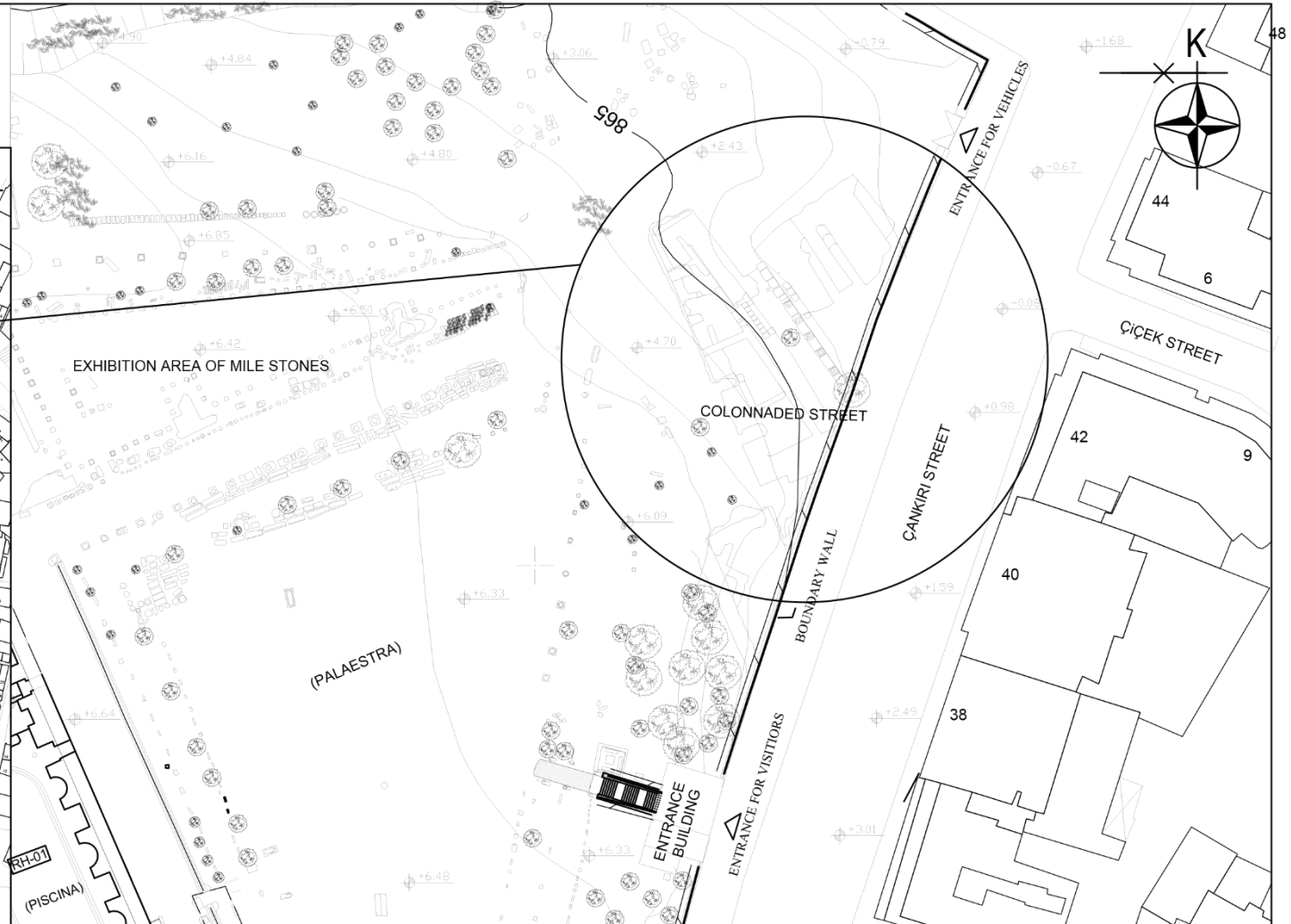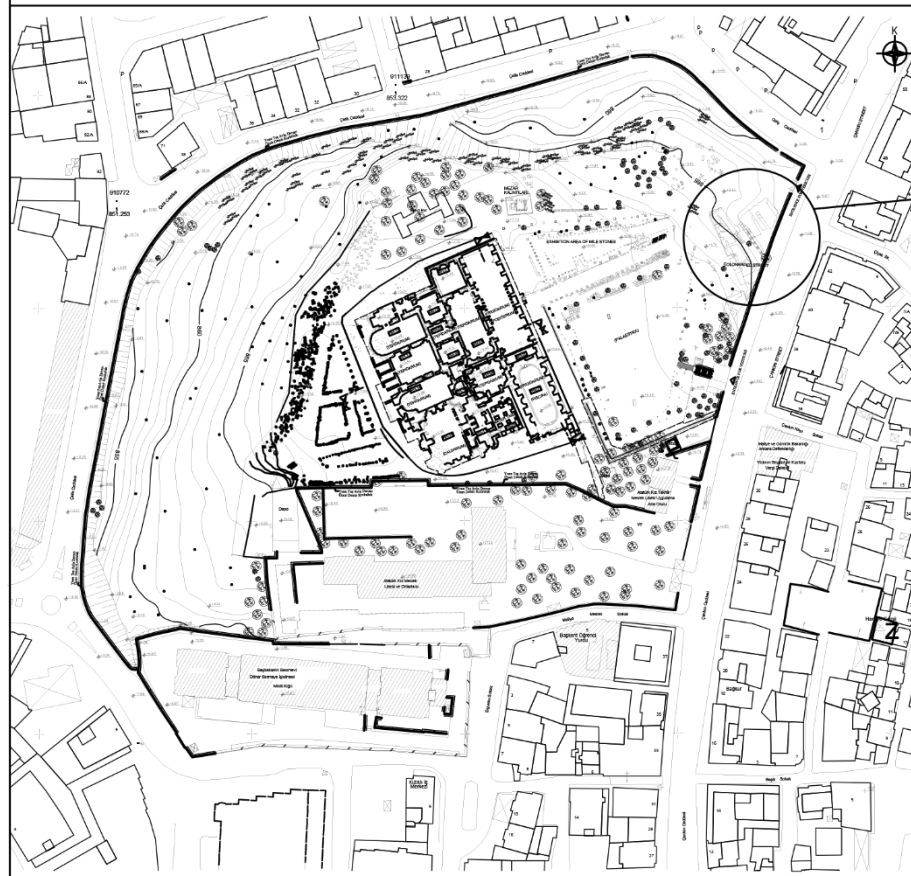
PLAN S:1/20

M.K. and MİYAR ARCHITECTURAL OFFICE
(KESKİN, 2012; NALBANT, 2014)

Drawing B.6 The Remains of Colonnaded Street, Location Plan S: 1/1000 and Site Plan S:1/200
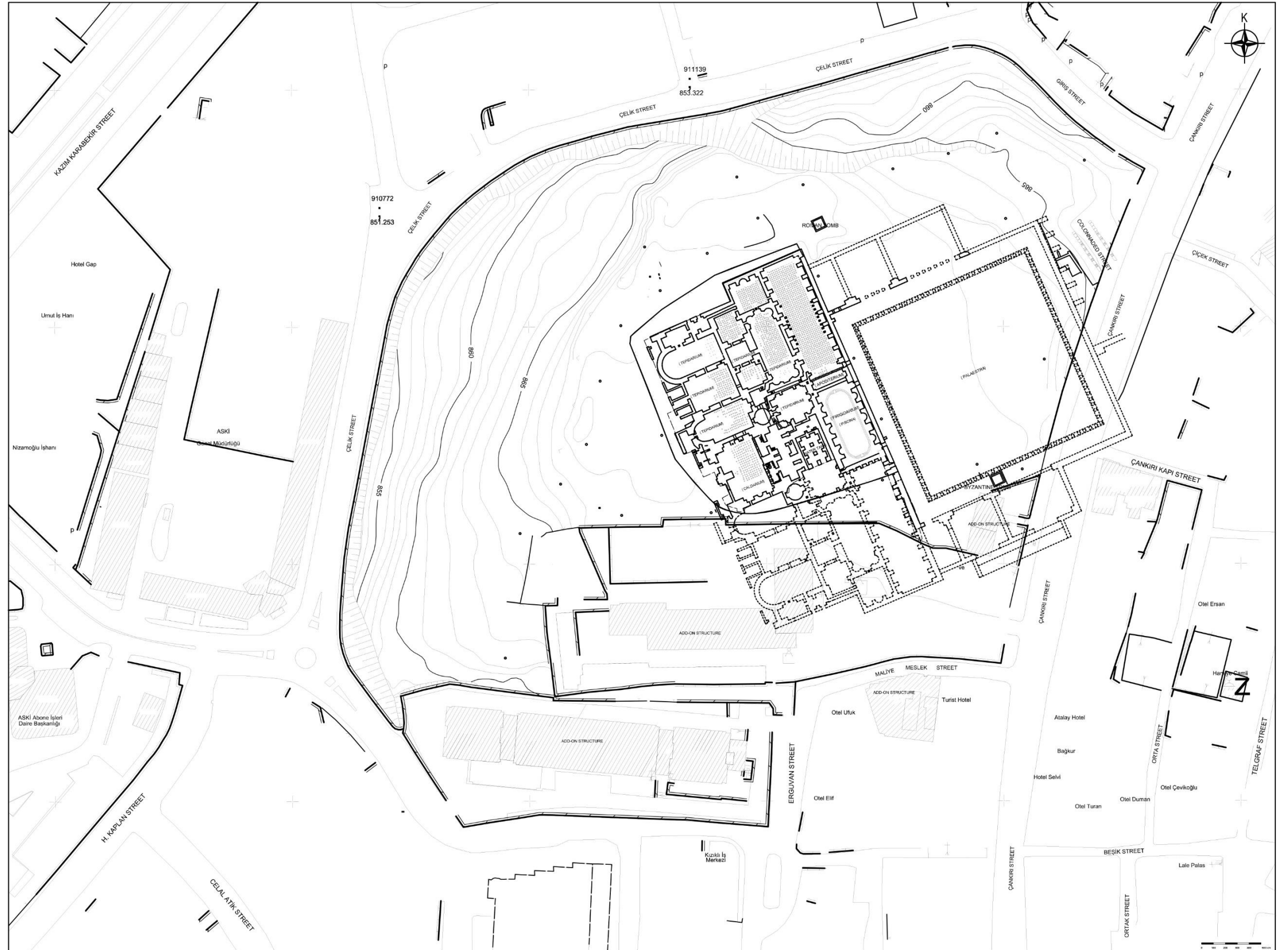
251

Drawing B.7 Restitution Site Plan of the Bath S:1/500
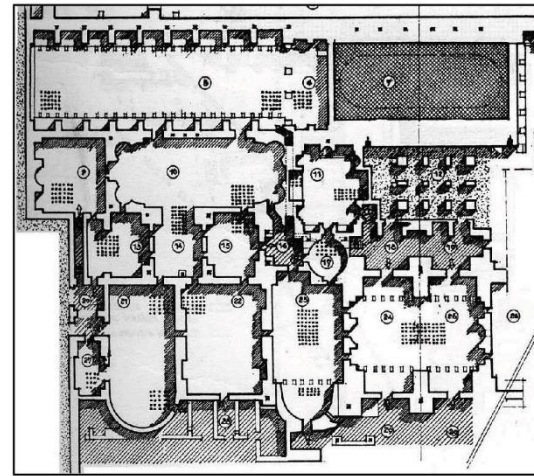
CLOSED BUILDING PART PLAN OF THE BATH (AKOK, 1955)
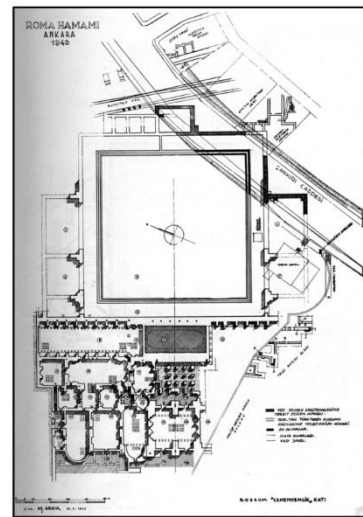
LOCATION PLAN OF THE BATH (AKOK, 1955)
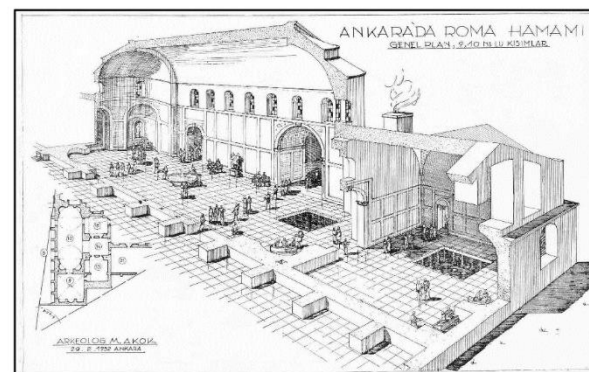
DRAWING OF INTERIOR PERSPECTIVE OF THE BATH (AKOK, 1955)
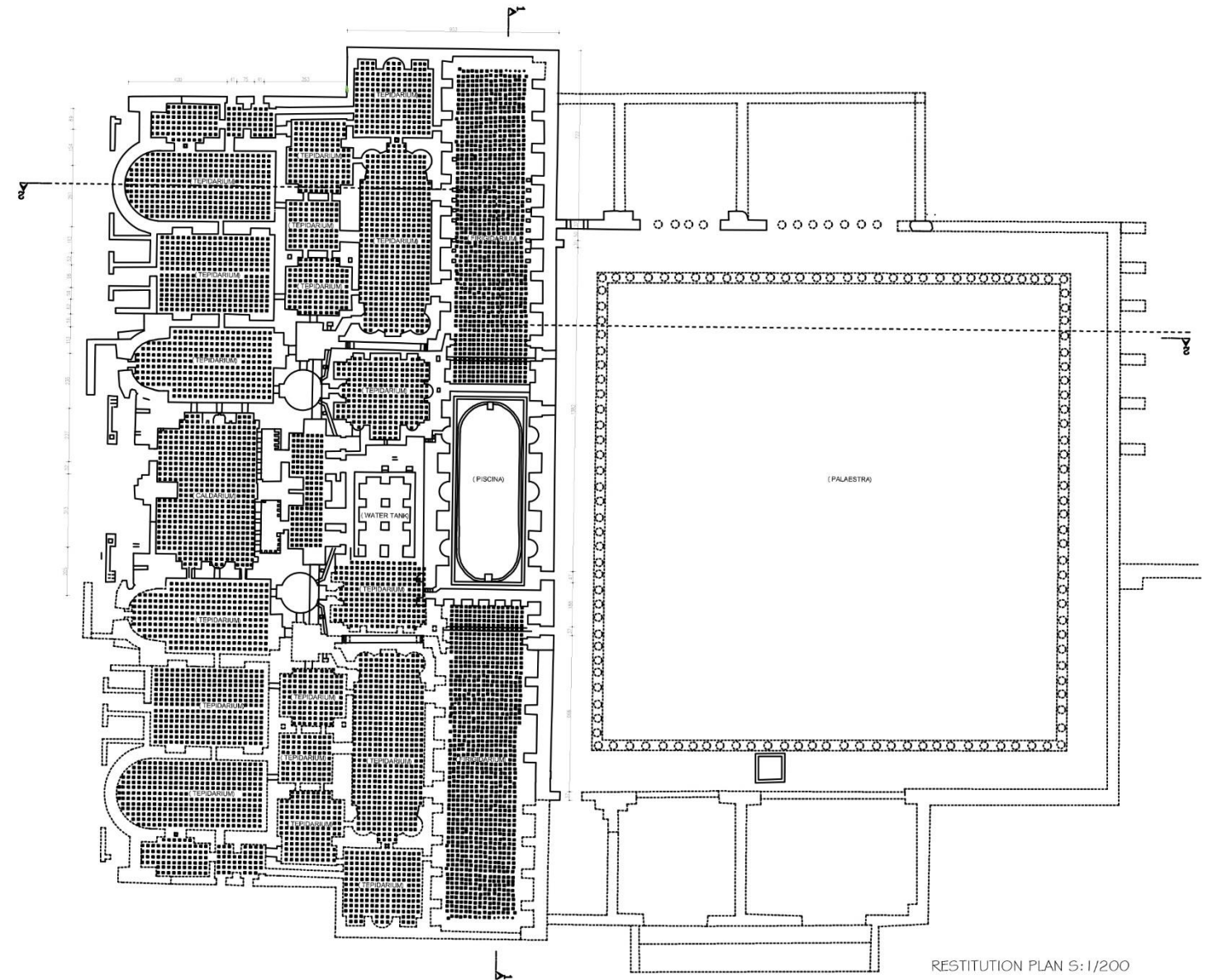
RESTITUTION PLAN S:1/200
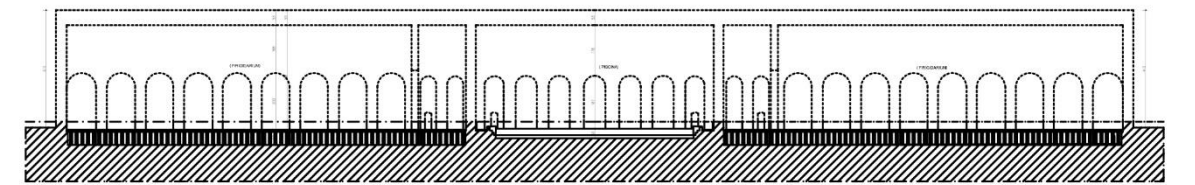
1-1 SECTION S:1/200
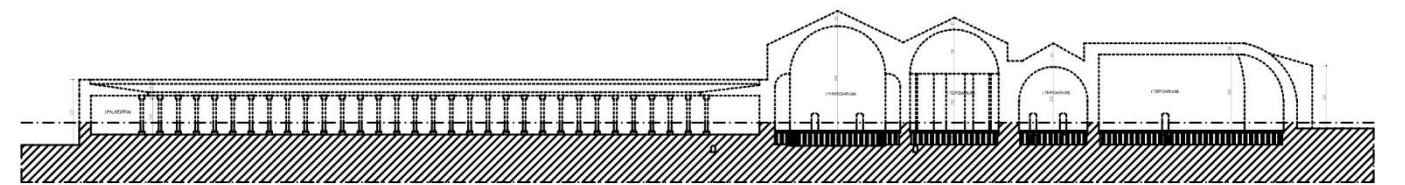
2-2 SECTION S:1/200

M.K. and MÍYAR ARCHITECTURAL OFFICE
(KESKÍN, 2012; NALBANT, 2014)

Drawing B.8 Restitution Plan and Sections of the Bath S:1/200

253
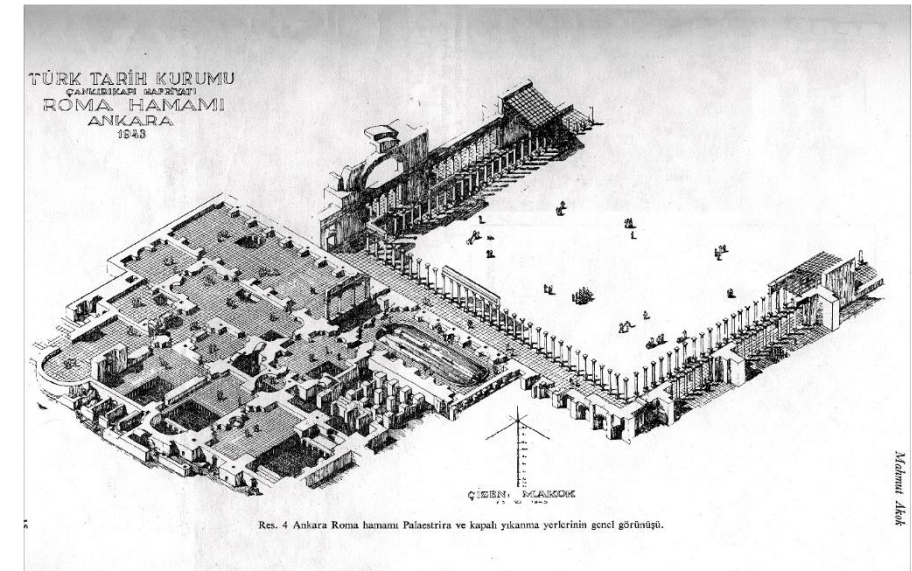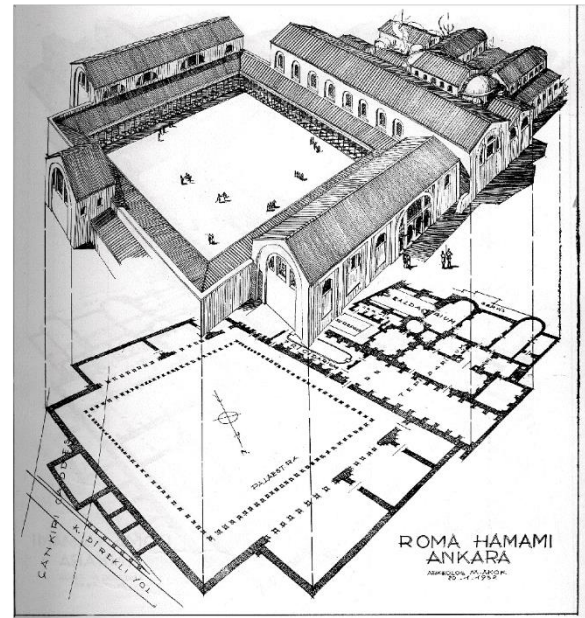
DRAWING OF PERSPECTIVE OF THE BATH (AKOK, 1955)
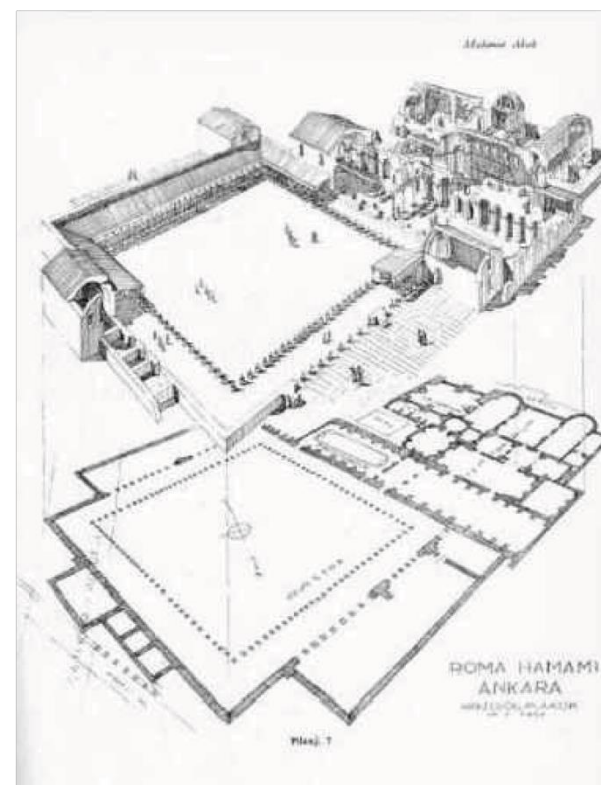
DRAWINGS OF PLAN and PERSPECTIVE OF THE BATH (AKOK, 1955)
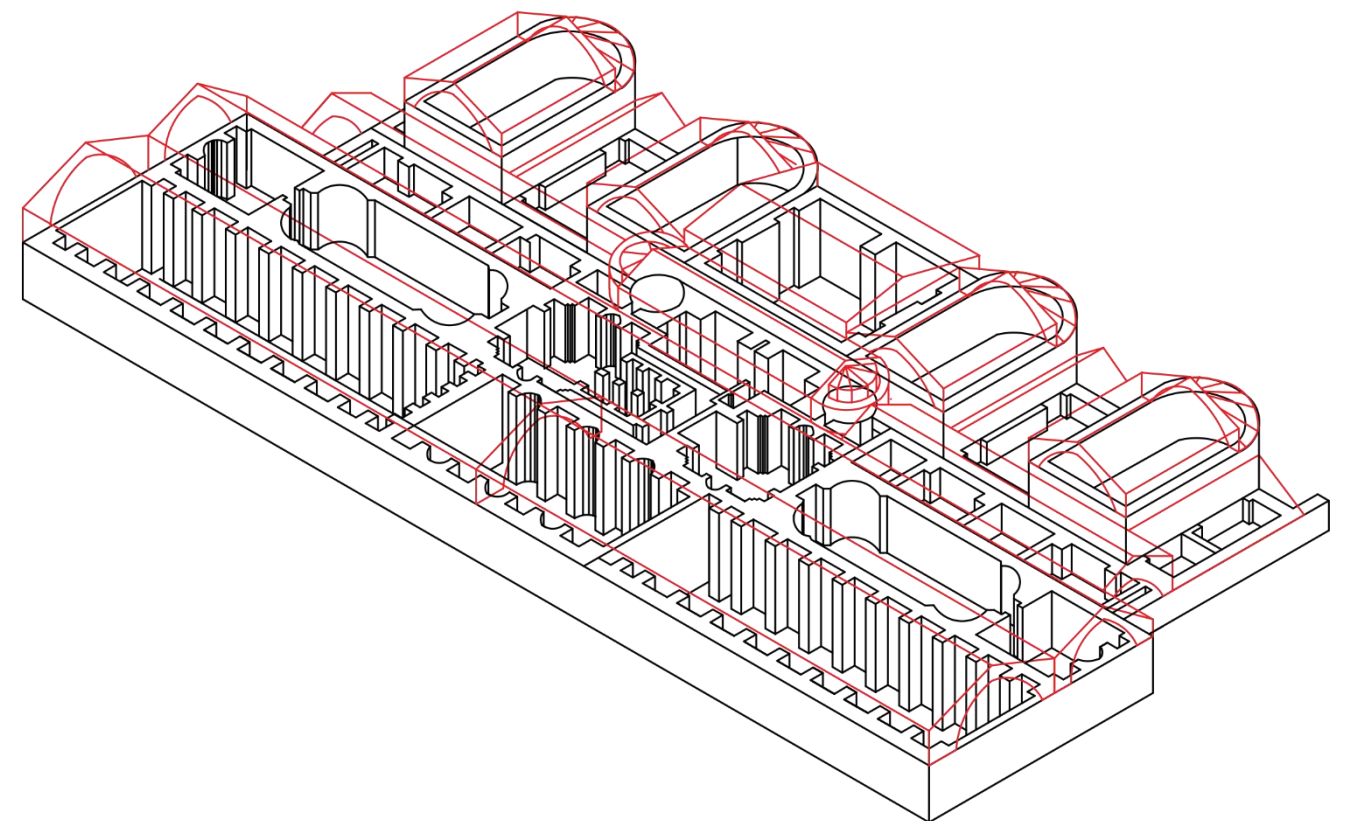
Drawing B.9 ISOMETRIC PERSPECTIVE OF THE CLOSED SPACES OF THE BATH S:1/200

Drawing B.9 IsometricPerspective of the Closed Spaces of the Bath S: 1/200

254

CURRICULUM VITAE

PERSONAL INFORMATION

Surname, Name: Tanrıverdi, Zeynep
Nationality: Turkish Rebuplic (TC)
Date and Place of Birth: 26 June 1981, Ankara
Marital Status: Single
Phone: +90 312 484 78 69
email: ztanriverdi.arch@gmail.com

EDUCATION

Degree	Institution	Year of Graduation
MS	Yıldız Technical University, Restoration Program of Architecture Department, Istanbul, Turkey	2012
BArch	Anadolu University, Department of Architecture, Eskişehir, Turkey	2007
High School	Kocatepe Mimar Kemal High School, Ankara Turkey	1999

WORK EXPERIENCE

Year	Place	Enrollment
2015- 2017	Atılım University, Faculty of Fine Arts and Design, Department of Architecture, Ankara, Turkey	Instructor
2012-2015	Hamamcıoğlu Waterside Restoration Work Sarıyer, Istanbul, Turkey	Architect
	Mister Osman Hamdi Boathouse Restoration Work, Gebze, Istanbul, Turkey	Architect
	Masonry Residential Building Restoration Work, Balat, Istanbul, Turkey	Architect

2012-2013	"City Dreams- 8, Saraçoğlu Neighborhood" Evaluation Project National Idea Competition	Jurry Member
2009-2011	Gürsoy Group Companies-Restoration Group Çengelköy, Istanbul, Turkey	Site Architect

2009-2011   Gürsoy Group Companies-Restoration Group   Site Architect
Çengelköy, Istanbul, Turkey

Participated Projects

Süleymaniye Mosque Restoration Work,
Fatih, Istanbul, Turkey

Yenikapı Mevlevi Lodge Restoration Work,
Zeytinburnu, Istanbul, Turkey

Egyptian Consulate (Hidiva Palace)
Restoration Work, Bebek, Istanbul, Turkey

Award of Building Branch Mister Uğur Reyhan Kiosk
Restoration Work, Çengelköy, Istanbul, Turkey

Archers Lodge Restoration Work,
Okmeydanı, Istanbul, Turkey

2009   Restoration Education Program of (KOREFD)   Architect
Conservation and Restoration Firms Solidarity
Fatih, Istanbul, Turkey

Theoretical training from Restoration Academic Staff
of METU, ITU, and YTU, Turkey

Hands-on training (hand-drawn, gold foil etc.)
in Dolmabahçe Palace and Yıldız Palace
Beşiktaş, Istanbul Turkey

Aynalıkavak Palace Restoration Work,
Beyoğlu, Istanbul, Turkey

2008   Fema Architectural Office, Ankara, Turkey   Intern Architect

2007   Housing Development Administration of Turkey   Intern Architect
Ankara, Turkey

RESEARCH INTERESTS

Conservation of cultural heritage, protection and restoration of historical sites, conservation and restoration techniques, structural and material analyses of historical and archaeological places, arhaeology, archaeometry.

PUBLICATIONS

National Articles

Tanrıverdi, Z., Akyol, A.A., Atalay, Ü., "Ankara Roma Hamamı Yapı Malzemelerinde Arkeometrik Çalışmalar", 39. Uluslararası Kazı, Araştırma ve Arkeometri Sempozumu, Cilt: 1, s. 13-37, Bursa, Türkiye, 2018.

PRESENTATIONS

Invited Seminars

2018, Ankara Roma (Caracalla) Hamamı Yapı Malzemelerinin Arkeometrik Olarak İncelenmesi, ODTÜ Arkeometri Semineri, Ankara, Türkiye.

2017, A study on the Historic Environmental Analysis and Protection of Saraçoğlu Quarter in Ankara, Seminar for 3rd Year Design Studio of Arhitectural Department, Reconsidering Urban Assets of Ankara: The Saracoglu Quarter Architecture that Heals: An Extention to Namık Kemal Primary School, METU, Ankara, Turkey.

2017, Ankara Saraçoğlu Mahallesi'nin Çevre ve Yapı Bazında İncelenmesi, ODTÜ Arkeometri Semineri, Ankara, Türkiye.